THESIS ON NATURAL AND EXACT SCIENCES B127

Variability of Thermohaline Structure in the Gulf of Finland in Summer

TAAVI LIBLIK

TUT
PRESS

TALLINN UNIVERSITY OF TECHNOLOGY
Marine Systems Institute

Dissertation was accepted for the commencement of the degree of Doctor of Philosophy in Earth Sciences on January 13, 2012

Supervisor: Prof. Urmas Lips, Marine Systems Institute at Tallinn University of Technology, Estonia

Opponents: Dr. Johannes Karstensen, Helmholtz Centre for Ocean Research Kiel (GEOMAR), Germany

Dr. Hanno Ohvril, Institute of Physics, University of Tartu, Estonia

Defence of the dissertation: April 17, 2012 at the Marine Systems Institute at Tallinn University of Technology, Akadeemia tee 15a, Tallinn, Estonia

Declaration:

Hereby I declare that this doctoral dissertation, my original investigation and achievement, submitted for the doctoral degree at Tallinn University of Technology has not been submitted for any academic degree.

Taavi Liblik

ISSN 1406-4723
ISBN 978-9949-23-258-1 (publication)
ISBN 978-9949-23-259-8 (PDF)

LOODUS- JA TÄPPISTEADUSED B127

Termohaliinse struktuuri muutlikkus Soome lahes suvekuudel

TAAVI LIBLIK

TTÜ
KIRJASTUS

Contents

LIST OF ORIGINAL PUBLICATIONS

I. Liblik, Taavi; Lips, Urmas. (2011). Characteristics and variability of the vertical thermohaline structure in the Gulf of Finland in summer. Boreal Environment Research, 16A, 73 – 83.

II. Liblik, Taavi; Lips, Urmas (2012). Short-term variations of thermohaline structure in the Gulf of Finland. Ocean Sci. Discuss., 9, 877-908.

III. Lips, Inga; Lips, Urmas; Liblik, Taavi (2009). Consequences of coastal upwelling events on physical and chemical patterns in the central Gulf of Finland (Baltic Sea). Continental Shelf Research, 29, 1836- 1847.

IV. Lips, Urmas; Lips, Inga; Liblik, Taavi; Elken, Jüri (2008). Estuarine transport versus vertical movement and mixing of water masses in the Gulf of Finland (Baltic Sea). US/EU-Baltic Symposium "Ocean Observations, Ecosystem-Based Management & Forecasting", Tallinn, 27-29 May, 2008. IEEE, 2008, (IEEE Conference Proceedings), 1 - 8.

V. Lips, Urmas; Lips, Inga; Liblik, Taavi; Kikas, Villu; Altoja, Kristi; Buhhalko, Natalja; Rünk, Nelli (2011). Vertical dynamics of summer phytoplankton in a stratified estuary (Gulf of Finland, Baltic Sea). Ocean Dynamics, 61, 903 - 915.

VI. Lips, Urmas; Lips, Inga; Liblik, Taavi; Kuvaldina, Natalja. (2010). Processes responsible for the formation and maintenance of sub-surface chlorophyll maxima in the Gulf of Finland. Estuarine, coastal and shelf science, 88, 339 - 349.

Author's contribution

I – The author was responsible for data analysis and writing of the manuscript

II – The author was responsible for organization of measurements, data analysis and writing of the manuscript

III – The author participated in the field measurements, processed and analysed temperature and salinity data, made the analysis of vertical profiles and contributed to the writing of the manuscript

IV – The author participated in the field measurements, processed and analysed temperature and salinity data and contributed to the writing of the manuscript

V – The author was responsible for organization of measurements at the autonomous buoy station, processed and analysed temperature, salinity and fluorescence data, made analysis of vertical profiles and contributed to the writing of the manuscript

VI – The author participated in the field measurements, processed and analysed temperature and salinity data, made analysis of vertical profiles and contributed to the writing of the manuscript

Approbations of the results

The results have been presented in the following international conferences:

1. European Geosciences Union General Assembly 2009 on 19-24 April 2009, Vienna, Austria. Inter-annual variability of vertical distribution of temperature and salinity in the Gulf of Finland (with U. Lips).
2. 7th Baltic Sea Science Congress on 17-21 August 2009, Tallinn, Estonia. Wind-forced variability of vertical structure of temperature and salinity fields in the Gulf of Finland (with U. Lips).
3. Joint meeting with ASLO and NABS 2010 on 6-11 June 2010, Santa Fe, USA. High-resolution observations of vertical structure and variability of hydrophysical fields and related changes in phytoplankton community behavior (with U. Lips, I. Lips, V. Kikas and K. Altoja).
4. 8th Baltic Sea Science Congress on 22-26 August 2011, St. Petersburg, Russia. Short-term variability of vertical thermohaline structure and currents in the Gulf of Finland (with U. Lips).
5. 21st Biennial Conference of the Coastal and Estuarine Research Federation on 6-10 November 2011, Daytona Beach, USA. Changes in thermohaline structure from hours to years in the Gulf of Finland in summer (with U. Lips).

Structure of thesis

The content of the thesis is as follows. In the first chapter, the background and importance of thermohaline structure in the Gulf of Finland is described. Subsequently, the motivation and objectives of the thesis are explained and formulated. In the second chapter, material and methods are described.

The results of the thesis are presented in chapters 3-5. In subsection 3.1 mainly long term descriptive thermohaline parameters of the Gulf of Finland are under investigation (paper I), such as the overall long term mean values, the mean changes along the Gulf or partial (summer only) seasonal course are presented. The results regarding long term variations in the Gulf are revealed in subsections 3.2 and 3.3 (paper I). Mesoscale, synoptic and diurnal scale variability is under consideration in subsection 4 (papers II, III, IV, V and VI) and its effects to the nutrient fields (papers III, IV and V), phytoplankton dynamics and vertical distribution (papers V and VI) are under discussion in chapter 5.

Concluding remarks are given in the chapter 6.

Acknowledgements

First, I would like to thank my supervisor Prof. Urmas Lips for guiding me during the last decade. Also, I take this opportunity to express my gratitude to the coauthors of the papers included in the study: Kristi Altoja, Natalja Buhhalko, Jüri Elken, Villu Kikas, Inga Lips and Nelli Rünk. I am grateful to Jüri Elken, Jaan Laanemets and Mairi Uiboaed for reviewing the thesis and their helpful comments.

I am thankful to colleagues in Marine Systems Institute at TUT and its predecessors who have participated in collecting of analyzed CTD data in 1987-2009. I also wish to thank the crew of research vessel Salme for their helpfulness and smooth cooperation.

This work was financially supported by the Estonian Science Foundation (grants ETF6752, ETF6955, ETF8930 and ETF9023), ESF Doctoral Studies and Internationalisation Programme DoRa and Doctoral School on Earth Sciences and Ecology.

Finally, I would like to thank my family, especially my partner Katrin, for always supporting me.

1. INTRODUCTION

1.1. Background

The Baltic Sea is a semi-enclosed, brackish and non-tidal sea with remarkably positive fresh water flux. The Gulf of Finland covers approximately 29 600 km^2 and its volume is 1100 km^3. The Gulf is about 400 km long and 48-135 km wide basin without sill at the entrance area separating the Gulf from open Baltic Sea. The maximum cross-sectional depth decreases from >100 m at the entrance to <30 m in the eastern part of the Gulf. The bottom topography of the Gulf is quite complicated, especially in the coastal areas, where shoals, peninsulas and islands subdivide coastal area to smaller bays. There are two main sources that contribute to water exchange of the Gulf: the freshwater run-off from rivers and saltier water inflow from the northern Baltic Proper. The Gulf receives on average 3556 $m^3\ s^{-1}$ of river discharge that is mainly concentrated in the easternmost part of the Gulf (Bergström and Carlson 1994). The combination of large freshwater inflow in the eastern part and saltier water in the western boundary of the Gulf causes permanent salinity gradient along the Gulf axis — the horizontal salinity distribution in the surface layer is characterized by an increase from 1-3 in the east to 6 in the west. Also, a slight increase of salinity from north to south exists due to the mean (residual) cyclonic circulation in the upper layer. Since the water can freely exchange through the mouth of the Gulf, the renewal time of the water is about two years (Elken 2006) and the water age with respect to exchange with the Baltic Proper is at most two years (Andrejev *et al*. 2004).

The thermohaline structure of the Gulf and its features are considerably dependent on atmospheric forcing, especially on wind. Typically for the Baltic Sea area SW winds are the most dominant round the year (Mietus 1998; Soomere and Keevallik 2001). The secondary maximum is from NNW. The dominance of these two wind directions is distinct, when only stronger winds are taken into account (Soomere and Keevallik 2001). Additionally to the described Baltic Sea general wind field, the along-axis winds (from E and NE) have also notable occurrence, but SE winds are very weak and infrequent in the Gulf of Finland (Soomere and Keevallik 2003). However, local changes in the wind field have also been detected (Keevallik and Soomere 2010).

The mesoscale features (mesoscale eddies, fronts etc.) are characterised by the horizontal scales determined by the baroclinic Rossby radius $R_d = NH/f$, where N is the mean buoyancy frequency, f is the inertial frequency (Coriolis parameter) and H is the depth. Since R_d depends on the vertical stratification and the depth of the sea, it varies from 50 km (typical scale in the oceans) to a few kilometres in the Baltic Sea (Pavelson 2005). The typical baroclinic Rossby radius in the Gulf of Finland was found to vary from 2–4 km in the eastern and central Gulf to about 5 km in the western part of the Gulf (Alenius *et al*. 2003).

Since the width of the Gulf is well larger than the baroclinic Rossby radius, the meso-scale processes and related changes in the vertical thermohaline structure are dominant dynamical features of the Gulf of Finland. Coastal coupled upwelling and downwelling events remarkably affect the spatial distribution of the sea surface temperature that is well visible on remote sensing images (see e.g. an analysis by Uiboupin and Laanemets 2009) or in the upper layer temperature and salinity measured across the Gulf (Lips *et al*. 2008). Normally upwelling event along the southern coast is coupled with downwelling event along the northern coast and *vice versa*. Upwelling along the northern coast of the Gulf of Finland is induced by south-westerly winds and near the southern coast by north-easterly winds. It has been found that winds must usually prevail for at least 60 hours to generate upwelling; however, required wind impulse depends on stratification (Haapala 1994). Since south-westerly winds are dominant in the region, the northern coast of the Gulf of Finland has been noticed by observations (Kononen and Niemi 1986; Haapala 1994) and modelling (Myrberg and Andrejev 2003) as one of the main upwelling areas in the Baltic Sea.

Since the Gulf has remarkable salinity gradients, the area is suitable for the generation of fronts. The most prominent, quasi-permanent density (salinity) front is located at the entrance area of the Gulf. The thermohaline structure in that area has been studied thoroughly (Talpsepp 1993; Pavelson *et al*. 1997; Laanemets *et al*. 2005 and others). The front separates the northern Baltic Proper more saline waters spreading along the Estonian coast and fresher waters originating from the Gulf of Finland. The front is highly sensitive to the wind direction. Easterly winds (parallel to the front) induce offshore movement of denser water, while with westerly winds, the water mass with lower density moves onshore and overrides the denser water, thus forming shallower secondary pycnocline (Pavelson 2005).

The water column in the deeper areas of the Gulf reveals a three-layer vertical structure in summer – the upper mixed layer (UML), the cold intermediate layer (CIL), known also as a Baltic Winter Water (e.g. Hagen and Feistel 2007) and a saltier and slightly warmer near-bottom layer (NBL) can be distinguished. These layers are separated by thermocline and halocline situated at the depths of 10-20 m and 60-70 m, respectively.

The inter-annual variability of temperature in the upper layer of the Gulf of Finland is remarkable. Lips and Lips (2008) showed that summer mean upper layer temperature along Tallinn-Helsinki transect varied in a range 14-18 °C in 1997-2005. On the background of the variability, an increase in average surface layer temperature has been observed during the last couple of decades (e.g. Suikkanen *et al.* 2007). It has been reported that the summer sea surface temperature of the North and Baltic seas has increased since 1985 at a rate of 0.07-0.08 °C yr^{-1}, which is 2-5 times faster than that in other seasons (MacKenzie and Schiedek 2007). Analyses of remote sensing data from 1990-

2004 (Siegel *et al.* 2006), 1990-2008 (Lehmann *et al*. 2011) and 1986-2005 (Bradtke *et al*. 2010) have revealed a strong positive trend of the sea surface temperature in the Baltic Sea in summer. However, according to the study by Voss *et al*. (2011) the positive trend was not confirmed in the upper layer (0-10 m) in May and August from 1979 to 2005.

The formation of cold intermediate layer (CIL) occurs in autumn-winter, when convective and wind-induced vertical mixing increases the upper layer thickness and breaks the sharp vertical temperature gradients formed in summer in the upper layer. This process leads to the period with thick (from surface to 60 m) (Haapala and Alenius 1994) mixed layer in winter. Thus, the meteorological forcing in winter months presumably has a considerable effect to the characteristics of cold intermediate layer. Hinrichsen *et al*. (2007) have shown a remarkable correlation between sea surface temperature in winter months and cold intermediate layer temperature in summer for several areas of the Baltic Sea (Gulf of Finland was not investigated in that study), which indicates that winter severity greatly determines the inter-annual variability of CIL. This variability can be well seen, for example, in the Baltic Sea maximum sea-ice extent (Seinä and Palosuo 1996) or in the sum of negative-degree-days in the central Gulf of Finland (Pärn 2011). The range of variability is very large — the Baltic Sea maximum ice extent in extremely severe winter (1986/1987) and the mildest winter since 1720 (2007/2008) were 405 000 km^2 (Seinä and Palosuo, 1996) and 49 000 km^2 (Vainio and Isemer 2008), respectively. Though large scale atmospheric forcing in winter appears to be the main influencing factor to the CIL formation, also local process could considerably contribute — denser surface water dives from shallow areas during autumn cooling and early spring heating to the deeper parts of the sea (Chubarenko and Demchenko 2010). In addition, the mixing intensity in spring and summer, as well the up- and downwelling events could also influence summer CIL temperature.

Though there is no evidence of summer CIL temperature trend in the Gulf of Finland, temperature increase was reported (Hinrichsen *et al*. 2007; Voss *et al*. 2011) in the southern Baltic Sea basins at the depths of 40-60 m during the last couple of decades.

The long term changes in temperature and salinity in the deep layers of the Baltic Sea are largely related to the major barotropic inflows (Matthäus and Franck 1992) and baroclinic inflows (Matthäus *et al*. 2008) from the North Sea. The stagnation period, which occurred since the major inflow in 1976, was ended with a very strong inflow in 1993 (Matthäus and Lass 1995; Jakobsen 1995), which was followed by a weaker event in 1997 (Matthäus *et al*. 2008) and moderate event in 2003 (Meier *et al*. 2003; Lehmann *et al*. 2003; Feistel *et al*. 2003a). The baroclinic warm water inflows have been documented in summer-early autumn 2002 (Feistel *et al*. 2003b; Lehmann *et al*. 2003), 2003 (Feistel *et al*. 2004), 2006 (Nausch *et al*. 2007) and 2009/10 (Nausch *et al*. 2010). According to the HELCOM monitoring data a decrease of salinity in the

deep layers of the Gulf of Finland, observed from the late seventies, was replaced by a salinity increase in the nineties (HELCOM 2002). This could be related to the end of the stagnation in the deep waters of the Baltic Proper.

According to Elken *et al.* (2003) also short-term variability exists in the deep layer temperature and salinity of the Gulf of Finland. They showed that depending on prevailing wind conditions, an ordinary estuarine circulation may be altered or even reversed if the south-westerly wind component exceeds the mean value by at least 4-5.5 m s^{-1}. Reversal of the estuarine circulation resulted in lower salinity in the deep layer and drastic weakening of the vertical stratification in the Gulf of Finland in August 1998. Inversely, the prevalence of north-easterly winds induces stronger estuarine flow, higher salinity values in the near bottom layer and stronger stratification through the water column.

Meier and Kauker (2003) have found that about half of the decadal variability of the average salinity of the Baltic Sea is related to the accumulated freshwater inflow. According to the model results (Graham 1999), no significant annual runoff trend was found during the period 1950-2009 in the Gulf (Kronsell and Andersson 2010). The BACC group (BACC 2008) analysed the runoff to the whole Baltic Sea during 1921-1998 and their outcome was similar — even the decadal mean values vary in a wide range, no statistical trend can be found.

In the present state, the Gulf of Finland ecosystem is extremely sensitive to increased sediment effluxes of nutrients (Gran and Pitkanen 1999; Jantti *et al*. 2011). After the spring bloom, the inorganic nutrients are almost depleted in the UML, and strong stratification prevents mixing between the nutrient depleted upper layer and the nutrient rich lower layers. One of the most important processes, which bring nutrient rich waters from deeper layers to the surface in summer, is upwelling. Direct measurements of changes of nutrient concentrations in the surface layer caused by coastal upwelling events are relatively rare in the Gulf of Finland. Haapala (1994) reported that during upwelling events in the coastal area near the Hanko Peninsula, the nutrient concentrations increased from 0.03-0.06 μmol l^{-1} to 0.13-0.26 μmol l^{-1} of phosphate-phosphorus and from 0.04-0.14 μmol l^{-1} up to 1.4 μmol l^{-1} of ammonium-nitrogen. The consequences of upwelling along the northern coast in the western Gulf of Finland were described on the basis of data collected during an intensive measurement campaign in July-August 1999 (Vahtera *et al*. 2005). An increase of phosphate-phosphorus concentration in the surface layer from 0.02 μmol l^{-1} up to 0.32 μmol l^{-1} was observed. The simulations of this upwelling event suggested that the total amount of phosphorus and nitrogen transported and left into the upper 10 m layer of the Gulf as a result of the upwelling event was 387 and 36 tons, respectively (Zhurbas *et al*. 2008).

The distribution of phytoplankton in water bodies (including the Baltic Sea) is highly heterogeneous, both horizontally and vertically. Horizontal distribution of phytoplankton in the euphotic layer is often related to the meso-scale

hydrophysical processes and structures – meso-scale eddies, fronts and coastal upwelling events (in the Gulf of Finland e.g. Talpsepp *et al*. 1994; Kononen *et al*. 1996; Kanoshina *et al*. 2003; Lips *et al*. 2005). Vertical distribution of phytoplankton is determined by availability of major resources – light and nutrients – as well as grazing and divergence/convergence of sinking and buoyancy (see e.g. Fennel and Boss 2003). In a stratified water column, the contrasting gradients of resources – light that is supplied from above and nutrients that are often supplied from below – will lead to the development of a sub-surface biomass/chlorophyll (Chl *a*) maximum (Klausmeier and Litchman 2001).

The sub-surface Chl *a* maxima have been observed in the Baltic Sea quite often (e.g. Kahru *et al*. 1982; Kuosa 1990; Kononen *et al*. 1998; Pavelson *et al*. 1999) and a variety of mechanisms of their formation has been suggested. Development of measuring equipment in the last years has triggered an enhanced interest to sub-surface maximum layers of phytoplankton and zooplankton biomass, their fine-scale structure (e.g. "thin layers"), and ecology. Typical fine-scale layers range in thickness from a few centimetres to a few metres and are described in literature as "thin layers" (e.g. McManus *et al*. 2003). Physical processes and vertical stratification can play an important role in the formation of such layers. A two-layer current, temporal and spatial variation of pycnocline depth, caused by meso-scale physical processes and estuarine structure of hydrographic fields, and minimum of turbulent mixing are conditions favourable for the formation of thin layers (Dekshenieks *et al*. 2001; McManus *et al*. 2003; Lund-Hansen *et al*. 2006). Vertical stratification characterized by two strong pycnoclines and a weak, estuarine circulation pattern superimposed by quite energetic, wind-driven meso-scale motions serve as pre-requisites for the formation of sub-surface Chl *a* maxima and thin layers in the Gulf of Finland.

1.2. Motivation and objectives

Changes in temperature and salinity and corresponding variations in density are crucial factors for the physics of the Gulf of Finland. The physical background and processes, such as stratification or dynamics of the water masses are relevant for many chemical and biological processes. A number of studies have reported the importance of thermohaline structure to several processes or components related to the ecological status/environmental problems of the Gulf of Finland, such as nutrients distribution (Zhurbas *et al*. 2008) and eutrophication, phytoplankton species composition (Rantajärvi *et al*. 1998), macrozoobenthos abundance (Laine *et al*. 2007), cyanobacteria blooms (Lips and Lips 2008), distribution of pelagic fish (Stepputtis *et al*. 2011) or oxygen concentration (Maximov 2006). Since many environmental problems appear in summer, the present thesis is focused on the thermohaline variability in that season.

The general motivation of the thesis is to enhance the present knowledge and predictability of the Gulf of Finland in different time scales. The data set with more than 2000 CTD casts collected during a period of twenty years was analysed to link the long-term changes and respective forcing factors, which should allow to estimate potential changes of thermohaline structure in case of different future climate projections, and also, compare the results with already projected changes in temperature and salinity (BACC 2008). The CTD profiles collected with high temporal resolution and intensive inter-disciplinary measurement campaigns gave an opportunity to enlarge the present knowledge of nutrient and phytoplankton dynamics in relation to changes in thermohaline structure at time scales from days to months.

The hydrography of the Gulf of Finland was quite thoroughly described by Alenius *et al.* (1998 and 2003) using data collected until 1996, but the latest descriptions of the hydrographic conditions in the Gulf of Finland have been based (see review paper by Soomere *et al.* 2008) mainly on modelling (e.g. Andrejev *et al.* 2004) or remote sensing (e.g. Uiboupin and Laanemets 2009).

A series of interdisciplinary field studies have been carried out in 1990's in the western Gulf of Finland (Kononen *et al*. 1996; Laanemets *et al*. 1997; etc.) resulting in a considerable increase in knowledge regarding the impact of meso-scale physical processes on nutrients and phytoplankton dynamics at a mesoscale. There has been growing demand on seasonal forecasts and continuous assessment of the state of the Baltic Sea, including the Gulf of Finland. Thus, ship-based interdisciplinary measurements and high-resolution observations should be extended to have large enough coverage (e.g. covering the entire cross-section of the Gulf) and long enough duration (seasonal) to elucidate the role of different mechanisms/processes and typical patterns in the termohaline structure influencing the nutrients and phytoplankton dynamics.

In comparison to the earlier studies (e.g. Alenius *et al*. 1998, 2003; Kononen *et al*. 1996; Laanemets *et al*. 1997; etc.), the present analysis includes also the years after the mid-1990s when according to the HELCOM monitoring data, an increase of salinity in the deep layers of the Gulf of Finland has occurred. Intensive interdisciplinary measurement campaigns were also carried out across the Gulf and vertical CTD measurements were performed with high temporal resolution at a buoy station in the open Gulf – a technology that allows to measure diurnal variability in thermohaline structure over a long period.

The main aim of the thesis was to improve the knowledge on the thermohaline structure of the Gulf of Finland in summer and to identify the main driving factors and processes causing its variability. Secondly, the influence of these processes and vertical stratification on the nutrient fields and phytoplankton dynamics were analysed.

The main objectives are:

- to describe the vertical structure of temperature and salinity fields and its inter-annual variations in the Gulf of Finland in summer (June-August) on the basis of data collected in 1987-2008 (paper I);
- to relate the observed inter-annual changes in thermohaline structure to changes in atmospheric forcing and suggest possible future changes in the vertical thermohaline structure of the Gulf of Finland taking into account the climate change projections (paper I);
- to define distinct stratification patterns (TS-curves) for the upper mixed layer and thermocline using CTD-measurements with high temporal resolution and explain in what conditions these situations/patterns occur (paper II);
- to specify the influence of upwelling on the changes of thermohaline structure of the Gulf, focusing on short-term variations at a buoy station (paper II) and weekly variations at a cross-gulf section (paper III);
- to show that the dynamics of the whole water column and corresponding salt and phosphorus fluxes in the deep layer reveal variations in accordance with variations in wind speed and direction (paper IV);
- to estimate how different patterns in the thermohaline structure and/or the processes shaping the structure affect the distributions and dynamics of nutrients and phytoplankton community (papers III, V, VI).

2. MATERIAL AND METHODS

The data analysed in the present thesis were collected in the frames of various research projects and monitoring programs of the Marine Systems Institute at Tallinn University of Technology and its predecessors in 1987-2009 (see Fig. 1.).

The CTD data used in the thesis could be divided as follows:

- data collected aboard research vessels all around the Gulf of Finland before 2006 (used in paper I),
- data collected aboard the research vessel along the section from Tallinn to Helsinki in 2006 (papers I, III, IV and VI) and 2007 (papers I and IV),
- data collected aboard the research vessel from the other areas in the Gulf from 2007 to 2008 (paper I),
- data collected aboard the research vessel and by autonomous water column profiler from the central part of the Gulf in 2009 (papers II and V).

The CTD data until 2008 were collected by CTD probes Neil Brown Mark III and Sea-Bird SBE 19*plus*. The data collected aboard the research vessel and at autonomous buoy station in 2009 were acquired by Idronaut S.r.l CTD probes Ocean Seven 320*plus* and Ocean Seven 316*plus*, respectively. The number of CTD profiles and study period for each publication is given in table 1.

CTD casts were processed and stored as vertical profiles with a resolution of 0.5 m (1 m corresponds roughly to 1 dbar). The salinity values were calculated using algorithms from Fofonoff and Millard Jr. (1983) and are presented without units on the Practical Salinity Scale 1978.

Table 1. The measurement period and the total number of CTD profiles used in each publication.

Papers	**Period**	**Total number of CTD casts**
I	1987-2008	2143
II, V	01.07-28.08.2009	314
III, VI	11.07-29.08.2006	189
IV	11.07-29.08.2006 and 26.04-07.06.2007	378

Additionally, the following data sets were used in the thesis:

- upper layer (4 m depth) temperature, salinity and Chl *a* fluorescence measurements by the Ferrybox system installed aboard the ferry "Baltic Princess" travelling twice a day between Tallinn and Helsinki (paper V),

- nutrient concentrations (phosphates and nitrates+nitrites) and Chl *a* determined from water samples collected by Ferrybox (paper V),
- current measurements in the central Gulf of Finland (papers II and V),
- wind data from Kalbådagrund meteostation were used in all papers,
- coastal temperature measurements at Loksa and Pakri (paper III),
- Baltic Sea Index (difference of normalized sea level pressure anomalies between Szczecin in Poland and Oslo in Norway) – BSI (Lehmann *et al*. 2002) (paper I),
- the annual maximum ice extent of the Baltic Sea (paper I),
- Chl *a* fluorescence and Chl *a* determined from water samples (papers V and VI),
- nutrient concentrations (phosphates and nitrates+nitrites) data determined from water samples collected by the research vessel (papers III, IV, V, VI),
- phytoplankton biomass and composition determined from water samples (paper V),
- hydrometeorological data from coastal stations (paper II).

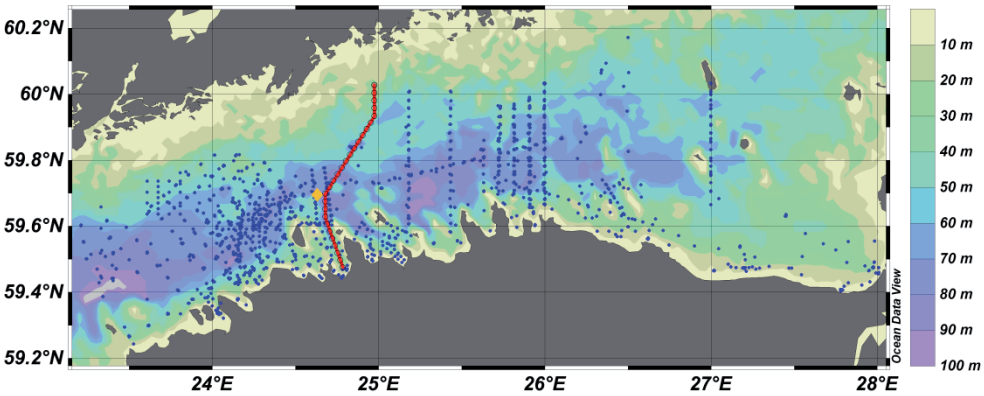

Figure 1. Map of the Gulf of Finland. CTD data collected in 1987-2008 (blue dots), cross-section sampled at 27 stations in 2006 and 2007 (red line), and autonomous buoy station in 2009 (yellow diamond).

Historical CTD data were collected as surveys on a horizontal grid of stations, sections or single stations visited in the frames of monitoring programmes. Measurements in July-August 2006-2007 were designed as stations of vertical profiles across the Gulf from Tallinn to Helsinki. Surveys were carried out on a weekly basis and with the spatial resolution (distance between stations) of about 2.6 km in order to reveal mesoscale variability and to cover the entire cross-section. For the measurements in July-August 2009, new autonomous systems with near real time data delivery were applied – a profiling buoy and a Ferrybox system. Vertical profiles at the buoy station were acquired with a time resolution of 3 hours in order to reveal the diurnal variability. The average vertical

resolution of profiles was 10 cm. Such technology – autonomous acquisition of fine-scale vertical profiles with a time reolution of 3 hours during a 2-months period – was applied for the first time in the Baltic Sea.

Autonomously collected data using the profiling buoy and Ferrybox were transmitted near real time after every CTD cast and every evening, respectively. During a two-month-long study period altogether 314 CTD-profiles were collected in 2009 by autonomous profiler.

In order to characterize the vertical thermohaline structure the following parameters were calculated:

- the upper mixed layer (UML) depth, which is equivalent also to the shallower border of thermocline (papers I, II, V and VI);
- the base of thermocline (BT), the difference between BT and UML is defined as the thermocline thickness (papers I, II and VI);
- the temperature and depth of the cold intermediate layer (CIL) were determined as the minimum temperature of the current profile and the depth corresponding to this minimum record (paper I, III and VI);
- the centre of the halocline was defined using smoothed salinity profiles (2.5 m moving average) as the maximum salinity gradient below the coldest point at the current profile. The halocline was determined only in case if the smoothed salinity gradient exceeded 0.07 m^{-1} (paper I);
- the depth of the strongest density gradient was defined as the depth of maximum Brunt-Väisälä frequency (h_{maxN}) (paper V).

The exact calculation procedures of parameters can be found in material and methods chapter in papers I-VI. Slightly different algorithms have been applied for the detection of the UML depth and base of the thermocline depending on the used data sets. For instance, since it was not always possible to detect the CIL temperature and depth for profiles acquired at autonomous buoy station (due to profiling depth of 45-50 m), the BT was defined simply as the depth of the isotherm 5 °C. It was checked that for those profiles, where application of both methods was possible, outcomes of used methods did not differ significantly.
The potential energy anomaly was calculated following Simpson and Bowers (1981) and Simpson *et al.* (1990) as:

$$P = \frac{1}{h}\int_{-h}^{0}(\rho_A - \rho)gzdz, \quad \rho_A = \frac{1}{h}\int_{-h}^{0}\rho dz; \qquad (1)$$

where $\rho(z)$ is the density profile over the water column of depth h. The stratification parameter P (J m^{-3}) is the work required to bring about complete mixing of the water column under consideration.

The time development of potential energy anomaly was modelled as the sum of the following four terms:

$$\frac{dP}{dt} = S_b + S_m + S_a + S_e, \quad (2)$$

where the first term on the right S_b is the increase or decrease of stratification due to the upper layer heating or cooling, respectively. The second term S_m is the decrease of stratification due to wind mixing and the third term S_a is the parameter, which describes the decrease or increase of stratification due to the wind induced transport in the surface layer. The last term on the right S_e is the parameter describing the mean estuarine flow that always increases the stratification. The calculation of these terms is shown in material and methods chapter of paper II.

For volume transport estimates in the Gulf of Finland in spring-summer 2006-2007, the results of operational oceanographic model HIROMB (High Resolution Operational Model for the Baltic Sea, Elken *et al.* 2008) were used. The model version domain covered the whole Baltic Sea area with grid steps 1' by latitude and 5/3' by longitude and had 16 vertical layers.

The intensity of sub-surface Chl *a* maxima was estimated as the difference between the maximum Chl *a* value below 10 m depth and the minimum above it at each vertical profile. The thickness of maximum layer was defined as the difference between the depth of local minimum and the depth where the Chl *a* values below the maximum decreased back to the same (minimum) concentration (see excact calculation procedure in paper VI). In addition, phosphacline and nitracline depths were defined on the basis of water sample analyses (collected in the thermocline with a vertical resolution of 2.5 m) as the deepest depth at which the phosphate (PO_4^{3-}) or nitrate-nitrite (NO_x) concentration, respectively, below the lower detection range was measured (paper VI).

The methods of water sample analyses for nutrient, Chl *a*, phytoplankton species composition and biomass are presented in papers III-VI. The lower detection range for phosphate-phosphorus and nitrate+nitrite-nitrogen was 1 ppb (parts per billion; with a measurement uncertainty of 20% near the detection limit). It corresponds to the concentration of 0.03 μmol l^{-1} for PO_4^{3-} and 0.07 μmol l^{-1} for NO_x, which were used also in the transport estimates below.

3. THERMOHALINE STRUCTURE IN THE GULF OF FINLAND

3.1. Hydrographic characteristics

3.1.1. Upper mixed layer

The overall mean UML depth on the basis of available CTD casts in the Gulf of Finland in summers 1987-2008 was 12.8 m. On average, the UML depth was the shallowest in June, slightly deeper in July and the deepest in August. Along the Gulf, the mean UML depth had relatively uniform distribution— the deepest UML depth (15.1 m) was found in the westernmost part of the Gulf, between longitudes 23.2 to 24.2 E, while in the two other regions, the mean UML depth was close to 13.0 m (Fig. 2). Across the Gulf, the UML depth was on average deeper near the southern coast than that in the off-shore areas. A remarkably higher variation of the UML depth was found in the coastal area. The deeper UML depth near the southern coast could be explained by south-westerly winds prevailing in the region and corresponding dominance of downward movement along the southern coast (Myrberg and Andrejev 2003).

The mean UML water temperature and salinity in summer in the Gulf of Finland were 15.2 °C and 5.2, while those in June were 11.8 °C and 4.9, in July 16.9 °C and 5.3, and in August 16.9 °C and 5.4. The mean UML temperature did not reveal any regular changes along the Gulf, however, notably higher average annual maximum sea surface temperatures have been reported (Alenius *et al*. 1998) in the eastern part of the Gulf, the area which was not included in the present study. The mean UML salinity distribution was characterized by an increase from 4.3 in the eastern part of the study area (25.7-26.2° E) to 5.7 in the mouth of the Gulf of Finland (Fig. 2).

Cross-gulf changes of the mean UML temperature and salinity were in the ranges of 15.7-16.4 °C and 5.1-5.3, respectively. The highest variations of the UML temperature and salinity were found near the coast. Obviously this feature could be explained by occasional coastal upwelling events, which remarkably affect the upper mixed layer temperature and salinity in summer.

3.1.2. Thermocline

The base of the thermocline was situated on average at 27.2 m and, as a result, an average thickness of the thermocline of 14.4 m was obtained. The monthly mean depth of the base of the thermocline and corresponding thicknesses of the thermocline were 23.6 m and 12.2 m in June, 26.5 m and 14.4 m in July, and 31.6 m and 16.7 m in August. The similar seasonal deepening of thermocline during the summer was well evident also in average seasonal variations of isotherms (Haapala and Alenius 1994).

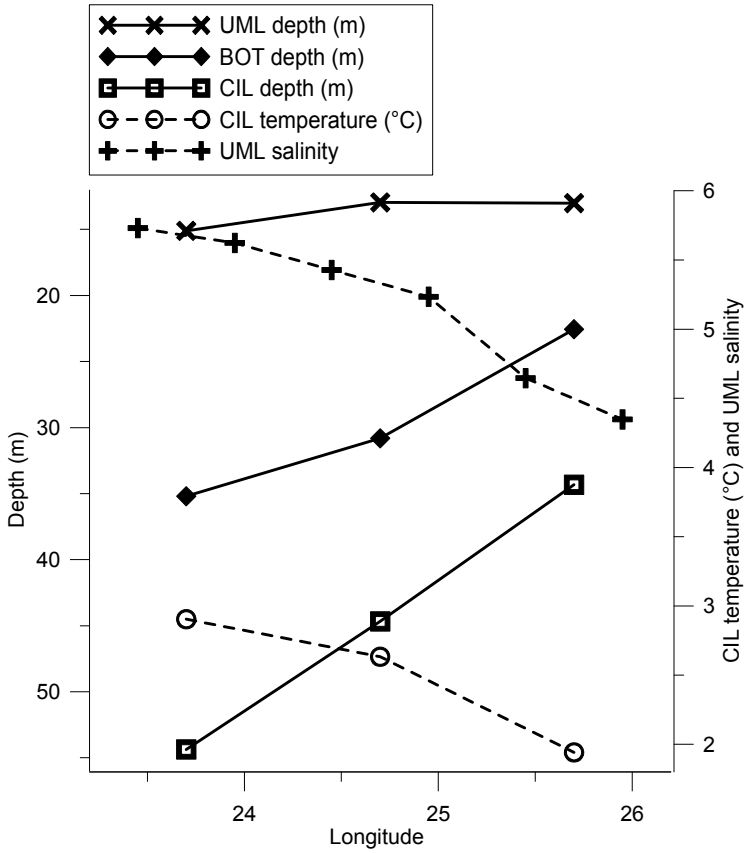

Figure 2. Mean along-gulf changes of the UML depth (solid line with crosses), the base of the thermocline (solid line with diamonds), the CIL depth (solid line with open squares), the UML salinity (dashed line with crosses) and the CIL temperature (dashed line with circles) in the Gulf of Finland in summers 1987-2008. Estimates are made within the three longitudinal intervals (23.2-24.2° E, 24.2-25.2° E and 25.2-26.2° E while for the UML salinity a longitudinal step of 0.5° was used).

The base of the thermocline was deeper in the mouth of the Gulf and shallower in the eastern part of the study area changing from 35.2 to 22.6 m (Fig. 2). Since the UML depth varied less in comparison with the rise of the base of the thermocline, the thermocline was remarkably thicker in the mouth area and thinner in the eastern part of the study area. Thus, similarily to a wind induced mixing event, a movement of the entire water column above the halocline to the east (in the southern part of the Gulf, for instance) will also cause the deepening of the thermocline at a certain measurement site.

3.1.3. Cold intermediate layer

The mean temperature of the coldest point of temperature profiles (CIL temperature) and its depth (CIL depth) in the Gulf of Finland in summers 1987-2008 were 2.5 °C and 42 m, respectively. On average, the CIL temperature rose during the summer as fast as 0.01 °C per day increasing from 2.0 in June to 2.8 in August. The CIL depth was deepening on average from 35 m depth in June to 47 m depth in August.

The average CIL temperature was 2.9 °C in the mouth of the Gulf and 1.9 °C in the eastern part of the study area (Fig. 2). The CIL depth was on average 54 m in the mouth area and 34 m in the eastern part of the study area (Fig. 2). Thus, the CIL temperature and depth in the western part of the study area are affected by the northern Baltic Proper water and its distinctive characteristics (Elken *et al.* 2006).

It has to be mentioned that the CIL depth may vary in a quite wide range during the summer, but CIL temperature is rather stable. Therefore, the long term mean profiles such as, for example, presented in Fig. 3, do not show the coldest temperature of the profile correctly, since the smoothing during averaging process will result in a CIL temperature (coldest temperature value on the average profile) which is always slightly warmer than the average of coldest values at profiles.

3.1.4. Halocline and deep layer

The mean temperature and salinity at the 70 m depth in the Gulf of Finland in summers 1987-2008 were 3.5 °C and 8.3, respectively. On average, a slight decrease of salinity from June to August about 0.2 units and a slight increase of temperature about 0.1 °C were detected. The average along-gulf changes of the deep layer temperature and salinity were also as low as 0.1 °C for temperature and 0.3 units for salinity between the mouth area and the eastern part of the study area. Such small or even hardly distinguishable change along the Gulf in the deeper layer salinity and temperature comparing to the upper layer can be well seen in the long term mean TS-diagrams at stations LL3 and LL7 (Liblik 2008; data from the Finnish Institute of Marine Research).

The centre of the halocline defined as the depth of maximum salinity gradient was on average in the Gulf of Finland in summers 1987-2008 at the depth of 67 m.

3.2. Long-term changes

Two distinct periods with different temperature and salinity distributions – one with a fresher and the second with saltier deep layer – have been identified on the basis of data from 1987-2008. Sub-sets of data from both groups — years 1987-1990 and years 1997, 2006-2008 from the geographical area between 23.2

E and 25.2 E, were extracted. It was done to secure that all summer months in all years are well covered and the data are collected from the same area within both periods. The overall scatter plot of the vertical temperature and salinity profiles available from those summers in the western Gulf of Finland (Fig. 3) revealed a quite large variability of temperature and salinity throughout the whole water column, especially in the surface and thermocline layer for temperature and in the surface and deep layer for salinity. Although a positive UML temperature trend could be detected (if comparing the years 1987-1990 and 2006-2008) supporting the earlier results (Siegel *et al.* 2006; Suikkanen *et al.* 2007) the variability of the UML temperature was too large to confirm the increase of the sea surface temperature.

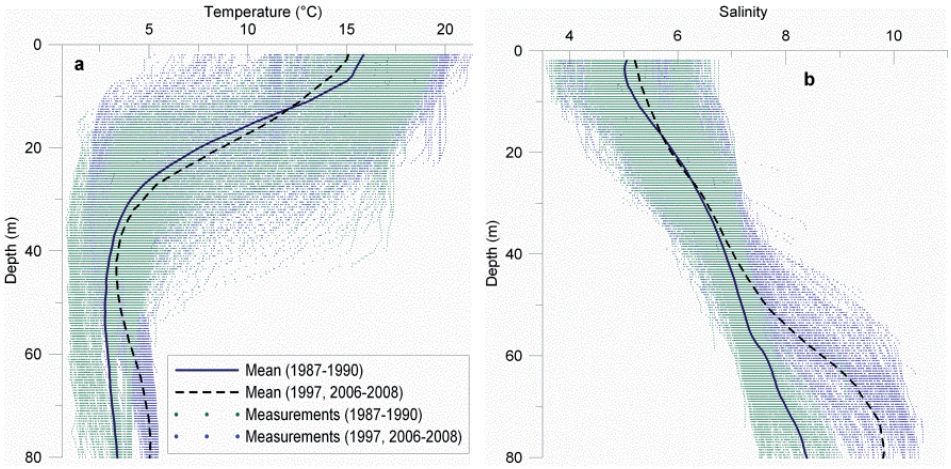

Figure 3. Scatter plots of vertical temperature (a) and salinity (b) profiles in the Gulf of Finland in summers 1987-2008, between longitudes 23.2 E and 25.2 E. Years 1987-1990 are shown as green dots and years 1997, 2006-2008 are shown as blue dots. The average vertical profiles for both groups of the years are indicated as solid lines (1987-1990) and dashed lines (1997, 2006-2008).

The years 1997 and 2006-2008 grouped clearly as the years with saltier and warmer waters in the deep layer of the Gulf of Finland. The estimated mean values of temperature and salinity at the 70 m depth in years 1987-1990 were 3.1 °C and 8.0 and in years 1997, 2006-2008 4.9 °C and 9.5. The hypothesis testing of the difference in means of two samples confirmed (*t*-test, $p < 0.05$) that the estimates of the mean deep layer salinity and temperature for these two groups are statistically different. In addition, the saltier years had a higher CIL temperature and a shallower CIL depth. The mean values of the CIL depth, CIL temperature and salinity at the CIL depth in the western Gulf (from 23.2 E to 25.2 E) in the less saline and more saline years were 46 m and 39 m, 2.5 °C and 2.9 °C, and 7.0 and 7.0, respectively.

Since statistically not different UML salinity and temperature were observed in years with a saltier deep layer, the vertical density gradient through the seasonal thermocline was close or even less during the latter years than in years with a fresher deep layer. At the same time, a significantly stronger vertical stratification was present in the deep layer in 1997, 2006-2008. The estimates of the mean density difference between the deep layer (70 m) and the intermediate layer (40 m) in these two groups of years were 1.1 kg m^{-3} (1987-1990) and 2.1 kg m^{-3} (1997, 2006-2008) and between intermediate layer (40 m) and surface layer (3 m) 2.8 kg m^{-3} and 2.7 kg m^{-3}. In conclusion, the vertical structure of the water column in the Gulf of Finland could be approximated mainly as a two-layer structure in 1987-1990 and as a clearly three-layer structure in the group of years 1997, 2006-2008. The detected clear difference between the years 1987-1990 and 1997, 2006-2008 was most probably caused by a major inflow of the North Sea waters into the Baltic Sea in 1993 that interrupted the stagnation in the Baltic Proper deep layers (Matthäus and Lass 1995; Jakobsen 1995) and further inflows, as those observed in 1997 (Matthäus *et al*. 2008) and 2003 (Feistel *et al.* 2003a). Also baroclinic inflows (Matthäus *et al*. 2008) could play an important role.

By analyzing historical monitoring data and numerical modelling results, simultaneous temporal changes of salinity have been shown throughout the whole water column in the Gulf of Finland (Omstedt and Axell 2003) and such simultaneous changes of salinity are predicted also in the Baltic Sea in case of the scenario with a salinity decrease (e.g. Meier 2006). We showed that while large changes were observed in the deep layer, the mean intermediate layer salinity remained almost unchanged. This feature could be explained by the different mixing depths in winter in years with a stronger halocline and years with a weaker halocline. Weaker stratification probably allows winter mixing to penetrate into the deeper layers causing an upward salt flux and in turn almost the same salinity in the cold intermediate layer of the Gulf of Finland than that in the years with more saline deep water and strong stratification (and consequently a shallower mixing depth in winter). On the other hand, this phenomenon could also be caused by an increase of accumulated fresh-water discharge from rivers. However, latter is not supported by the fact, that higher annual fresh-water inflow volumes, which were observed in eighties (Bergström and Carlsson 1994), were replaced by lower river discharge since mid-nineties (Graham 1999; Kronsell and Andersson 2010).

However, that leads to an important conclusion for the planktonic ecosystem — the vertical stratification in the seasonal thermocline will not change very much even if the salinity of deep layers changes remarkably.

The climate change scenarios predict that the Baltic Sea will be most probably warmer and fresher in the end of this century (Meier 2006; BACC 2008). The large variability of temperature and salinity fields observed within the last 22 years enables us to assume the possible changes in the vertical thermohaline

structure. It can be suggested that if the above scenario will be realized then the Gulf of Finland water column will be mixed down to the greater depths during winter and it will most likely have the two-layer structure in summer. However, if the water temperature will rise both in winter and summer (see in BACC 2008), the vertical gradients in the seasonal thermocline will rather increase than decrease, due to the fact that an increase of the CIL temperature (which is close to the temperature of maximum density) will influence the density less than that in the UML.

3.3. Inter-annual changes

Inter-annual variations of the summer UML temperature, salinity and depth were large, but no significant correlation was found with the BSI (paper I). The result is similar to the correlation analysis between North Atlantic Oscillation (NAO) and water temperature along the southern coast of the Baltic Sea — significant correlation was not found in summer (Girjatowizc 2008).

Large inter-annual variations of the CIL temperature were observed (Fig. 4) in the Gulf of Finland during the analyzed period 1987-2008. The lowest summer mean CIL temperature (1.3 °C) was observed in 1987 and the highest in 1990 and 2008 (3.6 and 3.4 °C, respectively).

Summer CIL temperature depends strongly on the severity of the previous winter. The correlation between the summer CIL temperature and the winter BSI was positive, and the best correlation ($r^2 = 0.81$, $p < 0.01$) was found if the mean BSI from January to February was used. The summer CIL temperature and the maximum ice extent of the Baltic Sea had a similar (as expected), but negative correlation ($r^2 = 0.72$, $p < 0.01$). A similar relationship between the winter atmospheric forcing and the CIL temperature in the Baltic Sea basins (but not the Gulf of Finland) was described by Hinrichsen *et al.* (2007). Considering the strong relationship between winter severities and CIL temperature and the fact that winters 1988/89, 1989/90 and 2007/08 were among the mildest (Seinä and Palosuo 1996; Vainio and Isemer 2008) and 1986/87 was one of the most severe winters (Seinä and Palosuo 1996) since 1720 according to the Baltic Sea maximum ice extent, it could be expected that the mean summer CIL temperature will vary between the minimum and maximum temperature values found within the period under investigation 1987-2008: 1.25 °C (1987) and 3.58 °C (1990).

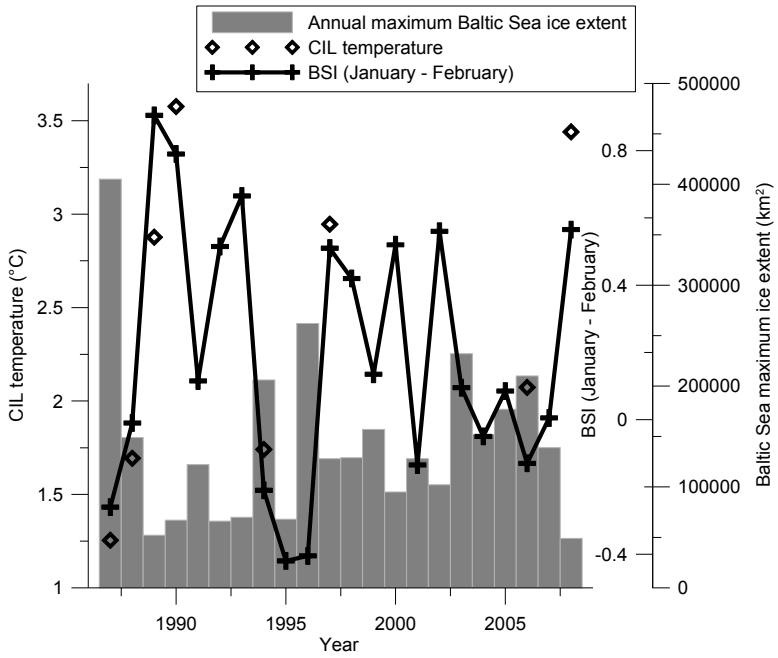

Figure 4. Inter-annual variability of the summer CIL temperature (diamonds; °C), the (January-February) BSI (dashed line with crosses) and the annual maximum Baltic Sea ice extent (bars; km^2).

Inter-annual variability of the deep layer (70 m) temperature and salinity was quite high (Fig. 5). As noted above, a group of years — 1997, 2006 and 2008 — with a higher summer mean salinity in a range of 9.1-9.8 and temperature in a range of 3.9-5.0 °C can be distinguished. Fresher and colder years with a summer mean salinity in a range of 7.7-8.2 and temperature in a range of 2.2-3.9 °C were 1987-1990 and 1994. The highest mean deep layer salinity and the strongest mean vertical salinity gradient were recorded in 2006. In years described above as the years with fresher deep layer waters, the centre of the halocline was found on average at the 71 m depth and in years 1997-2008 on average at the 64 m depth. It has to be mentioned also that at 22 % of analyzed profiles in the years before 1997, the maximum vertical salinity gradient was <0.07 m^{-1} and the halocline was not detected at all, while in years 1997, 2006 and 2008 the halocline was present at all profiles.

The changes in the deep layer temperature and salinity are related to two processes/reasons. First, the detected clear difference between the years 1987-1990 and 1997, 2006-2008 was mainly caused by major inflows described already in previous subchapter. On the other hand, Elken *et al.* (2003) described a relationship between the deep layer salinity changes and the wind-driven circulation in the Gulf of Finland. In 2006, when the northerly and easterly winds dominated for a long period, a large inflow of saltier waters into the Gulf of Finland deep layer has been revealed, which is well in accordance with the

detected correlation (described in subchapter 4.2) between the prevailing wind direction and salinity gradients between surface and bottom layer.

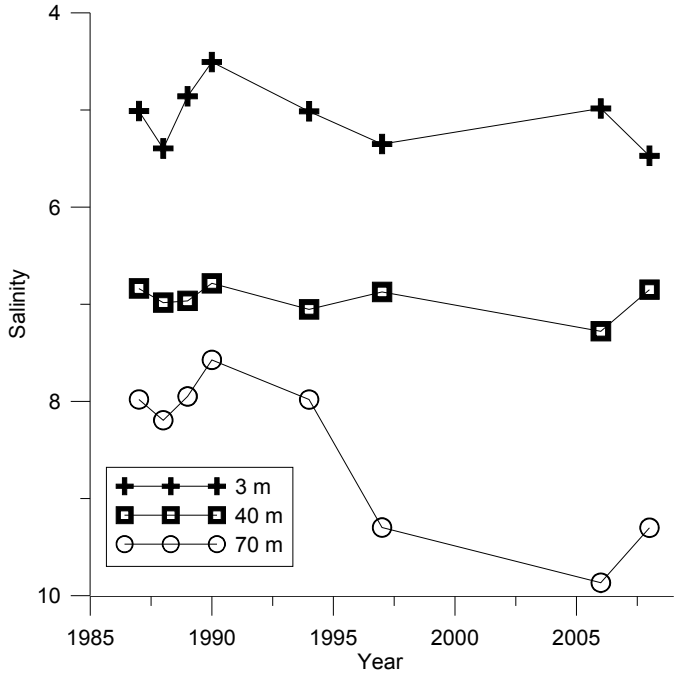

Figure 5. Inter-annual variation of the mean salinity at the 3 m (solid line with crosses), 40 m (solid line with squares) and 70 m (solid line with circles) depth in the Gulf of Finland in summers 1987-2008.

It has to be noted that the intermediate layer salinity (shown in Fig. 5 as the mean salinity at 40 m depth) had much lower inter-annual variations than those in the surface layer and, especially, in the deep layer.

4. WIND-DRIVEN CIRCULATION PATTERNS AND THEIR CONSEQUENCES TO THE THERMOHALINE STRUCTURE

4.1. Up- and downwelling events

The consequences of coastal upwelling events on physical and chemical patterns were studied in the Gulf of Finland by weekly mapping of hydrographical and -chemical (described in chapter 5) fields across the gulf between Tallinn and Helsinki in July-August 2006 (paper III). Subsequently, the formation and relaxation of a major upwelling event is described, starting from the pre-upwelling situation.

Before the upwelling event, on 25 July, a typical thermohaline structure with the seasonal thermocline at the depths of 10-20 m was observed (Fig. 6a, b). The cold intermediate water mass laid between the depths of 20 and 40 metres in the southern part and of 30 and 50 metres in the northern part of the study transect. The vertical structure of salinity field was characterised by low values in the surface layer – from 4.5 to 5.1 – and by a continuous increase of salinity in the seasonal thermocline and below it. The halocline was situated at the depths of 50-70 m.

An intense upwelling of cold and more saline waters from below the thermocline, induced by dominated easterly winds, was observed on 8 August off the southern coast of the Gulf (Fig. 6c, d). Sea surface temperature and salinity in the southern part of the cross-section changed from 19.1-19.4 °C and 4.5-5.1 to 5.3-8.0 °C and 6.2-6.6, respectively. The upwelling front, which consisted of the sloping thermocline and an associated salinity rise, was situated 18-20 km off the southern coast near the sea surface and about 35 km off shore at the depth of 20 m. A coupled downwelling was developing off the northern coast where the thermocline was located below the 20-m depth – about 5-10 m deeper than during the previous survey. A low salinity surface water mass appeared just above the sloping upwelling front obviously due to the along-front (along-gulf) westward advection.

On 15-16 August, the upwelling zone broadened, and the front moved northward to more than 30 km off the southern coast (Fig. 6e, f), most likely due to the easterly wind pulse observed before the survey. A week later when the relaxation of the upwelling event took place the thermocline was established along the whole study transect (Fig. 6g). On 29 august, upwelling was re-established along the Estonian coast and the upwelling front bordered by very fresh upper layer water was situated even more northward.

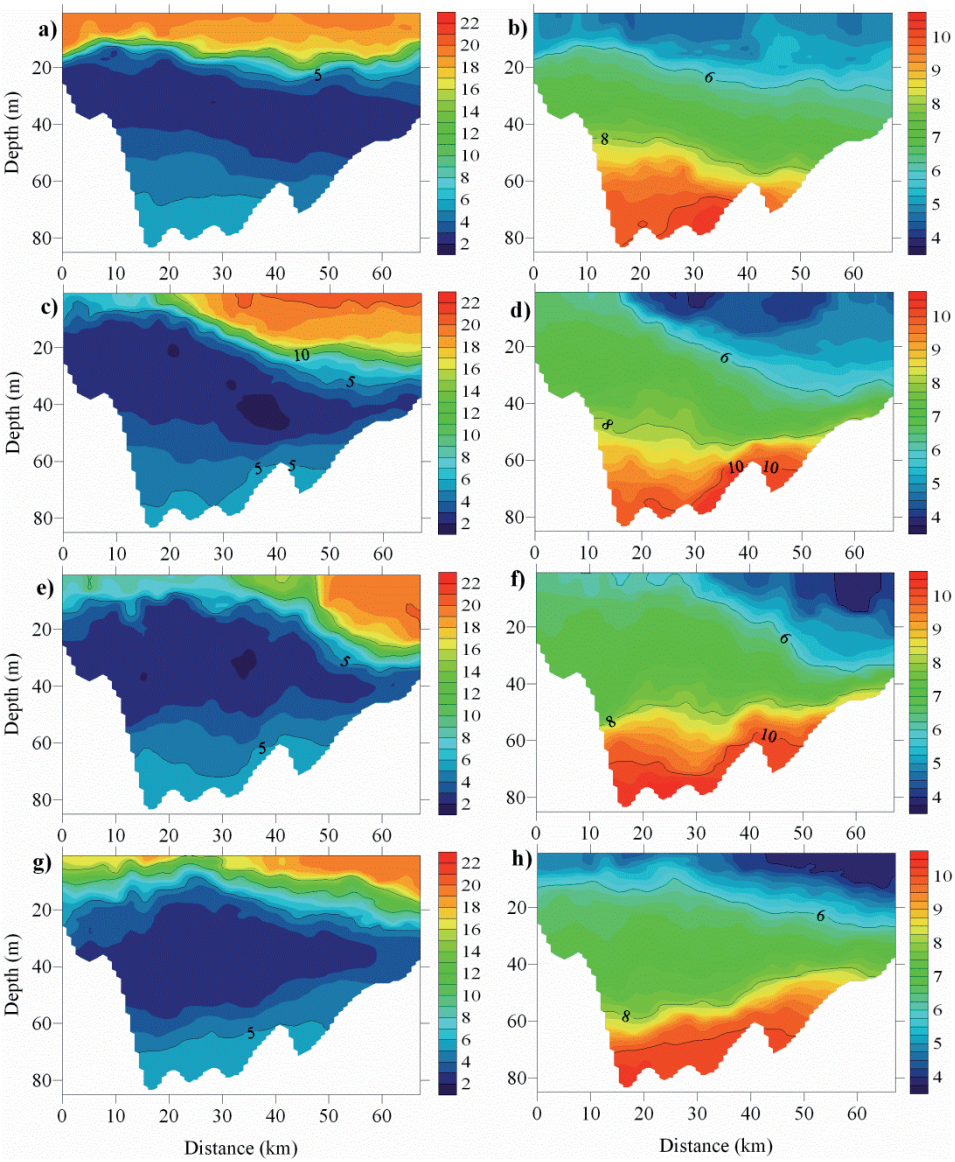

Figure 6. Vertical sections of temperature (°C) and salinity on 25 July (a, b), 8 August (c, d), 15-16 August (e, f) and 22 August (g, h) 2006. Values on x-axis are distance from the southernmost station (TH1, see paper III Fig. 1).

The most expressive feature of the coastal upwelling is the uplifted colder and saltier water along the coast. The upwelling formation in August 2006 was well seen in the data from the coastal stations Pakri and Loksa situated about 100 km apart (paper III) and it was observed also by Suursaar and Aps (2007) near Kunda (about 100 km to east from the study area). Uiboupin and Laanemets (2009) showed that the concerned upwelling event was the most extensive

upwelling along the southern coast among all observed upwelling events in 2000-2006. On 9 August 2006, it covered 6480 km^2 or about 20% of the total area of the Gulf.

The upwelling waters in the surface layer were bordered (Fig. 6d) with very fresh and warmer surface waters flowing to westward along the front. This phenomenon has not been observed in the case of upwelling along the northern coast. Thus, upwelling along the southern coast creates considerably steeper horizontal density gradients across the Gulf than those in the upwelling along the northern coast. The latter is in accordance with the results of horizontal temperature and salinity measurements in the surface layer carried out in 2007 using the Ferrybox system between Tallinn and Helsinki (Lips *et al*. 2008).

On the basis of TS-analysis (paper III), mixing of water masses during the upwelling event was estimated. The point corresponding to the TS-characteristics of upwelled water (5.41 °C and 6.47) was located quite exactly along a straight line connecting TS-values of the cold intermediate water and UML water at the southern stations before the initiation of upwelling. This is considered as evidence that the upwelling water could have been formed from these two water masses observed in the area before the upwelling event. According to this analysis the share of initial water masses mixed into the upwelling water was 15 % of the UML water and 85 % of the cold intermediate water. In addition, markedly weaker vertical gradients of salinity and density (Fig. 6c, d) were observed during the upwelling event in the southern part of the study transect if compared to those in the northern part. This weak stratification could favor vertical mixing in the layer below upwelling water.

The relaxation of upwelling comprises mixing of the water masses as well— it is evident from the TS-curves in and above the cold intermediate layer, which were almost straight lines after the relaxation of the upwelling on 22 August 2006 (paper III). As a conclusion, upwelling events contribute remarkably to the vertical mixing in the Gulf of Finland.

4.2. The consequences of wind-driven circulation in the deeper layers

Deepening of the halocline near the southern slope clearly seen on 15 August 2006 (Fig. 6f) suggests that within the halocline the cross-shore flow was directed northwards (offshore). Consequently, the onshore flow was concentrated in the intermediate layer which corresponds to the upwellings in the regions with strong stratification (Lentz and Chapman 2004). The changes of the shape of halocline and salinity of deep layers suggest also that inflow to the Gulf occurred in the deep layer of the northern part of the gulf during upwelling event (paper III). The latter shows that the upwelling favourable winds influence the dynamics of the whole water column of the Gulf of Finland. This finding does not agree with the Baltic-wide statement that the vertical extension of the

Ekman compensation below the mixed layer is restricted due to the existence of the halocline (Lehmann and Myrberg 2008).

The importance of the prevailing winds to the whole water column could be well seen in weekly hydrographical mapping in summer 2006 and spring, early summer 2007 (paper IV). Elken *et al*. (2003) showed that in the entrance of the Gulf north-easterly winds support the standard estuarine circulation and south-westerly winds work against the density-driven and riverine flow. Measurements in 2006-2007 showed that also north-westerly winds are favorable for the estuarine circulation. Obviously north-westerly winds directly initiate an outflow in the upper layer, which is compensated by the landward (eastward) flow in the deep layer. Northeasterly winds create a sea level difference which in turn causes an inflow in the lower layer.

Correlation analysis between the deep layer and surface layer salinity difference at individual CTD profiles and the average wind speed and direction from the period preceding the measurement was conducted (paper I). A significant correlation between the wind forcing and the salinity gradients was obtained if an average wind speed from a period of three weeks or longer (until a period of six weeks) before the CTD measurement was taken into account. The best (positive) correlation ($r^2 = 0.33$, $p < 0.01$) was found with the average wind component from north-north-east (20 degrees).

In order to estimate quantitatively the influence of prevailing wind conditions to the salt budget in spring-summer 2006-2007, the results of HIROMB were used. Cumulative volume transports through two cross-sections of the Gulf (see Fig. 1, paper IV, sections W and E), separately for layers above and below 30 m, were estimated using modeled current velocities, extracted daily from the model outputs. Estimates of cumulative upward transport of waters from below the 30 m depth to the surface layer were obtained for the 6 week period in July-August 2006 as high as 90 km^3 (paper IV). Similar estimates for summer 2007 resulted in much smaller volumes of vertical transport. The latter and the correlation analysis described above, gave rise to an important suggestion. Since lateral estuarine circulation is intensified and upward transport is many-fold more intense in case of long-lasting easterly–north-easterly winds, in comparison to usually prevailing westerly–south-westerly winds, these processes under described conditions could contribute significantly to the ventilation of deep layers of the northern Baltic Proper.

4.3. Short-term variations

High-resolution vertical profiling at the buoy station revealed remarkable temporal variations of the vertical distributions of temperature and salinity in the Gulf of Finland in July-August 2009 (Fig. 7). Although the general temporal pattern was superimposed by short-time variations, the deployment period could be divided into several sub-periods with distinct vertical structure (and/or

changes) of temperature and salinity fields (paper II and V). At the beginning of July, the UML temperature and depth were 13-15 °C and 5-9 m, respectively. Surfacing of colder and more saline sub-surface layer water was observed in the first half of July. Later, a less saline water mass with temperature and salinity ranging from 14 to 15.5 °C and from 4.2 to 4.5 m, respectively, appeared in the UML at the measurement site. A fast deepening of the UML from 7-9 m to 16-18 m occurred on 25 July, and a more saline water mass occupied the UML on 26 July – the UML salinity increased up to 5.0. After 31 July, considerable warming of the sea surface and formation of a secondary thermocline at 7-10 m depth was observed. It was followed by a drastic deepening of the UML from 13-15 m (on 15-16 August) to 26-30 m (on 20-21 August) accompanied by an increase of the UML salinity up to 5.7. While, in most cases, the depth of the strongest density gradient followed the temporal evolution of the UML depth, separation of about 10 m between these depths occurred from 29 July to 12 August.

By analysing of vertical thermohaline structure and current velocity profiles, five periods were selected according to their characteristic TS-curves (Fig. 8), were selected (see paper II, table 2 and Fig. 2.). These identified quasi-stationary stratification patterns lasted from 4 to 15 days and were dominated by distinct hydrophysical processes – upwelling, relaxation of the upwelling, reversal of the estuarine circulation, ordinary estuarine circulation, and downwelling. It is suggested that these patterns appear for long enough time periods to influence the phytoplankton dynamics in this stratified estuary.

First period was dominated by upwelling event, which is well seen in a rapid sea surface temperature drop, although the period's average heat flux into the sea was positive (131 W m^{-2}). However, three groups (TS-dots were grouped into three clouds) with characteristic TS-distribution were visible in the temperature and salinity scatter plots during the period (Fig. 8A). These groups can be regarded as the three phases in the development of the upwelling event or movement of upwelling waters into the study area. The TS-curves indicate a slightly larger salinity increase (at a fixed temperature) at the thermocline depths than that in the upper layer.

The thermohaline structure during the second period was determined by prevalation of south-easterly and south-westerly winds which caused upwelling relaxation. TS-curves (Fig. 8A) were mostly straight lines during this period; it supports the hypothesis that the relaxation of the upwelling could contribute to the vertical mixing of the Gulf of Finland waters (see also 4.1). Another feature in the second period's TS-curves is a remarkable shift of curves to the right (saltier), which indicates that south-westerly winds have induced eastward movement in the upper layer and thermocline. At the same time, the base of thermocline located clearly deeper than during the first period, which indicates that eastward transport could cause deepening of thermocline (see also 3.1.2).

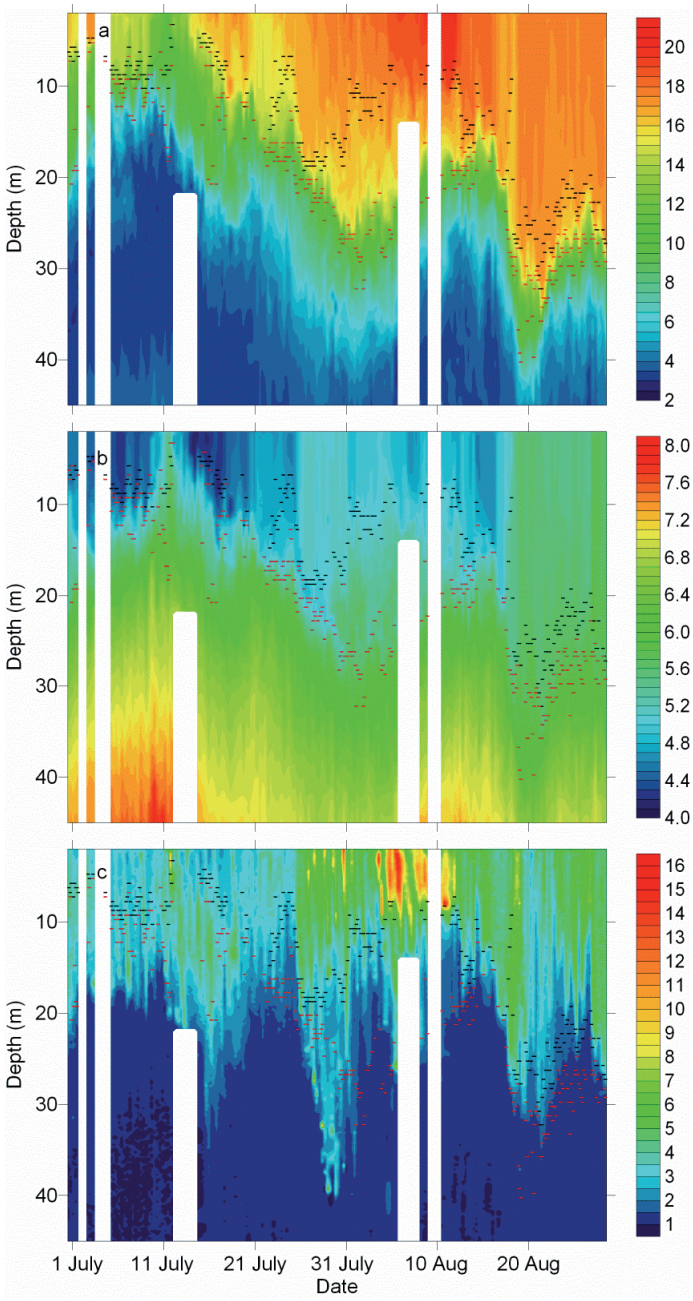

Figure 7. Variations of the vertical distribution of temperature (a, °C), salinity (b) and Chl *a* (c, milligram per cubic metre) as measured by autonomous profiler in the Gulf of Finland from 30 June to 28 August 2009. Blanked areas correspond to the periods when vertical profiles were not available for 24 h or more. Black dashes indicate the UML depth and red dashes the depth of the strongest density gradient.

It is seen in the third period TS-diagrams and vertical profiles (Fig. 8B and 8C) that the upper layer salinity has increased remarkably while the salinity at the thermocline depths has decreased if comparing to the earlier period. These changes are in accordance with the eastward flow in the upper layer and westward flow in the thermocline and below it (see paper II, Fig. 2). This flow pattern is known as the reversal of the estuarine circulation (Elken *et al*. 2003; subchapter 4.2).

The fourth period was characterized by weak winds from north and north-east and positive heat flux. This combination resulted in estuarine circulation – westward flow in the upper layer and eastward flow below the thermocline, and surface warming. The characteristic TS-curve (Fig. 8C and 8D) was close to a straight line due the increase of salinity at the thermocline depths and formation of a fresher and warmer near surface layer due to the calm conditions. The shift from the reversed to estuarine circulation is more thoroughly decribed in paper II.

The fifth period characteristic TS-curve (Fig. 8D) is strongly influenced by the occurred downwelling event. Due to the eastward transport in the upper layer and vertical mixing (TS-curve is nearly a straight line from surface to 40 metres), the upper layer salinity is relatively high and salinity gradient through the thermocline is relatively weak.

A comparison of the observed (calculated according to Eq. 1) and modelled changes of upper layer temperature and potential energy anomaly (Eq. 2) suggests that the upper layer dynamics and vertical stratification conditions in the Gulf of Finland can be simulated reasonably well when the surface transport along the Gulf prevails (see Figs. 4 and 6, paper II). The largest mismatches between the modelled and measurement-based changes of potential energy anomaly and upper layer temperature were found during the upwelling event, when the upwelling waters reached the study site (buoy station).

Thus, it is suggested that, in certain cases, the vertical stratification depends strongly on the water movement across the Gulf and associated vertical displacement of isopycnals. To advance the simple model presented in the paper II, an additional term should be added to the existing model (see Eq. 2). This term has to account for the wind induced drift of surface waters across the Gulf and resulting convergence or divergence of waters and vertical movement of isopycnals. If the wind impulse or cumulative along-gulf wind stress is strong enough for the surfacing of the thermocline (see e.g. Haapala 1994; Uiboupin and Laanemets 2009), the formation and behavior of the upwelling front has to be taken into account as well. Since these processes depend on the along-gulf wind stress, it is reasonable that the largest mismatches between the model and measurements were found in case of easterly winds (paper II).

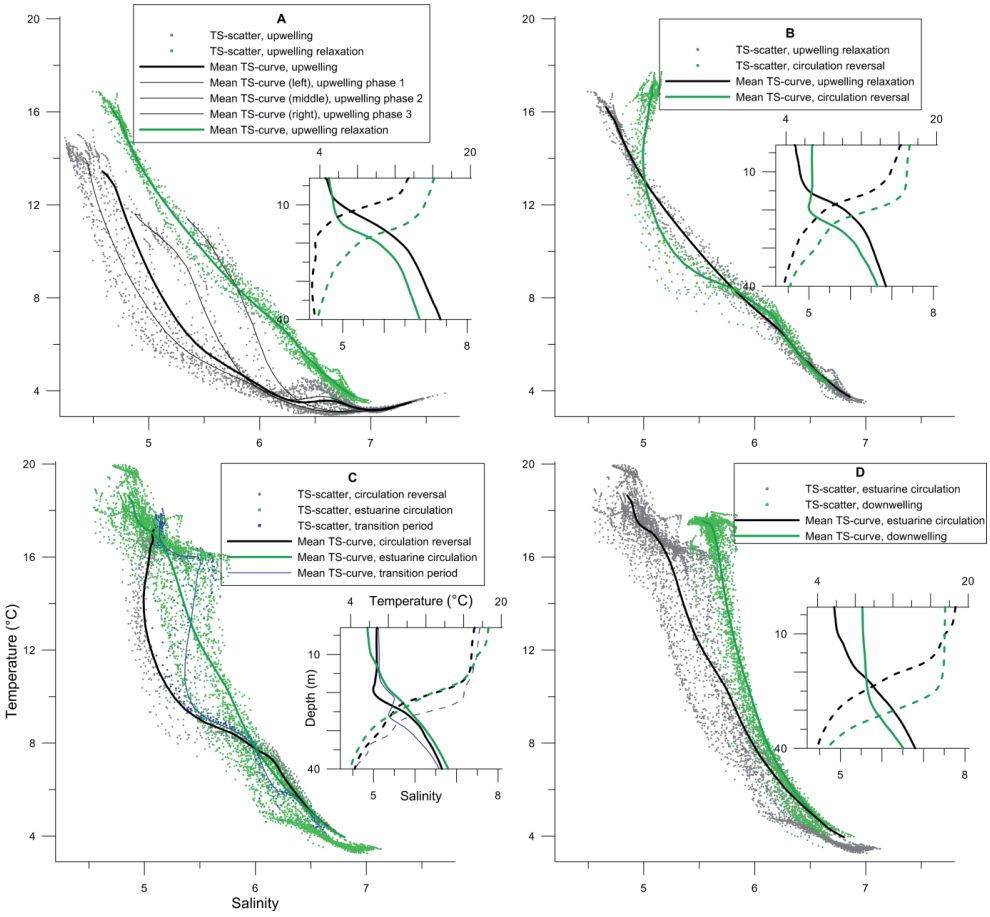

Figure 8. TS-diagrams. Temperature and salinity scatter plots, mean TS curves and mean temperature and salinity profiles in five periods: first and second period (A), second and third period (B), third and fourth period (C) and fourth and fifth period (D). In panel A, the three phases of the first period are indicated with black thin curves, in panel C transition period between third and fourth period is drawn out with blue dots and lines. Black curves and grey dots represent the earlier period and green curves and dots represent the later periods in each plot. In the panels of mean vertical profiles, the solid curves represent salinity and dashed curves represent temperature.

5. CONSEQUENCES OF THERMOHALINE VARIABILITY ON NUTRIENT PATTERNS AND PHYTOPLANKTON COMMUNITY

5.1. Nutrient patterns and transport estimates

Simultaneously with the temperature and salinity mapping described in chapter 4.1, vertical distribution of nutrients (phosphates, nitrates+nitrites) was investigated by weekly sampling across the Gulf of Finland in July-August 2006. In July, the nutrient concentrations were typically low in the surface layer where the phosphate (PO_4^{3-}) concentrations up to 0.10 μmol l^{-1} were measured, while nitrate+nitrite (NO_x) concentrations were below the detection limit (paper III). The upwelling event off the southern coast in the beginning of August caused a remarkable increase of $PO_4^{3-}$and NO_x concentrations with the maximum values of 0.48 and 0.79 μmol l^{-1}, respectively, observed on 8 August. A week later on 15 August, the PO_4^{3-} concentrations varied between 0.11 μmol l^{-1} and 0.24 μmol l^{-1} in the upwelling area while the NO_x concentrations had dropped below the detection limit again in the whole section. Relaxation of upwelling resulted in PO_4^{3-} and NO_x concentrations below the detection limit along the whole transect and re-establishment of upwelling on 29 August caused only a slight increase of PO_4^{3-} concentrations in the surface layer near the southern coast (paper III).

In July, the nutriclines were located mainly just below the thermocline, and PO_4^{3-} and NO_x vertical distributions coincided well with the density distribution (Fig. 9a, b). The nitracline and phosphacline were clearly separated off the northern coast but coincided in the open sea area and southern part of the study transect. Nutrient rich waters surfaced near the southern coast on 8 August (Fig. 9c, d). The border between the nutrient rich and nutrient depleted water masses coincided well with the upwelling front (exposed in Fig. 9c-f as a set of sloping isopycnals) on 8 and 15 August. After the upwelling relaxation, the nutriclines coincided in the open gulf but, in the Tallinn Bay, a clear separation of nitracline and phosphocline of about 7.5-10 m was observed (paper III). It shows that upwelling events contribute to the separation of the nitracline and phosphacline, often observed in the Gulf of Finland in summer and suggested being related mainly to the mixing depth during the spring bloom (Laanemets *et al*. 2004).

The simplest way to get a rough estimate of amounts of nutrients transported into the surface layer by an upwelling event is to multiply the average increase of nutrient concentrations and the volume of the upwelled water. The thickness of the surface layer in the estimates related to the upwelling event in August 2006 (paper III) was taken 12 metres. It corresponds to the average thickness of the UML water mass at the southernmost stations where the PO_4^{3-} and NO_x concentrations were below the detection limit before the upwelling initiation.

According to the CTD survey on 8 August, the seaward extension of the upwelling was ca 20 km. Taking into account the detection limits, the following average concentrations were obtained for the 20-km wide coastal area: 0.04 µmol l^{-1} of PO_4^{3-} and 0.07 µmol l^{-1} of NO_x on 25 July and 0.43 µmol l^{-1} of PO_4^{3-} and 0.59 µmol l^{-1} of NO_x on 8 August. Thus, the estimated nutrient amounts introduced into a 12 m thick, 20 km wide and 100 km long coastal stretch were equal to 290 tons of P-PO_4^{3-} and 175 tons of N-NO_x.

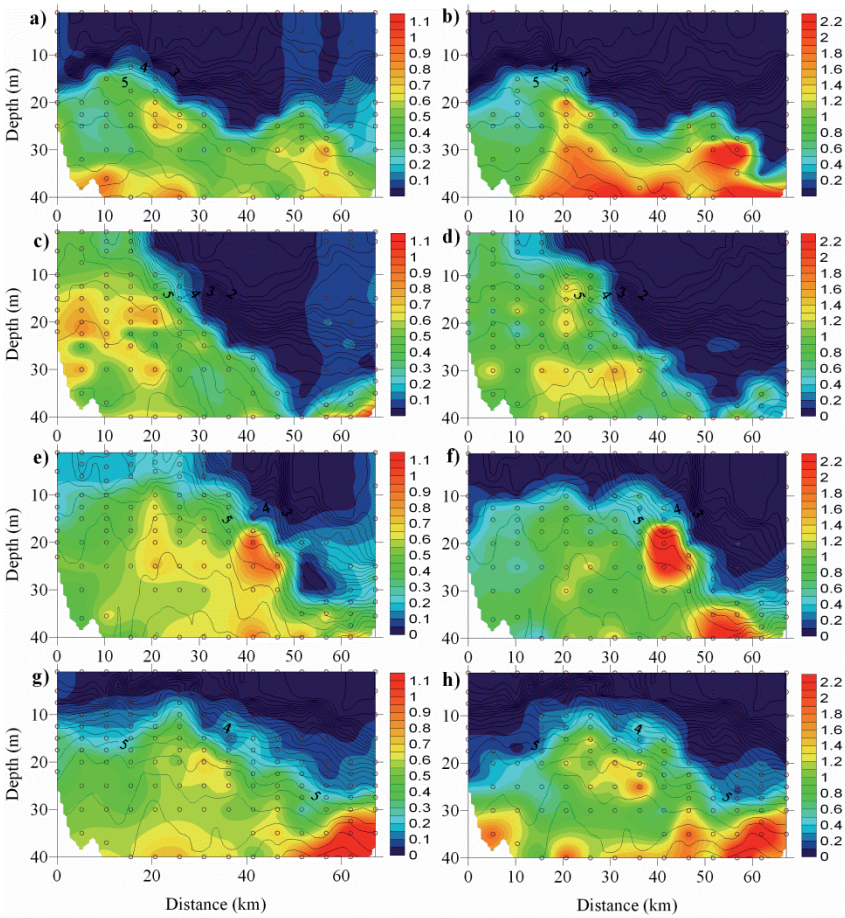

Figure 9. Vertical sections of phosphate-phosphorus (µmol l^{-1}) and nitrate-nitrite-nitrogen (µmol l^{-1}) in layer 0-40 m on 25 July (a, b), 8 August (c, d), 15 August (e, f) and 22 August (g, h) 2006. Dots indicate sampling points, values on x-axis are distance from the southernmost station (TH1, see paper III Fig. 1). Corresponding density anomaly distribution (density-1000 kg m^{-3}) is shown by black contour lines.

An alternative method used for the estimation of vertical nutrient transport by the upwelling event was based on the average nutrient concentrations in the water masses below and above the thermocline before the upwelling event and the estimated mixing ratio (paper III). Taking into account possible different off-shore extensions of the water masses under consideration (from 18 to 28 km), the estimated nutrient amounts introduced into a 12 m thick, 20 km wide and 100 km long coastal stretch were varying between 238-268 tons of $P\text{-}PO_4^{3-}$ and 175-255 tons of $N\text{-}NO_x$. A characteristic along-shore extent of the upwelling event in August 2006 was about 200 km (see e.g. http://wwwi4.ymparisto.fi/i4/eng/sst/ 2006/ sst_sat_2006_eng.html). Thus, both methods gave similar estimates of amounts of upwelled nutrients ranging from 480 to 580 tons of $P\text{-}PO_4^{3-}$ and from 350 to 510 tons of $N\text{-}NO_x$. In conclusion, the major upwelling event observed in August 2006 along the Estonian coast, brought phosphate-phosphorus into the surface layer in amounts equal to the monthly riverine load of total phosphorus to the Gulf of Finland (about 500 tons, see HELCOM 2004).

It was shown that dramatic alteration of vertical nutrient distribution can (may) occur in connection to changes in thermohaline structure during an upwelling event. As described in subchapter 4.2, the intensification or reversal of the estuarine flow could remarkably affect the thermohaline structure in the sub-surface and deep layers. The described changes in thermohaline structure and modelled volume transports through the selected cross-sections of the Gulf have indicated that the estuarine flow was clearly more intensive in late July and August 2006 than before (from May to mid July) and during the summer 2007 (paper IV). Since the northern Baltic Proper deep waters are oxygen depleted and phosphate rich (Lehtoranta 2003), such a strong inflow in the deep layer could potentially lead to a remarkable source of extra phosphorus for the Gulf of Finland. The measured deep layer phosphate concentrations indicated that phosphate rich deep layer water reached the study area in August — the near-bottom phosphate concentrations, which had been 2.6-2.7 μmol l^{-1} before the estuarine flow intensification, were in a range of 3.4-4.2 μmol l^{-1} during the entire August 2006 (see paper IV, Fig. 6). Thus, the intensification of estuarine circulation leads to higher salinity in the deep layers and stronger vertical stratification as well as supplies additional amounts of phosphorus into the Gulf of Finland.

5.2. Phytoplankton distribution and vertical dynamics

Phytoplankton dynamics affected by changes in the thermohaline structure is studied based on mapping in July-August 2006 and high-frequency measurements at autonomous buoy station in July-August 2009. The phytoplankton dynamics related to the major upwelling event is described by Lips and Lips (2010) and Kuvaldina *et al*. (2010). In the present thesis, the main

emphasis is on links between vertical distribution and dynamics of phytoplankton and thermohaline structure and physical processes forming it.

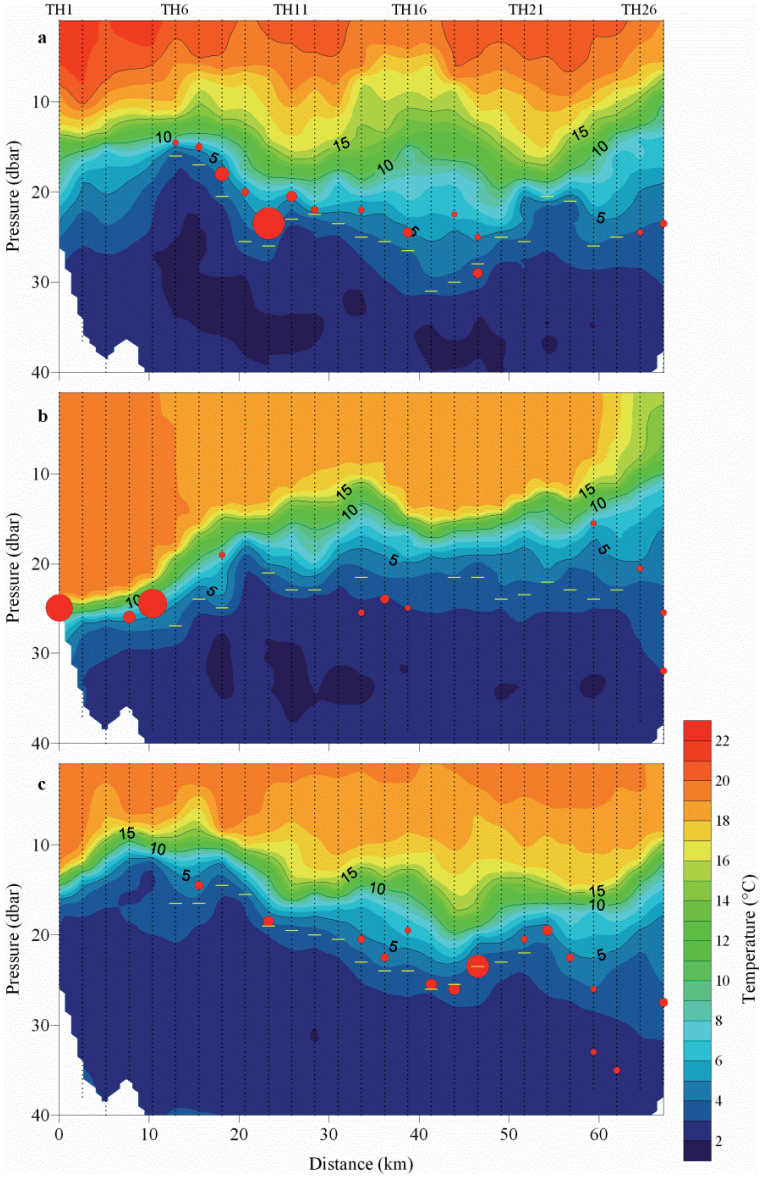

Figure 10. Vertical sections of temperature on 11 (a), 19-20 (b) and 25 (c) July 2006. Dotted lines indicate profiles; values on x-axis are distance from the southernmost station (TH 1, see paper III Fig. 1); station numbers are shown above. Observed sub-surface Chl *a* maxima are indicated as red circles scaled proportionally to the intensity of maxima; the base of thermocline is shown by yellow dashes (the base of thermocline was not determined if the profile did not reach the minimum temperature).

During three surveys in July 2006 sub-surface maxima of chlorophyll *a* (Chl *a*) with intensities ≥0.5 μg l^{-1} were observed at 37 vertical profiles out of measured 80 profiles (paper VI). As seen from the vertical cross-sections of temperature (Fig. 10) the Chl *a* maxima followed almost precisely the base of thermocline. On 11 July, the maxima were situated just above the base of thermocline and were related to the isotherm 5 °C. On 19 July, the most intensive maxima were observed in the thermocline in the downwelling area. The initial pattern of maxima distribution was re-established on 25 July when those were registered almost precisely at the base of thermocline and at slightly lower temperatures than on 11 July. The registered sub-surface Chl *a* maxima coincided well with the nutriclines, especially with the nitracline (paper VI) – the concentrations of NO_x were below the lower detection range in the samples taken above the Chl *a* maximum layer and detectable concentrations were measured in the samples taken just below the maxima.

In order to determine the stratification conditions favourable for the formation of sub-surface Chl *a* maxima, the vertical profiles were analysed in detail. The UML depth was on average 7 m on 11 July and 8 m on 25 July while the base of thermocline was situated at 24 m on 11 July and 21 m on 25 July. In comparison with the long-term mean characteristics of the UML and thermocline, the estimated values indicate that in 2006 the UML was thinner and the base of thermocline was at shallower depths. At the same time, the most intensive maxima were observed in areas where the base of thermocline was locally situated at deeper positions.

Cross-section geostrophic velocity distributions were calculated relative to the reference depth of 40 m (assumed level of no motion). The found distribution of alternating flow directions along the study transect (see Fig. 6, paper VI) could be interpreted as a sequence of meso-scale eddies or as a sequence of cyclonic and/or anti-cyclonic circulation cells. According to the location of Chl *a* maxima in relation to the geostrophic current distribution, it is concluded that the formation of pronounced maxima or "thin layers" are favoured by accumulation of phytoplankton along the depressed isopycnals at the base of anti-cyclonic circulation cells (paper VI).

High-frequency profiling at the autonomous buoy station in the Gulf of Finland (see location in Fig. 1) in July-August 2009 revealed three periods with deep distribution patterns of Chl *a* related to the deepening of the UML after 12 July, 25 July and 16 August. These periods of relatively high Chl *a* concentration in the sub-surface layer differed from each other regarding the depths of Chl *a* penetration and the concurrent UML depth and depth of the strongest density gradient (Fig. 7c). In the period after 12 July, the highest Chl *a* values were observed mainly in the thermocline between the UML depth and the depth of the strongest density gradient, i.e. the Chl *a* concentrations in the UML were lower than those in the thermocline. On 26-31 July, relatively high Chl *a* concentrations were observed in the UML while patches of very high Chl *a* were

detected also in the sub-surface layer below the depth of the strongest density gradient. During the third period of deep Chl *a* distribution (after 16 August), high Chl *a* concentrations were observed only in the UML (however, the UML was deep), and no patches of elevated Chl *a* content were detected below the depth of the strongest density gradient. Relatively high Chl *a* values were measured below the depth of the highest density gradient on 5-9 July when the UML was very shallow, and h_{maxN} was located close to the UML depth. The analysis of stratification parameters and TS-characteristics of the water column (paper II and V) showed that the periods with different Chl *a* dynamics differed also regarding to the thermohaline structure. Thus, it is suggested that the conditions caused by the prevailing atmospheric and oceanographic forcing (including vertical stratification) explain the vertical dynamics of phytoplankton.

In order to verify whether the observed short-term variations in Chl *a* distribution in July-August 2009 were consistent with a diurnal vertical migration pattern of phytoplankton, the average daily courses of Chl *a* were constructed for the entire deployment period and several distinct periods of atmospheric-oceanographic forcing, and species composition (paper V). Due to the high variability at other time scales, the amplitude of the diurnal cycle revealed using data from the entire deployment period was low in comparison to the overall variability. Clear diurnal patterns in the Chl *a* dynamics were detected in the period of dominance of euglenophytes (*Eutreptiella* spp.) at the beginning of July, and in the period of dominance of the dinoflagellate *Heterocapsa triquetra* in late July-early August (Fig. 11).

The observed Chl *a* dynamics can be interpreted as diurnal vertical migration of phytoplankton with a clear downward migration at night. In late July-early August the maximum Chl *a* concentrations at the surface were observed between noon and 6 p.m., and the minimum at 3 a.m. (Fig. 11c). The maximum Chl *a* values at 6-12 m were observed at 9 p.m. and the minimum at 3 p.m., while the maximum and minimum at 14-20 m were observed at 3 a.m. and 6-9 p.m. respectively. It suggests that, on average, after accumulation at the very surface at 3 p.m. the phytoplankton experienced downward migration reaching 20 m at 3 a.m., whereas sinking was faster in the almost mixed upper layer (see vertical density distribution in Fig. 11d). After 3 a.m. some part of the community continued downward migration and penetrated into the water layer below the strongest density gradient while some part returned, reaching the surface at noon. It can be assumed that part of the deep population could join the maximum at about 20 m depth at 3 a.m. the next day, and thus could have a bi-diurnal migration pattern.

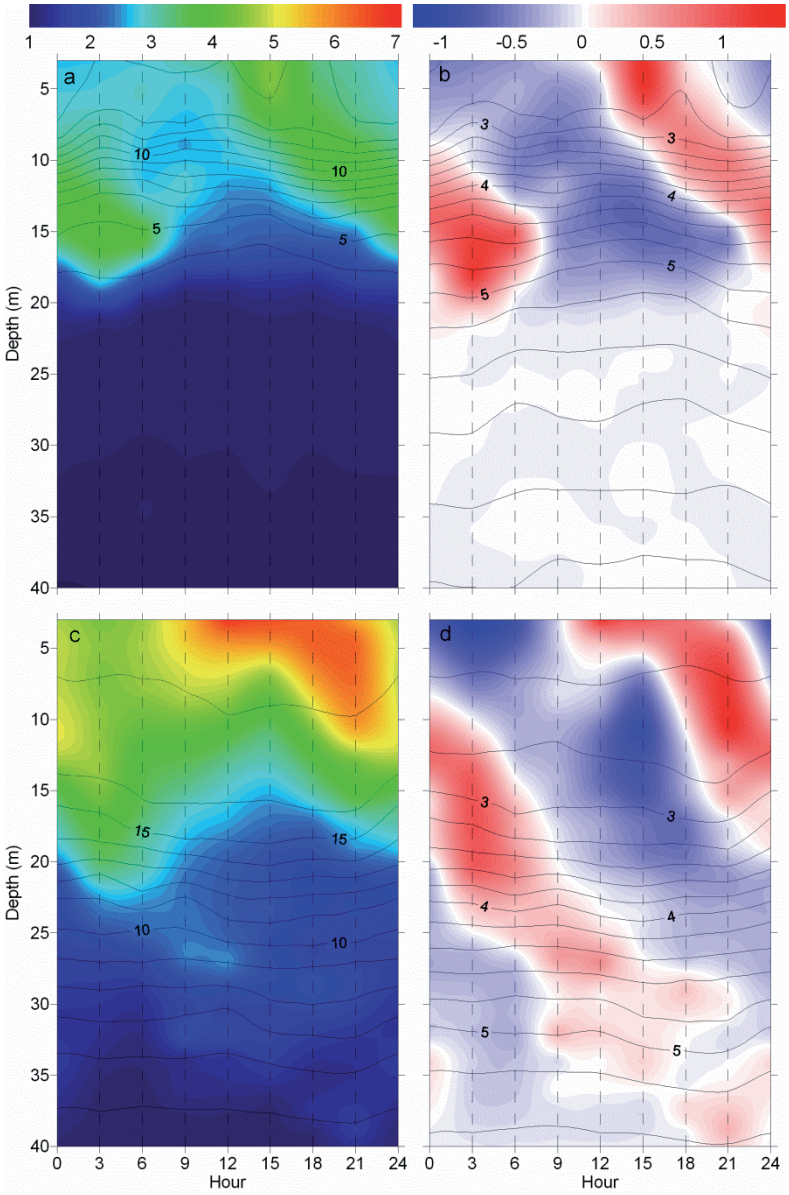

Figure 11. The daily average variations of Chl *a* and devations from the mean Chl *a* at each depth in the layer 3-40 m from 5 July to 9 July (a and b, respectively) and from 25 July to 2 August (c, d). Both Chl *a* scales are in milligram per cubic metre. Average temperature (°C; a, c) and density anomaly (kilogram per cubic metre; b, d) distributions are shown by *solid lines*.

Downward migration of phytoplankton can be characterised also by a series of consecutive vertical profiles of Chl *a* (see Fig. 7, paper V). According to this example from noon on 26 July to 6 p.m. on 27 July, the Chl *a* maximum was moving downward during the night with an approximate speed of 1.6 m h^{-1}. The

splitting of the community into two at 9 a.m. could indicate that part of the community returned to the sea surface and the other part continued downward migration until getting below the thermocline.

In many studies, it has been argued that physical processes are able to shape the vertical distribution of phytoplankton into thin layers of high biomass (e.g. Velo-Suarez *et al*. 2010). Sullivan *et al.* (2010) have concluded that even though physical forcing affects the spatial-temporal dynamics of thin phytoplankton layers, biological processes and behaviour can be equally, if not more important. Ross and Sharples (2007) showed that motility could give an advantage to the phytoplankton in competing for the nutrients in the thermocline. The results presented in this study indicate that the sub-surface maxima of *H. triquetra* were fuelled by synchronous downward migration of cells at night. It is suggested that this migration pattern occurs as an adaptation of phytoplankton to migrate to the deeper nutrient resources at low irradiances. On the other hand, the success of this strategy depends on physical background – vertical stratification and mesoscale processes. Similar suggestions on the importance of mesoscale processes were made also in earlier studies, e.g. by Kononen *et al*. (2003).

6. CONCLUSIONS

The main aim of the thesis was to improve the knowledge on the thermohaline structure of the Gulf of Finland in summer and to identify the main driving factors and processes causing its variability. Secondly, the influence of these processes and vertical stratification on the nutrient fields and phytoplankton dynamics were analysed. In comparison to other studies, three main advantages in used data and methods could be stressed: first, a quite long and extensive historical data set of CTD profiles collected in the Gulf of Finland was available from 1987 until 2009; secondly, new technologies were applied to measure vertical temperature, salinity and chlorophyll *a* profiles with high resolution in time, this type of autonomous buoy profiler was used for the first time in the Gulf of Finland; and the field measurements carried out in 2006-2009 included also sampling and analyses of nutrients as well as phytoplankton species composition and biomass – thus, the measurements had interdisciplinary character.

Parameters of vertical thermohaline structure and stratification were defined, and methods for their estimates were developed in the present thesis. Changes in UML temperature, salinity, and depth are mainly related to the short-term variability of local wind. Wind-induced movements of water masses along and across the Gulf, upward or downward movements of isopycnals, occurrence of up- or downwelling events along the coasts and vertical mixing can remarkably affect UML water characteristics (papers II-VI). The most rapid changes in UML temperature, salinity and stratification are related to the upward-downward movements of isopycnals related to up- and downwelling events. However, if such movements across the Gulf are not dominant, upper layer temperature and stratification can be simulated reasonably well with a simple model (paper II). Although upper layer thermohaline structure is mainly determined by the synoptic scale variability in summer, still seasonal warming in UML and deepening of its depth from June to August are evident (paper I). Furthermore, inter-annual variability can be detected both in UML temperature (Lips and Lips 2008) and salinity (paper I).

Changes in summer CIL temperature are mainly related to the inter-annual variability of winter severity (paper I). However, other processes (Chubarenko and Demchenko 2010) could also contribute to this inter-annual variability. Regarding spatial variability of CIL temperature and depth, the along-gulf gradients are evident (paper I). The changes in the deep layer temperature and salinity are related to two processes/reasons. First, the occurrence/absence of major inflows from North Sea to the Baltic Sea greatly determines deep layer salinity and temperature in the Gulf (paper I). Secondly, intensification or reversal of estuarine circulation (Elken *et al.* 2003, paper IV) could also remarkably influence deep layer thermohaline characteristics.

In the future studies of long-term changes, inclusion of fresh water inputs could be useful for a better understanding of the observed changes and possible future trends of the thermohaline structure of the Gulf of Finland. For instance, Meier and Kauker (2003) have found that about half of the decadal variability of the average salinity of the Baltic Sea is related to the accumulated freshwater inflow. Omstedt and Axell (2003) have suggested that simultaneous temporal changes of salinity occur throughout the whole water column in the Gulf of Finland, and such simultaneous changes of salinity are predicted also in the Baltic Sea in case of the scenario with a decrease in salinity (e.g. Meier 2006). In the present thesis, it is shown that the thermohaline structure at certain depth ranges (UML, thermocline, CIL, halocline, deep layer) is influenced by different factors or their combination, and simultaneous shifts in the same direction (e.g. decrease in salinity throughout the entire water column) are not obvious.

The main results of the present thesis can by summarised as follows:

- The vertical structure of the water column in the Gulf of Finland could be approximated mainly as a two-layer structure in 1987-1990 and clearly as a three-layer structure after mid-nineties. The latter was most probably caused by a major inflow of the North Sea waters into the Baltic Sea in 1993 that interrupted the stagnation in the Baltic Proper deep layers.
- The temperature of cold intermediate layer in the Gulf of Finland in summer depends strongly on the severity of the previous winter in the Baltic Sea area – the summer CIL temperature had significant correlation with the Baltic Sea Index in January-February and maximum ice extent of the Baltic Sea in winter.
- In case of climate change towards warmer and fresher Baltic Sea, the Gulf of Finland water column will most likely have the two-layer structure in summer, but the vertical gradients in the seasonal thermocline will rather increase than decrease.
- Estuarine circulation is intensified and upward volume transport in the Gulf is many-fold more intense in case of long-lasting easterly–north-easterly winds, in comparison to usually prevailing westerly–south-westerly winds. The intensification of estuarine circulation supplies additional amounts of phosphorus to the Gulf of Finland.
- The upwelling events cause vertical mixing and enlarge the vertical separation of the nitracline and phosphacline in the Gulf of Finland in summer. The share of initial water masses mixed into the upwelling water near the Estonian coast in August 2006 was determined as 15 % of the upper mixed layer water and 85 % of the cold intermediate water.
- The upwelling event observed in August 2006 along the Estonian coast brought phosphate-phosphorus into the surface layer in amounts equal to the monthly riverine load of total phosphorus to the entire Gulf of Finland.
- Distinct quasi-stationary stratification patterns, which lasted from 4 to 15 days and were dominated by certain hydrophysical processes – upwelling,

relaxation of the upwelling, wind induced reversal of the estuarine circulation, estuarine circulation, and downwelling, were distinguished in the Gulf of Finland in July-August 2009.

- A simple model for potential energy anomaly, where the heat flux through the sea surface, wind mixing, wind induced transport (parallel to the horizontal salinity gradient) in the upper layer and estuarine circulation were taken into account, simulated the observed changes in the vertical stratification reasonably well. The largest discrepancies between the observations and model results were found when water movement across the Gulf and associated vertical displacement of isopycnals (upwelling or downwelling) were dominant processes.
- The sub-surface maxima of Chl *a* almost precisely follow the base of thermocline and coincide with the nutriclines in the stratified Gulf of Finland in summer. It is suggested that the formation of pronounced Chl *a* maxima layers is favoured by meso-scale processes.
- Clear diurnal patterns in the Chl *a* dynamics were detected in the periods with certain vertical stratification. During the period of dominance of the dinoflagellate *H. triquetra*, the splitting of the community into two and downward movement of Chl *a* maximum with a speed of up to 1.6 m h^{-1} were observed.

REFERENCES

Alenius P., Myrberg K. and Nekrasov A. 1998. The physical oceanography of the Gulf of Finland: a review. Boreal. Env. Res. 3: 97-125.

Alenius P., Nekrasov A. and Myrberg K. 2003. Variability of the baroclinic Rossby radius in the Gulf of Finland. Cont. Shelf Res. 23: 563-573.

Andrejev O., Myrberg K., Alenius P. and Lundberg P.A. 2004. Mean circulation and water exchange in the Gulf of Finland - a study based on three-dimensional modeling. Boreal. Env. Res. 9: 1-16.

BACC. 2008. Assessment of climate change for the Baltic Sea basin. Springer, Berlin, Heidelberg.

Bergström S. and Carlsson B. 1994. River runoff to the Baltic Sea: 1950-1990. Ambio 23: 280-287.

Bradtke K., Herman A. and Urbański J. A. 2010. Spatial and interannual variations of seasonal sea surface temperature patterns in the Baltic Sea. Oceanologia 52(3): 345-362.

Chubarenko, I. and Demchenko, N. 2010. On contribution of horizontal and intra-layer convection to the formation of the Baltic Sea cold intermediate layer. Ocean Sci., 6, 285-299.

Dekshenieks, M. M., Donaghay, P. L., Sullivan J. M., Rines, J. E. B., Osborn, T. R., Twardowski, M. S. 2001. Temporal and spatial occurence of thin phytoplankton layers in relation to physical processes. Marine Ecology Progress Series 223, 261-271.

Elken, J. 2006. Läänemere veekonveier: kas korsten paikneb Soome lahe suudmes? Pulicationes Geophysicales Universitatis Tartuensis, 50, 74-84.

Elken. J., Kõuts, T., Lagemaa, P., Lips, U., Raudsepp, U. and Väli, G. 2008. Sub-regional observing and forecasting system for the NE Baltic: needs and first results. US/EU-Baltic International Symposium, 2008 IEEE/OES: 421-429.

Elken, J., Mälkki, P., Alenius, P. and Stipa, T. 2006. Large halocline variations in the Baltic Proper and associated meso- basin-scale processes. Oceanologia 48(S), 91-117.

Elken J., Raudsepp U. and Lips U. 2003. On the estuarine transport reversal in deep layers of the Gulf of Finland. J. Sea Res. 49: 267-274.

Feistel R., Nausch G., Heene T., Piechura J., Hagen E. 2004. Evidence for a Warm Water Inflow into the Baltic Proper in Summer 2003, Oceanologia 46, 581-598.

Feistel R., Nausch G., Matthäus W., Hagen E. 2003a. Temporal and Spatial Evolution of the Baltic Deep Water Renewal in Spring 2003, Oceanologia 45, 623-642.

Feistel R., Nausch G., Mohrholz, V., Łysiak-Pastuszak, E., Seifert, T., Matthäus, W., Krüger S., Sehested Hansen I. 2003b. Warm Waters of Summer 2002 in the Deep Baltic, Oceanologia 45, 571-592.

Fennel, K. and Boss, E. 2003. Subsurface maxima of phytoplankton and chlorophyll: Steady-state solutions from a simple model. Limnology and Oceanography, 48 (4), 1521-1534.

Fofonoff N. P., Millard Jr. R. C. 1983. Algorithms for computation of fundamental properties of seawater. Unesco Technical Papers in Marine Science 44: 1-58.

Girjatowicz, J. P. 2008. The relationships of the North Atlantic Oscillation to water temperature along the southern Baltic Sea coast.

Graham, P. 1999. Modeling runoff to the Baltic Sea. Ambio, 28(4), 328-334.

Gran, V. and Pitkanen, H. 1999. Denitrification in estuarine sediments in the eastern Gulf of Finland, Baltic Sea. Hydrobiologia, 393, 107-115.

Haapala, J. and Alenius, P. 1994. Temperature and salinity statistics for the northern Baltic Sea 1961-1990. Finnish Mar. Res., 262, 51-121.

Haapala, J. 1994. Upwelling and its influence on nutrient concentration in the coastal area of the Hanko Peninsula, entrance of the Gulf of Finland, Estuarine. Coastal and Shelf Science 38 (5), 507–521.

Hagen, E., Feistel, R. 2007. Synoptic changes in the deep rim current during stagnant hydrographic conditions in the Eastern Gotland basin, Baltic Sea. Oceanologia, 49 (2), 185-208.

HELCOM. 2004. The Fourth Baltic Sea Pollution Load Compilation (PLC-4). Baltic Sea Environment Proceedings, 93, 1-188.

HELCOM. 2002. Environment of the Baltic Sea area 1994-1998; background document. Baltic Sea Environment Proceedings 82B: 1-215.

Hinrichsen H.-H., Lehmann A., Petereit C. and Schmidt J. 2007. Correlation analysis of Baltic Sea winter water mass formation and its impact on secondary and tertiary production. Oceanologia 49: 381-395.

Jakobsen, F., 1995. The major inflow to the Baltic Sea during January 1993. Journal of Marine Systems, 6(3), 227-240.

Jantti, H., Stange, F., Leskinen, E. and Hietanen, S., 2011. Seasonal variation in nitrification and nitrate-reduction pathways in coastal sediments in the Gulf of Finland, Baltic Sea.

Kahru, M., Aitsam, A. and Elken, J., 1982. Spatio-temporal dynamics of chlorophyll in the open Baltic Sea. Journal of Plankton Research, 4 (4), 779-790.

Kanoshina, I., Lips U. and Leppänen, J-M., 2003. The influence of weather conditions (temperature and wind) on cyanobacterial bloom development in the Gulf of Finland (Baltic Sea). Harmful Algea, 2, 29-41.

Keevallik, S., Soomere, T.,2010. Towards quantifying variations in wind parameters across the Gulf of Finland. Estonian Journal of Earth Sciences, 59(4), 288-297.

Klausmeier C. A. and Litchman, E., 2001. Algal games: The vertical distribution of phytoplankton in poorly mixed water columns. Limnology and Oceanography, 46(8), 1998-2007.

Kononen K. and Niemi A. 1986. Variation in phytoplankton and hydrography in the outer archipelago at the entrance to the Gulf of Finland in1968–1975. Finnish Marine Research 253, 35–51.

Kononen, K., Hällfors, S., Kokkonen, M., Kuosa, H., Laanemets, J., Pavelson, J. and Autio, R., 1998. Development of a subsurface chlorophyll maximum at the entrance to the Gulf of Finland, Baltic Sea. Limnology and Oceanography, 43, 1089-1106.

Kononen, K., Kuparinen, J., Mäkela, K., Laanemets, J., Pavelson, J. and Nõmmann, S., 1996. Initiation of cyanobacterial blooms in a frontal region at the entrance of the Gulf of Finland, Baltic Sea. Limnology and Oceanography, 41, 98-112.

Kononen, K., Huttunen, M., Hällfors, S., Gentien, P., Lunven, M., Huttula, T., Laanemets, J., Lilover, M.-J., Pavelson, J., Stips, A., 2003. Development of a deep chlorophyll maximum of Heterocapsa triquetra Ehrenb. at the entrance to the Gulf of Finland. Limnol. Oceanogr., 48, 594-607.

Kronsell, J. and Andersson, P., 2011. Total and regional Runoff to the Baltic Sea. HELCOM Indicator Fact Sheets 2010. Online. 04.01.2012.

Kuosa, H., 1990. Subsurface chlorophyll maximum in the Northern Baltic Sea. Archiv fur Hydrobiologie, 118 (4), 437-447.

Kuvaldina, N., Lips, I., Lips, U., Liblik, T., 2010. The influence of a coastal upwelling event to the spatio-temporal distribution of nutrients and chlorophyll a in the Gulf of Finland, Baltic Sea: observational results. Hydrobiologia, 639(1), 221 - 230.

Laanemets, J., Kononen, K. and Pavelson, J., 1997. Nutrient intrusions at the entrance area to the Gulf of Finland. Boreal Environment Research, 2, 337-344.

Laanemets, J., Kononen, K., Pavelson, J. and Poutanen, E.-L., 2004. Vertical location of seasonal nutriclines in the Western Gulf of Finland. Journal of Marine Systems, 52, 1-13.

Laanemets, J., Pavelson J., Lips, U. and Kononen, K., 2005. Downwelling related mesoscale motions at the entrance of the Gulf of Finland: observations and diagnosis. Oceanological and Hydrobiological Studies, 34(2), 15-36.

Laine A.O., Andersin A.-B., Leiniö S., Zuur A. F., 2007. Stratification-induced hypoxia as a structuring factor of macrozoobenthos in the open Gulf of Finland (Baltic Sea). Journal of Sea Research 57 (1), 65-77.

Lehmann A., Krauss W. and Hinrichsen H.-H. 2002. Effects of remote and local atmospheric forcing on circulation and upwelling in the Baltic Sea. Tellus A54: 299-316.

Lehmann, A., Getzlaff, K., Harlass, J., 2011. Detailed assessment of climate variability in the Baltic Sea area for the period 1958-2009. Climate Research, 46(2), 185-196.

Lehmann, A., Lorenz, P. and Jacob, D., 2003. Modelling the exceptional Baltic Sea inflow events in 2002-2003.

Lehmann, A., Myrberg, K., 2008. Upwelling in the Baltic Sea – A review. Journal of Marine Systems, 74 (Suppl. 1), S3-S12.

Lehtoranta, J., 2003. Dynamics of sediment phosphorus in the brackish Gulf of Finland. Monographs of the Boreal Environment Research, 24, 1-58.

Lentz, S.J., Chapman D.C., 2004. The importance of nonlinear cross-shelf momentum flux during wind-driven coastal upwelling. Journal of Physical Oceanography, 34(11), 2444-2457.

Liblik, T., 2008. Temperatuuri ja soolsuse vertikaalse jaotuse iseärasused Soome lahes suvekuudel. Master's thesis in Tallinn University of Technology.

Lips, I. and Lips, U., 2008. Abiotic factors influencing cyanobacterial bloom development in the Gulf of Finland (Baltic Sea). Hydrobiologia, 614, 133 - 140.

Lips, I. and Lips, U., 2010. Phytoplankton dynamics affected by the coastal upwelling events in the Gulf of Finland in July–August 2006. Journal of Plankton Research, 32, 1269-1282.

Lips, U., Lips, I., Kikas, V., Kuvaldina, N. 2008. Ferrybox Measurements: a tool to study meso-scale processes in the Gulf of Finland (Baltic Sea). US/EU-Baltic International Symposium, 2008 IEEE/OES: 1-6. (DOI: 10.1109/BALTIC.2008.4625536).

Lips, I., Lips U., Kononen, K. and Jaanus, A., 2005. The effect of hydrodynamics on the phytoplankton primary production and species composition at the entrance to the Gulf of Finland (Baltic Sea) in July 1996. Proc. Estonian Acad. Sci. Biol. Ecol., 2005, 54, 3, 210-229.

Lund-Hansen, L.C., Ayala P.C.A. and Reglero A.F. 2006. Bio-optical properties and development of a sub-surface chlorophyll maxima (SCM) in south-west Kattegat, Baltic Sea. Est. Coast. Shelf Sci., 68: 372-378.

MacKenzie B.R. and Schiedek D. 2007. Daily ocean monitoring since the 1860s shows record warming of northern European seas, Global Change Biology **13**: 1335-1347.

Matthäus, W and Franck, H., 1992. Characteristics of major Baltic Inflows—a statistical analysis. Continental Shelf Research, 12(12), 1375-1400.

Matthäus, W. and Lass H.U., 1995. The recent salt inflow into the Baltic Sea. Journal of Physical Oceanography, 25(2), 280-286.

Matthäus, W., Nehring, D., Feistel, R., Nausch, G., Mohrholz, V., Lass, H.U., 2008, The inflow of highly saline water into the Baltic Sea. In Feistel, R., Nausch, G., Wasmund, N. (Eds.), State and Evolution of the Baltic Sea, 1952 – 2005. A Detailed 50-Year Survey of Meteorology and Climate, Physics, Chemistry, Biology, and Marine Environment. John Wiley and Sons, Inc., Hoboken, 265-309.

Maximov, A. A. 2006. Causes of the Bottom Hypoxia in the Eastern Part of the Gulf of Finland in the Baltic Sea. Oceanology 46 (2), 204-210.

McManus et al., 2003. Characteristics, distribution and persistence of thin layers over a 48 hours period. Mar. Ecol. Progr. Ser., 261: 1-19.

Meier H.E.M. 2006. Baltic Sea climate in the late twenty-first century: a dynamical downscaling approach using two global models and two emission scenarios. Climate Dynamics 27: 39-68.

Meier, H. E. M., Kauker, F., 2003. Modeling decadal variability of the Baltic Sea: 2. Role of freshwater inflow and large-scale atmospheric circulation for salinity. Journal of Geophysical Research- Oceans, 108(C11), 3368.

Meier, H.E.M., Doscher, R., Broman, B. and Piechura, J., 2003. The major Baltic inflow in January 2003 and preconditioning by smaller inflows in summer/autumn 2002: a model study. Oceanologia, 46(4), 557-579.

Mietus, M., 1998. The climate of the Baltic Sea basin, Marine Marine Meteorology and Related Oceanographic Activities. Report No. 41. World Meteorological Organisation, Geneva.

Myrberg, K., Andrejev, O., 2003. Main upwelling regions in the Baltic Sea – a statistical analysis based on three-dimensional modelling. Boreal Environment Research 8 (2), 97–112.

Nausch, G., Feistel, R., Lass, H.-U., Nagel, K., Siegel, H., 2007, Hydrographisch-chemische Zustandseinschätzung der Ostsee 2006. Meereswissenschaftliche Berichte Warnemünde 70, 2-91.

Nausch, G., Feistel, R., Umlauf, L., Nagel, K., Siegel, H., 2010, Hydrographisch-chemische Zustandseinschätzung der Ostsee 2009. Meereswissenschaftliche Berichte Warnemünde 80, 1-107.

Omstedt A. and Axell L.B. 2003. Modeling the variations of salinity and temperature in the large gulfs of the Baltic Sea. Cont. Shelf Res. 23, 265-294.

Pavelson J., Laanemets, J., Kononen, K., Nõmmann, S., 1997. Quasi-permanent density front at the entrance of the Gulf: response to wind forcing. Continental Shelf Reasearch, 17, 253-265.

Pavelson, J., 1988. Nature and some characteristics of thermohaline fronts in the Baltic Proper. Proceedings of the 16th Conference of the Baltic Oceanographers, Kiel, Germany, 796-805.

Pavelson, J., 2005. Mesoscale physical processes and the related impacts on the summer nutrient fields and phytoplankton blooms in the western Gulf of Finland. PhD-thesis. Marine Systems Institute, Tallinn University of Technology.

Pavelson, J., Kononen, K. and Laanemets, J., 1999. Chlorophyll distribution patchiness caused by hydrodynamical processes: a case study in the Baltic Sea. ICES Journal of Marine Science, 56, 87-99.

Pärn, O. Sea ice deformation events in the Gulf of Finland and their impact on shipping. PhD-thesis. Marine Systems Institute, Tallinn University of Technology.

Rantajärvi, E., Gran, V., Hällfors, S., Olsonen, R., 1998. Effects of environmental factors on the phytoplankton community in the Gulf of Finland — unattended high frequency measurements and multivariate analyses. Hydrobiologia, 363, 127-139.

Ross, O.N. and Sharples, J. 2007. Phytoplankton motility and the competition for nutrients in the thermocline. Mar. Ecol. Prog. Ser., 347, 21-38.

Seinä, A. and Palosuo, E., 1996. The classification of the maximum annual extent of ice cover in the Baltic Sea 1720-1995. MERI: Report Series of the Finnish Institute of Marine Research. 27: 79-91.

Siegel H. Gerth M. and Tschersich G. 2006. Sea surface temperature development of the Baltic Sea in the period 1990-2004. Oceanologia 48(S): 119-131.

Simpson, J.H. and Bowers D.G., 1981. Models of stratification and frontal movement in shelf areas. Deep-Sea Research, 28, 727-738.

Simpson, J. H., J. Brown, J. Matthews, and G. Allen. 1990. Tidal straining, density currents, and stirring in the control of estuarine stratification. Estuaries 13, 125-132.

Soomere, T., Keevallik, S., 2001. Anisotropy of moderate and strong winds in the Baltic Proper. Proc. Estonian Acad. Sci. Eng., 7, 35-49.

Soomere, T., Keevallik, S., 2003. Directional and extreme wind properties in the Gulf of Finland. Proc. Estonian Acad. Sci. Eng., 9 (2), 73-90.

Soomere, T., Myrberg, K., Leppäranta, M. and Nekrasov, A., 2008. The progress in knowledge of physical oceanography of the Gulf of Finland: a review for 1997-2007. Oceanologia, 50 (3), 287-362.

Stepputtis, D., Hinrichsen, H.-H., Bottcher, U., Gotze, E., Mohrholz, V, 2011. An example of meso-scale hydrographic features in the central Baltic Sea and their influence on the distribution and vertical migration of sprat, Sprattus sprattus balticus (Schn.). Fisheries oceanography, 20 (1), 82-88.

Suikkanen S., Laamanen M. and Huttunen M. 2007. Long-term changes in summer phytoplankton communities of the open northern Baltic Sea. Estuarine, Coastal and Shelf Science 71: 580-592.

Suursaar, Ü., Aps, R., 2007. Spatio-temporal variations in hydro-physical and -chemical parameters during a major upwelling event off the southern coast of the Gulf of Finland in summer 2006. Oceanologia, 49 (2), 209-228.

Sullivan, J.M., Donaghay, P.L., Rines, J.E.B. 2010. Coastal thin layer dynamics: consequences to biology and optics. Cont. Shelf Res., 30, 50-65.

Zhurbas V.M., Laanemets J., Vahtera, E., 2008. Modeling of the mesoscale structure of coupled upwelling/downwelling events and the related input of the nutrients to the upper mixed layer in the Gulf of Finland. Journal of Geophysical Reasearch-Oceans, 113 (C5).

Talpsepp, L., 1993. Investigations of mesoscale hydrophysical processes in the Gulf of Finland in 1985-1990. Proc. Eston. Acad. Sci. Ecol., 3 (3), 137-148.

Talpsepp, L., Nõges, T., Raid, T. and Kõuts, T., 1994. Hydrophysical and hydrobiological processes in the Gulf of Finland in summer 1987:

characterization and relationship. Continental Shelf Research, 14(7-8), 749-763.

Uiboupin R. and Laanemets J. 2009. Upwelling characteristics derived from satellite sea surface temperature data in the Gulf of Finland, Baltic Sea. Boreal Env. Res. 14: 297-304.

Vahtera, E., Laanemets, J., Pavelson, J., Huttunen, M., Kononen, K., 2005. Effect of upwelling on the pelagic environment and bloom-forming cyanobacteria in the Western Gulf of Finland, Baltic Sea. Journal of Marine Systems, 58 (1-2), 67-82.

Vainio, J and Isemer, HJ., 2008. Mildest ice winter ever in the Baltic Sea. BALTEX Newsl 11:6–7 www.baltex-research.eu/publications/newsletter. html

Velo-Suarez, L., Fernand, M., Gentien, P., Reguera, B. 2010. Hydrodynamic conditions associated with the formation, maintenance and dissipation of a phytoplankton thin layer in a coastal upwelling system. Cont. Shelf Res., 30, 193-202.

Voss, R., Hinrichsen, H.-H., Quaas, M.F., Schmidt, J.O. and Tahvonen, O., 2011. Temperature change and Baltic sprat: from observations to ecological - economic modelling. ICES J. Mar. Sci. 68 (6), 1244-1256.

PUBLICATIONS

Paper I

Liblik, Taavi; Lips, Urmas. (2011). Characteristics and variability of the vertical thermohaline structure in the Gulf of Finland in summer. Boreal Environment Research, 16A, 73 – 83.

BOREAL ENVIRONMENT RESEARCH 16 (suppl. A): 73–83
ISSN 1239-6095 (print) ISSN 1797-2469 (online)

Helsinki 31 March 2011

Characteristics and variability of the vertical thermohaline structure in the Gulf of Finland in summer

Taavi Liblik* and Urmas Lips

Marine Systems Institute at the Tallinn University of Technology, Akadeemia Road 21, EE-12618 Tallinn, Estonia (corresponding author's e-mail: taavi.liblik@gmail.com)

Received 21 Nov. 2009, accepted 19 Aug. 2010 (Editor in charge of this article: Kai Myrberg)

Liblik, T. & Lips, U. 2011: Characteristics and variability of the vertical thermohaline structure in the Gulf of Finland in summer. *Boreal Env. Res.* 16 (suppl. A): 73–83.

Vertical profiles of temperature and salinity collected in the summers of 1987–2008 were analyzed in order to describe the mean characteristics and variability of the vertical termohaline structure in the Gulf of Finland. Quantitative estimates of the mean characteristics of the upper mixed layer, seasonal thermocline, cold intermediate layer, halocline and deep layer as well as their along-gulf changes were obtained. Both the long-term (inter-annual) and short term variations in the thermohaline structure were related to the changes in the atmospheric forcing. Two distinct periods with statistically different mean temperature and salinity in the deep layer were detected among the analyzed 22 years. The overall vertical salinity (and density) gradient was much stronger and the halocline was sharper in the recent years than in the years 1987–1990. However, the summer mean vertical salinity and density gradients in the seasonal thermocline did not reveal large inter-annual variations. We suggest that a possible shift towards fresher waters in the Baltic Sea due to the climate change would result in the two-layer structure of water column in the deeper areas of the Gulf of Finland in summer. At the same time, a possible increase of sea surface temperature could lead to a strengthening of the vertical density stratification in the seasonal thermocline.

Introduction

The Gulf of Finland is a 400-km-long and 48–135-km-wide, elongated sub-basin of the Baltic Sea. It covers approximately 29 600 km^2 and its volume is 1100 km^3 (Alenius *et al*. 1998). It has no sill at the entrance area separating the Gulf from the open Baltic Sea and its maximum cross-section depth decreases from > 100 m at the entrance to < 30 m in the eastern part. The Gulf receives 3556 $m^3\ s^{-1}$ (70-year average) of river discharge (annually 10% of the volume of the Gulf) that is mainly concentrated in the easternmost part of the Gulf (Bergström and Carlsson 1994). Therefore, the salinity distribution in the surface layer is characterized by an increase from 1–3 in the east to 6 (on the Practical Salinity Scale) in the west. Also a slight decrease across the Gulf from south to north exists.

The characteristics and seasonal development of vertical stratification in the Gulf of Finland was quite thoroughly described by Alenius *et al*. (1998) using data collected until 1996. The water column in the deeper areas of the Gulf reveals a three-layer vertical structure in summer — the upper mixed layer, the cold intermediate layer and the near-bottom layer, which is saltier and slightly warmer, can be distinguished. These

layers are separated by the two pycnoclines — the seasonal thermocline usually situated at the depths of 10–20 m and the permanent halocline at the depths of 60–70 m.

According to the HELCOM monitoring data, a decrease in salinity of the deep layers of the Gulf of Finland, observed from the late 1970s, was replaced by a salinity increase in the 1990s (HELCOM 2002). During the same monitoring period an average surface layer temperature increase was observed (e.g. Suikkanen *et al*. 2007). It has been reported that the summer sea surface temperatures of the North and Baltic Seas have increased since 1985 at a rate equalling 3 times the global rate, and 2–5 times faster than in other seasons (MacKenzie and Schiedek 2007). An analysis of the remote sensing data from 1990–2004 has revealed strong positive trends in the sea surface temperature in the Baltic Sea in July and August as well (Siegel *et al*. 2006). These long-term salinity and temperature trends are superimposed by relatively large inter-annual variations in the Gulf of Finland, which are well visible, for instance, as variations in the ice conditions (Jaagus 2006) and deep layer salinity (Alenius *et al*. 1998). Both the long-term trends and inter-annual variations in hydrographic conditions affect the Gulf of Finland's ecosystem through, for instance, changes in inorganic phosphorus pool due to the benthic release of phosphorus (Pitkänen *et al*. 2001), changes in phytoplankton community composition (Suikkanen *et al*. 2007) or high inter-annual variability of the late-summer cyanobacteria blooms (e.g. Lips and Lips 2008).

Due to the variable wind forcing and the width of the Gulf, well greater than the internal Rossby radius (Alenius *et al*. 2003), the meso-scale processes and related changes in the vertical thermohaline structure are dominant dynamical features of the Gulf of Finland. Frequent coastal upwelling events affect remarkably the spatial distribution of the sea surface temperature that is visible on remote sensing images (*see* e.g. an analysis by Uiboupin and Laanemets 2009), and the vertical thermohaline structure (e.g. Lips *et al*. 2009). It has also been shown that, depending on prevailing wind conditions, an ordinary estuarine circulation may be altered or even reversed if the southwesterly wind component exceeds the mean value by at least 4–5.5 m s^{-1} (Elken *et al*. 2003) resulting in a drastic weakening of the vertical stratification in the Gulf of Finland. Thus, the wind induced circulation and mixing modify the thermohaline structure in both a short-term (synoptic) and a long-term (from a month to a season) scale. We assume that similarly to the inter-annual variations in the atmospheric forcing defined as the North Atlantic Oscillation (NAO) index (Jones *et al*. 1997) or the Baltic Sea Index (hereafter BSI) (Lehmann *et al*. 2002) it could be possible also to indicate related inter-annual variations in the vertical stratification of the Gulf of Finland water column.

The main aim of the present study was to describe the vertical structure of temperature and salinity fields and its inter-annual variations in the Gulf of Finland in summer (June–August) using the data collected in 1987–2008. The latest descriptions of the hydrographic conditions in the Gulf of Finland have mainly been based on modeling studies [*see* e.g. a paper by Andrejev *et al*. (2004) and a review by Soomere *et al*. (2009)]. In comparison with the study by Alenius *et al*. (1998), the present analysis includes also the years after the mid-1990s when according to the HELCOM monitoring data (HELCOM 2002) an increase of salinity in the deep layers of the Gulf of Finland has occurred. Based on the results we suggest possible changes in the vertical thermohaline structure of the Gulf of Finland taking into account the projections of future anthropogenic climate change (BACC 2008).

Data and methods

The data analyzed in the present paper were collected in 1987–2008 during various research projects and monitoring programs run by the Marine Systems Institute at Tallinn University of Technology and its predecessors. Vertical profiles of temperature and salinity were obtained using Neil Brown Mark III and Sea-Bird SBE-19 CTD (conductivity, temperature, depth) profilers. The salinity values were calculated using algorithms from Fofonoff and Millard (1983) and are presented without units on the Practical Salinity Scale 1978.

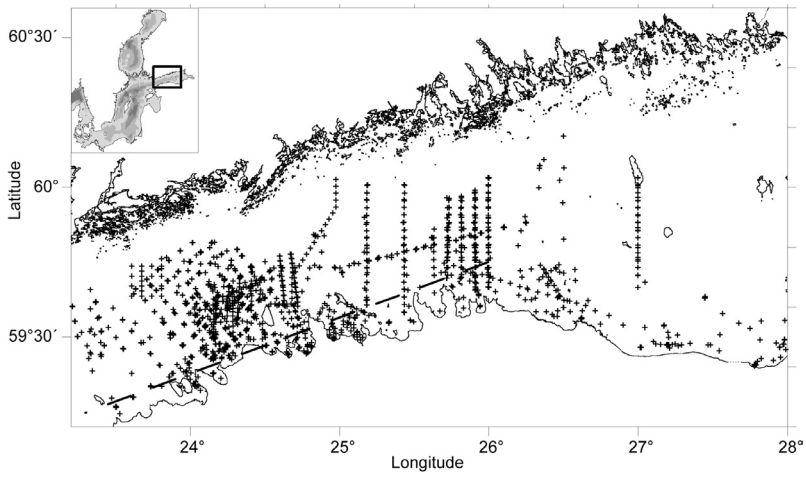

Fig. 1. Map of the Gulf of Finland. CTD cast locations are indicated with crosses and the reference line with a dashed line.

Altogether, the data from 2143 CTD casts, processed and stored as vertical profiles with a resolution of 0.5 m (1 m corresponds roughly to 1 dbar), were analyzed. A higher number of CTD casts was available from the south-western part of the Gulf of Finland (Fig. 1). The number of available profiles varied greatly from year to year (Table 1). We used only deep enough CTD casts in the analysis, whereas different depth limits were defined for different estimates. Profiles deeper or equal to 40 m were used in estimating the upper mixed layer (UML) depth, ≥ 60 m in estimating the base of thermocline and the cold intermediate layer parameters, ≥ 70 m in estimating the deep layer temperature and salinity and ≥ 80 m in estimating the gradients in halocline (and halocline presence).

We estimated the UML depth using smoothed (2.5 m moving average) vertical profiles of density. The UML depth was defined at each profile as the smallest depth where the density gradient exceeded a criterion defined on the basis of the density difference between the cold intermediate layer (CIL) and the UML (an example of the vertical temperature and density profiles and the corresponding estimates are shown in Fig. 2). This criterion (critical value) was calculated as follows:

$$\mathrm{Cr}_{\mathrm{up}} = (\rho_{\mathrm{cold}} - \rho_{\mathrm{min}})C_{\mathrm{up}}, \qquad (1)$$

where ρ_{cold} is the density in the CIL at the depth of minimum temperature, ρ_{min} is the minimum density in the UML and $C_{\mathrm{up}} = 1/30$ m^{-1}. The latter is a constant, which was determined empirically in order to obtain the best performance of the criterion. In case of the characteristic density difference between the UML and CIL of 3 kg m^{-3}, $\mathrm{Cr}_{\mathrm{up}}$ equals 0.1 kg m^{-4}. Thus, the used criterion

Table 1. The number of available CTD casts by year and depth.

		Depth range (m)				
Year	Total	≤ 40	40–60	60–70	70–80	≥ 80
1987	402	68	122	82	88	42
1988	78	23	27	12	10	6
1989	388	78	74	87	111	38
1990	448	89	139	106	86	28
1991	0	0	0	0	0	0
1992	0	0	0	0	0	0
1993	32	20	5	1	3	3
1994	142	91	19	13	8	11
1995	33	19	6	4	1	3
1996	18	11	1	2	2	2
1997	138	16	78	31	11	2
1998	4	0	0	0	4	0
1999	9	4	5	0	0	0
2000	18	12	3	0	3	0
2001	57	47	4	1	1	4
2002	16	14	2	0	0	0
2003	0	0	0	0	0	0
2004	0	0	0	0	0	0
2005	0	0	0	0	0	0
2006	187	32	84	28	36	7
2007	45	7	37	0	0	1
2008	128	17	23	8	59	21
Total	2143	548	629	375	423	168

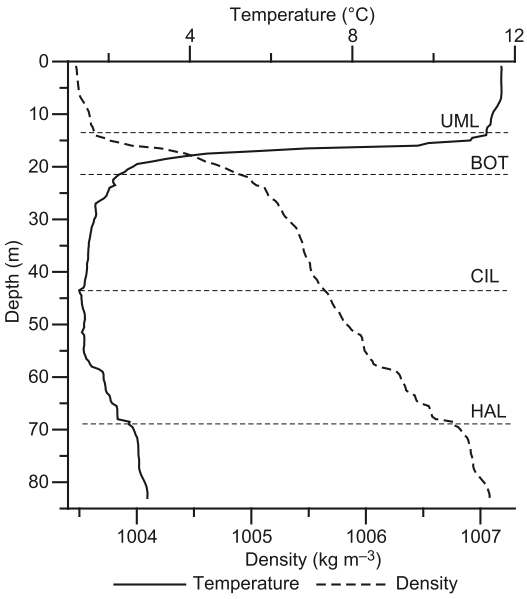

Fig. 2. An example of the vertical temperature and density profiles with the estimated characteristics of the termohaline structure: UML = upper mixed layer, BOT = base of the thermocline, CIL = cold intermediate layer, and HAL = center of the halocline.

was 3–10 times greater than that usually applied in estimating the open-ocean mixed-layer depth [*see* an overview by Thomson and Fine (2003)]. The base (lower border) of the thermocline was determined as the smallest depth where the temperature was below a critical value. The critical value was calculated as follows:

$$\mathrm{Cr}_{dp} = T_{min} + (T_{max} - T_{min})C_{dp}, \qquad (2)$$

where T_{min} is the minimum and T_{max} the maximum temperature at the current profile, and C_{dp} = 0.1. The latter constant was also determined empirically in order to obtain the best performance of the criterion.

The CIL temperature and depth were determined as the minimum temperature at the current profile and the depth corresponding to this minimum temperature record. Non-smoothed temperature profiles were used. The deep layer temperature, salinity and density were estimated at each profile as average temperature, salinity and density in the layer between 68 and 70 meters.

The center of the halocline was defined using smoothed salinity profiles (2.5-m moving average) as the maximum salinity gradient below the coldest point at the current profile. The halocline was determined only in case if the smoothed salinity gradient exceeded 0.07 m^{-1}.

The wind data were obtained from the Kalbådagrund meteorological station (Finnish Meteorological Institute) located in the central part of the Gulf. To characterize the large-scale meteorological forcing conditions in the region, we used the monthly-averaged BSI values calculated as the difference of normalized sea level pressure anomalies between Szczecin in Poland and Oslo in Norway (Lehmann *et al*. 2002; values provided by Andreas Lehmann).

Mean values of studied parameters were calculated stepwise as follows: first, monthly mean values of parameters as simple arithmetic means in a month in each year were found, secondly, monthly mean values for the whole study period were calculated taking into account only years with sufficient number of measurements and, finally, an overall mean was calculated on the basis of the obtained three monthly mean values. The sufficient number of measurements was defined as from > 7 CTD casts for the UML characteristics to > 3 CTD casts for the deep layer characteristics. Along-gulf and cross-gulf spatial variations were estimated using the above-mentioned procedures, respectively, for three longitudinal intervals (23.2–24.2°E, 24.2–25.2°E and 25.2–26.2°E, while for the UML salinity a longitudinal step of 0.5 was used) and for four distance intervals (0–10, 10–20, 20–30 and 30–40 km) where the distances were calculated from a reference line shown in Fig. 1.

Inter-annual variations of estimated parameters are presented and analyzed using the calculated, yearly (summer) mean values taking into account only these years where measurements from at least two summer months were available. The missing monthly-mean values were found by interpolation (extrapolation) using the existing monthly mean values from the same year and the average temporal evolution during the summer months (constructed for each parameter as described above). In order to relate the observed inter-annual changes to the atmospheric forcing, simple linear correlation coefficients between the characteristics of the vertical thermohaline structure and the BSI were

calculated. Significance of diferences in salinity and temperature between years was tested with a *t*-test, under an assumption that data are normally distributed.

Results

Upper mixed layer

The overall mean UML derived from the available CTD casts in the Gulf of Finland in the summers of 1987–2008 was 12.8 m. On average, the UML depth was the smallest in June (11.4 m), slightly greater in July (12.1 m) and the greatest in August (14.9 m). Along the Gulf, the mean UML depth had relatively uniform distribution — the greatest UML depth (15.1 m) was found in the westernmost part of the Gulf between longitudes 23.2°E and 24.2°E, while in the two other regions the mean UML depth was close to 13.0 m (Fig. 3). Across the Gulf, the UML depth was on average greater near the southern coast than in the off-shore areas changing from 14.1 to 10.7 m. A remarkably higher variation of the UML depth was found in the coastal area — the standard deviation of the UML depth there was 7.4 m while in the off-shore areas (30–40 km from the reference line) it was 5.1 m.

The mean UML water temperature and salinity in summer in the Gulf of Finland were 15.2 °C and 5.2, respectively, while those in June were 11.8 °C and 4.9, respectively, in July 16.9 °C and 5.3, respectively, and in August 16.9 °C and 5.4, respectively. The mean UML temperature did not reveal any regular changes along the Gulf, but the mean UML salinity distribution increased from 4.3 in the eastern part of the study area (25.7–26.2°E) to 5.7 in the mouth of the Gulf of Finland (Fig. 3). Cross-gulf changes of the mean UML temperature and salinity were in the ranges of 15.7–16.4 °C and 5.1–5.3, respectively. The highest variations of the UML temperature and salinity were found near the coast where within the first distance interval of 0–10 km the corresponding standard deviations were 3.1 °C and 0.8, respectively.

Inter-annual variations in the UML temperature, salinity and depth were large, but no significant correlation was found with the BSI.

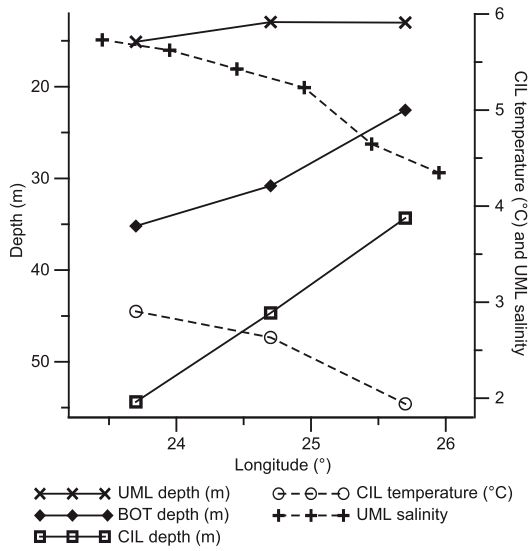

Fig. 3. Mean along-gulf changes of the UML, BOT, and CIL depths, as well as UML salinity and CIL temperature in the Gulf of Finland in the summers of 1987–2008. Estimates were made within the three longitudinal intervals (23.2–24.2°E, 24.2–25.2°E and 25.2–26.2°E) while for the UML salinity a longitudinal step of 0.5° was used.

Long-term changes of the mean UML temperature and salinity were estimated using the data from the two best covered periods: 1987–1990 and 2006–2008. The average July–August UML temperature and salinity were in 1987–1990 (mean ± SD) 16.42 ± 2.27 °C and 4.94 ± 0.68, respectively (the data from 862 CTD casts were used), and in 2006–2008 (mean ± SD) 16.91 ± 2.86 °C and 5.17 ± 0.70, respectively (253 CTD casts). Although an increase in both the UML temperature and salinity was found, due to the large short-term variability of these UML characteristics, the calculated mean values did not differ significantly.

Thermocline

The shallower border of the thermocline was defined to be equal to the UML depth, which was on average 12.8 m while the base of the thermocline was situated on average at 27.2 m; hence, the thermocline thickness was 14.4 m. The monthly mean depth of the base of the thermo-

cline and corresponding thicknesses of the thermocline were in June 23.6 m and 12.2 m, respectively, in July 26.5 m and 14.4 m, respectively, and in August 31.6 m and 16.7 m, respectively. The base of the thermocline was at a greater depth in the mouth of the Gulf and smaller in the eastern part of the study area changing from 35.2 to 22.6 m (Fig. 3). Since the UML depth varied less in comparison with the rise of the base of the thermocline, the thermocline was remarkably thicker in the mouth area and thinner in the eastern part of the study area.

In order to quantify the variability of the thermocline characteristics, the probability distributions for some selected parameters were constructed. With a 75% probability, the UML depth was between 5 and 19 m, the base of the thermocline in a depth range of 17–37 m and the thickness of the thermocline between 6 and 22 m. For some thermocline parameters, clear maximum frequency ranges existed in probability distributions in a specific month (June, July or August) but in some other cases the distributions were more uniform and the variability was higher. For instance, the most frequent depth interval, where the base of the thermocline was detected, was in June 18–21 m (25% of cases) and in July 21–24 m (26% of cases) while in August no distinct maximum in the frequency distribution was observed. The thickness of the thermocline was in June in 83% of the cases between 4 and 16 m, but in July and August the variability of the thermocline thickness was much higher.

The mean vertical temperature gradient in the thermocline was –0.99 °C m^{-1} and the mean vertical salinity gradient 0.09 m^{-1}. In more than 70% of the cases, the absolute values of mean gradients in the thermocline were < 1.5 °C m^{-1} for temperature and < 0.2 m^{-1} for salinity. The mean vertical salinity gradient in the thermocline was stronger in June (0.12 m^{-1}) and weaker in July (0.08 m^{-1}) and August (0.07 m^{-1}). Although the smoothed density profiles revealed stable stratification, the negative vertical salinity gradients could be observed locally. At 5.5% of the profiles, inverse local salinity gradients exceeding 0.5 m^{-1} were detected. The steepest temperature gradient in the thermocline was most probably situated in a depth range of 12–21 m (52%). The steepest temperature gradients in each profile were mostly (75%) between 1 and 5 °C m^{-1}. The gradients > 8 °C m^{-1} were detected at < 5% of profiles.

Cold intermediate layer

The mean temperature of the coldest point of temperature profiles (CIL temperature) and its depth (CIL depth) in the Gulf of Finland in the summers of 1987–2008 were 2.5 °C and 42 m, respectively, whereas remarkable seasonal and inter-annual variations were detected. On average the CIL temperature rose during the summer as fast as 0.01 °C per day increasing from 2.0 in June to 2.8 in August. The CIL depth was increasing on average from 35 m in June to 47 m in August. The average CIL temperature was 2.9 °C in the mouth of Gulf and 1.9 °C in the eastern part of the study area (Fig. 3). The CIL depth revealed on average a similar trend: it was 54 m in the mouth area and 34 m in the eastern part of the study area (Fig. 3).

Large inter-annual variations in the CIL temperature were observed (Fig. 4) in the Gulf of Finland during the analyzed period 1987–2008. The lowest summer mean CIL temperature (1.3 °C) was measured in 1987 and the highest in 1990 and 2008 (3.4 and 3.6 °C, respectively). It could be expected that the summer CIL temperature depends strongly on the severity of previous winter. The correlation between the summer CIL temperature and the winter BSI was positive and the best correlation ($n = 8$, $r^2 = 0.81$, $p < 0.01$) was found if the mean BSI from January to February was used. The summer CIL temperature and the maximum ice extent in the Baltic Sea were (as expected) also correlated, but the correlation was negative ($n = 8$, $r^2 = 0.72$, $p < 0.01$).

Halocline and deep layer

The mean temperature and salinity at the 70 m depth in the Gulf of Finland in summer in 1987–2008 were 3.5 °C and 8.3, respectively. On average, a slight decrease in salinity from June to August of about 0.2 units and a slight increase in temperature of about 0.1 °C were detected. The average along-gulf changes in the deep layer temperature and salinity were also as

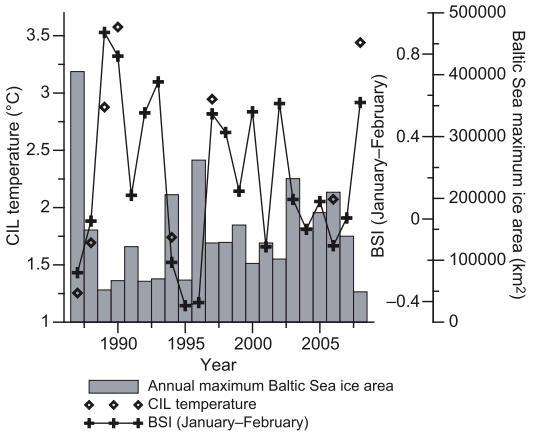

Fig. 4. Variability of the summer CIL temperature, BSI, and the annual maximum Baltic Sea ice area.

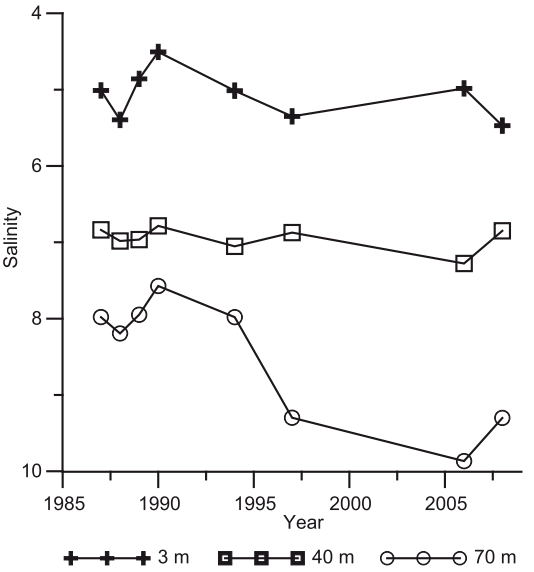

Fig. 5. Variation of the mean salinity at 3 m, 40 m and 70 m depths in the Gulf of Finland in the summers of 1987–2008.

low as 0.1 °C and 0.3, respectively, between the mouth area and the eastern part of the study area.

Inter-annual variability of the deep layer (70 m) temperature and salinity was quite high (Fig. 5). A group of years (1997, 2006 and 2008) with a higher summer mean salinity in a range of 9.1–9.8 and temperature in a range of 3.9–5.0 °C could be distinguished. On the other hand, in 1987–1990 and 1994 summer mean salinity was in a range of 7.7–8.2 and temperature in a range of 2.2–3.9 °C. Inter-annual variability of the salinity difference between the upper and deeper layers was in accordance with the mean deep layer (70 m) salinity changes (Fig. 5) although a slight increase in surface layer salinity between the years with a fresher and saltier deep layer could be noticed as well. The highest mean deep-layer salinity and the strongest mean vertical salinity gradients were recorded in 2006. However, it has to be noted that the intermediate-layer salinity (shown in Fig. 5 as the mean salinity at the 40-m depth) had much lower inter-annual variations than those in the surface layer and especially in the deep layer.

In order to elucidate the possible dependence of salinity gradients on the wind conditions, a correlation analysis between the deep layer and the surface-layer salinity difference at individual profiles, and the average wind speed and direction in the period preceding the measurement was performed. A significant correlation between the wind forcing and the salinity gradients was obtained if an average wind speed from a period of three weeks or longer (until a period of six weeks) before the CTD measurement was taken into account. The best (positive) correlation (n = 586, $r^2 = 0.33$, $p < 0.01$) was found with the average wind component from N-NE (20°).

The halocline was detected only if the smoothed vertical salinity gradient exceeded the value of 0.07 m^{-1}. The center of the halocline defined as the depth of the maximum salinity gradient was in the Gulf of Finland in the summers of 1987–2008 on average at the depth of 67 m. In the years described above as those with fresher deep layer waters, the center of the halocline was found on average at the 71-m depth, and in the years 1997–2008 on average at the 64-m depth. It has to be mentioned that also at 22% of analyzed profiles in the years before 1997, the maximum vertical salinity gradient was < 0.07 m^{-1}, and the halocline was not detected at all, while in the years 1997, 2006 and 2008, the halocline was present at all profiles.

Vertical structure

In order to compare the vertical temperature and salinity distribution in the two distinct periods (fresher and saltier deep layer in the Gulf

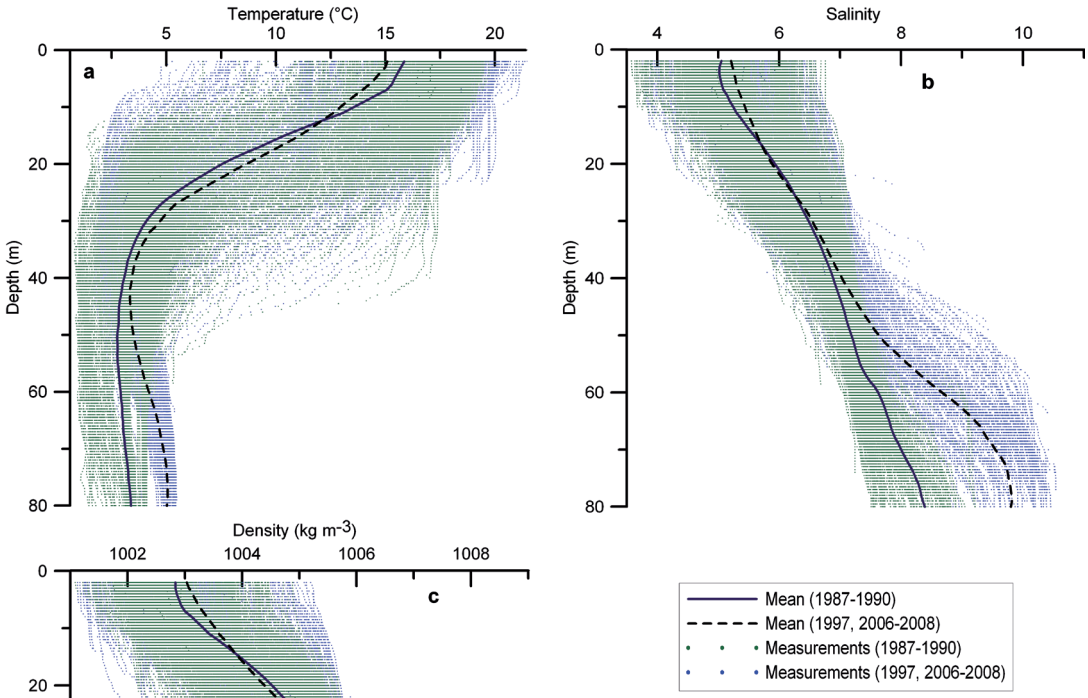

Fig. 6. Scatter plots of (**a**) vertical temperature, (**b**) salinity and (**c**) density profiles in the Gulf of Finland in the summers of 1987–2008 between 23.2°E and 25.2°E.

of Finland) we extracted sub-sets of data from both groups (years 1987–1990 and years 1997, 2006–2008), and restricted the geographical area to the longitudes between 23.2°E and 25.2°E. It was done to be sure that all summer months are well covered and the data are collected from the same area within both periods. The overall scatter plot of the vertical temperature and salinity profiles available from those summers in the western Gulf of Finland (Fig. 6) revealed a quite large variability of temperature and salinity throughout the entire water column, especially in the surface and thermocline layer for temperature and in the surface and deep layer for salinity. Although the variability was high in the surface layer, the profiles did not form two separate groups in the upper layers down to the CIL depth. At the same time, the years 1997 and 2006–2008 grouped clearly as those with saltier and warmer waters in the deep layer of the Gulf of Finland.

The mean vertical profiles showed a clear difference in the temperature and salinity distribution in the deep layer as well (Fig. 6). The estimated mean values of temperature and salinity at the 70 m depth in the years 1987–1990 were 3.1 °C and 8.0, respectively, and in the years 1997, 2006–2008, 4.9 °C and 9.5, respectively. The mean deep-layer temperature and salinity for these two groups are statistically different (*t*-test: df = 544, $p < 0.05$). In addition, in the years with saltier waters, the CIL temperature was higher and the CIL depth lower. The mean values of the

CIL depth, CIL temperature and salinity at the CIL depth in the western Gulf (from 23.2°E to 25.2°E) in the years with less-saline and more-saline waters were 46 m and 39 m, 2.5 °C and 2.9 °C, and 7.0 and 7.0, respectively.

Since UML salinity and temperature observed in the years with a saltier deep layer did not differ statistically, the vertical density gradient through the seasonal thermocline during those years was close to or even smaller than that in the years with a fresher deep layer. At the same time, a significantly stronger vertical stratification was present in the deep layer in 1997, 2006–2008 (Fig. 6c). The estimates of the mean density difference between the deep layer (70 m) and the intermediate layer (40 m) in these two groups of years were 1.1 kg m^{-3} (1987–1990) and 2.1 kg m^{-3} (1997, 2006–2008), and between the intermediate layer (40 m) and the surface layer (3 m) 2.8 kg m^{-3} (1987–1990) and 2.7 kg m^{-3} (1997, 2006–2008). In conclusion, the vertical structure of the water column in the Gulf of Finland could be approximated in 1987–1990 mainly as a two-layer structure, and in the years 1997, 2006–2008 clearly as a three-layer structure.

We also divided the years into two groups on the basis of the CIL temperature. The years 1989, 1990, 1997 and 2008 were classified as those with a higher CIL (2.8–3.6 °C), and the years 1987, 1988, 1994 and 2006 as those with a lower CIL (1.3–2.1 °C). Vertical profiles of temperature did not form clear groups in the scatter plot but the mean CIL temperature differed statistically between the warmer (3.2 °C) and colder years (1.5 °C), and in the colder years the mean temperature was lower throughout the entire water column.

Discussion and conclusions

Inter-annual variations in the UML temperature and salinity in the Gulf of Finland were estimated using the available CTD casts from 1987–2008. Although a positive UML temperature trend could be detected supporting the earlier results (Siegel *et al*. 2006, Suikkanen *et al*. 2007), the variability in the UML temperature within the groups of years (1987–1990 and 2006–2008) was too large to unequivocally confirm the increase in the sea surface temperature. Thus, the CTD casts collected during different programs and projects could not serve as a basis for long-term trend estimates (if used alone) due to high variability in the UML characteristics.

The inter-annual variations in CIL temperature agreed quite well with severity of a preceding winter and the BSI in January–February. According to the classification of the maximum annual extent of ice cover in the Baltic Sea (Seinä and Palosuo 1996), the winter 1986/1987 was extremely severe and the winters 1988/1989 and 1989/1990 were extremely mild. These extremes resulted in the lowest CIL temperature in summer 1987 and much higher CIL temperatures in 1989 and 1990. The highest CIL temperature was observed in 1990 probably due to the two preceding consecutive mild winters. A similar relationship between the winter atmospheric forcing and the CIL temperature in the Baltic Sea basins (except the Gulf of Finland and the Gulf of Bothnia) was described by Hinrichsen *et al*. (2007).

The changes in deep-layer temperature and salinity depend on two processes. The detected clear difference between the years 1987–1990 and 1997, 2006–2008 was most probably caused by a major inflow of the North Sea waters into the Baltic Sea in 1993 that interrupted the stagnation in the Baltic Proper deep layers (Matthäus and Lass 1995) and further inflows, as that observed in 2003 (Feistel *et al*. 2003). On the other hand, Elken *et al*. (2003) described a relationship between the deep-layer salinity changes and the wind-driven circulation in the Gulf of Finland. They showed that the wind-induced surface transport out of the Gulf is most intensive in case of the winds from NE while the reaction time is about 15 hours. In 2006, when the northerly and easterly winds dominated for a long period, a large inflow of saltier waters into the Gulf of Finland deep layer took place (Lips *et al*. 2008). In accordance with those findings, we showed that a linear correlation exists between the average wind component from N-NE and the salinity difference between the deep layer and the surface layer. This relationship was significant when the averaging period longer than three weeks was used indicating that the wind forcing effect is seen in the vertical salinity distribution

after a relatively long period of winds supporting or working against the ordinary estuarine circulation with an inflow in the surface layer and an outflow in the deeper layers.

The most evident difference in the vertical temperature and salinity distributions between the years 1987–1990 and 1997, 2006–2008 was observed in the deep layer: in the earlier period, the halocline was weak or absent, while in the latter one the halocline was much stronger. By analyzing historical monitoring data and numerical modeling results, simultaneous temporal changes of salinity have been shown to take place throughout the entire water column in the Gulf of Finland (Omstedt and Axell 2003), and such simultaneous changes of salinity are predicted also in the Baltic Sea in case of the scenario with a salinity decrease (e.g. Meier 2006). We showed that while large changes were observed in the deep layer, the intermediate-layer mean salinity remained almost unchanged. This feature can be explained by the different mixing depths in winter in the years with a strong halocline and in the years with a weak halocline. Weak stratification allows for winter mixing to penetrate into deeper layers causing an upward salt flux and in turn almost the same salinity in the cold intermediate-layer of the Gulf of Finland than that in the years with more saline deep water and strong stratification (and consequently a shallower mixing depth in winter). It leads to an important consequence for the planktonic ecosystem: the vertical stratification in the seasonal thermocline will not change very much even if the salinity of deep layers changes remarkably.

The climate change scenarios predict that the Baltic Sea will be most probably warmer and fresher at the end of this century (Meier 2006, BACC 2008). The large variability of the temperature and salinity fields observed within the last 22 years enables us to foresee the possible changes in the vertical thermohaline structure. We suggest that if the above scenario realizes, the Gulf of Finland water column will be mixed down to the greater depths during winter and it will have most likely the two-layer structure in summer. However, if the water temperature rises both in winter and summer (*see* BACC 2008), the vertical gradients in the seasonal thermocline will rather increase than decrease, due to the fact that an increase of the CIL temperature (which is close to the temperature of maximum density) will influence the density less than that in the UML.

In conclusion, we showed that the vertical structure of temperature and salinity fields has experienced large variations. The years under consideration (1987–2008) can be divided into two distinct groups of years with the statistically different mean temperature and salinity in the deep layer (1987–1990: fresher and colder deep layer; 1997, 2006–2008: saltier and warmer deep layer). While the overall salinity (and density) gradient in 1997, 2006–2008 was much stronger as well as the halocline was sharper, the intermediate layer salinity and consequently the vertical salinity (density) gradient in the seasonal thermocline did not reveal large changes between these two periods. We suggest that a possible change towards fresher waters in the Baltic Sea will lead to a weakening of the halocline in the Gulf of Finland deeper areas and the water column (and flow pattern) will have a two-layer structure in summer. At the depths of the seasonal thermocline, the vertical gradient of salinity will not decrease simultaneously and a possible increase of sea surface temperature could lead to a strengthening of the vertical density stratification in the thermocline.

Acknowledgements: The work was financially supported by Estonian Science Foundation (grants no. 6955 and 6752). We thank our colleagues who have participated in collecting of analyzed CTD data in 1987–2008. We are grateful to Andreas Lehmann, who provided the BSI data, and to the Finnish Meteorological Institute for wind data.

References

Alenius P., Myrberg K. & Nekrasov A. 1998. The physical oceanography of the Gulf of Finland: a review. *Boreal Env. Res.* 3: 97–125.

Alenius P., Nekrasov A. & Myrberg K. 2003. Variability of the baroclinic Rossby radius in the Gulf of Finland. *Cont. Shelf Res.* 23: 563–573.

Andrejev O., Myrberg K., Alenius P. & Lundberg P.A. 2004. Mean circulation and water exchange in the Gulf of Finland — a study based on three-dimensional modeling. *Boreal Env. Res.* 9: 1–16.

BACC 2008. *Assessment of climate change for the Baltic Sea basin*. Springer, Berlin, Heidelberg.

Bergström S. & Carlsson B. 1994. River runoff to the Baltic Sea: 1950–1990. *Ambio* 23: 280–287.

Elken J., Raudsepp U. & Lips U. 2003. On the estuarine transport reversal in deep layers of the Gulf of Finland. *J. Sea Res.* 49: 267–274.

Feistel R., Nausch G., Matthäus W. & Hagen E. 2003. Temporal and spatial evolution of the Baltic deep water renewal in spring 2003. *Oceanologia* 45: 623–642.

Fofonoff N.P. & Millard R.C.Jr. 1983. Algorithms for computation of funda- mental properties of seawater. *Unesco Technical Papers in Marine Science* 44: 1–58.

HELCOM 2002. Environment of the Baltic Sea area 1994–1998; background document. *Baltic Sea Environment Proceedings* 82B: 1–215.

Hinrichsen H.-H., Lehmann A., Petereit C. & Schmidt J. 2007. Correlation analysis of Baltic Sea winter water mass formation and its impact on secondary and tertiary production. *Oceanologia* 49: 381–395.

Jaagus J. 2006. Trends in sea ice conditions in the Baltic Sea near the Estonian coast during the period 1949/1950–2003/2004 and their relationships to large-scale atmospheric circulation. *Boreal Env. Res.* 11: 169–183.

Jones P.D., Jonsson T. & Wheeler D. 1997. Extension to the North Atlantic Oscillation using early instrumental pressure observations from Gibraltar and south-west Iceland. *International Journal of Climatology* 17: 1433–1450.

Lehmann A., Krauss W. & Hinrichsen H.-H. 2002. Effects of remote and local atmospheric forcing on circulation and upwelling in the Baltic Sea. *Tellus A* 54: 299–316.

Lips I. & Lips U. 2008. Abiotic factors influencing cyanobacterial bloom development in the Gulf of Finland (Baltic Sea). *Hydrobiologia* 614: 133–140.

Lips I., Lips U. & Liblik T. 2009. Consequences of coastal upwelling events on physical and chemical patterns in the central Gulf of Finland (Baltic Sea). *Cont. Shelf Res.* 29: 1836–1847.

Lips U., Lips I., Liblik T. & Elken J. 2008. Estuarine transport *versus* vertical movement and mixing of water masses in the Gulf of Finland (Baltic Sea). In: *US/EU Baltic Symposium "Ocean Observations, Ecosystem-Based Management & Forecasting", Tallinn, 27–29 May, 2008*, IEEE Conference Proceedings, doi:10.1109/BALTIC.2008.4625535.

MacKenzie B.R. & Schiedek D. 2007. Daily ocean monitoring since the 1860s shows record warming of northern European seas, *Global Change Biology* 13: 1335–1347.

Matthäus W. & Lass H.-U. 1995. The recent salt inflow into the Baltic Sea, *Journal of Physical Oceanography* 25: 280–286.

Meier M.H.E. 2006. Baltic Sea climate in the late twenty-first century: a dynamical downscaling approach using two global models and two emission scenarios. *Climate Dynamics* 27: 39–68.

Omstedt A. & Axell L.B. 2003. Modeling the variations of salinity and temperature in the large gulfs of the Baltic Sea. *Cont. Shelf Res.* 23: 265–294.

Pitkänen H., Lehtoranta J. & Räike A. 2001. Internal nutrient fluxes counteract decreases in external load: the case of the estuarial eastern Gulf of Finland, Baltic Sea. *Ambio* 30: 195–201.

Seinä A. & Palosuo E. 1996. The classification of the maximum annual extent of ice cover in the Baltic Sea 1720–1995. *MERI — Report Series of the Finnish Institute of Marine Research* 27: 79–91.

Siegel H., Gerth M. & Tschersich G. 2006. Sea surface temperature development of the Baltic Sea in the period 1990–2004. *Oceanologia* 48(S): 119–131.

Soomere T., Leppäranta M. & Myrberg K. 2009. Highlights of the physical oceanography in the Gulf of Finland reflecting potential climate changes. *Boreal Env. Res.* 14: 152–165.

Suikkanen S., Laamanen M. & Huttunen M. 2007. Long-term changes in summer phytoplankton communities of the open northern Baltic Sea. *Estuarine, Coastal and Shelf Science* 71: 580–592.

Thomson R.E. & Fine I.V. 2003. Estimating mixed layer depth from oceanic profile data *J. Atm. Oceanic Tech.* 20: 319–329.

Uiboupin R. & Laanemets J. 2009. Upwelling characteristics derived from satellite sea surface temperature data in the Gulf of Finland, Baltic Sea. *Boreal Env. Res.* 14: 297–304.

Paper II

Liblik, Taavi; Lips, Urmas (2012). Short-term variations of thermohaline structure in the Gulf of Finland. Ocean Sci. Discuss., 9, 877-908.

Ocean Sci. Discuss., 9, 877–908, 2012
www.ocean-sci-discuss.net/9/877/2012/
doi:10.5194/osd-9-877-2012

Ocean Science Discussions

Short-term variations of thermohaline structure in the Gulf of Finland

T. Liblik and U. Lips

Marine Systems Institute, Tallinn University of Technology, Akadeemia Road 15a, 12618 Tallinn, Estonia

Received: 29 February 2012 – Accepted: 5 March 2012 – Published: 12 March 2012

Correspondence to: T. Liblik (taavi.liblik@gmail.com)

Published by Copernicus Publications on behalf of the European Geosciences Union.

Abstract

We present and analyze high-frequency observational data of thermohaline structure and currents acquired in the Gulf of Finland (Baltic Sea) using an autonomous buoy profiler and a bottom mounted acoustic Doppler current profiler in July–August 2009. Vertical profiles of temperature and salinity were measured in the upper 50-m layer with a time resolution of 3 h and vertical profiles of current velocity and direction were recorded with a time resolution of 10 min. Although high temporal variations of the vertical temperature and salinity distributions were revealed, it was possible to define several periods with quasi-stationary vertical thermohaline structure. These quasi-stationary stratification patterns lasted from 4 to 15 days and were dominated by certain hydrophysical processes – upwelling, relaxation of the upwelling, wind induced reversal of the estuarine circulation, estuarine circulation, and downwelling. Vertical profiles of current velocities supported the concept of synoptic-scale quasi-stationary periods of hydrophysical fields. The periods with distinct layered flow structures and current oscillations with the prevailing period of 26 h were revealed. A simple model, where the heat flux through the sea surface, wind mixing, wind induced transport (parallel to the horizontal salinity gradient) in the upper layer and estuarine circulation were taken into account, simulated the observed changes in the vertical stratification reasonably well. The largest discrepancies between the observations and model results were found when water movement across the Gulf and associated vertical displacement of isopycnals (upwelling or downwelling) were dominant processes.

1 Introduction

The vertical stratification of the water column in the oceans and seas is a key factor shaping the distribution and transport of substances. The Gulf of Finland, a 400-km long and 48–135-km wide sub-basin of the Baltic Sea, is dominated by the fresh water discharge at the eastern end and free water exchange with the Baltic Proper through

its western border (Alenius et al., 1998). This creates both horizontal and vertical gradients of salinity. The surface layer salinity varies from 1–3 in the east to 6 (on the Practical Salinity Scale) in the west whereas also a slight decrease across the Gulf from south to north exists. The water column in the deeper areas of the Gulf consists of the three layers – the upper mixed layer (UML), the cold intermediate layer (CIL) and a saltier and slightly warmer near-bottom layer, separated by two pycnoclines – the thermocline at the depths of 10–20 m and the permanent halocline at the depths of 60–70 m.

Based on analysis of vertical profiles of temperature and salinity collected in the Gulf of Finland in 1987–2008, the long-term average parameters of the vertical thermohaline structure have been estimated (Liblik and Lips, 2011). The average UML depth, temperature and salinity were 12.8 m, 15.2 °C and 5.2, respectively. The base of the thermocline (BT) was situated on average at 27.2 m, and the thickness of the thermocline was 14.4 m. The mean temperature of the coldest point of temperature profiles (CIL temperature) and its depth (CIL depth) were 2.5 °C and 42 m. The center of the halocline defined as the depth of maximum salinity gradient was on average at the depth of 67 m. It has been shown that all stratification parameters reveal temporal variations influenced by different factors (Liblik and Lips, 2011). For instance, CIL temperature depended strongly on the preceding winter severities and the Baltic Sea Index in January–February, although it has been shown that denser surface waters diving from shallow areas during autumn and spring could also influence CIL temperature next summer (Chubarenko and Demchenko, 2010). A clear difference between the deep layer salinity in the years until and after the mid-1990s was suggested to be mostly caused by a major inflow of the North Sea waters into the Baltic Sea in 1993 that interrupted the stagnation in the Baltic Proper deep layers (Matthäus and Lass, 1995) and further inflows, as that observed in 2003 (Feistel et al., 2003).

Due to the variable wind forcing and the width of the Gulf of Finland, well larger than the internal Rossby radius (Alenius et al., 2003), the mesoscale processes are dominant dynamical features of the Gulf. The intensity or even reversal of the estuarine

circulation, characterized by an inflow in the deeper layers and an outflow in the surface layer, is depending on the prevailing winds as well (Elken et al., 2003; Liblik and Lips, 2011). Thus, the wind induced changes in the vertical thermohaline structure are visible throughout the entire water column.

Simpson et al. (1990) have introduced a model to describe the vertical stratification in a tidal estuary by adapting the energy considerations used in the surface heating problem to describe the competition between the stabilizing effect of fresh water and the vertical mixing by tidal and wind stirring. A simulation of the monthly cycle based on this model including straining, stirring, and the estuarine circulation was in qualitative agreement with the main features of the observations in the Liverpool Bay. Although the tidal stirring is not an issue in the Gulf of Finland, predicting the development of stratification is even more difficult problem since the stratification at a certain point is depending very much also on the across Gulf movements of water masses. The latter leads often to pronounced upwelling or downwelling events along the coasts (Lips et al., 2009) while in some cases in up to 38 % of the surface area of the Gulf of Finland the surface waters are replaced by the upwelled waters (Uiboupin and Laanemets, 2009).

The simulations of the vertical stratification using 3-D numerical models are not so reliable yet (Myrberg et al., 2010). However, a number of studies have reported the importance of the vertical thermohaline structure to the ecosystem components of the Gulf of Finland, such as phytoplankton species composition (Rantajärvi et al., 1998) and sub-surface maxima of phytoplankton biomass (Lips et al., 2010), cyanobacteria blooms (Lips and Lips, 2008), distribution of pelagic fish (Stepputtis et al., 2011), macrozoobenthos abundance (Laine et al., 2007) or oxygen concentrations in the near bottom layer (Maximov, 2006). Thermohaline structure and related processes in the Gulf of Finland have been mainly studied using classical observations aboard research vessels. The remote sensing methods and Ferrybox systems do not reveal the vertical structure of water column. Because of the narrow width and high marine traffic intensity widespread technologies for water column profiling (like ARGO floats) have not been applied here. An autonomous profiling buoy station was first used in the Gulf of Finland

in summer 2009. An analysis of autonomously collected data together with phytoplankton sampling and counting results suggested that the phytoplankton dynamics was to a large extent determined by stratification conditions (Lips et al., 2011).

In this study, we present and analyze high-frequent observational data of thermohaline structure and currents in the Gulf of Finland (Baltic Sea). The main aim of the paper is to define distinct stratification patterns in the water layer from the sea surface until to the 40–50 m depth, including the seasonal thermocline and to explain in what conditions these patterns occur.

2 Data and methods

2.1 Observations

The CTD-data analyzed in the present paper were collected by an autonomous vertical water column profiler (Idronaut s.r.l) mounted on the specially designed surface buoy (Flydog Solutions Ltd.). The buoy was anchored in the central part of the Gulf of Finland, between Tallinnamadal and Uusmadal shoals at the depth of 85 m (Fig. 1).

Vertical temperature and salinity profiles were obtained using Idronaut s.r.l OS316 CTD probe. The salinity values were calculated using algorithms from Fofonoff and Millard Jr. (1983) and are presented without units on the Practical Salinity Scale 1978. The autonomously collected salinity data were compared with the data collected by OS320*plus* CTD probe (Idronaut s.r.l) aboard the research vessel and the quality of salinity data was checked against the water sample analyses by a high precision salinometer AUTOSAL (Guildline). Altogether 314 CTD profiles in the water layer from 2 (3) to 50 (45) m were collected from 30 June until 28 August 2009. Data acquired with a vertical resolution of about 10 cm were processed and stored for further analysis as vertical profiles of temperature, salinity and density with a resolution of 0.5 m.

CTD profiles were collected with a time resolution of 3 h, but due to maintenance and technical problems some longer breaks occurred. Data on current velocity and direction

were collected by acoustic Doppler current profiler (ADCP, Teledyne RD Instruments). The ADCP was mounted close to the buoy profiler and was set to separate 36 vertical bins by 2 m step. The shallowest bin was at the depth range of 9–11 m and the deepest bin at the depth range of 79–81.

Wind data from June to August were obtained from the Kalbådagrund meteorological station (Finnish Meteorological Institute) located in the central part of the Gulf and other hydrometeorological data (cloudiness, partial pressure of water vapor, relative humidity, air temperature, solar irradiation) at Harku meteostation in Estonia (Estonian Meteorological and Hydrological Institute).

Information on the data sets used in the present paper is summarized in Table 1.

2.2 Definitions

In order to characterize the vertical thermohaline structure measured by the buoy profiler in the upper 50-m layer, the following parameters were defined and estimated: upper mixed layer depth (UML depth), the base of the thermocline (BT), the thickness of the thermocline and the depth of the strongest density gradient. The UML depth was defined as the minimum depth, where the criterion $\rho_z \geq \rho_4 + 0.25\,\mathrm{kg\,m^{-3}}$ was satisfied (ρ_z is the density at the depth z and ρ_4 is the density at the 4 m depth). The base of the thermocline was defined as the maximum depth, where the temperature was $\geq 5\,^{\circ}\mathrm{C}$.

The thermocline thickness was defined as the difference between the BT and UML depth and the depth of the strongest density gradient was defined as the depth where the greatest density increase between the consecutive horizons, calculated over the 0.5 m depth step, was observed.

The periods characterizing dominance of a few distinct processes were selected qualitatively on the basis of the observed variations in the vertical temperature and salinity distributions (Fig. 2) and TS-diagrams (Fig. 3). The mean values of parameters for a certain period were estimated as arithmetic averages over all profiles within the period while the wind characteristics presented in Sect. 3.1 were calculated with advanced time lag of 15 h (Elken et al., 2003). A number of criteria and parameters, such

as the UML depth, BT depth and depth of a certain isohaline were tested to define the limits of the periods with specific quasi-stationary stratification patterns described in Sect. 3.1. Finally, the similarity of TS-curves was chosen as a qualitative criterion for separating the periods. Although, depending on the chosen criterion, the periods and estimated mean parameters in each period varied slightly, it does not affect the basic idea of the study – to show that it is possible to detect a number of quasi-stationary stratification patterns in the Gulf of Finland. However, some time slots between the detected periods were not assigned to any of them to keep the similarity of TS-curves within each period. A shift between the periods is discussed separately in Sect. 3.1.3.

Vertical stratification was described by the potential energy anomaly P (Simpson and Bowers, 1981; Simpson et al., 1990) calculated as:

$$P = \frac{1}{h}\int_{-h}^{0}(\rho_A - \rho)gz\mathrm{d}z, \quad \rho_A = \frac{1}{h}\int_{-h}^{0}\rho\mathrm{d}z; \tag{1}$$

where $\rho(z)$ is the density profile over the water column of depth h. The stratification parameter P ($\mathrm{J\,m^{-3}}$) is the work required to bring about complete mixing of the water column under consideration. The stratification parameter in the estuaries has been estimated usually over the entire water column. In the present study, the integration was conducted until the depth of 40 m. This choice was defined by the aim to study the changes in the stratification pattern at the depths of the seasonal thermocline. The water column, characterized by the three-layer structure in the Gulf of Finland in summer (see e.g., Alenius et al., 1998), was divided into two. The calculations were restricted to the upper 40 m, that is close to the long-term mean depth of the cold intermediate layer (coldest point at the vertical temperature profile) of 42 m (Liblik and Lips, 2011).

2.3 Model setup

The time development of P was modeled in the present study as the sum of the following four terms:

$$\frac{\mathrm{d}P}{\mathrm{d}t} = S_b + S_m + S_a + S_e, \tag{2}$$

where the first term on the right S_b is the increase or decrease of stratification due to the upper layer heating or cooling, respectively. The second term S_m is the decrease of stratification due to wind mixing and the third term S_a is the parameter, which describes the decrease or increase of stratification due to the wind induced transport in the surface layer. The last term on the right S_e is the parameter describing the mean estuarine flow that always increases the stratification.

The first two terms on the right S_b and S_m were calculated as suggested by Simpson et al. (1990):

$$S_b = \frac{\alpha g Q_{TOT}}{2c_p} \tag{3}$$

$$S_m = -\delta k_s \rho_a \frac{W^3}{h} \tag{4}$$

These terms are dependent on the surface heating/cooling rate Q_{TOT} (see below) and wind speed W, respectively. In the calculations, the depth $h = 40$ m was considered and the following constants were used: thermal expansion coefficient $\alpha = 1.5 \times 10^{-4}$, specific heat of seawater $c_p = 4000\,\mathrm{J\,(kg\,C)^{-1}}$, air density $\rho_a = 1.3\,\mathrm{kg\,m^{-3}}$, effective drag coefficient $k_s = 10^{-3}$ and efficiency of mixing $\delta = 10^{-3}$.

The third term S_a was calculated using the equation given by Oey et al. (1987) and applied earlier by Pavelson et al. (1997) in the Gulf of Finland:

$$S_a = \frac{g\rho_y \tau^x h}{2f\rho_0}, \tag{5}$$

where ρ_0 is the reference density of seawater – 1003 kg m^{-3} and f is the Coriolis parameter. S_a depends on wind stress τ_x, which can increase the seaward flow in the surface layer and, thus, stratification or vice-versa. The following assumptions and choices of parameters were made: the most appropriate wind direction for seaward flow intensification was 25° (see Elken et al., 2003; Lips et al., 2008), the along-gulf horizontal density gradient was $\rho_y = 5 \times 10^{-6}$ kg m^{-4} (Alenius et al., 1998) and the upper mixed layer depth h was 15 m (Liblik and Lips, 2011).

The fourth term S_e was considered as a constant over the study period – 5.5 $\times^{-5}$ J m^{-3}. It corresponds to a permanent outflow at the rate of 2 cm s^{-1} in the upper 15-m layer.

Without taking into account the advective heat fluxes, we can represent the total heat flux as it follows:

$$Q_{TOT} = Q_{SW} + Q_{LW} + Q_S + Q_L, \quad (6)$$

where Q_{SW} is the short wave radiation, Q_{LW} is the net long-wave radiation, Q_S is the sensible heat flux and Q_L is the latent heat flux.

Short-wave radiation was roughly considered as 90 % (constant sea surface *Albedo* of 10 % was assumed) of measured solar irradiation at Harku meteostation.

The outgoing long-wave radiation is calculated by Stefan Boltzmann law and incoming long-wave radiation as Omstedt (1990) whereby following input data were used: air temperature, sea surface temperature, cloudiness and partial pressure of water vapor.

Sensible heat flux was calculated by bulk formula:

$$Q_S = \rho_a c_{pa} c_{aw}^s W(T_a - T_w), \quad (7)$$

c_{pa} is the specific heat of air (J kg^{-1} K^{-1}), c_s^{aw} is the Stanton number, T_a is the air temperature and T_w is the sea surface temperature. Stanton numbers for stable ($T_a > T_w$) and unstable ($T_a < T_w$) atmospheric boundary layer are 0.66 and 1.13, respectively (Large and Pond, 1982).

The latent heat flux was calculated as it follows:

$$Q_L = L_{aw} E, \quad (8)$$

where L_{aw} is the specific heat of evaporation and E is evaporation.

Evaporation was calculated from the specific humidity difference at the 2 m height and just above the sea level. Specific humidity values were calculated as by Maykut (1986) and input variables such as air temperature, sea surface temperature and relative humidity were used.

Considering strong stratification in summer and assuming that the heat exchange between the upper mixed layer and lower layers is not as important we can express the temporal change in temperature as it follows:

$$\frac{dT}{dt} = \frac{1}{C_p \rho H} Q_{TOT}, \quad (9)$$

where H is the upper mixed layer depth (m).

3 Results

3.1 Temperature and salinity distribution

3.1.1 General description

The UML depth, its temperature and salinity, as well the seasonal thermocline, revealed very high variability over the study period (Fig. 2). The overall mean temperature in the surface layer (3 m) in July–August 2009 was close to the long-term average, while salinity was lower than on average in July–August 1987–2008: 16.9 °C and 4.9, respectively. The monthly mean surface layer temperature and salinity were lower in July (15.7 °C and 4.7) and higher in August (18.1 °C and 5.2). The mean UML was considerable thinner in July (10.3 m) than that in August (17.4 m). When comparing these

estimates with the average monthly values of the UML depth in 1987–2008, 12.1 m in July and 14.9 m in August, the UML was shallower in July and deeper in August than the long-term mean. Similar tendencies were revealed in the mean BT depths: it was slightly shallower in July (25.1 m) and deeper in August (34.9 m) than the mean values in 1987–2008 (respectively 26.5 and 31.6 m). Nevertheless, the thicknesses of thermocline in both months (14.8 and 17.5 m) were similar to the long-term mean values (14.4 and 16.7 m).

The strongest density gradient was situated on average at 15 m depth in July and at 26 m depth in August, as the mean of the strongest gradient at profiles was in July 0.38 kg m^{-4} and in August 0.39 kg m^{-4}.

The average flow pattern of the study period was characterized with the movement to the north-east and east in the upper 60 m and to the north-west below that depth. The average current speed varied in a range of 7.3–12.6 cm s^{-1}, whereas it was > 10 cm s^{-1} in the upper layer, above 20 m and in the deep layer, below 62 m depth.

The observed variations in the vertical distribution of temperature, salinity and current velocity can be interpreted as a result of influence of different hydrophysical processes. A qualitative description of the processes in response to the atmospheric forcing was presented by Lips et al. (2011) and can be summarized as the following. South-easterly winds, which are favourable for upwelling near the southern coast, caused an upwelling event near the southern coast on 7–13 July, and the upwelling waters reached the buoy station on 10 July resulting in a temporal temperature decrease and salinity increase measured by the profiler on 10–12 July (Fig. 2). Mainly westerly-south-westerly winds prevailed in the area from 15 July until the end of July and caused the deepening of the thermocline and south-eastward flow in the 20 m upper layer and north-westward flow below the thermocline. The appearance of more saline water in the UML on 26 July was related to this flow structure.

A period of weak winds was observed during the first 10 days of August. The flow structure was characterized by a northward (north-westward) flow in the surface layer, and an eastward flow below the thermocline. The temperature increase in the surface

layer and the strengthening of stratification occurred in response to the calm weather. Strong wind pulses, observed from 10 August until the end of the measurement period, caused, first, strong current oscillations in the whole water mass and later, when westerly and north-westerly winds prevailed, an intense downwelling event, which was detected at our measurement site as the sharp deepening of the UML from 17 to 19 August.

Considering this qualitative description of the dynamics of the thermohaline structure, the five periods were selected within the whole study period (see Fig. 2 and Table 2), which could be related to the following dominant processes: 1 – upwelling, 2 – relaxation of the upwelling, 3 – wind induced reversal of the estuarine circulation, 4 – estuarine circulation, and 5 – downwelling.

3.1.2 Characterization of the selected periods

Upwelling. In the first period, the thermohaline structure was affected by upwelling, resulting in a thin, cold and saltier UML and shallow base of the thermocline (BT; see Table 2). The mean UML and BT depths, and the thickness of the thermocline were 8.4 m, 14.3 m and 5.9 m, respectively. In the temperature and salinity scatter plots for the first selected period (Fig. 3a), three groups with characteristic TS-distribution were visible (TS-dots were grouped into three clouds). These groups can be regarded as the three phases in the development of the upwelling event or movement of upwelling waters into the study area. The TS-curves indicate a slightly larger salinity increase (at a fixed temperature) at the thermocline depths than that in the upper layer. Due to the upwelling event, the sea surface temperature dropped during the period (Fig. 4), although the period's average heat flux into the sea was positive (131 W m^{-2}). The mean temperature in the surface layer was the lowest and consequently the temperature gradient through the water column (difference at 3 and 40 m) was the smallest (9.9 °C) out of the five periods, but the density difference was still 3.0 kg m^{-3}. The latter was due to the high salinity at 40 m depth, which resulted in a very strong salinity gradient through

the thermocline. The strongest density gradients of the each profile were situated at relatively shallow depths, the mean was only 10.7 m in the first period.

Upwelling relaxation. In the second period, the meteorological conditions were characterized by a clearly positive heat flux (109 W m^{-2}) and relatively strong winds from south-west, though occasional strong wind pulses from south-east occurred as well. The south-westerly winds caused relaxation of the upwelling and thereafter BT depth shortly began to decline while UML depth even became slightly thinner through the period. The UML depth varied in a range of 6.5–16 m and BT in a range of 22.5–35 m while the mean values were estimated at 11.0 m and 29.4 m, respectively, and the mean thickness of the thermocline was 18.4 m.

The sea surface temperature, varying in the ranges 14.7–16.8 °C, was clearly higher than that in the first period and salinity, varying in the ranges 4.6–4.8, was close to those values in the first period. Since the temperature gradient through the water column (12.5 °C; difference at 3 and 40 m) was stronger and the salinity gradient (2.2) weaker than in the first period, the density gradient (3.0 kg m^{-3}) was similar to the upwelling period. The second period's TS-diagrams (Fig. 3a and b) show, that ordinary summer stratification was re-established in the area. TS-curves were mostly straight lines in this period, which could indicate that the relaxation of the upwelling contributes well to the vertical mixing of the Gulf of Finland waters (Lips et al., 2009).

Reversed circulation. Moderate and strong winds mostly from south and west prevailed in the third period. The mean E-W wind component was 5.6 m s^{-1}, N-S component 1.9 m s^{-1} and the mean speed 6.7 m s^{-1}. The latter is in accordance with the observed flow pattern (Fig. 2): eastward flow occurred in the upper layer and a strong outflow from the Gulf in the deep layer (Fig. 2). The mean heat flux into the sea was 91 W m^{-2} that led to the corresponding surface layer temperature increase during the period. The surface layer temperature and salinity varied from 16.7 to 17.7 and from 4.9 to 5.2, respectively. The mean salinity gradient through the water column had dropped to 1.6, a slightly stronger temperature gradient (12.8 °C) was detected and the mean density gradient (2.6 kg m^{-3}) had decreased. The UML and BT depth varied in ranges

15–19.5 and 34–39.5 m and were on average 18.4 and 36 m, respectively. As the BT situated deeper than typically, the mean thickness of the themocline was as high as 17.6 m.

It is seen in the TS-diagrams and mean vertical profiles (Fig. 3b and c) that the upper layer salinity has increased remarkably while the salinity at the thermocline depths has decreased if comparing to the earlier period. These changes are in accordance with the eastward flow in the upper layer and westward flow in the thermocline and below it (Fig. 2). This flow pattern, known as the reversal of the estuarine circulation (Elken et al., 2003; Lips et al., 2008), caused also most probably the observed deepening of the base of the thermocline (Figs. 2 and 3b).

Estuarine circulation. The fourth period was characterized by weak winds from north and north-east. On average, the E-W wind component was 1.5 m s^{-1}, N-S wind component was 0.6 m s^{-1} and the mean wind speed (4.8 m s^{-1}) was lowest of the five periods. The mean heat flux was 48 W m^{-2} and the highest daily heat fluxes up to 128 W m^{-2} were found in this period. The currents were directed most of the time out from the Gulf in the upper layer and into the Gulf in the deeper layer (Fig. 2).

Relatively calm wind conditions and positive heat flux resulted in a thin upper mixed layer. Though the salinity varied around the study periods overall mean (4.5–5.0), the sea surface temperature was clearly the highest of five periods varying from 17.4 to 19.9. The UML depth was as low as 7.5–10 m during the most of the period. The BT depth was close to 40 m during the first days of the period, but gradually moved to the shallower position up to 25 m depth. As a result, the thermocline, which was thicker than 20 m in the beginning, became thinner than 10 m at some point during the period. Since the temperature gradient (14.7 °C) through the water column was clearly the largest of five periods due to the warm surface layer, the density gradient (3.2 kg m^{-3}) was the strongest as well.

The changes seen in the TS-diagram (Fig. 3c and d) can be explained by the influence of estuarine circulation – westward flow in the upper layer and eastward flow below the thermocline, and surface warming. The characteristic TS-curve was close to

the straight line due the increase of salinity at the thermocline depths and formation of a fresher and warmer near surface layer due to the calm conditions.

Downwelling. Wind regime in the final period was characterized by strong wind pulses blowing mainly from the west and with the mean wind speed of 6.5 m s^{-1}. The daily mean heat fluxes varied around the zero, but on average the heat flux was slightly negative (−19 W m^{-2}). The strong winds from the west caused downwelling near the Estonian coast and as a result, the mean UML and BT were deepest of five periods: 25.8 and 38.7 m, respectively. The depth of the maximum density gradient was located on average at 30.1 m depth. Due to changes in wind forcing, strong oscillations with amplitude > 30 cm s^{-1} occurred in the entire water column. The study period's maximum current speed of 48 cm s^{-1} was measured in the beginning of this period.

Since the isopycnals were forced deeper by downwelling, the mean salinity gradient through the water column and, therefore, density gradient as well, were lowest of five periods – 1.0 and 2.2 kg m^{-3}, respectively. The fifth period characteristic TS-curve (Fig. 3d) is strongly influenced by the occurred downwelling event. Due to the eastward transport in the upper layer and vertical mixing (TS-curve is nearly a straight line from surface to 40 m), the upper layer salinity is relatively high and salinity gradient through the thermocline is relatively weak.

3.1.3 Shift from reversed to estuarine circulation

The stratification pattern during the third period was influenced by the dominating flow in the upper layer to the east and in the thermocline to the west resulting in a characteristic TS- curve (Fig. 3b) with slightly fresher waters in the thermocline beneath the saltier water mass in the upper layer. The water column in the fourth period had a clearly different characteristic TS-curve, which was almost a straight line in the TS-plot. The shift from the third to fourth period could be defined differently based on TS-characteristics and flow structure. As seen in the TS-plot (Fig. 3c), a saltier water masses appeared in the upper part of the thermocline (depth range 20–25 m; marked as "transition period" in Fig. 3c) and a slightly fresher water mass in the deeper part

(30–35 m) of the thermocline. These changes were well in accordance with the vertical distribution of current vectors: an eastward flow dominated in the upper part and a westward flow in the lower part of the thermocline. The strongest eastward current was observed exactly between the same depth range (20–25 m), where the mentioned saltier water mass appeared.

The flow structure (Fig. 5) during the transition period was very variable in the upper 60-m layer, but the strong current was almost permanently directed to the north-west in the deep layer (below 60 m depth), similarly to that during the third period of reversed circulation. The flow in the upper layer was affected by anticyclonic oscillations, which caused variations of the current speed from 0 to 15 cm s^{-1}. The flow in the thermocline depths was stronger and more stable in the upper part of the thermocline (upper 25 m), but weak and variable in the deeper part of the thermocline (25–40 m). The period of observed oscillations coincided well with the most pronounced spectral peak in the whole study period – 26 h. A fast transition of the flow structure occurred on 31 July–1 August – the layered flow was replaced with an eastward current, synchronously oscillating in the entire upper 60 m layer and the westward flow ceased in the deep layer. Further on, a typical estuarine circulation scheme was established gradually with a westward flow in the upper layer and eastward in the deeper layers (see Fig. 2). As a result, the TS-curve was straightened (Fig. 3c), although a saltier water mass was appearing occasionally in the thermocline until 2 August.

3.2 Comparison between observed and modeled upper layer dynamics

In the present subchapter, we present a comparison between the measured and modeled changes in the stratification and upper layer temperature. Calculation techniques were described in the methods Sect. 2.2–2.3. For the temperature estimates, the upper layer was assumed to be 18 m thick. This choice was based on the best agreement between the observed and modeled temperature changes, and the chosen value was close to the observed mean UML depth in August (17.4 m).

The observed temperature was clearly more variable than the modeled one (Fig. 4), especially in the first half of July when the upwelling waters caused a considerable decrease of temperature followed by a rapid temperature increase related to the upwelling relaxation. The dynamics of the modeled temperature was defined by the heat flux through the sea surface – an increase continued until the heat flux into the sea was positive. Coincidence between the modeled and measured temperature was better when the upper mixed layer depth according to the observations was close to the assumed upper layer depth in the calculations (18 m). The largest discrepancies were found when the advective heat exchange, which was not taken into account in the estimates, was dominating in the temperature variations, e.g. during the upwelling event in the beginning of the study period.

The stratification parameter (potential energy anomaly P) estimated on the basis of vertical profiles of density varied during the study period as it could be expected intuitively (Fig. 6). Both, upwelling and downwelling caused a decrease of stratification. The reversed circulation and estuarine circulation, which dominated during the third and fourth period, respectively, caused the observed stratification decrease in the third period and increase in the fourth period. The modeled stratification was relatively well in accordance with the measurements during these two periods – a decrease in stratification in the middle of the study period, followed by an increase due to the upper layer heating and estuarine circulation, is clearly detectable in the modeled time-series of stratification.

The largest discrepancies between the modeled and measurements-based changes of stratification parameter were found during the upwelling event. Although the positive heat flux and easterly winds should increase the stratification according to Eqs. (3) and (4), most probably, the passage of the upwelling front through the measurement site caused a rapid decrease of stratification. The other inconsistency is related to the transition between the fourth and fifth periods – the observed stratification decrease was much larger than the modeled one. Partly it is related to an underestimate of the stratification increase during the fourth period (estuarine circulation) when according to

the measurements the secondary thermocline was established. But mostly, the stratification decrease caused by the downwelling was not reproduced by the model since the downward and upward movements of isopycnals (and pycnoclines) due to the near shore convergence/divergence were not included into the model.

4 Discussion and conclusions

High-resolution vertical profiling has revealed remarkable variations of the vertical distribution of temperature and salinity in the Gulf of Finland in July–August 2009. Based on the known synoptic scale variability in the atmospheric forcing, we assumed that the variations in the vertical thermohaline structure could also reveal the variability characterized with some quasi-stationary stratification patterns occurring for the time periods with the same length of several days. Five periods with characteristic vertical temperature and salinity distributions (and TS-curves) were selected and mean parameters of thermohaline structure in each period were estimated. While the mean temperature and salinity in the upper layer, UML and BT depths for the entire study period differed only slightly from the long-term mean values (estimated by Liblik and Lips (2011) on the basis of data from 1987–2008), the average parameters for a certain selected period could differ from each other and the long-term average considerably. It shows that the prevailing synoptic scale forcing and related processes alter the vertical stratification significantly, which in turn could lead to the certain vertical dynamics of phytoplankton community in this stratified estuary (Lips et al., 2011).

The selected quasi-stationary stratification patterns lasted from 4 to 15 days and were dominated by distinct hydrophysical processes – upwelling, relaxation of the upwelling, reversal of the estuarine circulation, ordinary estuarine circulation, and downwelling. Some of these mentioned processes occur in mesoscale while some are related to the estuarine (basin-scale) circulation pattern, which can be reversed depending on the prevailing wind forcing (Elken et al., 2003). In case of the reversed circulation scheme, the thickness of the thermocline was increasing and the stratification

decreasing, and a clear change of the direction of current velocity was observed in the thermocline. Although the layered flow structure was superimposed by remarkable current oscillations, this observational result supports the suggestion that the winds, which generate along-gulf flow in the upper layer, cause in turn opposite flow beneath, and changes in stratification can be modeled as proposed by Simpson et al. (1990). We note that the sub-surface biomass maxima in the vertical distribution of phytoplankton were detected during this period at the same depths in the thermocline (Lips et al., 2011) as the change in current direction. Similar links between the vertical structure of hydrophysical fields and occurrence of sub-surface maxima of phytoplankton biomass have been observed also in other regions (e.g., Velo-Suarez et al., 2010).

Temporal changes of TS-curves give indications about the circulation pattern in the Gulf of Finland bearing in mind the existing horizontal gradients of salinity (Lips et al., 2009). If a section of the TS-curve was shifted to lower (higher) salinities in comparison with that recorded at the same location and density range earlier, a movement of waters from east to west (from west to east) should have been occurred. The observed changes of TS-curves have demonstrated the sensitivity of stratification (vertical thermohaline structure) to the prevailing wind events, especially when estuarine circulation or its reversal were dominant processes. This is another approval for using wind-dependent term in the stratification model in the form of Eq. (5), where the flow in the upper layer along the Gulf (parallel to the average salinity gradient) is taken into account.

Vertical profiles of current velocities supported the concept of synoptic-scale quasi-stationary periods of hydrophysical fields. Strong in- and outflow events, with speed up to 48 cm s^{-1} from/to the Gulf both in the upper and deeper layer alternated during periods of dominance of different quasi-stationary stratification patterns. The flow structure in shorter time-scales was often affected by oscillations with most pronounced spectral peak at 26 h that is close to 27 h, which is one of the dominating oscillation periods in the Gulf of Finland suggested by Jönsson et al. (2008), and revealed also during earlier field studies, e.g. by Lilover et al. (2011).

A comparison of the observed and calculated changes of upper layer temperature and potential energy anomaly suggests that the upper layer dynamics and vertical stratification conditions in the Gulf of Finland can be simulated reasonably well when the surface transport along the Gulf prevails. The largest mismatches between the modeled and measurement-based changes of potential energy anomaly and upper layer temperature were found during the upwelling event, when the upwelling waters reached the study site (buoy station). However, according to the Ferrybox data (Lips et al., 2011), the upwelling front extended a couple of kilometers to the north from the buoy station. Thus, it could be expected that in the central part of the Gulf, the accordance between the model and measurements would be still relatively good. Nevertheless, during major upwelling events, such as has occurred in August 2006 (Lips et al., 2009), the model would still miss the significant decrease in stratification and upper layer temperature.

Thus, we suggest that in certain cases the vertical stratification depends strongly on the water movement across the Gulf and associated vertical displacement of isopycnals. To advance the simple model presented in the present paper, an additional term should be added to the existing model (Eq. 2). This term has to account for the wind induced drift of surface waters across the Gulf and resulting convergence or divergence of waters and vertical movement of isopycnals. If the wind impulse or cumulative along-gulf wind stress is strong enough for the surfacing of the thermocline (see e.g., Haapala, 1994; Uiboupin and Laanemets, 2009), the formation and behavior of the upwelling front has to be taken into account as well. Since these processes depend on the along-gulf wind stress, it is reasonable that the largest mismatches between the model and measurements were found in case of easterly winds (see Figs. 4 and 6). A series of high-resolution CTD sections across the Gulf, such as those presented by Lips et al. (2009), are needed for the parameterization of the influence of upwelling/downwelling to the stratification depending on the along-gulf wind stress and distance of the site from the shore.

Although the movements across the Gulf seem to be the main reason of inconsistency, other sources, such as spatial variability in atmospheric forcing, irregularity of

advective heat and salt transport or parameterization errors could also contribute to the mismatches. For instance, the meteorological data for heat flux estimates were obtained from the on-shore station and the sea surface temperature was taken from a single site (buoy station). Furthermore, we mostly described the processes at the thermocline depths knowing that in the deeper parts of the Gulf the water column has three-layer structure and the dynamics should be more complicated. However, we showed that in certain conditions the simple stratification model is able to simulate the observed changes.

In conclusion, on the basis of the high-resolution profiling of the water column in July–August 2009, the quasi-stationary stratification patterns, which lasted from 4 to 15 days and were dominated by certain hydrophysical processes – upwelling, relaxation of the upwelling, wind induced reversal of the estuarine circulation, estuarine circulation, and downwelling, were distinguished. Vertical profiles of current velocities supported the concept of synoptic-scale quasi-stationary periods of hydrophysical fields. The periods with distinct layered flow structures and current oscillations with the prevailing period of 26 h were revealed. The layered flow structures as well as sub-mesoscale intrusions of waters with different temperature and salinity along the isopycnals were principal features in the period of reversed estuarine circulation and its transformation back to the ordinary scheme. A simple model, where the heat flux through the sea surface, wind mixing, wind induced transport (parallel to the horizontal salinity gradient) in the upper layer and estuarine circulation were taken into account, simulated the observed changes in the vertical stratification reasonably well. The largest discrepancies between the observations and model results were found when water movement across the Gulf and associated vertical displacement of isopycnals (upwelling or downwelling) were dominant processes.

Acknowledgement. The study was financially supported by the Estonian Science Foundation (projects G6955, G9023). We appreciate the help of our colleagues participating in the field measurements. We thank the Finnish Meteorological Institute for wind data from the Kalbådagrund and the Estonian Meteorological and Hydrological Institute for meteorological data from the coastal stations.

References

Alenius, P., Myrberg, K., and Nekrasov, A.: The physical oceanography of the Gulf of Finland: a review, Boreal. Env. Res., 3, 97–125, 1998.

Alenius, P., Nekrasov, A., and Myrberg, K.: Variability of the baroclinic Rossby radius in the Gulf of Finland, Cont. Shelf Res., 23, 563–573, 2003.

Chubarenko, I. and Demchenko, N.: On contribution of horizontal and intralayer convection to the formation of the Baltic Sea cold intermediate layer, Ocean Sci., 6, 285–299, 2010, http://www.ocean-sci.net/6/285/2010/.

Elken, J., Raudsepp, U., and Lips, U.: On the estuarine transport reversal in deep layers of the Gulf of Finland, J. Sea Res., 49, 267–274, 2003.

Feistel, R., Nausch, G., Matthäus, W., and Hagen, E.: Temporal and spatial evolution of the Baltic deep water renewal in spring 2003, Oceanologia 45, 623–642, 2003.

Fofonoff, N. P. and Millard Jr., R. C.: Algorithms for computation of fundamental properties of seawater, Unesco Tech. Pap. Mar. Sci., 44, 1–58, 1983.

Haapala, J.: Upwelling and its influence on nutrient concentration in the coastal area of the Hanko Peninsula, entrance of the Gulf of Finland, Estuar. Coast. Shelf Sci., 38 (5), 507–521, 1994.

Jönsson, B. K., Döös, K., Nycander, J., and Lundberg, P.: Standing waves in the Gulf of Finland and their relationship to the basin-wide Baltic seiches, J. Geophys. Res., 113, C03004, doi:10.1029/2006JC003862, 2008.

Laine, A. O., Andersin, A.-B., Leiniö, S., and Zuur, A. F.: Stratification-induced hypoxia as a structuring factor of macrozoobenthos in the open Gulf of Finland (Baltic Sea), J. Sea Res., 57(1), 65–77, 2007.

Large, W. G. and Pond, S.: Sensible and latent heat flux measurements over the ocean, J. Phys. Oceanogr., 12, 464–482, 1982.

Liblik, T. and Lips, U.: Characteristics and variability of the vertical thermohaline structure in the Gulf of Finland in summer, Boreal Environ. Res. A, 16, 73–83, 2011.

Lilover, M.-J., Pavelson, J., and Kõuts, T.: Wind forced currents over the shallow Naissaar Bank in the Gulf of Finland, Boreal Environ. Res. A, 16, 164–174, 2011.
Lips, I. and Lips, U.: Abiotic factors influencing cyanobacterial bloom development in the Gulf of Finland (Baltic Sea), Hydrobiologia, 614, 133–140, 2008.
Lips, U., Lips, I., Liblik, T., and Elken, J.: Estuarine transport versus vertical movement and mixing of water masses in the Gulf of Finland (Baltic Sea), US/EU-Baltic International Symposium, 2008 IEEE/OES, 1–8, doi:10.1109/BALTIC.2008.4625535, 2008.
Lips, I., Lips, U., and Liblik, T.: Consequences of coastal upwelling events on physical and chemical patterns in the Central Gulf of Finland (Baltic Sea), Cont. Shelf Res., 29, 1836–1847, 2009.
Lips, U., Lips, I., Liblik, T., and Kuvaldina, N.: Processes responsible for the formation and maintenance of sub-surface chlorophyll maxima in the Gulf of Finland, Estuar. Coast Shelf Sci., 88, 339–349, 2010.
Lips, U., Lips, I., Liblik, T., Kikas, V., Altoja, K., Buhhalko, N., and Rünk, N.: Vertical dynamics of summer phytoplankton in a stratified estuary (Gulf of Finland, Baltic Sea), Ocean Dynam., 61, 903–915, 2011.
Myrberg, K., Ryabchenko, V., Isaev, A., Vankevich, R., Andrejev, O., Bendtsen, J., Erichsen, A., Funkquist, L., Inkala, A., Neelov, I., Rasmus, K., Medina, M. R., Raudsepp, U., Passenko, J., Söderkvist, J., Sokolov, A., Kuosa, H., Anderson, T. R., Lehmann, A., and Skogen, M. D.: Validation of three-dimensional hydrodynamic models of the Gulf of Finland, Boreal Env. Res., 15, 453–479, 2010.
Matthäus, W. and Lass, H. U.: The recent salt inflow into the Baltic Sea, J. Phys. Oceanogr., 25(2), 280–286, 1995.
Maximov, A. A.: Causes of the Bottom Hypoxia in the Eastern Part of the Gulf of Finland in the Baltic Sea, Oceanology, 46(2), 204–210, 2006.
Maykut, G.: The sea surface heat and mass balance, in: The Geophysics of Sea Ice, edited by: Untersteiner, N., NATO ASI Series, Plenum Press, New York and London, 395–464, 1986.
Oey, L. Y., Atkinson, L. P., and Blanton, J. O.: Shoreward intrusion of upper Gulf Stream water onto the US southeastern continental shelf, J. Phys. Oceanogr., 17, 2318–2333, 1987.
Omstedt, A.: A coupled one-dimensional sea ice model applied to a semi-enclosed basin, Tellus A, 42, 568–582, 1990.
Pavelson, J., Laanemets, J., Kononen, K., and Nõmmann, S.: Quasi-permanent density front at the entrance to the Gulf of Finland: response to wind forcing, Cont. Shelf Res., 17, 253–265,

1997.
Rantajärvi, E., Gran, V., Hällfors, S., and Olsonen, R.: Effects of environmental factors on the phytoplankton community in the Gulf of Finland – unattended high frequency measurements and multivariate analyses, Hydrobiologia, 363, 127–139, 1998.
Simpson, J. H. and Bowers, D. G.: Models of stratification and frontal movement in shelf areas, Deep-Sea Res., 28, 727–738, 1981.
Simpson, J. H., Brown, J., Matthews, J., and Allen, G.: Tidal straining, density currents, and stirring in the control of estuarine stratification, Estuaries, 13, 125–132, 1990.
Stepputtis, D., Hinrichsen, H.-H., Bottcher, U., Gotze, E., and Mohrholz, V.: An example of meso-scale hydrographic features in the Central Baltic Sea and their influence on the distribution and vertical migration of sprat, *Sprattus sprattus balticus* (Schn.), Fish. Oceanogr., 20(1), 82–88, 2011.
Uiboupin, R. and Laanemets, J.: Upwelling characteristics derived from satellite sea surface temperature data in the Gulf of Finland, Baltic Sea, Boreal Env. Res., 14, 297–304, 2009.
Velo-Suarez, L., Fernand, M., Gentien, P., and Reguera, B.: Hydrodynamic conditions associated with the formation, maintenance and dissipation of a phytoplankton thin layer in a coastal upwelling system, Cont. Shelf Res., 30, 193–202, 2010.

Table 1. Measurement information.

Data type	Data availability		Measuring interval
	From	To	
CTD profiler	30 Jun 2009	28 Aug 2009	1 or 3 h
Current profiler	23 Jul 2009	31 Aug 2009	10 min
Wind data	1 Jun 2009	31 Aug 2009	3 h
Cloudiness	1 Jun 2009	31 Aug 2009	3 h
Other meteorological data	1 Jun 2009	31 Aug 2009	1 h

Table 2. Mean upper mixed layer depth and the base of thermocline depth in different periods.

Period number	Period	The state and/or development of thermohaline structure	Mean UML depth (m)	Mean BT depth (m)
1	5 Jul–12 Jul	Upwelling	8.4	14.3
2	20 Jul–25 Jul	Upwelling relaxation	11.0	29.4
3	25 Jul–28 Jul	Estuarine circulation reversal	18.4	36.0
4	31 Jul–15 Aug	Estuarine circulation	11.3	31.5
5	18 Aug–29 Aug	Downwelling	25.8	38.7

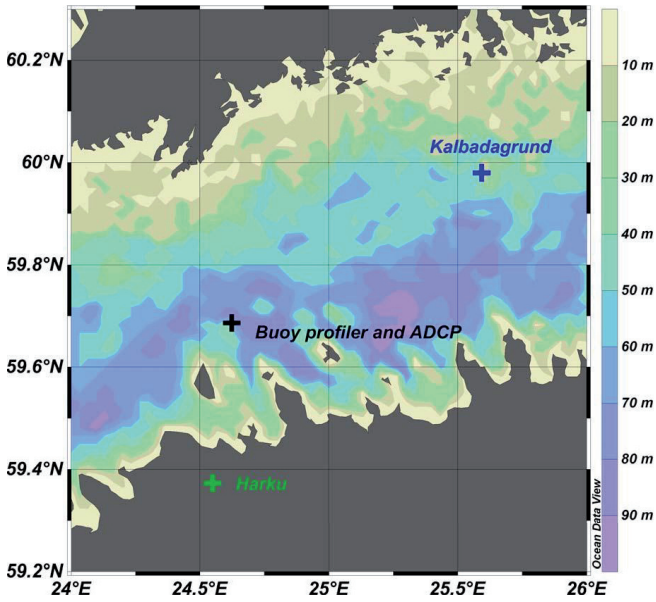

Fig. 1. Locations of the buoy profiler and ADCP mooring, Kalbådagrund and Harku meteorological stations.

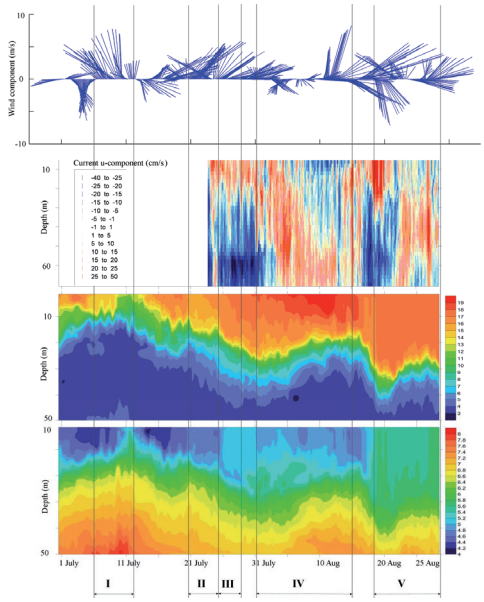

Fig. 2. Wind vectors in Kalbådagrund, E-W component of horizontal current velocity, temperature and salinity at the buoy station (see location in Fig. 1) in summer 2009.

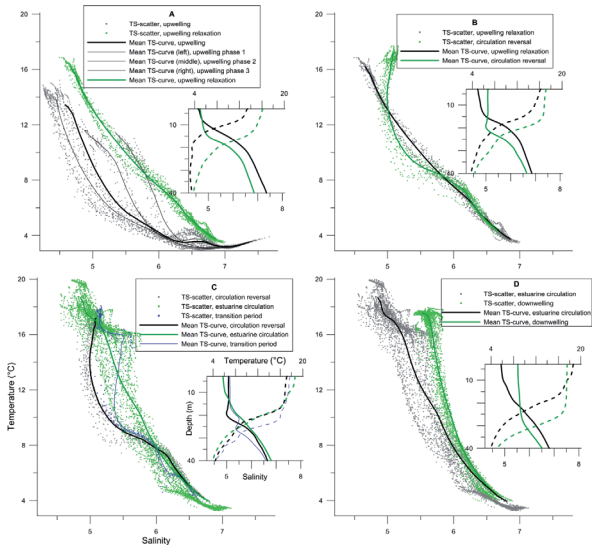

Fig. 3. TS-diagrams. Temperature and salinity scatter plots, mean TS curves and mean temperature and salinity profiles in five periods: first and second period **(A)**, second and third period **(B)**, third and fourth period **(C)** and fourth and fifth period **(D)**. In panel **(A)**, the three phases of the first period are indicated with black thin curves, in panel **(C)** transition period between third and fourth period is drawn out with blue dots and lines. Black curves and grey dots represent the earlier period and green curves and dots represent the later periods in each plot. In the panels of mean vertical profiles the solid curves represent salinity and dashed curves represent temperature.

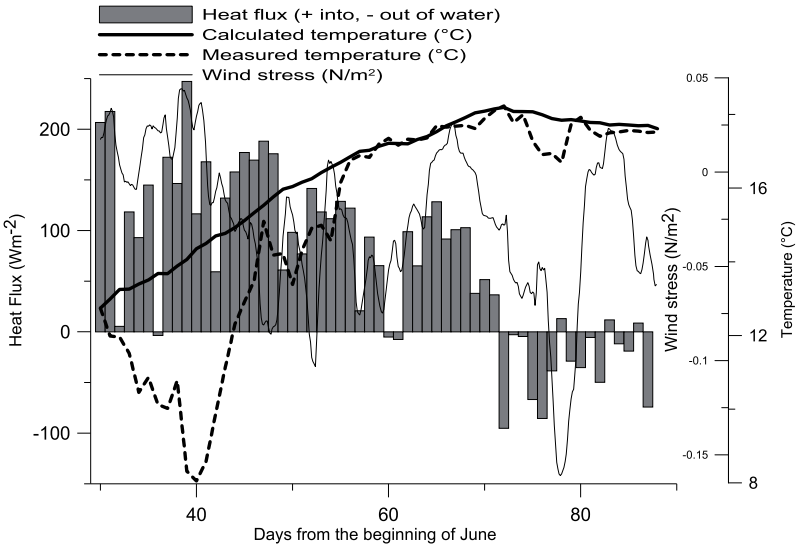

Fig. 4. Development of calculated and measured temperature, along-gulf (70°) wind stress and total heat flux. Total heat flux and temperature are presented as 1-day mean values and wind stress as 3-day running mean.

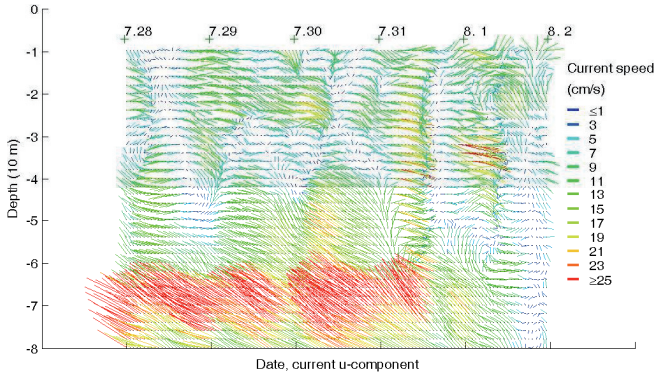

Fig. 5. Vertical distribution of vectors of horizontal current from 28 July to 2 August. Current vectors are averaged with the time step of 1 h.

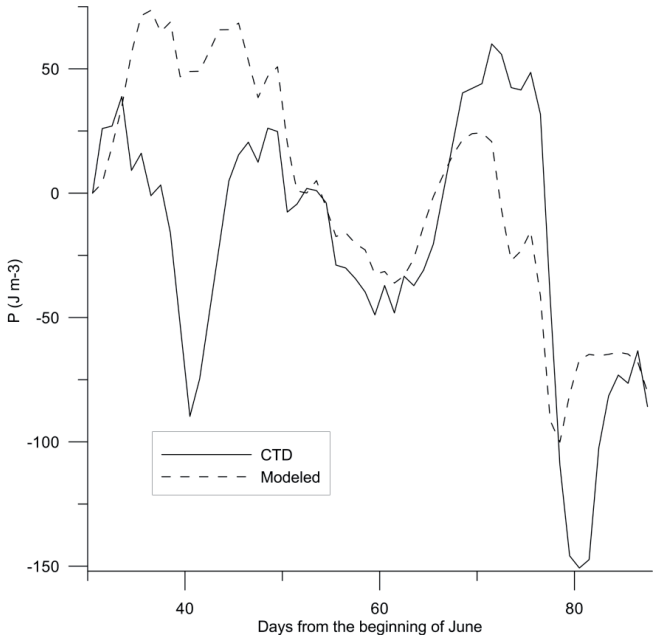

Fig. 6. Development of potential energy anomaly (*P*). Potential energy anomalies, modeled (Eq. 2) and calculated from CTD data (Eq. 1), are presented as 1-day mean values. Modeling started from zero and the first value was subtracted from the whole CTD-based dataset to synchronize both time-series.

Paper III

Lips, Inga; Lips, Urmas; Liblik, Taavi (2009). Consequences of coastal upwelling events on physical and chemical patterns in the central Gulf of Finland (Baltic Sea). Continental Shelf Research, 29, 1836- 1847.

Continental Shelf Research 29 (2009) 1836–1847

Contents lists available at ScienceDirect

Continental Shelf Research

journal homepage: www.elsevier.com/locate/csr

Consequences of coastal upwelling events on physical and chemical patterns in the central Gulf of Finland (Baltic Sea)

Inga Lips *, Urmas Lips, Taavi Liblik

Marine Systems Institute, Tallinn University of Technology, Akadeemia Road 21B, 12618 Tallinn, Estonia

ARTICLE INFO

Article history:
Received 7 January 2009
Received in revised form
17 June 2009
Accepted 26 June 2009
Available online 2 July 2009

Keywords:
Upwelling
Nutrients
TS-characteristics of water masses
Vertical transport and mixing
Gulf of Finland
Baltic Sea

ABSTRACT

The consequences of a coastal upwelling event on physical and chemical patterns were studied in the central Gulf of Finland. Weekly mapping of hydrographical and -chemical fields were carried out across the Gulf between Tallinn and Helsinki in July–August 2006. In each survey, vertical profiles of temperature and salinity were recorded at 27 stations and water samples for chemical analyses (PO_4^{3-}, NO_2^-+NO_3^-) were collected at 14 stations along the transect. An ordinary distribution of hydrophysical and -chemical variables with the seasonal thermocline at the depths of 10–20 m was observed in the beginning of the measurements in July. Nutrient concentrations in the upper mixed layer were below the detection limit and nutriclines were located just below or in the lower part of the thermocline. In the first half of August, a very intense upwelling event occurred near the southern coast of the Gulf when waters with low temperature and high salinity from the intermediate layer surfaced. High nutrient concentrations were measured in the upwelled water – 0.4 μmol l^{-1} of phosphates and 0.6 μmol l^{-1} of nitrates+nitrites. We estimated the amount of nutrients transported into the surface layer as 238–290 tons of phosphorus (P)-PO_4^{3-} and 175–255 tons of N-NO_x for a 12 m thick, 20 km wide and 100 km long coastal stretch. Taking into account a characteristic along-shore extension of the upwelling of 200 km, the phosphate-phosphorus amount is approximately equal to the average total monthly riverine load of phosphorus to the Gulf of Finland. It is shown that TS-characteristics of water masses and vertical distribution of nutrients along the study transect experienced drastic changes caused by the upwelling event in the entire studied water column. TS-analysis of profiles obtained before and during the upwelling event suggests that while welled up, the cold intermediate layer water was mixed with the water from the upper mixed layer with a share of 85% and 15%. We suggest that the coastal upwelling events contribute remarkably to the vertical mixing of waters in the Gulf of Finland. Intrusions of nutrient-rich waters along the inclined isopycnal surfaces in the vicinity of upwelling front were revealed. The upwelling event widened the separation of phosphocline and nitracline which in turn prevented surfacing of nitrate+nitrite-nitrogen during the next upwelling event observed a week after the upwelling relaxation. A suggestion is made that such widening of nutricline separation caused by similar upwelling events in early summer could create favourable conditions for late summer cyanobacterial blooms.

1. Introduction

Eutrophication, i.e. an excess supply of nutrients leading to increased biological productivity, is considered one of the main problems in aquatic environments (e.g. Smith et al., 1999). The Gulf of Finland is one of the most eutrophied parts of the Baltic Sea (HELCOM, 2002). Relative to the surface area of the Gulf of Finland, its external nutrient load is 2–3 times the average for the Baltic (Pitkänen et al., 2001). Although the external phosphorus (P) load to the Gulf declined by about 30% during the 1990s, water dissolved inorganic phosphorus (DIP) concentrations increased rather than decreased at the monitoring stations during the same period (Lips et al., 2002; Fleming-Lehtinen et al., 2008). There are two main reasons for the poor correlation between the external P loading and the DIP concentration observed in water: first, the benthic flux of DIP in the Gulf has increased in the late 1990s and, second, the inflow of saline water rich in DIP has brought a large amount of this nutrient from the Baltic Proper to the Gulf (Lehtoranta, 2003).

In the present state, the Gulf of Finland is very sensitive to increased sediment effluxes of nutrients. The DIN:DIP ratio in the near-bottom water is about 2 by mass in late summer (Lehtoranta, 2003), which is well below the Redfield ratio of 7 by mass, the optimum for phytoplankton production. It suggests that the

* Corresponding author. Tel.: +372 6204303; fax: +372 6204301.
E-mail address: inga@sea.ee (I. Lips).

0278-4343/$ - see front matter © 2009 Elsevier Ltd. All rights reserved.
doi:10.1016/j.csr.2009.06.010

intensified sediment efflux of P is probably responsible for the observed extensive cyanobacterial blooms in the Gulf from the late 1990s (Lips, 2005). Therefore, it is necessary to investigate more closely the hydrophysical processes responsible for nutrient fluxes into the upper mixed layer (UML) to be able to differentiate and demonstrate the importance of internal loading to the Gulf's ecosystem.

During autumn–winter the water column in the Gulf of Finland is mixed down to the bottom in shallow areas or down to the permanent halocline (at depth 50–70 m) in deeper areas. This process is responsible for transporting large amounts of nutrients from the deep layers to the near-surface layer. The winter level of inorganic nutrients directly controls the intensity of the spring phytoplankton bloom following the formation of stratification. After the spring bloom the inorganic nutrients are almost depleted in the UML and strong stratification (formation of seasonal thermocline) prevents mixing between the nutrient-depleted upper layer and the nutrient-rich lower layers.

Important processes which bring nutrient-rich waters from deeper layers to the surface in summer are wind-induced vertical mixing and upwelling events (both coastal and off-shore). Upwelling near the northern coast of Gulf of Finland is associated with along-shore south-westerly winds and near the southern coast with along-shore north-easterly winds. Haapala (1994) have found that the wind events must usually prevail for at least some 60 h in order to generate upwelling and that the required wind impulse depends of the stratification of the water column. Studies at the Gulf of Finland entrance area (Laanemets et al., 2004) have shown that the seasonal nutricline depths in summer in the Gulf of Finland decrease from south to north which point to the higher probability of nutrient transport from lower layers to the UML by different hydrophysical processes (upwelling, turbulent mixing) near the northern coast. This area is suggested also as one of the main wind-driven upwelling areas in the Baltic Sea as follows from the observational results (Kononen and Niemi, 1986; Haapala, 1994), model simulations (Myrberg and Andrejev, 2003), and can be expected from the mean wind direction in the Baltic Sea area in summer (Leppäranta and Myrberg, 2009). The southern coast is, respectively, one of the main downwelling areas (Laanemets et al., 2004). However, it is estimated on the basis of wind data from 2000 to 2005 that on an average about two north-westerly wind events in June–September with large enough cumulative wind stress might generate upwellings along the Estonian coast (Uiboupin and Laanemets, 2009).

Direct measurements of changes of nutrient concentrations in the surface layer caused by coastal upwelling events are relatively rare in the Gulf of Finland. Haapala (1994) reported that during upwelling events in the coastal area near the Hanko Peninsula the nutrient concentrations increased from 0.03–0.06 to 0.13–0.26 $\mu mol\,l^{-1}$ of phosphate-phosphorus and from 0.04–0.14 up to 1.4 $\mu mol\,l^{-1}$of ammonium-nitrogen. The consequences of upwelling along the northern coast in the western Gulf of Finland were described on the basis of data collected during an intensive measurement campaign in July–August 1999 (Vahtera et al., 2005). An increase of phosphate-phosphorus concentration in the surface layer from 0.02 up to 0.32 $\mu mol\,l^{-1}$ was observed. The simulations of this upwelling event by applying the Princeton Ocean Model suggested that the total amount of phosphorus and nitrogen transported and left into the upper 10 m layer of the Gulf as a result of the upwelling event was 387 and 36 tons, respectively (Zhurbas et al., 2008).

The main goal of studies in summer 2006 was to map the spatio-temporal variability of nutrient concentrations in the central Gulf of Finland and to relate the observed patterns and changes to the overall hydrographic and meteorological regime in the area and to occurred mesoscale processes. The main aim of the present paper is to demonstrate the consequences of an observed intense costal upwelling event on physical and chemical patterns and to estimate the related amounts of nutrients transported into the surface layer.

2. Study area

The study was conducted in the Gulf of Finland. It is the easternmost elongated and narrow basin of the Baltic Sea and has no sill towards open Baltic Proper. The Gulf of Finland becomes shallower toward its eastern end. The deepest areas (>80 m) are located in the western and southern parts of the Gulf (the maximum depth being 123 m).

The sampling transect was located in the central part of the Gulf between Tallinn and Helsinki (Fig. 1). The southernmost sampling station TH1 was located <2 km off the coast in the Tallinn Bay and the northernmost station TH27 about 5 km from the archipelago area off Helsinki. The width of the gulf in the study area is <80 km. The water depths are 25–40 m in the inner Tallinn Bay followed by a steep bottom slope to about 90 m in the southern part of the open gulf and a general northward rise of the bottom with remarkable irregularities of the sea bed.

About 75% of the total freshwater inflow into the Gulf of Finland comes from the River Neva in the easternmost end of the Gulf (Pitkänen et al., 2008). Due to the estuarine character of the Gulf of Finland and the residual cyclonic circulation (Alenius et al., 1998), the salinity increases from east to west along the gulf and from north to south across the Gulf. The vertical structure of temperature and salinity fields in the study area in July–August is characterised by a warm and less saline upper mixed layer, a strong seasonal thermocline at the depths of 10–20 m, a cold intermediate layer at the depths of 20–50 m and a permanent halocline below the depth of 50–60 m. The nutrient concentrations in the UML are usually under the detection limit in July–August while below the seasonal thermocline high reserves of nutrients are present.

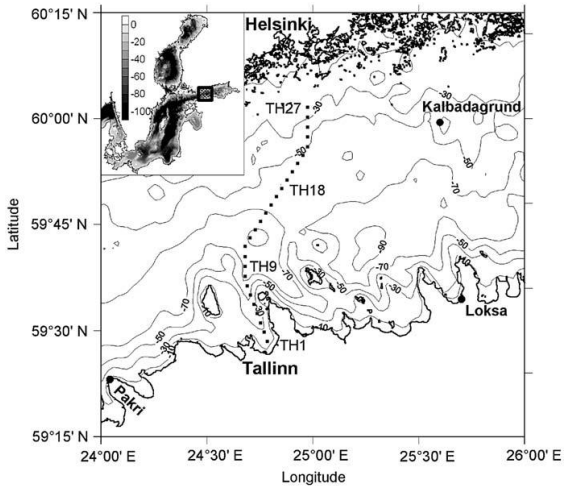

Fig. 1. Map of the study area. Location of sampling stations TH1-TH27. Location of Kalbådagrund meteorological station and coastal stations Pakri and Loksa are shown by filled circle.

3. Materials and methods

3.1. Meteorological information

Meteorological conditions during the study period are characterised by wind data from the Kalbådagrund meteorological station (see Fig. 1) provided by the Finnish Meteorological Institute. Ten-minute average wind speed and direction measured every 3 h at the level of 32 m above the sea surface in July–August 2006 were analysed.

Along-gulf wind stress was estimated by standard quadratic formula, where the values of drag coefficient $c_D = 1.2 \times 10^{-3}$ and air density $\rho_a = 1.2\,\mathrm{kg\,m^{-3}}$ were used. The positive direction of the chosen axis had an azimuth of 70°. Thus, positive values of wind stress correspond to the Ekman drift in the surface layer toward the southern coast and negative values toward the northern coast.

3.2. Surveys and sampling

Seven surveys along a transect of 27 stations were conducted in the sea area between Tallinn and Helsinki (Fig. 1) from 11 July up to 29 August 2006 – on 11 July, 19–20 July, 25 July, 8 August, 15–16 August, 22 August and 29 August. Each survey to map the hydrophysical and -chemical fields was completed within 12–16 h.

At all stations (distance between stations ca 2.6 km) vertical profiles of temperature and salinity were recorded using a NBIS Mark III probe and a Sea-Bird SBE 19 CTD probe. The salinity values were calculated using algorithms from Fofonoff and Millard Jr. (1983) and are presented in the paper without units. Salinity data were quality checked against the water sample analyses by a high precise salinometer AUTOSAL (Guildline).

Water samples for chemical analyses were collected at every second station (distance between measurement points ca 5.2 km) using Niskin water samplers (volume 1.7 l). To represent the UML, the samples were prepared by pooling three (in case of a shallow UML – two) samples taken from the surface layer from the 1 m depth down to the seasonal thermocline, the depth of which was determined from the CTD casts. In addition to the samples from UML the water samples for nutrient analyses were collected from the thermocline with a vertical resolution of sampling of 2.5–5 m and from the near-bottom layer.

3.3. Nutrient analyses

Nutrient analyses were carried out according to the guidelines of American Public Health Association (APHA, 1992; methods 4500-NO3 F and 4500-P F). Samples for phosphates (PO_4^{3-}) were mostly analysed immediately after the sampling onboard *r/v* Kake and samples for dissolved nitrogen compounds (NO_2^-+NO_3^-; henceforth called as NO_x) determination were deep-frozen after collection and analysed later in the on-shore laboratory. Phosphates and nitrates+nitrites were analysed using automatic nutrient analyser μMac 1000 (Systea S.r.l.). The detection limits for phosphate-phosphorus and nitrate+nitrite-nitrogen were 0.06 and $0.14\,\mu\mathrm{mol\,l^{-1}}$, respectively.

3.4. Data analysis methods

CTD data are presented as vertical sections of temperature and salinity over the entire water column along the transect. TS-diagrams from successive surveys are used to define the original water masses along the transect in ordinary conditions, transport of water masses with different TS-characteristics into the study area and the origin of or relative amount of upper and lower layer waters in an upwelled water mass with observed characteristics. For these estimates. it has been assumed that the spatial variation of TS-characteristics of water masses in the vicinity of the study area corresponded to the ordinary structure where salinity gradually increases from east to west along the gulf and from north to south across the gulf. We also assumed that to some extent temperature and salinity can be treated as conservative tracers although some heating of the surfaced cold water was obvious and its effects are discussed.

Distributions of nutrient concentrations with depth and versus density are presented and the reasons for observed changes are discussed. The phosphocline (nitracline) depth was defined as the shallowest depth where PO_4^{3-} (NO_x) concentration was above the detection limit. Estimates of vertical nutrient transport into the upper layer caused by the upwelling event were obtained in two different ways. The first estimate was obtained on the basis of the direct measurements of nutrient concentrations in the upper layer before and during the upwelling event. The second approach was based on the estimated mixing ratio of upper and lower layer waters obtained from the TS-analysis. An attempt was made to explain discrepancies between the two estimates by an initial inhomogeneous distribution of nutrients and by the uptake of nutrients by phytoplankton.

4. Results

4.1. Wind forcing

A number of periods with distinctly different wind conditions were identified in July–August 2006 (Fig. 2a and b). In the first half of July the south-westerly winds with a moderate speed of $3–8\,\mathrm{m\,s^{-1}}$ prevailed. From 14 July to 21 July a period with north-westerly winds of $5–10\,\mathrm{m\,s^{-1}}$ speed can be distinguished. Later, weak winds from variable directions followed by moderate westerly winds were observed. Starting from 29 July until the end of the study period mainly easterly winds prevailed. An exception was the period from 16 to 20 August when south-westerly winds were observed.

Three stronger wind pulses, which were responsible for the initiation and development of the observed upwelling event, are evident from 29 July to 3 August, from 12 to 15 August and from 22 to 26 August. A characteristic wind speed within these periods was from 6 to $12\,\mathrm{m\,s^{-1}}$.

According to the wind stress estimates southward cross-gulf Ekman drift prevailed in July and northward cross-gulf Ekman drift prevailed in August (with an exception from 15 to 20 August) in the surface layer of the Gulf of Finland. The mentioned three periods of stronger wind pulses in August are also clearly seen from the time series of wind stress. Therefore, the physical patterns in July and August should be different and the coastal upwelling should be a dominating feature near the southern coast of the gulf almost throughout the entire August.

4.2. Temporal variations in the surface layer

The temporal variations of surface layer temperature along the transect were consistent with the variations in the wind characteristics. The sea surface temperature was over 20 °C at almost all stations on 11 July and a slight temperature decrease in the surface layer along the whole transect as well as an upwelling event off northern coast observed on 19 July (Fig. 3a) could be explained by a relatively strong north-westerly wind pulse on 14–21 July. The former was most likely caused by more intense vertical mixing and the latter by off-shore Ekman drift near the

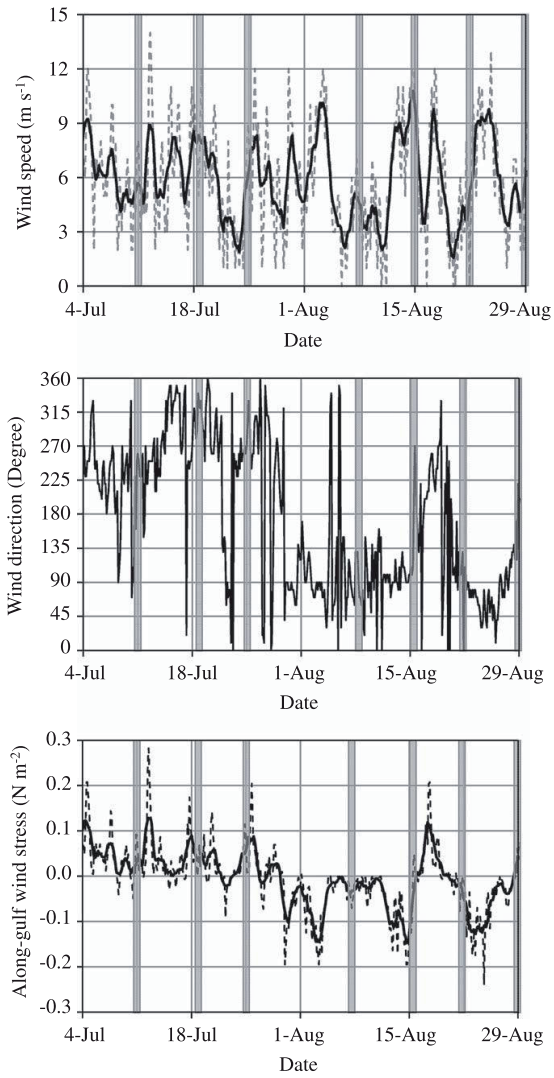

Fig. 2. Wind speed (a, dashed line) and direction (b) at Kalbådagrund meteorological station and estimated along-gulf wind stress (c, dashed line) in July–August 2006. Daily average wind speed and wind stress are indicated as solid lines. Vertical grey areas on panels indicate the periods of hydrographic sampling.

northern coast. On the basis of measurements on 25 July the temperature distribution in the surface layer was almost uniform along the transect. A drastic temperature decline up to 6–8 °C observed off the southern coast on 8 August was caused by the strong easterly wind pulse on 29 July–3 August, which led to a coastal upwelling in this sea area. A widening of the low-temperature area observed on 15 August, a temporal increase of temperature recorded on 22 August and re-establishment of low-temperature surface layer on 29 August could all be explained by the Ekman drift in the surface layer and the related compensating circulation. The relaxation of the upwelling event was forced by the south-westerly winds that prevailed on 16–20 August and due to the next easterly wind pulse on 22–26 August the upwelling intensified again. However, according to the survey on 29 August in the latter case the surface water temperature did not drop below 10 °C.

The most pronounced temporal variations of salinity along the study transect were also related to the wind-forced coastal upwelling event off the southern coast where salinity rose from about 5 to 6.3–6.5. A more saline surface layer, which was separated from the less saline waters by a narrow area of strong salinity gradients (later referred as upwelling front) and extended about 20 km off-shore on 8 August and over 30 km on 15 august (Fig. 3b), was observed in the southern part of the transect. Although the upwelling event was detected near the northern coast on 19 July on the basis of temperature recordings, no changes were detected in the salinity field. A low-salinity water mass (salinity as low as <4.4) appeared in the study area close to the upwelling front as revealed by the measurements on 8 August. Later this low-salinity water mass occupied the entire northern half of the transect. After relaxation of the upwelling (observed on 22 August) the next event led to an increase in surface layer salinity in the southern part of the study transect but according to the survey on 29 August the salinity values exceeded 5.8 units only at the southernmost station in the Tallinn Bay.

In the beginning of the study period the phosphate (PO_4^{3-}) concentrations were below the detection limit in the coastal areas and varied between 0.06 and 0.10 $\mu mol\,l^{-1}$ in the open gulf (Fig. 3c). Similar low, but detectable values were observed at the northernmost stations starting from the second survey almost throughout the whole study period. The upwelling event off the southern coast affected significantly the PO_4^{3-} distribution in the surface layer of the study area. The highest concentrations of PO_4^{3-} were measured on 8 August – maximum of 0.48 $\mu mol\,l^{-1}$ at Station TH1 and the average value of 0.41 $\mu mol\,l^{-1}$ in the upwelling area at Stations TH1-TH7. A week later PO_4^{3-} concentrations varied between 0.11 and 0.24 $\mu mol\,l^{-1}$ in the upwelling area at Stations TH1-TH15 with a maximum at Station TH9. Northward from the upwelling front the surface layer was depleted of phosphate-phosphorus except at the northernmost station where a concentration of 0.13 $\mu mol\,l^{-1}$ was measured. Relaxation of upwelling resulted in PO_4^{3-} concentrations below the detection limit along the whole transect on 22 August. After re-establishment of upwelling on 29 August the concentrations exceeding the detection limit were observed at the southernmost stations and at Stations TH15 and TH17.

The nitrates+nitrites (NO_x) concentrations were below the detection limit in the surface layer throughout the whole study period except the southernmost 18 km of the transect on 8 August and at Station TH17 on 29 August (Fig. 3d). The maximum concentration of 0.79 $\mu mol\,l^{-1}$ was measured on 8 August at Station TH3 and the average value at Stations TH1-TH7 in the upwelling waters was 0.52 $\mu mol\,l^{-1}$. Although on 15 August the upwelling area widened and was clearly seen in the temperature and salinity distributions, the NO_x concentrations dropped below the detection limit again. After relaxation and re-establishment of upwelling on 29 August, the NO_x concentrations remained under the detection limit at the southernmost stations.

4.3. *Vertical temperature and salinity distribution*

An ordinary cross-gulf vertical structure of temperature, salinity (Fig. 4a and b) and density fields (Fig. 5a and b) was observed on 25 July, 2006. The seasonal thermocline was relatively sharp and it was located at the depths of 10–20 m. The cold intermediate water mass laid between the depths of 20 and 40 m in the southern part and of 30 and 50 m in the northern part of the study transect. The vertical structure of salinity field

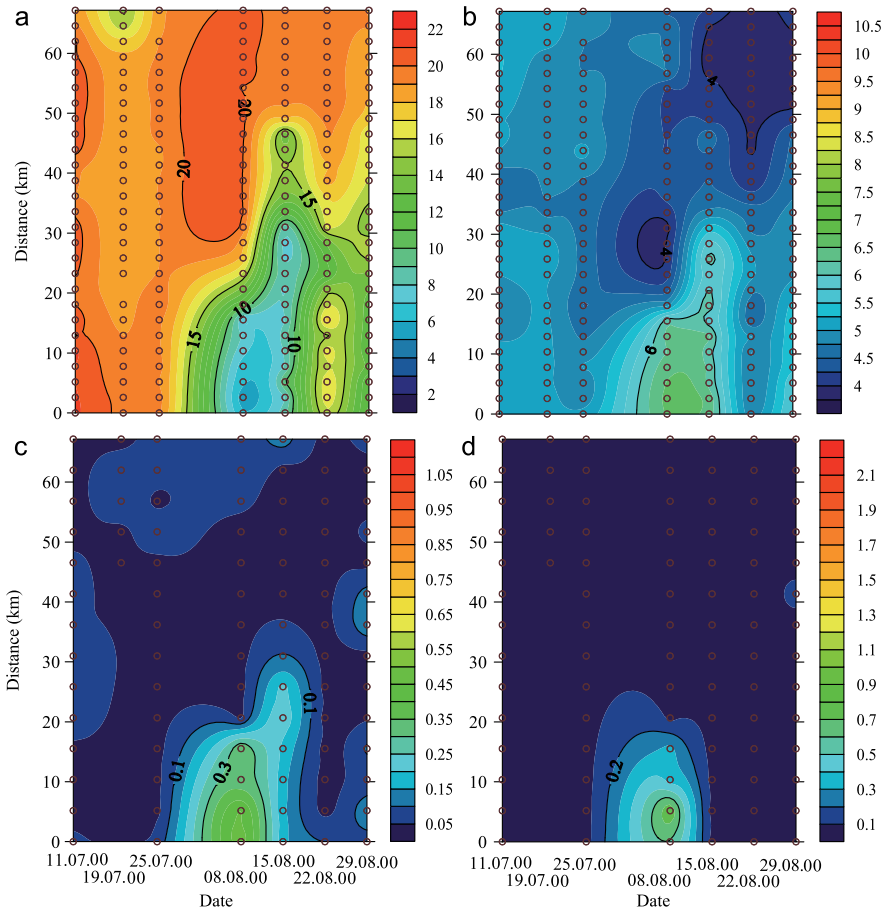

Fig. 3. Temporal changes of temperature (a, °C), salinity (b), phosphate-phosphorus (c, μmol l^{-1}) and nitrate+nitrite-nitrogen (d, μmol l^{-1}) concentration in the upper mixed layer along the study transect from 11 July to 29 August 2006. Dots indicate measurement (a,b) or sampling (c,d) points, values on *y*-axis are distance from the southernmost station (TH1), hydrographic sampling dates are indicated on *x*-axis.

was characterised by low values in the surface layer – from 4.5 to 5.1 – and by a continuous increase of salinity in the seasonal thermocline and below it. The halocline was situated at the depths of 50–70 m. The isotherms and isohalines under the seasonal thermocline had generally a shallower position in the southern part and a deeper position in the northern part of the study transect. It resulted in a stronger vertical gradient of salinity and density in the Tallinn Bay compared to that along the rest of the transect and in a horizontal salinity and density gradient in the intermediate layer of the open gulf.

An intense upwelling of cold and more saline waters from below the thermocline was observed on 8 August off the southern coast of the Gulf (Fig. 4c and d). The upwelling front, which consisted of the sloping thermocline and an associated salinity rise, was situated 18–20 km off the southern coast near the sea surface and about 35 km off-shore at the depth of 20 m. A coupled downwelling was developing off the northern coast where the thermocline was located below 20 m depth – about 5–10 m deeper than during the previous survey. Low-salinity surface water mass appeared just above the sloping upwelling front obviously due to the along-front (along-gulf) westward advection. Markedly weaker vertical gradients of salinity and density (Fig. 5c and d) were observed in the southern part of the study transect if compared to those in the northern part.

On 15–16 August the upwelling zone broadened and the front moved northward to more than 30 km off the southern coast (Fig. 4e and f) most likely due to the easterly wind pulse observed before the survey. The shape of the upwelling front was influenced by the presence of a patch of colder and more saline water – probably an upwelling filament. Thus, the upwelling front consisted of two branches and the northern one which separated the filament and the low-salinity surface water was sharper and very steep. The downwelling was further deepened in the northernmost part of the study transect. The halocline slope was opposite to that observed on 25 July and as a result, the vertical stratification in the intermediate and halocline layer was very weak in the southern part and strong in the northern part of the study transect.

A week later when the relaxation of the upwelling event took place the thermocline was established along the whole study transect (Fig. 4g). It had the shallowest position in the southern part of the open gulf whereas its depth was between 10 and 20 m

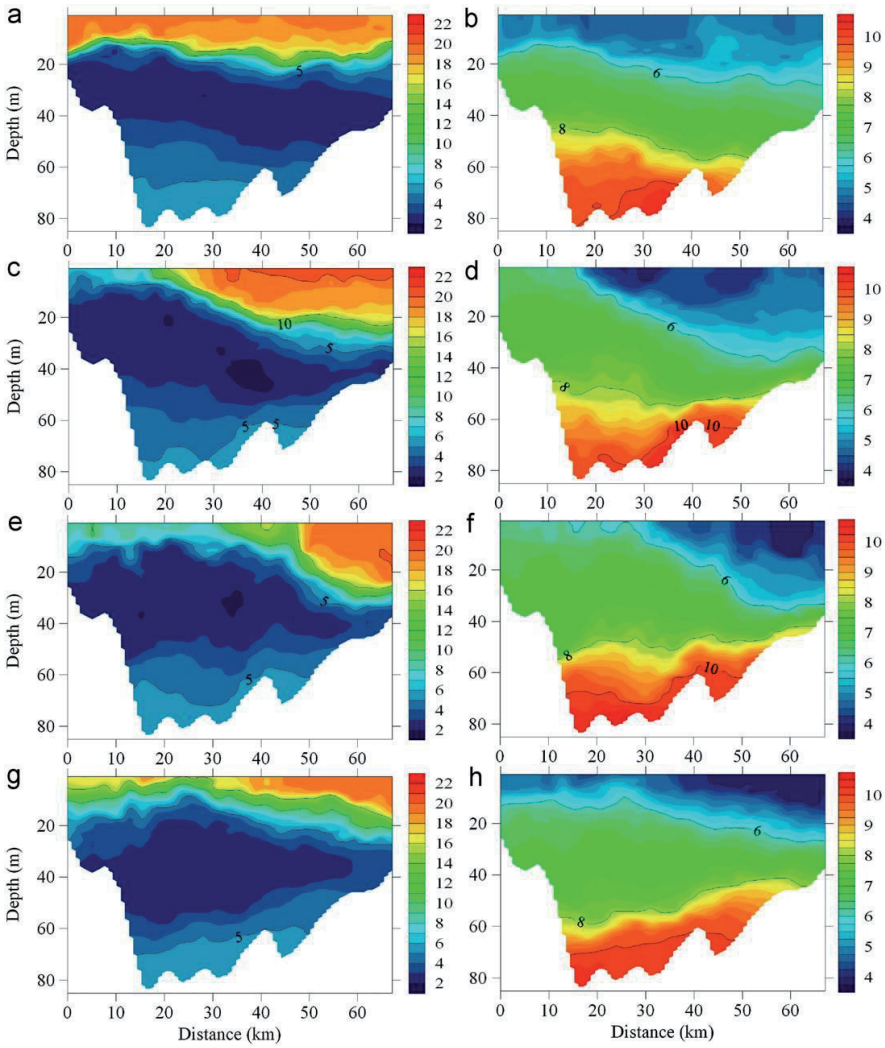

Fig. 4. Vertical sections of temperature (°C) and salinity on 25 July (a,b), 8 August (c,d), 15–16 August (e,f) and 22 August (g,h) 2006. Values on *x*-axis are distance from the southernmost station (TH1).

in the southernmost section of the study transect. The inclination of the halocline was steepened – compared to the previous survey the halocline had fallen deeper in the southern part and risen up in the northern part (Fig. 4h).

4.4. Vertical distribution of nutrients

According to the survey on 25 July the nutriclines were located mainly just below the thermocline and both PO_4^{3-} and NO_x vertical distributions below the thermocline coincided well with the density distribution in the open gulf section of the study transect (Fig. 5a and b) – simultaneous upward shift of thermocline, isopycnal surfaces and nutriclines were observed at certain locations. However, in the lower layers in the Tallinn Bay the nutrient concentrations were lower than at the same isopycnals in the central gulf. It resulted in PO_4^{3-} and NO_x gradients along the isopycnals between the Tallinn Bay and the open gulf. A similar zone of along-isopycnals gradients was observed in the northern half of the open gulf – from 40 to 50 km. At the northernmost stations opposite gradients along the isopycnals were evident, especially for NO_x – the nitracline was observed as deep as at the 35 m depth. Thus, the separation of nutriclines was clear off the northern coast but could not be identified for the open sea area on the basis of our measurements with 2.5 m vertical resolution of sampling on 25 July. Off southern coast a detectable PO_4^{3-} concentration was measured in the UML at Station TH1 and a separation of nutriclines was found also at Station TH7 where PO_4^{3-} concentration of 0.20 $\mu mol\,l^{-1}$ was measured at 12.5 m depth while NO_x concentration was still below the detection limit.

Nutrient-rich waters surfaced in the upwelling area on 8 August (Fig. 5c and d). The border between the nutrient-rich and

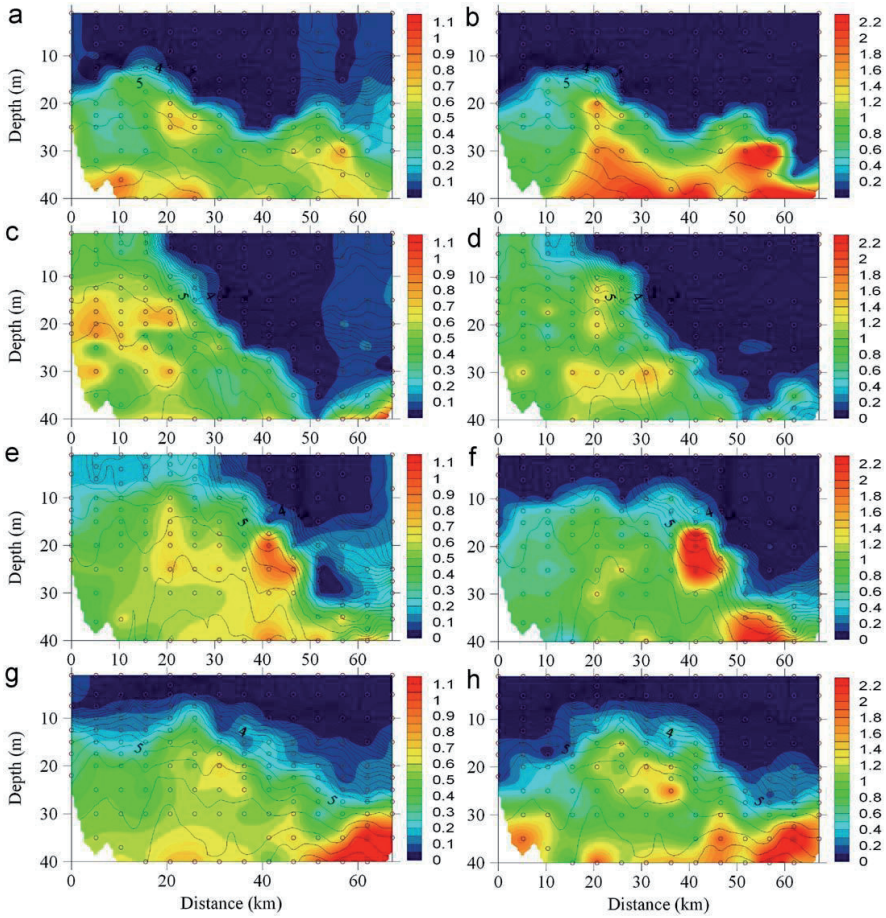

Fig. 5. Vertical sections of phosphate-phosphorus (μmol l^{-1}) and nitrate+nitrite-nitrogen (μmol l^{-1}) in layer 0–40 m on 25 July (a), 8 August (b), 15 August (c) and 22 August (d) 2006. Dots indicate sampling points, values on *x*-axis are distance from the southernmost station (TH1). Corresponding density anomaly distribution (density—1000 kg m^{-3}) is shown by black contour lines.

nutrient-depleted water masses coincided well with the upwelling front exposed in Fig. 5c and d as a set of sloping isopycnals. In the intermediate layer between the depths of 10 and 40 m the distribution of nutrients was relatively patchy in the Tallinn Bay and in the open gulf under the sloping upwelling front. In the northern part of the study transect the nutrient-depleted layer reached the depths of 30–40 m although in the northernmost stations low but detectable concentrations of PO_4^{3-} were observed. It has to be noted also that under the low-salinity surface water mass in the frontal zone relatively high nutrient concentrations, especially of NO_x, were observed in comparison with the other areas within the same density interval.

Although both PO_4^{3-} and NO_x distributions were quite patchy, a general coincidence of the border between nutrient-rich and nutrient-depleted water masses and the upwelling front was exposed also on 15 August (Fig. 5e and f). An extraordinary patch of water with high nutrient concentrations – NO_x up to 3.15 μmol l^{-1} and PO_4^{3-} up to 1.07 μmol l^{-1} – was observed in the sloping frontal zone at the depth of 17.5–25 m between isopycnals 4.6 and 5.4 below the low-salinity water mass confined between the front and the filament.

The surface layer was nutrient depleted down to at least 7.5 m depth along the whole transect on 22 August (Fig. 5g and h), except for PO_4^{3-} at the southernmost station. After the relaxation of the upwelling event the nutriclines had quite shallow position (7.5–10 m) and coincided in the open gulf. However, in the Tallinn Bay a clear separation of nitracline and phosphocline of about 7.5–10 m was observed. The nutriclines were separated by 2.5–5 m also in the northern part of the transect at Stations TH19TH23.

4.5. *TS-analysis*

Two distinct water layers exist in the central Gulf of Finland above the halocline—the warm UML and the cold intermediate layer. The water masses in both layers are characterised by a general salinity decrease from west to east and from south to north. The shapes and the temporal changes of TS-curves give indications about the mixing and circulation patterns in the area. If a TS-curve differs from the straight line, the observed water masses above and below the thermocline cannot form the thermocline water and consequently those water masses originate

from different areas of the gulf or some heating (or cooling) of the UML water has occurred. If a TS-curve is shifted to lower (higher) salinities in comparison with that recorded at the same location earlier, a general movement of waters from east to west (from west to east) occurs in the area under consideration.

To characterise the water masses in the study area in July–August 2006 as well as their transformations in relation to the initiation, development and relaxation of the observed coastal upwelling event, the TS-diagrams of surveys on 25 July, 8 August, 15–16 August and 22 August were analysed (Fig. 6a–d). To estimate the initial TS-characteristics of the two water masses, we placed the border between the UML water and the cold intermediate water along the isotherm of 11 °C which corresponded to the sharpest part of the thermocline on 25 July. The deeper border of the cold intermediate water was chosen as the depth of the isotherm of 3 °C below the temperature minimum.

The TS-characteristics of the UML water and the cold intermediate water estimated on the basis of measurements along the entire study transect on 25 July were 17.74 °C, 4.92 and 3.38 °C, 6.52, respectively. The average thickness of the UML water mass was 16 m and the cold intermediate water was situated between the depths of 16 and 45 m. If only the 7 southernmost stations were taken into account, the corresponding TS-characteristics 18.04 °C, 4.97 and 3.19 °C, 6.75, the thickness of the UML water of 12 m, and the depth range of the cold intermediate water of 12–39 m were obtained. The shapes of the TS-curves differ from a straight line in a manner indicating that the water mass above the thermocline had more westward origin than the water mass below the thermocline (Fig. 6a). At the southernmost stations TH1-TH7 the salinity values in the thermocline were approximately 0.5 units higher than those (at the same temperatures) at the other stations and the TS-curves were closer to straight lines.

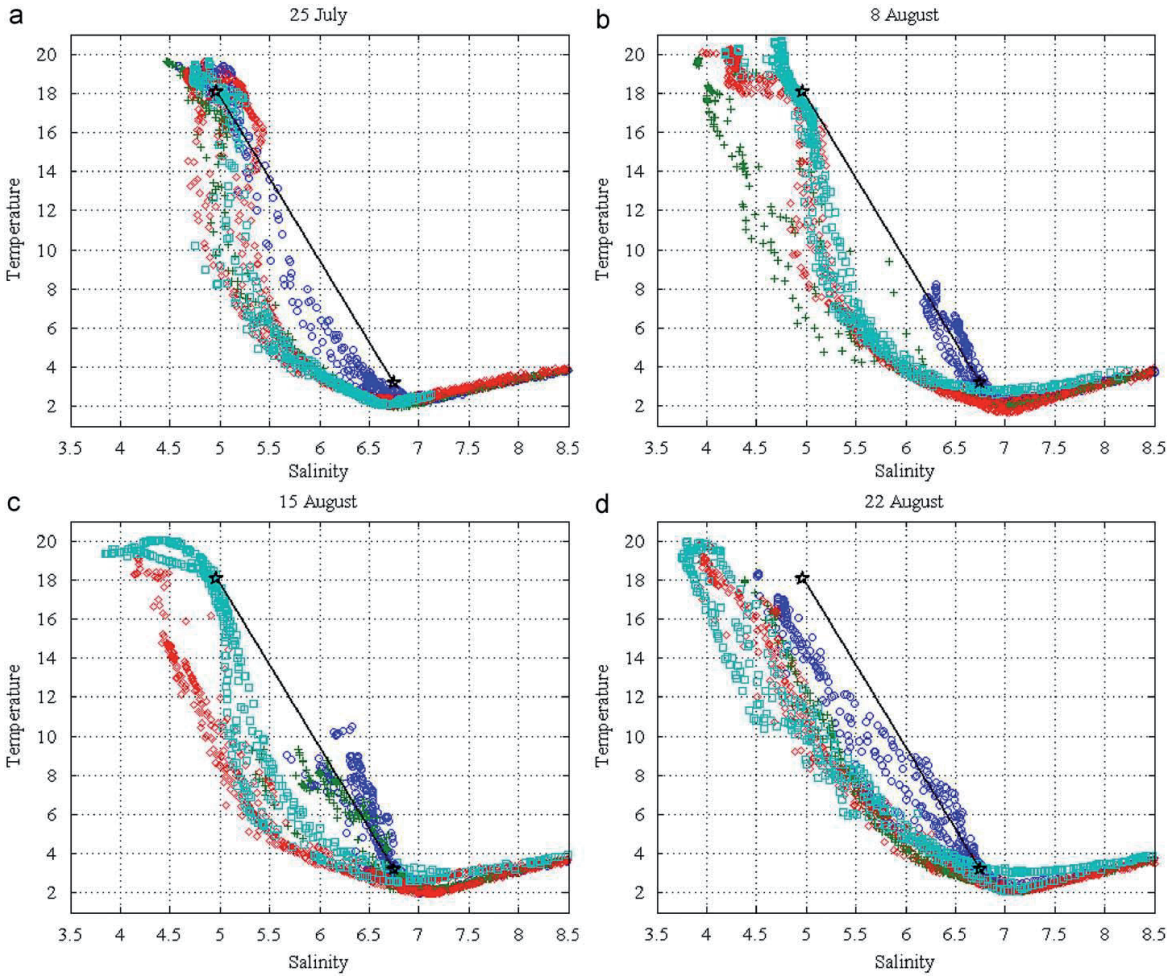

Fig. 6. TS-diagrams on 25 July (a), 8 August (b), 15–16 August (c) and 22 August (d) 2006. Stations TH1-TH7 are marked by blue circles, TH8-TH13 by green crests, TH14-TH21 by red diamonds and TH22-TH27 by cyan squares. The initial upper mixed layer water mass (0–12 m) and the water mass below the thermocline (12–40 m) in the southern part of the study area – Stations TH1-TH7 – are indicated as pentagrams connected with a solid line. Temperature in °C. (For interpretation of the references to colour in this figure legend, the reader is referred to the web version of this article.)

TS-characteristics of water masses observed on 8 August after the initiation of the upwelling event in the study area were much more diverse than those two weeks earlier (Fig. 6b). TS-curves of Stations TH1-TH7, which were influenced by the upwelling event, were located quite exactly along a straight line connecting TS-values of the cold intermediate water and of the UML water at the southern stations before the initiation of upwelling. This is an evidence that the upwelling water with the estimated average TS-characteristics in the upper 12 m layer of 5.41 °C and 6.47 could have been formed from these two water masses observed in the area before the upwelling event. On the basis of these estimates, the share of initial water masses mixed into the upwelling water was obtained as: 15% of the UML water and 85% of the cold intermediate water.

At Stations TH8TH12, TS-curves were shifted to far lower salinities than at the other stations on 8 August and at all stations two weeks earlier. This fact indicates that a less saline water mass was transported into the study area from east most probably along the upwelling front. At the stations in the northern half of the open gulf, the TS-curves were similar to the curves observed on 25 July with an exception of a low-salinity water mass at high temperatures.

On 15 August a similar pattern was revealed in the TS-diagram – the curves characterising upwelling waters at Stations TH1TH13, the curves shifted to the lower salinities at Stations TH14TH20, and the curves comparable to the initial ones but with a low-salinity water mass at high temperatures at the northernmost stations. In comparison with the previous survey, the upwelling front and the described pattern has moved northwards. At some stations in the upwelling region the points of the TS-curves in the surface layer were relocated to the right from the mentioned straight line connecting the TS-values of initial water masses. It could indicate some heating of the upwelling waters near the sea surface. At the same time at some stations near the upwelling front the upwelling waters had lower salinity suggesting that these waters had mixed with waters of more eastward origin.

The relaxation of the upwelling event led to the more uniform TS-curves along the whole study transect (Fig. 6d). The curves are in general almost straight lines with slightly higher position of curves representing southernmost stations. The main difference between the results of this survey and that of four weeks earlier was that the surface layer in the northern part of the study area got remarkably less saline after upwelling relaxation.

4.6. Estimates of vertical transport of nutrients

The simplest way to get a rough estimate of amounts of nutrients transported into the surface layer by an upwelling event is to multiply the average increase of nutrient concentrations and the volume of the upwelled water. The thickness of the surface layer in the estimates was taken 12 m which corresponds to the average thickness of the UML water mass at the southernmost stations where the PO_4^{3-} and NO_x concentrations were below the detection limit before the upwelling initiation on 25 July. According to the vertical section of temperature on 8 August the upwelling event occupied seven southernmost stations; hence, the seaward extension of the upwelling was ca 20 km. To get the average concentrations of PO_4^{3-} and NO_x in the initial water masses and in the upwelling water, first the interpolation of measured values onto a regular grid was carried out (method of interpolation was Kriging; graphical presentation see in Fig. 5). Before the interpolation the values below the detection limit were replaced by the values equal to the $\frac{1}{2}$ of the detection limit – 0.03 $\mu mol\,l^{-1}$ of PO_4^{3-} and 0.07 $\mu mol\,l^{-1}$ of NO_x.

The following average concentrations were obtained for the southernmost 18 km of the transect (corresponds to 20 km wide coastal area): 0.04 $\mu mol\,l^{-1}$ of PO_4^{3-} and 0.07 $\mu mol\,l^{-1}$ of NO_x in the UML water with an average thickness of 12 m on 25 July and 0.43 $\mu mol\,l^{-1}$ of PO_4^{3-} and 0.59 $\mu mol\,l^{-1}$ of NO_x in the upper 12 m layer on 8 August. On the basis of the obtained increase of concentrations, the estimated nutrient amounts introduced into a 12 m thick, 20 km wide and 10 km long coastal stretch were equal to 290 tons of P-PO_4^{3-} and 175 tons of N-NO_x. Thus, for a 200 km coastal stretch corresponding to a characteristic along-shore extent of the upwelling event in August 2006 (see e.g. http://wwwi4.ymparisto.fi/i4/eng/sst/2006/sst_sat_2006_eng.html) the estimates of amounts of upwelled nutrients were 580 tons of P-PO_4^{3-} and 350 tons of N-NO_x.

An alternative method used for the estimation of vertical nutrient transport by the upwelling event was based on the mixing estimate obtained from the TS-analysis and related calculations of average nutrient concentrations in the identified water masses. Average values of PO_4^{3-} and NO_x concentration in the cold intermediate water at the seven southernmost stations corresponding to 18 km of the study transect on 25 July were 0.41 $\mu mol\,l^{-1}$ of PO_4^{3-} and 0.70 $\mu mol\,l^{-1}$ of NO_x. As it was pointed out above, an along-isopycnal gradient of nutrient concentrations was observed outside the Tallinn Bay. Thus, the estimates of nutrient content in the initial water masses which formed the upwelling water mass could be different, if a wider area is taken into account. The following characteristics of the cold intermediate water mass were obtained for a 23 km wide area (corresponding to 9 stations) and for a 28 km wide area (11 stations): 3.16 °C, 6.74, 0.86 $\mu mol\,l^{-1}$, 0.44 $\mu mol\,l^{-1}$ and 3.16 °C, 6.71, 0.96 $\mu mol\,l^{-1}$, 0.46 $\mu mol\,l^{-1}$ for temperature, salinity, PO_4^{3-} and NO_x, respectively.

Assuming that the two initial water masses were mixed as estimated above – 15% and 85% – the nutrient content in the upwelling water should be 0.36 $\mu mol\,l^{-1}$ of PO_4^{3-} and 0.60 $\mu mol\,l^{-1}$ of NO_x (in case the initial cold intermediate water characteristics corresponded to those of waters from southernmost 18 km); 0.38 $\mu mol\,l^{-1}$ of PO_4^{3-} and 0.74 $\mu mol\,l^{-1}$ of NO_x (southernmost 23 km) and 0.40 $\mu mol\,l^{-1}$ of PO_4^{3-} and 0.83 $\mu mol\,l^{-1}$ of NO_x (southernmost 28 km). These estimated values are close to the average concentrations in the upwelling water calculated on the basis of water samples analyses on 8 August – 0.43 and 0.59 $\mu mol\,l^{-1}$. However, slightly lower values for PO_4^{3-} and equal to the average or higher values for NO_x were obtained. As a result, the estimated nutrient amounts introduced into a 12 m thick, 20 km wide and 100 km long coastal stretch varied between 238–268 tons of P-PO_4^{3-} and 175–255 tons of N-NO_x.

5. Discussion

A very intense upwelling event was observed along the southern coast of the Gulf of Finland in August 2006. According to the data from the coastal stations Pakri and Loksa situated about 100 km apart (see Fig. 1; data of the Estonian Meteorological and Hydrological Institute) the near coast water temperature dropped from about 19 to 5–8 °C simultaneously at both locations within three days from 31 July up to 3 August (Fig. 7). Suursaar and Aps (2007) estimated a maximum along-shore extension of upwelling as 360 km and cross-shore extent as 25 km. On the basis of available satellite images from years 2000 to 2006 this event was considered as the most extensive upwelling along the southern coast which on 9 August 2006 covered 6480 km^2 or about 20% of the total area of the Gulf (Uiboupin and Laanemets, 2009). According to our measurements the cross-shore extent of the upwelling was about 20 km on 8 August and exceeded 30 km on 15 August.

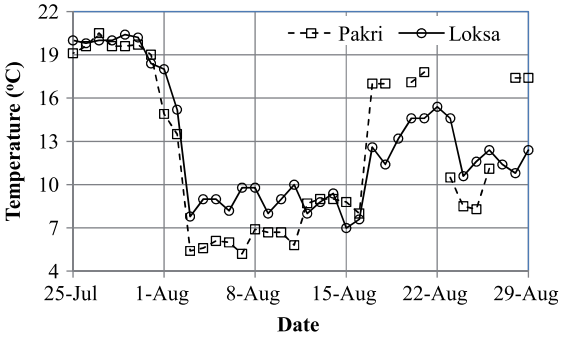

Fig. 7. Surface water temperature at coastal stations Pakri and Loksa (Estonian Meteorological and Hydrological Institute) from 25 July up to 29 August, 2006.

The most pronounced signal of the upwelling in the thermohaline fields is surfacing of cold and more saline waters from below the seasonal thermocline. This very dynamic process involves both the vertical advection of the lower layer water mass as a compensation of off-shore Ekman drift of the surface layer water mass and mixing of these water masses. On the basis of our data and applied approximations we estimated that the upwelling water consisted of 85% of the cold intermediate water mass and 15% of the initial upper mixed layer water mass. Vertical mixing could be also important in the layer below the upwelling water where very low vertical gradients of density were observed, especially on 15 August (note southernmost 20 km in Fig. 5c–f). The relaxation process comprises mixing of water masses as well – it is evident from the TS-curves which were almost straight lines on 22 August. As a conclusion, we suggest that the coastal upwelling events contribute remarkably to the vertical mixing of waters in the Gulf of Finland.

Coastal upwelling is associated with intense jet-like along-shore currents. We have observed a low-salinity water mass close to the upwelling front on the basis of both surveys during the upwelling event on 8 and 15 August (Figs. 3b and 4d and f). The successive TS-curves at Stations TH8-TH13 (Fig. 6a and b) and at Stations TH14-TH21 (Fig. 6b and c) indicate that the westward movement of waters close to the upwelling front prevailed in the whole water column at least down to the temperature minimum. Deepening of the halocline near the southern slope clearly seen on 15 August (Fig. 4f) suggests that within the halocline the cross-shore flow was directed northwards (off-shore). Consequently the on-shore flow was concentrated in the intermediate layer which corresponds to the upwellings in the regions with strong stratification (Lentz and Chapman, 2004).

As a response of a stratified elongated basin to constant along-axis wind, also an along-shore jet in the downwelling area and a slow return flow in the central basin should appear (Krauss and Brügge, 1991). In case of the intense upwelling event observed in August 2006 the vertical cross-sections of density (Fig. 5c–f) and variations of TS-characteristics (Fig. 6b and c) indicate that the return flow in the surface layer was relatively narrow on 8 August and totally absent on 15 August. At the same time the changes of the shape of halocline and salinity of deep layers suggest that a return flow could occur in the deep layer of the northern part of the gulf. The latter shows that the upwelling favourable winds influence the dynamics of the whole water column of the Gulf of Finland and it is not restricted to the water layer above the halocline where the Ekman compensation flow exists (Lehmann and Myrberg, 2008).

We estimated amounts of nutrients transported into the surface layer by means of two methods as 290 or 238–268 tons of P-PO_4^{3-} and 175 or 175–255 tons of N-NO_x for a 12 m thick, 20 km wide and 100 km long coastal stretch. Taking into account a characteristic along-shore extension of the upwelling of 200 km, the phosphate-phosphorus amount is approximately equal to the average total monthly riverine load of phosphorus of 500 tons to the Gulf of Finland (HELCOM, 2004). Discrepancies between the two estimates which were $<20\%$ for P-PO_4^{3-} and $<40\%$ for N-NO_x, could be explained by high patchiness of nutrient distribution and by differences in assumptions made. The average PO_4^{3-} concentration in the initial cold intermediate waters mass could be higher than obtained by the measurements on 25 July–we did not have data from the deeper areas of the Tallinn Bay where below our deepest sampling points of 25–35 m PO_4^{3-} concentrations could be higher. Similarly, on 11 July just outside the Tallinn Bay below 30–40 m depth the PO_4^{3-} concentrations rose remarkably while NO_x concentrations did not. As an indication of this for PO_4^{3-} is a patch of higher concentrations observed at Stations TH1-TH9 between the depths of 15 and 20 (22.5) m on 8 August. The higher estimates of N-NO_x when using mixing arguments if compared to the estimates when actual measured concentrations were used can be explained by some uptake of nutrients. Our primary survey of the upwelling was conducted on 8 August, thus during five days from 3 to 8 August some amount of nutrients could have been used for the phytoplankton growth and if we assume the uptake was in accordance with the Redfield ratio, it should be seen more clearly in changes of N-NO_x amounts.

The uptake of nutrients is responsible also for a drop of NO_x concentrations below the detection limit and a decrease of PO_4^{3-} concentrations in the upwelling water within a week between surveys on 8 and 15 August (Figs. 3c and d and 5c–f). After the relaxation of the upwelling the surface water is depleted of inorganic nutrients. However, the question stays open: How much nutrients was left (consumed) in the upper layer and what amount was transported back down? Zhurbas et al. (2008) estimated by a model simulation of an upwelling observed in 1999 along the northern coast of the Gulf of Finland that as a result of the event 387 tons of P-PO_4^{3-} and only 36 tons of N-NO_x was introduced into the upper 10 m layer of the gulf. No nutrient uptake was included in the model and the mechanical mixing alone was responsible for nutrient retention in the upper layer. Our data suggest that for a realistic estimate of nutrient amounts channelled to the food web in the euphotic layer also nutrient uptake during the upwelling, especially for such a long event as observed in August 2006, has to be taken into account.

When estimating amounts of upwelled inorganic nitrogen compounds we have to keep in mind that only the N-NO_x measurements were included in our study as well as in the estimates by Zhurbas et al. (2008). Haapala (1994) measured NH_4^- concentrations up to 1.43 $\mu mol\,l^{-1}$ in the upwelling water. According to the marine monitoring data the NH_4^- concentrations in the lower layers of the Gulf of Finland are comparable to the NO_x concentrations and did have an increasing trend during last decades in the near-bottom layer (Pitkänen et al., 2008). Hence, in the above calculations the amounts of dissolved inorganic nitrogen brought from the lower layers during the observed upwelling event were underestimated. The fact that we did not consider NH_4^- content could also serve as a reason why a relatively larger decrease of inorganic phosphorus than that of nitrogen in relation to the Redfield ratio was observed in the upwelling water between 8 and 15 August, respectively, from 0.43 to 0.24 $\mu mol\,l^{-1}$ and from 0.59 to 0.14 $\mu mol\,l^{-1}$ on the basis of average concentrations in the upper 12 m layer at Stations TH1-TH7.

Relatively more inorganic phosphorus than nitrogen is transported into the surface layer first of all due to the low inorganic nitrogen to inorganic phosphorus ratio in the lower layer waters

of the Gulf of Finland. The separation of phosphocline and nitracline depth (Laanemets et al., 2004) is also responsible for that and in cases when upwelling waters are mostly from the layer with some PO_4^{3-} content but almost depleted of inorganic nitrogen, amounts of nutrients brought into the upper layer differ drastically (Zhurbas et al., 2008). In our study, the depths of nutriclines were only slightly separated in the southern part of the transect and the NO_x to PO_4^{3-} ratio in the upwelling water on 8 August was somewhat less than that observed below the thermocline on 25 July. After the relaxation of the upwelling event much wider separation of nutriclines at the southernmost stations was observed. The latter was a quite expected result because a week earlier the surface layer was NO_x depleted while PO_4^{3-} concentrations were still above the detection limit. Taking into account the observed separation of nutriclines on 22 August the lack of NO_x in the surface layer on 29 August when the next but less intense upwelling event has occurred was also predictable. As a conclusion, we suggest that upwelling events could markedly widen the separation of nutriclines which initially would be formed due to a difference between the spring bloom depth and the seasonal thermocline depth as proposed by Laanemets et al. (2004). Thus, a positive impact of early summer upwelling events on the development of late summer cyanobacterial blooms in the Gulf of Finland as showed by Lips and Lips (2008) could be caused by the widening of separation of nutriclines after these upwelling events which in turn will lead to relatively larger amounts of inorganic phosphorus brought into the surface layer either by vertical turbulent mixing or any transport of waters along sloping isopycnals.

Finally, we would like to stress the relatively high patchiness of nutrient distribution in the thermocline and below it (Fig. 5). The most pronounced patches were observed in the vicinity of the inclined upwelling front and they were tracked by a few water samples at 2–3 neighbouring stations between the same isopycnal surfaces while at different depths. Thus, these patches of nutrient-rich waters obviously had origin from lower layers and were brought into the study area along the sloping isopycnals. Our extensive data set confirms the suggestion by Laanemets et al. (2004) that colder and nutrient-rich waters transported along the inclined isopycnal surfaces in the northern part of the gulf could spread into the gulf's interior as intrusions due to the flow instability at the front.

6. Conclusions

The long-lasting easterly winds led to a very intense upwelling event along the southern coast of the Gulf of Finland in August 2006. We have mapped vertical distributions of temperature, salinity and nutrient concentration before, during and after the event which gave us a valuable data set to study the consequences of the upwelling on physical and chemical patterns in the Gulf of Finland. The off-shore extent of upwelling of 20 and >30 km a week later as well as its coupling with the downwelling along the opposite coast was documented. TS-analysis of profiles obtained before and during the upwelling event suggests that while welled up the cold intermediate water was mixed with the water from the upper mixed layer with a share of 85% and 15%. High nutrient concentrations were measured in the upwelled water – 0.4 μmol l^{-1} of phosphates and 0.6 μmol l^{-1} of nitrates+nitrites. We estimated the amount of nutrients transported into the surface layer as 238–290 tons of P-PO_4^{3-} and 175–255 tons of N-NO_x for a 12 m thick, 20 km wide and 100 km long coastal stretch. Taking into account a characteristic along-shore extension of the upwelling of 200 km, the phosphate-phosphorus amount is approximately equal to the average total monthly riverine load of phosphorus to the Gulf of Finland. The signs of intense vertical mixing caused by the upwelling and transport of nutrient-rich waters along the inclined isopycnal surfaces in the vicinity of the upwelling front were revealed. The upwelling event widened the separation of phosphocline and nitracline which in turn prevented surfacing of nitrate+nitrite-nitrogen during the next upwelling event observed a week after the upwelling relaxation.

Acknowledgements

This work was financially supported by the Estonian Science Foundation (Grant no. 6752) and Foundation Innove (Grant no. 1.0101-0279). Authors appreciate the help of colleagues and crew members who participated at the field measurements in the frame of this study. Special thanks to the Finnish Meteorological Institute for providing us with wind data at Kalbådagrund station and to Estonian Meteorological and Hydrological Institute for water temperature data at Pakri and Loksa stations.

References

Alenius, P., Myrberg, K., Nekrasov, A., 1998. Physical oceanography of the Gulf of Finland: a review. Boreal Environment Research 3, 97–125.
APHA, A., 1992. APHA, AWWA, and WPCF Standard Methods for the Examination of Water and Wastewater, 18th ed American Public Health Association, Washington, DC.
Fleming-Lehtinen, V., Laamanen, M., Kuosa, H., Haahti, H., Olsonen, R., 2008. Long-term development of inorganic nutrients and chlorophyll a in the open northern Baltic Sea. Ambio 37 (2), 86–92.
Fofonoff, N.P., Millard Jr., R.C., 1983. Algorithms for computation of fundamental properties of seawater. Unesco Technical Papers in Marine Science 44 58 p.
Haapala, J., 1994. Upwelling and its influence on nutrient concentration in the coastal area of the Hanko Peninsula, entrance of the Gulf of Finland, Estuarine. Coastal and Shelf Science 38 (5), 507–521.
HELCOM, 2002. Environment of the Baltic Sea area 1994–1998; background document. Baltic Sea Environment Proceedings 82B 215 p.
HELCOM, 2004. The fourth Baltic Sea pollution load compilation (PLC-4). Baltic Sea Environment Proceedings 93 188 p.
Kononen, K., Niemi, Å., 1986. Variation in phytoplankton and hydrography in the outer archipelago at the entrance to the Gulf of Finland in 1968–1975. Finnish Marine Research 253, 35–51.
Krauss, W., Brügge, B., 1991. Wind produced water exchange between the deep basins of the Baltic Sea. Journal of Physical Oceanography 21 (3), 373–384.
Laanemets, J., Kononen, K., Pavelson, J., Poutanen, E.-L., 2004. Vertical location of seasonal nutriclines in the western Gulf of Finland. Journal of Marine Systems 52 (1), 1–13.
Lehmann, A., Myrberg, K., 2008. Upwelling in the Baltic Sea – a review. Journal of Marine Systems 74 (Suppl. 1), S3–S12.
Lehtoranta, J., 2003. Dynamics of sediment phosphorus in the brackish Gulf of Finland. Monographs of the Boreal Environment Research 24 58 p.
Lentz, S.J., Chapman, D.C., 2004. The importance of nonlinear cross-shelf momentum flux during wind-driven coastal upwelling. Journal of Physical Oceanography 34 (11), 2444–2457.
Leppäranta, M., Myrberg, K., 2009. Physical Oceanography of the Baltic Sea. Praxis Publishing Ltd., Chichester, UK.
Lips, I., 2005. Abiotic factors controlling the cyanobacterial bloom occurrence in the Gulf of Finland. Dissertationes Biologicae Universitatis Tartuensis 108 47 p.
Lips, I., Lips, U., 2008. Abiotic factors influencing cyanobacterial bloom development in the Gulf of Finland (Baltic Sea). Hydrobiologia 614, 133–140.
Lips, U., Pitkänen, H., Poutanen, E.-L., Kauppila, P., Basova, S., 2002. Hydrochemistry of the Gulf of Finland. In: Environment of the Baltic Sea area 1994–1998. Baltic Sea Environment Proceedings 82B, pp. 76–78.
Myrberg, K., Andrejev, O., 2003. Main upwelling regions in the Baltic Sea – a statistical analysis based on three-dimensional modelling. Boreal Environment Research 8 (2), 97–112.
Pitkänen, H., Lehtoranta, J., Räike, A., 2001. Internal nutrient fluxes counteract decreases in external load: the case of the estuarial eastern Gulf of Finland, Baltic Sea. Ambio 30 (4), 195–201.
Pitkänen, H., Lehtoranta, J., Peltonen, H., 2008. The Gulf of Finland. In: Schiewer, U. (Ed.), Ecology of Baltic Coastal Waters. Ecological Studies, vol. 197. Springer, Berlin Heidelberg, pp. 285–308 Chapter 13.

Smith, V.H., Tilman, G.D., Nekola, J.C., 1999. Eutrophication: impacts of excess nutrient inputs on freshwater, marine, and terrestrial ecosystems. Environmental Pollution 100 (1–3), 179–196.

Suursaar, Ü., Aps, R., 2007. Spatio-temporal variations in hydro-physical and -chemical parameters during a major upwelling event off the southern coast of the Gulf of Finland in summer 2006. Oceanologia 49 (2), 209–228.

Uiboupin, R., Laanemets, J., 2009. Upwelling characteristics derived from satellite sea surface temperature data in the Gulf of Finland, Baltic Sea. Boreal Environment Research 14, 297–304.

Vahtera, E., Laanemets, J., Pavelson, J., Huttunen, M., Kononen, K., 2005. Effect of upwelling on the pelagic environment and bloom-forming cyanobacteria in the western Gulf of Finland, Baltic Sea. Journal of Marine Systems 58 (1–2), 67–82.

Zhurbas, V., Laanemets, J., Vahtera, E., 2008. Modeling of the mesoscale structure of coupled upwelling/downwelling events and related input of nutrients to the upper mixed layer in the Gulf of Finland, Baltic Sea. Journal of Geophysical Research 113, C05004, doi:10.1029/2007JC004280 1–8.

Paper IV

Lips, Urmas; Lips, Inga; Liblik, Taavi; Elken, Jüri (2008). Estuarine transport versus vertical movement and mixing of water masses in the Gulf of Finland (Baltic Sea). US/EU-Baltic Symposium "Ocean Observations, Ecosystem-Based Management & Forecasting", Tallinn, 27-29 May, 2008. IEEE, 2008, (IEEE Conference Proceedings), 1 - 8.

Estuarine Transport *versus* Vertical Movement and Mixing of Water Masses in the Gulf of Finland (Baltic Sea)

Urmas Lips, Inga Lips, Taavi Liblik and Jüri Elken
Marine Systems Institute, Tallinn University of Technology
Akadeemia tee 21
12618 Tallinn, Estonia

Abstract- **Weekly mapping of vertical temperature and salinity fields was carried out across the Gulf of Finland in summer 2006 and spring 2007. Using successive cross-gulf vertical sections of salinity and wind data from the region the variations of estuarine and transverse circulation are described. Changes of deep layer phosphate-phosphorus concentrations are found to be related to the described variations in circulation patterns in a season with strong vertical stratification of water column. Cumulative volume transport estimates were obtained using the results of a 3D baroclinic circulation model (HIROMB). We suggest that the north-easterly winds, which intensify the estuarine circulation and lead to the upwelling events along the southern coast of the Gulf of Finland, could have a major impact to the Gulf's ecosystem by importing more saline and phosphorus rich waters. These events with many-fold more intense upward movement and mixing of deep waters (upward diapycnal transport) could contribute significantly to the ventilation of deep layers of the northern Baltic Proper.**

INTRODUCTION

The Gulf of Finland is a 400-km long and 80-120-km wide elongated sub-basin of the Baltic Sea. It has no sill at the entrance area separating the Gulf from the open Baltic Sea and its maximum cross-section depth decreases from > 100 m at the entrance to < 30 m in the eastern part. Since the main fresh-water source – the Neva River – is located in the easternmost end of the Gulf the salinity distribution in the surface layer is characterized by an increase from 1-3 in the east to 6 (psu) in the west [1,2]. Below the seasonal thermocline salinity increases slowly with the depth and the permanent halocline exists at the depths of 60-70 m in the deeper areas of the Gulf. Seasonal thermocline develops in spring-summer at the depths of 10-20 meters.

General residual circulation in the Gulf of Finland is typical for stratified and wide estuaries. Landward flow dominates in the lower layer and along the southern coast while seaward flow dominates in the upper layer and along the northern coast. [3]. Along-gulf (along-channel) winds force a cross-gulf flow in the upper layer that leads to coupled upwelling-downwelling events in the coastal areas and associated vertical movements of thermocline and halocline as well as vertical mixing of water masses.

Eutrophcation is considered as one of the most important environmental problems of the Gulf of Finland. To be able to suggest adequate measures for reduction of nutrient inputs from land the governing processes and fluxes in the sea itself must be understood and modeled. Nutrient budgets of seven sub-basin of the Baltic Sea, including Gulf of Finland, have been constructed by Shavchuk [4]. It has been estimated that about $14.0 * 10^3$ tons of phosphorus (P) is imported to the Gulf from the Baltic Proper and $12.7 * 10^3$ tons of P is exported annually. However in that study internal load from the bottom sediments in the Gulf of Finland [5,6] was not taken into account. Some other studies (e.g. [6,7]) have estimated much higher net import of phosphorus from the open Baltic Proper – up to 7800 tons annually. These very different estimates show that understanding of dynamics of estuarine circulation and quantification of related nutrient transports is one of the keys for building the nutrient budget of the Gulf of Finland.

Wind-dependent variation of estuarine transport in the Gulf of Finland has been studied by Elken et al. [8]. A simple formula for estimating volume transport in the layer below 40 m on the basis of wind data has been introduced and a reversal of estuarine circulation caused by strong south-westerly winds was reported. Similar effects of reversal of estuarine transport has been documented or modeled by other authors [9]. The role of vertical turbulent mixing mainly related to tides and related fortnightly fluctuations in residual estuarine circulation has been shown in several studies (e.g. [10]). In many cases the estuarine circulation reveals seasonal variation caused by seasonality in wind field, fresh water inflow from rivers or buoyancy flux through the sea surface (e.g. [11]).

The main aim of the present paper is to show that the volume transport and corresponding salt and phosphorus fluxes in the deep layer reveal variations in accordance with the variations in wind speed and direction. Our main hypothesis is that the north-easterly winds, which intensify the estuarine circulation and lead to the upwelling events along the southern coast of Gulf of Finland, have a major impact to the pelagic ecosystem of the Gulf as well as to the water and material transport in the whole Baltic Sea. These processes transport more saline and phosphorus rich waters to the Gulf, and due to the many-fold more intense upward movement and mixing of deep waters (upward diapycnal transport) ventilate the deep layers of the northern Baltic Proper.

978-1-4244-2268-5/08/$25.00 ©2008 IEEE

MATERIAL AND METHODS

A. Measurements

Field measurement campaigns were conducted in two successive years – 2006 and 2007 – in the sea area between Tallinn and Helsinki (see Fig. 1). In 2006 six surveys along a transect of 27 stations were carried out from 11 July until 29 August. In 2007 the measurements were conducted 7 times along the same transect with some westward positions of Stations TH24-TH27 in spring from 26 April to 7 June. At all stations vertical profiles of temperature, salinity and chlorophyll *a* fluorescence (not presented here) were recorded. Water samples for phytoplankton chlorophyll *a* content, biomass and species composition (not presented here), and chemical analyses were collected at every second station. One survey consisting of 27 stations was completed within 12-16 hours.

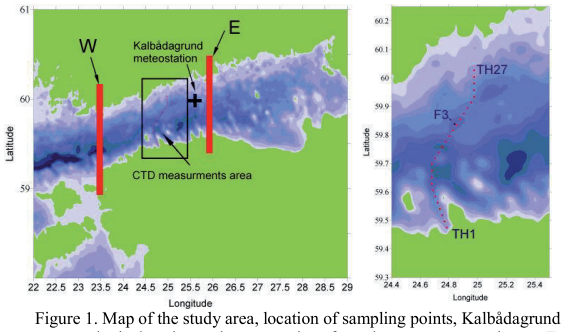

Figure 1. Map of the study area, location of sampling points, Kalbådagrund meteorological station and cross-sections for volume transport estimates E and W.

Temperature and salinity profiles were recorded using Neil Brown Mark III CTD probe and SeaBird Electronics Ltd CTD probe SBE 19. Temperature and salinity values obtained using both probes were compared, and water samples were taken and analyzed using high precision salinometer to control the performance of temperature and conductivity sensors of probes. In this study mainly Neil Brown Mark III data preliminary processed and interpolated into profiles with a vertical resolution of 0.5 m are used.

Samples for analyses of phosphate-phosphorus content were collected from the near bottom layer. Because of complicated bottom topography in the study area and drifting of research vessel while working at the stations and taking water samples the sampling depths were not constant at a particular station throughout the study period and water depths as well as distances from the bottom for samples have to be taken into account when analyzing the results. Analyses of phosphate-phosphorus concentration were conducted with MicroMAC 1000 (Systea S.r.l.) partly onboard and partly in on-shore laboratory. In latter case, the samples were kept deep frozen.

Wind data from Kalbådagrund meteorological station located in the northern part of the Gulf, eastward from the cross-section (Fig. 1), were obtained from the Finnish Meteorological Institute. Wind speed and direction with a time step of 3 hours were used for calculations within this study.

Estimates of the wind induced Ekman drift in the surface layer were obtained by standard quadratic formula. The following values of drag coefficient c_D = 1.2 10^{-3} and air density ρ_a = 1.2 kg m^{-3} were used. Direction of the Ekman transport in the surface layer was obtained by rotating wind stress vector 90 degrees to the right.

Wind-dependent landward volume transport in the deep layer below 40 m depth was estimated using a formula derived by Elken et al. [8]. It was assumed that the deep layer flow is driven by the cross-gulf sea level difference, which was created by the north-easterly or south-westerly winds. We note that in [8] wind data from Utö meteorological station were used to get the best fit between estimates by this simple formula and 3D model results. Utö is located in the entrance area to the Gulf of Finland but in the present study the data from Kalbådagrund were used.

B. Model results

The time series of vertical profiles of temperature and salinity at a grid point closest to the monitoring station F3 (close to the Station 18, see Fig. 1) have been extracted daily from the operational oceanographic model HIROMB (High Resolution Operational Model for the Baltic Sea). The core of the model system is a 3D baroclinic circulation model that calculates currents, temperature, salinity and turbulence in the water column. The model domain covers the whole Baltic Sea area with grid steps 1' by latitude and 5/3' by longitude and has 16 vertical layers [12].

Cumulative volume transports through 2 different cross-sections of the Gulf (see Fig. 1; sections W and E) were estimated using modeled currents, separately in the surface layer (from sea surface to 30 m depth) and in the deep layer (below 30 m).

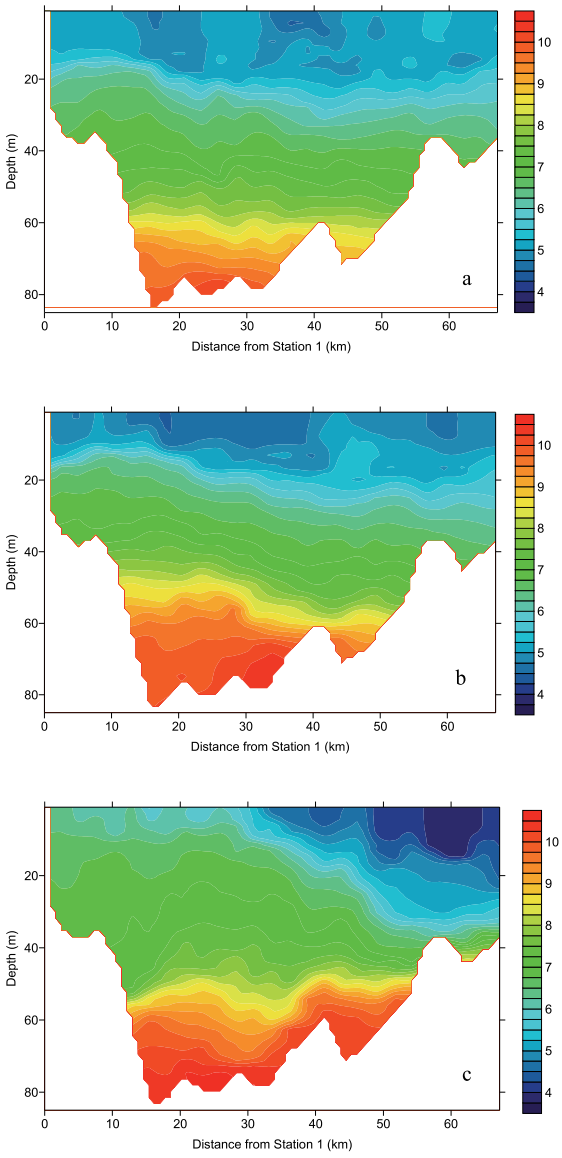

Figure 2. Vertical sections of salinity along the study transect on 11 July, 25 July and 15 August 2006.

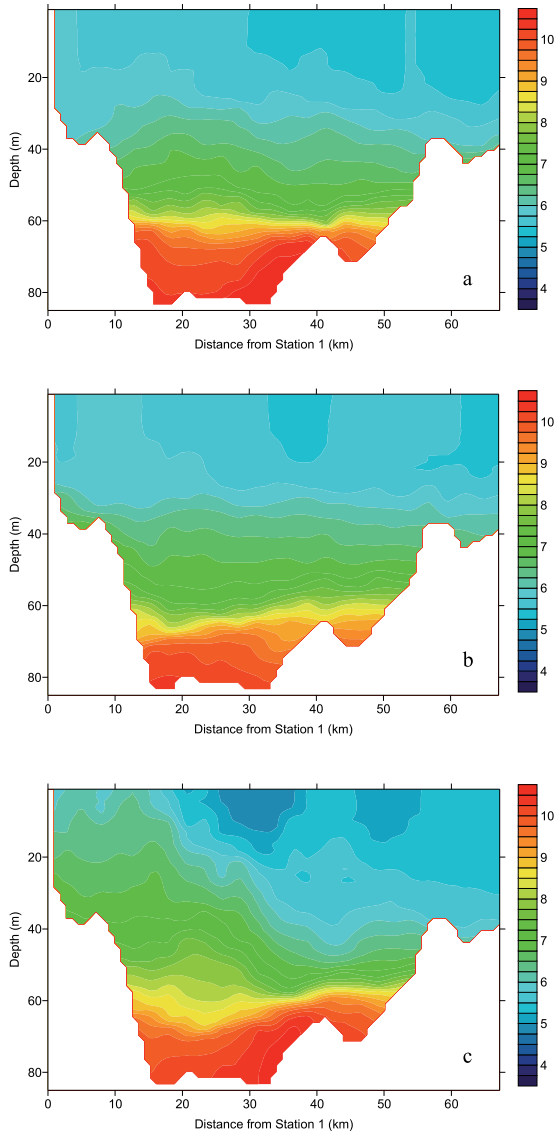

Figure 3. Vertical sections of salinity along the study transect on 10 May, 24 May and 7 June 2007.

RESULTS

A. *Vertical sections of salinity in July-August 2006*

Vertical structure of temperature, salinity and density fields were quite variable in the central part of the Gulf of Finland in July-August 2006 depending on the wind forcing. An ordinary temperature distribution with the seasonal thermocline at the depths of 10-20 m was observed in July while a major upwelling event caused by long-lasting easterly winds was observed near the southern coast in August [13]. In the beginning of the study period, the salinity distribution was characterized by salinity values of 4.5 to 5.5 in the upper 20-m layer and with a continuous increase of salinity with the depth below that (Fig. 2a). Halocline was situated at the depths below 60 meters on 11 July.

A remarkable increase of salinity in the deep layers of the gulf was observed in the second half of July when northerly – north-westerly winds prevailed (Fig. 2b) and during the pronounced and dynamic upwelling event in August (Fig. 2c). The observed changes of salinity in the deep layer had a distinguished transverse structure – between surveys on 11 and 25 July an upward shift of halocline occurred in the southern and central parts of the cross-section while during the upwelling event the halocline rose near the northern slope and dropped near the southern slope. In the surface layer the most pronounced transverse structure was observed in August when more saline waters occupied the southern part of the Gulf and low salinity waters were pushed toward the northern shore and the layer itself was deepened. This structure corresponds to the upwelling along the southern coast and associated downwelling along the northern coast.

B. *Vertical sections of salinity in April-June 2007*

Vertical structure and variations of temperature, salinity and density fields in the study area in April-June 2007 were typical for the spring season. Salinity distribution was characterized by a low salinity surface layer with the thickness of about 30 meters, a continuous increase of salinity with the depth below 30 m and a relatively sharp halocline at the depths of 60-70 meters (Fig. 3). If compared with the vertical salinity distribution in July-August 2006, then significantly thicker surface layer with clearly higher salinity values was observed in spring 2007. A relatively thick high-salinity deep layer observed on 10 May (Fig. 3a) was lowered and halocline was weakened before the survey on 24 May (Fig. 3b).

An upwelling event caused by easterly winds was observed near the southern coast on 7 June 2007 (Fig. 3c). The transverse structure in the surface and intermediate layer was characterized by more saline waters reaching the sea surface and elevated positions of isolines in the southern part of the Gulf. A low salinity water jet appeared close to the salinity front separating the upwelled waters from the surface layer waters. A downwelling was observed near the northern coast of the Gulf.

Salinity distribution in the deep layer on 7 June was characterized by the transverse structure as well but with an opposite horizontal salinity gradient. The halocline was elevated near the northern slope while the vertical salinity gradient was significantly decreased in the southern part of the deep region.

C. *Wind-dependent transport estimates and observed temporal changes of salinity and phosphate-phosphorus content*

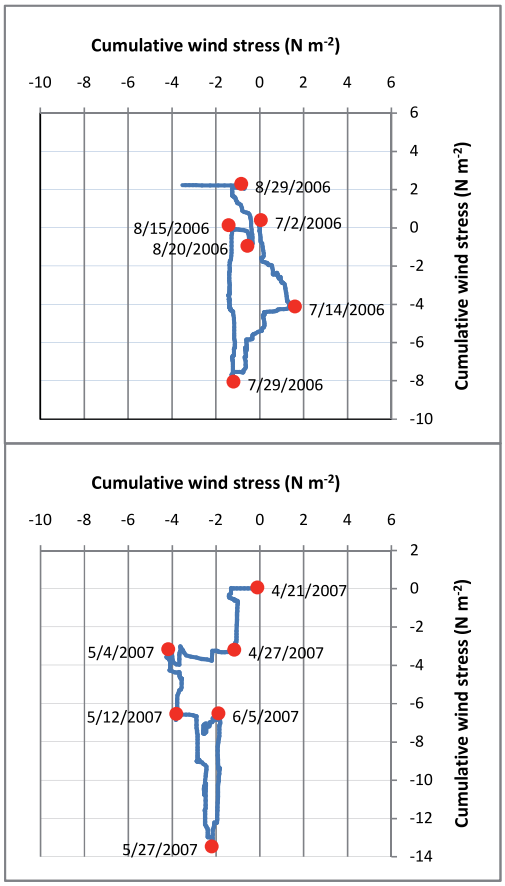

Figure 4. Estimates of surface layer Ekman transport using Kalbådagrund wind data in July-August 2006 and April-June 2007. Wind stress vector is turned 90º to the right; positive direction of x-axis corresponds to the eastward and positive direction of y-axis to the northward Ekman transport.

Cumulative wind stress estimates rotated by 90º to the right (to point to the direction of the Ekman transport in the surface layer; see Fig. 4) indicate that cross-gulf (cross-channel) drift flows occur in the study area more frequently than along-gulf flows, at least according to wind data from Kalbådagrund.

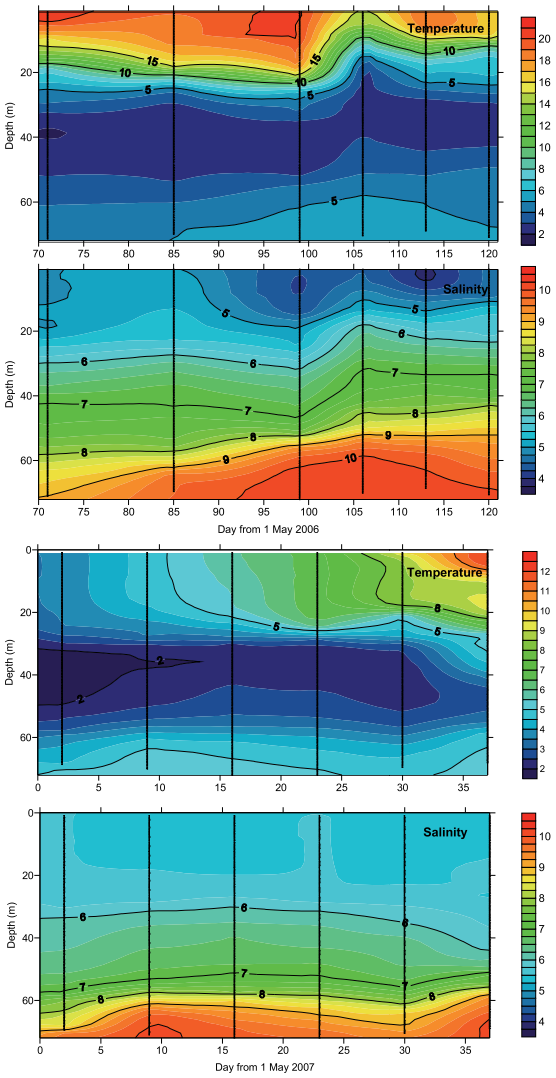

Figure 5. Temporal changes of vertical temperature and salinity distribution at Station TH18 (see Fig. 1) in July-August 2006 and April-June 2007.

In July-August 2006 periods with a southward drift flow in the surface layer were observed in the beginning of July until 14 July and from 15 August to 20 August. A two-week period in the second half of July from 14 July to 29 July was characterized by outflow favorable winds. In the rest of study period a northward Ekman flow was dominating with a very strong cross-gulf surface layer transport within two weeks starting from 29 July.

During the study period in 2007 mainly southward drift flow dominated in the area. Only two shorter periods with different flow directions were observed. Wind induced outflow occurred in the surface layer from 27 April to 4 May. A northward Ekman transport in the surface layer favorable for upwelling along the southern coast occurred from 27 May until 5 June 2007.

Vertical temperature and salinity distributions at Station TH18 in the central gulf (Fig. 5) revealed temporal changes well corresponding to the described wind dependent flow structure in the area. In July-August 2006 salinity (and temperature) started to increase in the deep layer during the period of dominating outflow in the surface layer when north-westerly winds prevailed (after 14 July). During the upwelling event, when easterly and north-easterly winds prevailed salinity and temperature continued to increase. In the surface layer of the central gulf a water mass with very low salinity (< 4) appeared indicating to an outflow jet there. An exception was the survey on 15 August when an upwelling filament was observed at Station 18.

In 2007 salinity in the deep layer increased during mentioned two periods when outflow occurred in the surface layer in the beginning of May and during the upwelling event along the southern coast in the beginning of June. In between salinity in the deep layer dropped slightly in accordance to suggested reversal of estuarine circulation due to prevailing westerly – south-westerly winds.

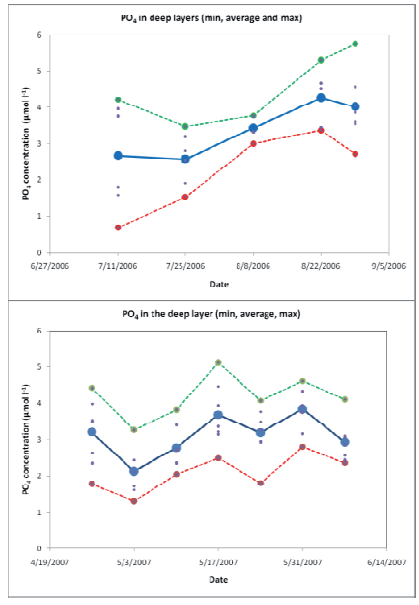

Figure 6. Temporal changes of phosphate-phosphorus content in the deep layer of the central Gulf of Finland in July-August 2006 and April-June 2007

Phosphate-phosphorus concentrations in the deep layer followed generally the described flow structure in July-August 2006. When estuarine circulation was intensified due to the favorable winds the average PO_4 concentration rose simultaneously with increase of salinity. In spring 2007 when summer stratification was not well developed yet the variations of phosphate-phosphorus concentration were not well correlated to the changes of deep layer salinity.

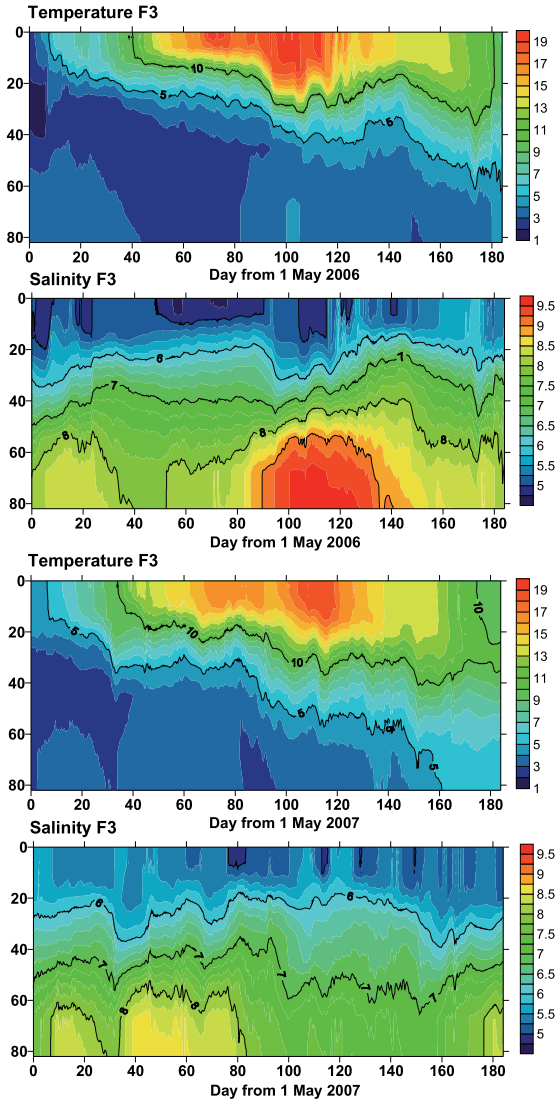

Figure 7. Temporal changes of vertical temperature and salinity distribution in the central gulf (station F3, see Fig. 1) in the basis of 3D modeling results in May-September 2006 and 2007.

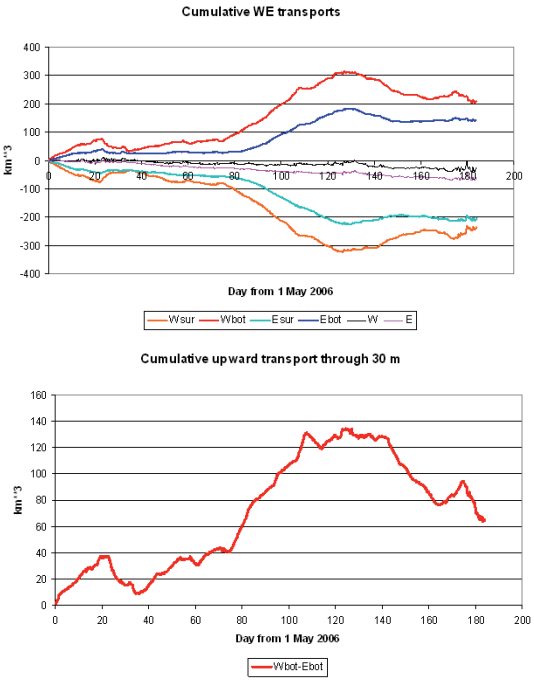

Figure 8. Cumulative west-east transport in the deep layer of the Gulf through the sections W and E (see Fig. 1) and cumulative upward transport through 30-m level from 1 May 2006.

D. *Model results: temporal changes in salinity field and transport estimates*

Variations of vertical profiles of temperature and salinity in the central area of the Gulf of Finland according to model results (Fig. 7) showed a quite well coincidence with the measurement results (Fig. 5). The same increase of salinity in the deep layer was evident from the model in the second half of July and August 2006. Lower absolute values of salinity comparing to the measurements were obtained in the deep layer of the Gulf in April-June 2007 from the model output. However the changes – an increase of salinity in the beginning of May followed by a decrease and next increase in the beginning of June – were qualitatively coinciding with the measurement results.

Cumulative volume transports through two cross-sections of the Gulf of Finland (see Fig. 1) were estimated on the basis of current velocities extracted from the model outputs daily. These results show very clearly that a major event of intensification of estuarine circulation occurred in the study area in the second half of July – August 2006 (Fig. 8). Cumulative volume transport through the western section was estimated up to 200 km^3 during this 6-week period. Since transport values through the eastern section were much lower (but still quite high) the rest of the volume had to be transported back to the Baltic Proper as a surface layer flow. Estimates of cumulative upward transport of waters from below 30-m depth to the surface layer were obtained for this 6-week period as high as 90 km^3 – cumulative transport increased from 40 km^3 to 130 km^3.

Similar estimates for the study period in 2007 revealed much lower volume transport values. Cumulative volume transport curve revealed a maximum of 130 km^3 in June but for the period from 1 May to 31 August the resulting value was only 80 km^3. For comparison the same period in 2006 had a cumulative volume transport in the deep layer about 320 km3. Cumulative upward transport for the whole season in 2007 was close to zero. The upwelling event in the beginning of June gave an upward volume flux of 40 km^3.

DISCUSSION AND CONCLUSIONS

Time series of vertical sections of salinity in general and time series of vertical profiles at a central station were in a good agreement with the estimates of Ekman transport in the surface layer and directions of associated compensating flow in the deep layer of the Gulf of Finland. However, estimates of Ekman transport indicated that cross-gulf (cross-channel) drift flows occur more frequently than along-gulf flows that is in accordance with earlier studies in regard of upwelling statistics [14]. Since the cross-channel wind stress creates also cross-channel sea level gradients, the resulting flow patterns relative to wind direction and Ekman transport are more complex. For the section at the Gulf of Finland entrance, Elken et al. [8] have estimated that maximum inflow takes place in deep layers during northeasterly winds but in the central gulf such estimates are missing. We have showed that both north-westerly and north-easterly winds lead to the increase of salinity in the deep layer of the central gulf, and suggest that this is because of intensified estuarine circulation under these conditions. North-easterly winds initiate directly the seaward drift flow in the upper layer, which is compensated by the landward flow in the deep layer. North-easterly winds create a sea level difference which in turn causes an inflow in the lower layer.

Vertical sections of salinity revealed also that distinct transverse structures exist in the salinity distribution when cross-gulf drift flows dominate in the surface layer. Northward Ekman transport force an upwelling to appear along the southern coast and downwelling along the northern coast. Halocline behaves in an opposite manner – it lifts up near the northern slope and goes deeper near the southern slope. Our conclusion is that the deep layer has a very clear opposite response to the wind forcing and distinct vertical separation of flows should exist in the Gulf of Finland.

The present study supports the earlier findings that wind forcing is a very important factor affecting the estuarine circulation in stratified wide estuaries (e.g. [11]). The results suggest that intensification of estuarine circulation due to the long-lasting north-easterly winds could have a major influence on the pelagic ecosystem in the Gulf of Finland. Imported more saline water in the deep layer has higher phosphorus concentration than the waters flowing out of the gulf in the surface layer.

Estimates of cumulative volume transport through two cross-sections in the gulf and resulting upward volume transport (by upwelling and associated vertical mixing) between these cross-sections gave rise to the other important suggestion. Since upward transport is many-fold more intense in case of long-lasting easterly–north-easterly winds, in comparison to usually prevailing westerly–south-westerly winds, these processes under described conditions could contribute significantly to the ventilation of deep layers of the northern Baltic Proper.

ACKNOWLEDGMENT

This study was supported by the Estonian Science Foundation, grants No. 6752, 6955 and 7328. The wind data were provided by the Finnish Meteorological Institute. We thank colleagues and crews of research vessels participated in the measurement campaigns as well as HIROMB consortium partners.

REFERENCES

[1] P. Mälkki and R. Tamsalu, R., "Physical features of the Baltic Sea.", *Finn. Mar. Res.*, 252, 110 pp, 1985.

[2] J. Haapala and P. Alenius, "Temperature and salinity statistics for the northern Baltic Sea 1961–1990", *Finn. Mar. Res.* 262, pp. 51–121, 1994.

[3] O. Andrejev, K. Myrberg, P. Alenius and P. Lundberg. “Mean circulation and water exchange in the Gulf of Finland - a study based on three-dimensional modeling”, *Boreal Env. Res.,* 6, pp. 1-16, 2004.

[4] O. Savchuk. “Resolving the Baltic Sea into seven subbasins: N and P budgets for 1991-1999.”, *J. Mar. Systems,* 56, pp. 1-15, 2005.

[5] M. Kiirikki, J. Lehtoranta, A. Inkala, H. Pitkänen, S. Hietanen, P. Hall, A Tenberg, J. Koponen and J. Sarkkula. “A simple sediment process description suitable for 3D-ecosystem modelling - Development and testing in the Gulf of Finland”, *J. Mar. Systems,* 61, pp. 55-66, 2006.

[6] H. Pitkänen, J. Lehtoranta and A. Räike, “Internal nutrient fluxes counteract decreases in external load: the case of the estuarial eastern Gulf of Finland, Baltic Sea,” *Ambio*, 30, pp. 195-201, 2001.

[7] M. Perttilä, L. Niemistö and K. Mäkelä, “Distribution, development and total amounts of nutrients in the Gulf of Finland”, *Estuar. Coast. Shelf Sci.* 41, pp. 345-360, 1995.

[8] J. Elken, U. Raudsepp and U. Lips, “On the estuarine transport reversal in the deep layers of the Gulf of Finland”, *J. Sea Res.,* 49, pp. 267-274, 2003.

[9] X. A. Alvarez-Salgado, J. Gago, B. M. Miguez, M. Gilcoto, and F. F. Perez, ”Surface Waters of the NW Iberian Margin: Upwelling on the Shelf versus Outwelling of Upwelled Waters from the Rias Baixas.”, - *Estuar. Coast. Shelf Sci.*, 51, pp. 821-837, 2000.

[10] D. A. Griffin and P. H. LeBlond, “Estuary/ocean exchange controlled by spring-neap tidal mixing”, *Estuar. Coast. Shelf Sci.*, 30, pp. 275-297, 1990.

[11] R. E. Thomson, S. F. Mihaly and E. A. Kulikov, “Estuarine versus transient flow regimes in Juan de Fuca Strait”, *J. Geophys. Res.,* 112, C09022, 2007.

[12] A. Jönsson, “Status of operational HIROMB”, *7th HIROMB-Scientific Workshop, December 7-9, 2004 in Helsinki, http://www.environment.fi/ download.asp? contentid=28920&lan=en*, 2004.

[13] I. Lips, U. Lips, T. Liblik and N. Kuvaldina “Consequences of summer upwelling events on hydrophysical and biogeochemical patterns in the western Gulf of Finland (Baltic Sea)”, 2008, manuscript.

[14] K. Myrberg and O. Andrejev, “Main upwelling regions in the Baltic Sea – a statistical analysis based on three-dimensional modeling,” *Boreal Environ. Res.*, vol. 8, pp. 97-112, 2003.

.

Paper V

Lips, Urmas; Lips, Inga; Liblik, Taavi; Kikas, Villu; Altoja, Kristi; Buhhalko, Natalja; Rünk, Nelli (2011). Vertical dynamics of summer phytoplankton in a stratified estuary (Gulf of Finland, Baltic Sea). Ocean Dynamics, 61, 903 - 915.

Ocean Dynamics (2011) 61:903–915
DOI 10.1007/s10236-011-0421-8

Vertical dynamics of summer phytoplankton in a stratified estuary (Gulf of Finland, Baltic Sea)

Urmas Lips · Inga Lips · Taavi Liblik · Villu Kikas · Kristi Altoja · Natalja Buhhalko · Nelli Rünk

Received: 30 September 2010 / Accepted: 31 March 2011 / Published online: 20 April 2011

Abstract We present the results of multiparametric observations designed to follow the phytoplankton dynamics and interrelated physical, chemical and biological processes in the Gulf of Finland (Baltic Sea). Data were acquired by an autonomous moored water column profiler, an acoustic Doppler current profiler, a flow-through system installed aboard a ferry and by profiling and discrete water sampling aboard research vessels in July and August 2009. The main aim of the study was to investigate the processes responsible for the formation and maintenance of sub-surface maxima of phytoplankton biomass. We suggest that the environmental conditions caused by the prevailing atmospheric and oceanographic forcing (wind; vertical stratification; basin-wide, mesoscale and sub-mesoscale processes) are preferred by certain species/taxonomic groups and explain the migration patterns of phytoplankton. Nocturnal downward migration of phytoplankton with a swimming speed up to 1.6 mh^{-1} occurred when the community was dominated by the dinoflagellate *Heterocapsa triquetra*. The observed splitting of the population into two vertically separated biomass maxima suggests that the *H. triquetra* cells, which reached the sub-surface layers with high nutrient concentrations, experienced bi-diurnal or asynchronous (when swimming upwards) vertical migration. The most intense sub-surface biomass maxima, on some occasions with the biomass much higher than that in the surface layer, were detected in connection to the sub-mesoscale intrusions below the depth of the strongest vertical density gradient.

Keywords Phytoplankton dynamics · Stratification · *Heterocapsa triquetra* · Vertical migration · Autonomous profiler · Gulf of Finland

Responsible Editor: Aida Alvera-Azcárate

This article is part of the Topical Collection on *Multiparametric observation and analysis of the Sea*

U. Lips (✉) · I. Lips · T. Liblik · V. Kikas · K. Altoja · N. Buhhalko · N. Rünk
Marine Systems Institute, Tallinn University of Technology, Akadeemia Rd. 15A,
12168 Tallinn, Estonia
e-mail: urmas.lips@phys.sea.ee

1 Introduction

The Gulf of Finland is a stratified and wide estuary with considerable fresh water inflow at the eastern end and relatively open water exchange with the Baltic proper through the gulf's western boundary. In April–May, a seasonal thermocline begins to form, and during the productive season, the Gulf is strongly stratified. The upper mixed layer depth is typically 10–20 m, and temperature drops in summer from about 15–20°C at the top of the thermocline to about 2–4°C in the cold intermediate layer. Estuarine circulation is characterized by an inflow into the Gulf in the deeper layers and an outflow in the surface layer; however, depending on the prevailing winds, the circulation pattern might be reversed (Elken et al. 2003). Residual circulation in the surface layer consists of an outflow of gulf water in the northern part and an inflow of open Baltic Sea water to the southern part of the Gulf (Alenius et al. 1998).

The seasonal dynamics of nutrient concentrations in the surface layer of the Gulf of Finland is characterized by a maximum in winter and a minimum in summer. After the spring bloom, in the middle of May, the euphotic layer becomes depleted of dissolved inorganic nitrogen (DIN). Dissolved inorganic phosphorus (DIP) concentration usu-

ally reaches a minimum in late June–early July before the late summer bloom that is dominated by cyanobacteria or, in some years, by the dinoflagellate *Heterocapsa triquetra* (Ehrenberg) Stein (Kononen et al. 1996; HELCOM 2002).

The wind-driven circulation in the Gulf of Finland is highly variable and characterized by intense mesoscale features—eddies, upwelling/downwelling and coastal and frontal jet currents. Upwelling events cause substantial vertical nutrient transport (Zhurbas et al. 2008; Lips et al. 2009) and influence the phytoplankton dynamics in the upper layer in the Gulf of Finland (Vahtera et al. 2005; Lips and Lips 2010). The upward transport of nutrients from below the seasonal thermocline could create favourable conditions for the growth of nitrogen-fixing cyanobacteria due to the low DIN/DIP ratio in the upwelled waters. Furthermore, any vertical mixing could support the growth of cyanobacteria, since the phosphacline is usually located in the upper part of the seasonal thermocline (Laanemets et al. 2004). Less attention has been paid to downwelling events, although they are associated with the horizontal convergence of waters and substances that could lead to vertical transport and mixing and, for instance, to support the formation of sub-surface phytoplankton biomass maxima (Lips et al. 2010).

Earlier studies in the Gulf of Finland carried out during the late summer phytoplankton bloom have mostly dealt with cyanobacteria (Kononen et al. 1996; Kanoshina et al. 2003; Lips and Lips, 2008). A few studies only have investigated the dynamics of communities dominated by cyanobacteria/dinoflagellates (e.g. Kononen et al. 2003) or the dynamics of the whole phytoplankton community (e.g. Lips and Lips 2010). The co-dominance of functionally different phytoplankton species (*Aphanizomenon* sp. (L.) Ralfs and *H. triquetra*) in the summer community in the upper layer has been explained by Kononen et al. (2003) by the dynamic hydrographic field and species-specific adaptation to water movements.

The sub-surface maxima of phytoplankton biomass, among them the relatively deep biomass maxima of *H. triquetra*, have been observed in the Gulf of Finland in summer (e.g. Pavelson et al. 1999; Kononen et al. 2003). In July 2006, sub-surface chlorophyll *a* (Chl *a*) maximum layers with thicknesses varying between 1.5 and 9 m and an intensity up to 7.6 mg m^{-3} were observed in the lower part of the seasonal thermocline within the depth range of 14.5 to 35 m (Lips et al. 2010). Nutrient analyses of water samples collected from the thermocline revealed the coincidence of the location of Chl *a* maxima and nutriclines. However, until 2009, continuous/high-resolution vertical profiling data were not available for the Gulf of Finland, and we did not have observational evidence of the formation of sub-surface biomass maxima by vertical migration of phytoplankton.

Studies of sub-surface maxima of phytoplankton biomass or "thin layers" have been carried out in many coastal regions of the world, for example, in Monterey Bay (e.g. Sullivan et al. 2010) and in Ria de Pontevedra (Velo-Suarez et al. 2010). The conditions in these coastal ocean regions and in our study area differ due to the relatively turbid waters in the Gulf of Finland and occurrence of sub-surface phytoplankton maxima (dominated by *H. triquetra*) in the water layer below the euphotic depth. However, many questions are common to the studies of sub-surface biomass maxima at all sites, such as, is it possible to explain the formation and maintenance of maxima mainly by physical processes, and what is the role of vertical migration due to different physiological states of the phytoplankton cells?

The main motivation of the present study was to show that knowledge of the links between phytoplankton dynamics and meteorological and oceanographic forcing can be improved by using high-resolution autonomous in situ observations. We aimed to define more precisely the physical, chemical and biological processes responsible for the formation of sub-surface maxima of phytoplankton biomass in the Gulf of Finland.

2 Materials and methods

A multiparametric observation program was designed to follow the phytoplankton dynamics and interrelated physical, chemical and biological processes in the Gulf of Finland (Baltic Sea) in the summer, 2009. The measurements were performed using an autonomous moored water column profiler, a bottom mounted acoustic Doppler current profiler (ADCP), an autonomous system installed aboard a ferry (Ferrybox system) and measurement and sampling devices aboard the research vessel SALME and hydrographic vessel EVA-318. The data collected with the autonomous systems were transferred via mobile phone network immediately after every profiling from the buoy station and once a day from the ferry. The operational data gathering enabled us to perform additional measurements and sampling aboard the research vessel within the periods of special interest.

The autonomous profiler (Idronaut S.r.l.; surface buoy designed by Flydog Solutions Ltd.) was deployed in the Gulf of Finland from 30 June to 28 August in a sea area with a bottom depth of 86 m (see location in Fig. 1). Vertical profiles of temperature, salinity and Chl *a* fluorescence in the water layer from 2 to 45 (50) m were acquired with a time resolution of 3 h and a vertical resolution of 10 cm. Measurements were conducted using an Ocean Seven 316*plus* CTD probe (Idronaut S.r.l.) equipped with a Seapoint Chl *a* fluorometer. An ADCP (Teledyne RDI, 300 kHz) was deployed close to the buoy

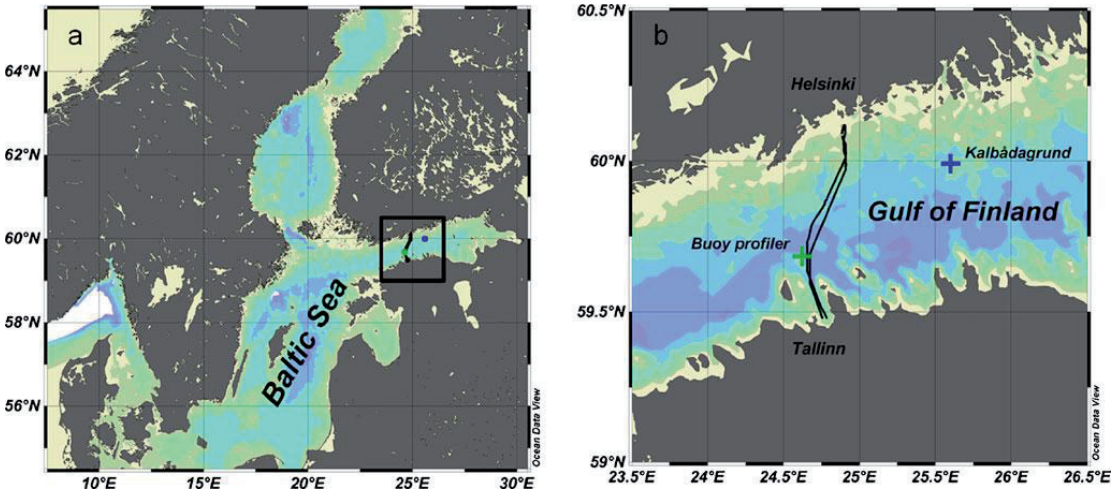

Fig. 1 Map of the Baltic Sea (**a**) and observation sites in the Gulf of Finland (**b**) where locations of moored profiler and ADCP (*green cross*), ferry track from Tallinn to Helsinki and back (*solid curves*) and Kalbådagrund meteorological station (*blue cross*) are shown. Maps are created using ODV software (Shlitzer 2010)

profiler from 23 July until 24 September to measure flow structure in the whole water column with a vertical resolution of 2 m.

The Ferrybox system installed aboard the passenger ferry "Baltic Princess" (AS Tallink Group) travelling between Tallinn and Helsinki was used for measurements and sampling in the surface layer. Water intake was located approximately at 4 m depth. Temperature, salinity and Chl *a* fluorescence were recorded along the ferry route (Fig. 1) twice a day with a time resolution of 20 s corresponding approximately to a spatial resolution of 150 m. Water sampling at 17 locations distributed evenly along the ferry route was conducted on 5, 12 and 19 July and 2, 9 and 23 August. The collected water samples were analysed for Chl *a* content and phytoplankton species composition and biomass.

CTD measurements using an Ocean Seven 320*plus* CTD probe (Idronaut S.r.l.) equipped with a Seapoint Chl *a* fluorometer and water sampling aboard the research vessel were performed on 28 July, 31 July and 11–12 August. The locations of stations and the sampling depths were defined on the basis of autonomously acquired data and vertical profiles of Chl *a* fluorescence at each sampling station. Vertical resolution of water sampling was from 2 to 5 m. Water samples were analysed for inorganic nutrient (PO_4^{3-} and $NO_2^- + NO_3^-$) concentrations, Chl *a* content and phytoplankton species composition and biomass.

Nutrient analyses were carried out according to the guidelines of the American Public Health Association (APHA 1992; methods 4500-NO3 F and 4500-P F). The samples were deep-frozen after collection and analysed at the on-shore laboratory using an automatic nutrient analyser (μMac 1000, Systea S.r.l.). The lower detection range for phosphate–phosphorus and nitrate + nitrite–nitrogen was 1 ppb (parts per billion; 0.03 and 0.07 μM, respectively; with a measurement uncertainty of 20% near detection limit).

Chl *a* concentration in the water samples was determined on Whatman GF/F glass fibre filters following extraction at room temperature in the dark with 96% ethanol for 24 h. Chl *a* content from the extract was measured spectrophotometrically (Thermo Helios γ) in the laboratory (HELCOM 1988). Phytoplankton samples were preserved with acid Lugol's solution and analysed using the Utermöhl (1958) technique and PhytoWin software by Kahma Ky. Cyanobacterial filaments were counted as 100-μm segments and other phytoplankton species as single cells or colonies. All biomass data are given in wet weight concentrations.

Fluorescence data were calibrated against Chl *a* measured in the water samples collected aboard the research vessel on 28 July, 31 July and 11–12 August. Sixty data pairs were used to find the best linear fit (using least mean square criteria) between fluorescence and Chl *a*: Chl $a = 2.11 \times F + 0.63$ ($r^2 = 0.69$, where F is fluorescence in arbitrary units and Chl *a* content is obtained in milligram per cubic metre). The applicability of the same equation to convert the fluorescence values measured by another Seapoint fluorometer attached to the moored profiler was confirmed by very good agreement between the simultaneous vertical Chl *a* fluorescence profiles obtained by the moored profiler and the profiler aboard the research vessel.

Two stratification parameters were calculated for each vertical density profile measured at the buoy station—upper mixed layer (UML) depth (h_{UML}) and depth of the strongest density gradient (depth of the maximum Brunt-Väisälä frequency—h_{maxN}). Profiles with a vertical resolution of 0.5 m were used, and only those profiles were taken into account where the profiling depth was ≥30 m. The UML depth was derived as the depth at which the density exceeded the surface density (taken at 4 m depth) by 0.25 kg m^{-3}.

Wind data with a time resolution of 3 h obtained from the Kalbådagrund meteorological station (Finnish Meteorological Institute; see location in Fig. 1) were used to characterize local atmospheric forcing.

3 Results

3.1 Vertical temperature, salinity and Chl *a* distribution

High-resolution vertical profiling at the buoy station revealed remarkable temporal variations of the vertical distributions of temperature and salinity in the Gulf of Finland in July–August 2009 (Fig. 2a, b). Although the general temporal pattern was superimposed by short-time variations, the deployment period could be divided into several sub-periods with distinct vertical structure (and/or changes) of temperature and salinity fields. At the beginning of July, the UML temperature and depth were 13–15°C and 5–9 m, respectively. Surfacing of colder and more saline subsurface layer water was observed in the first half of July. Later, a less saline water mass with temperature and salinity ranging from 14°C to 15.5°C and from 4.2 to 4.5 m, respectively, appeared in the UML at the measurement site. A fast deepening of the UML from 7–9 to 16–18 m occurred on 25 July and a more saline water mass occupied the UML on 26 July—the UML salinity increased up to 5.0. After 31 July, considerable warming of the sea surface and formation of a secondary thermocline at 7–10 m depth were observed. It was followed by a drastic deepening of the UML from 13–15 m (on 15–16 August) to 26–30 m (on 20–21 August) accompanied by an increase of the UML salinity up to 5.7. While in most cases the depth of the strongest density gradient followed the temporal evolution of the UML depth, separation of about 10 m between these depths occurred from 29 July to 12 August.

The general dynamics of Chl *a* were characterized by an interchange of periods with different Chl *a* distribution patterns (Fig. 2c). Three periods with deep distribution patterns of Chl *a* were related to the deepening of the UML after 12 July, 25 July and 16 August. The highest Chl *a* concentrations in the UML were observed on 3–10 August when the highest UML temperature (up to 19.2°C) and

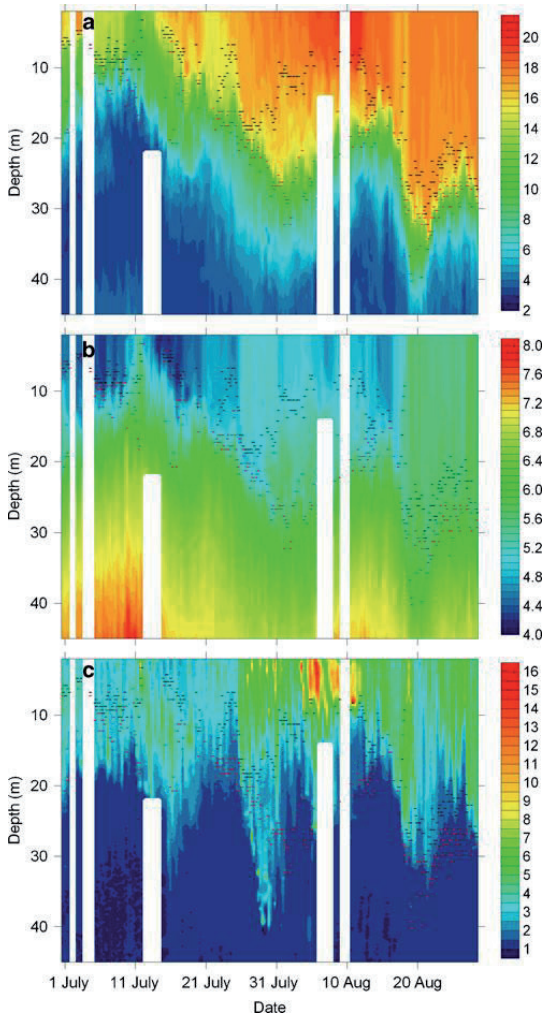

Fig. 2 Variations of the vertical distribution of temperature (**a**, degree Celsius), salinity (**b**) and Chl *a* (**c**, milligram per cubic metre) as measured by autonomous profiler in the Gulf of Finland from 30 June to 28 August 2009. *Blanked areas* correspond to the periods when vertical profiles were not available for 24 h or more. *Black dashes* indicate the UML depth and *red dashes* the depth of the strongest density gradient

secondary thermocline occurred. The three mentioned periods of relatively high Chl *a* concentration in the subsurface layer differ from each other regarding the depths of Chl *a* penetration and the concurrent UML depth and depth of the strongest density gradient (Fig. 2c). In the period after 12 July, the highest Chl *a* values were observed mainly in the thermocline between the UML depth and the depth of the strongest density gradient, i.e. the Chl *a* concentrations in the UML were lower than those in the

thermocline. On 26–31 July, relatively high Chl *a* concentrations were observed in the UML, while patches of very high Chl *a* were detected also in the sub-surface layer below the depth of the strongest density gradient. The overall Chl *a* concentration maximum, measured by the buoy profiler, was registered also within this period in the sub-surface layer (19.8 mg m^{-3} at 32 m on 28 July). During the third period of deep Chl *a* distribution (after 16 August), high Chl *a* concentrations were observed only in the UML (however, the UML was deep), and no patches of elevated Chl *a* content were detected below the depth of the strongest density gradient. Relatively high Chl *a* values were measured below the depth of the highest density gradient on 5–9 July when the UML was very shallow and h_{maxN} was located close to the UML depth. It has to be pointed out that the described general Chl *a* dynamics was superimposed with short-term variations, often having a diurnal signal in the whole water column where noticeable Chl *a* concentrations were measured.

3.2 Atmospheric and oceanographic forcing

Wind measurements at the Kalbådagrund meteorological station (see location in Fig. 1) revealed high variability of the wind but some periods with characteristic wind forcing (Fig. 3) leading to certain current patterns (data available since 23 July) or coastal upwelling/downwelling events. South-easterly winds, which are favourable for upwelling near the southern coast, prevailed in the Gulf of Finland area from 6 to 12 July. The temperature and salinity data collected in the surface layer along the Tallinn–Helsinki ferry route confirmed that an upwelling event occurred near the southern coast on 7–13 July (Fig. 4) and that upwelling waters reached the buoy station on 10 July resulting in a temporal temperature decrease and salinity increase measured by the profiler on 10–12 July. Mainly westerly–south-

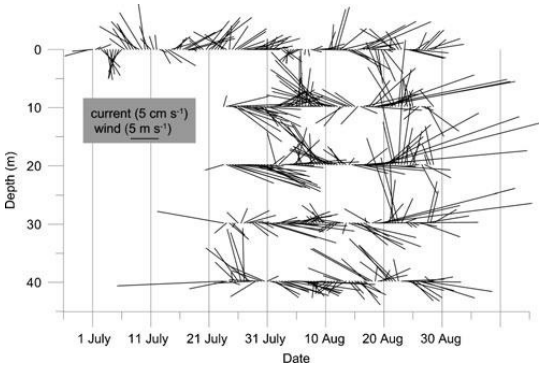

Fig. 3 Daily mean wind velocity measured at the Kalbådagrund meteorological station from 30 June to 28 August 2009 (upper row of vectors) and daily mean currents at the depths of 10, 20, 30 and 40 m

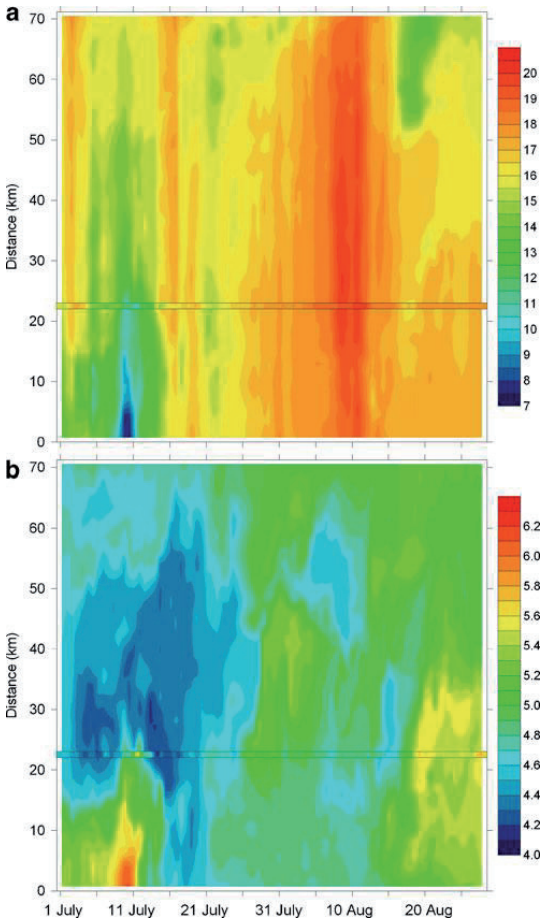

Fig. 4 Variations of temperature (**a**, degree Celsius) and salinity (**b**) in the surface layer along the ferry route Tallinn–Helsinki from 30 June until 28 August 2009. Distance in kilometres from a fixed starting point of Ferrybox measurements near Tallinn is shown on the *y*-axis. Simultaneous data acquired at the buoy profiler (at the depth of 4 m) are shown at the distance of 22–23 km

westerly winds prevailed in the area from 15 July until the end of July. This period was characterized by deepening of the thermocline (h_{maxN}, see Fig. 2a). South-eastward flow in the 20-m upper layer and north-westward flow below the thermocline were observed from 24 July (Fig. 3). The appearance of more saline water in the UML on 26 July (Figs. 2b and 4b) could be related to this flow structure.

A period of weak winds was observed during the first 10 days of August. The flow structure was characterized by a northward (north-westward) flow in the surface layer and an eastward flow below the thermocline (30 and 40 m in Fig. 3). Strong wind pulses from variable directions were observed from 10 August until the end of the measurement

period. First, simultaneous diurnal current oscillations occurred in the whole water mass (not seen in Fig. 3 where daily mean velocities are presented). Later, a clear two-layer flow structure was established with similar changes of current speed and direction in the upper 30 m layer and mostly opposite flow below. Strong westerly and north-westerly winds on 15–20 August caused downwelling near the southern coast of the Gulf, which was detected at our measurement site as the sharp deepening of the UML from 17 to 19 August. According to the Tallinn–Helsinki Ferrybox data, an intensive upwelling event developed simultaneously near the northern coast (Fig. 4).

3.3 Phytoplankton dynamics in the surface layer

Phytoplankton biomass and species composition in the surface layer changed during the study period and, according to the sampling using the Ferrybox system, differed between the regions along the ferry route. On the basis of combined Ferrybox and research vessel data collected near the buoy profiler (Fig. 5), phytoplankton biomass values were relatively low (420–880 mg m^{-3}, expressed as total wet weight concentrations) at the beginning of July. Euglenophytes *Eutreptiella* spp. de Cunha (16–30% of total wet weight biomass), the filamentous cyanobacterium *Aphanizomenon* sp. (13–26%) and the dinoflagellate *Dinophysis acuminata* Claparède and Lachmann (19–27%) were the dominant species in the phytoplankton community. In the area influenced by a coastal upwelling near the southern coast, *Eutreptiella* spp. were most prominent (28–58%) on 12 July, and the community was dominated by *Aphanizomenon* sp. (32–50%) and *D. acuminata* (12–27%) on 19 July. At the same time, the three Ferrybox samplings in July revealed that the dinoflagellate *H. triquetra* dominated at most of the stations in the northern Gulf (10–53% of total wet weight biomass). According to the research vessel data (used to fill in the gap in the Ferrybox data) collected from the upper layer (1–5 m) in the vicinity of the buoy profiler on 28 and 31 July, the community was clearly dominated by cyanobacteria and dinoflagellates (Fig. 5) in late July. Dominant species on both days were *Aphanizomenon* sp. (37% and 29%, respectively) and *H. triquetra* (32% and 27%). The biomass increase on 31 July was mainly due to the appearance of *Nodularia spumigena* Mertens and higher biomass of *D. acuminata* in the whole community.

On 2 August, *Aphanizomenon* sp. and *H. triquetra* were dominant in the southern Gulf (21–32% and 27–57% of total wet weight, respectively; Ferrybox data). The more saline water mass just northward from the buoy station (see Fig. 4b) was characterized by a lower *Aphanizomenon* sp. contribution (below 10%) and high dominance of *H. triquetra* (58–72%). One week later, on 9 August, *Aphanizomenon* sp. and *H. triquetra* were more or less evenly distributed across the Gulf (11–44% and 10–32%, respectively). The cyanobacterium *N. spumigena* had a significant share in the total biomass in the whole sampling area (6–46%). On 11 August, the samples collected aboard the research vessel showed an overall decrease in phytoplankton biomass and the dominance of filamentous cyanobacteria in the community. On 23 August, *Aphanizomenon* sp. continued to dominate in the southern part of the Gulf (40–50%); however, the total phytoplankton biomass was clearly lower than that of previous sampling days (Fig. 5).

3.4 Vertical migration of phytoplankton

To verify whether the observed short-term variations in Chl *a* distribution (Fig. 2) were consistent with a diurnal vertical migration pattern of phytoplankton, the average daily courses of Chl *a* were constructed for the entire deployment

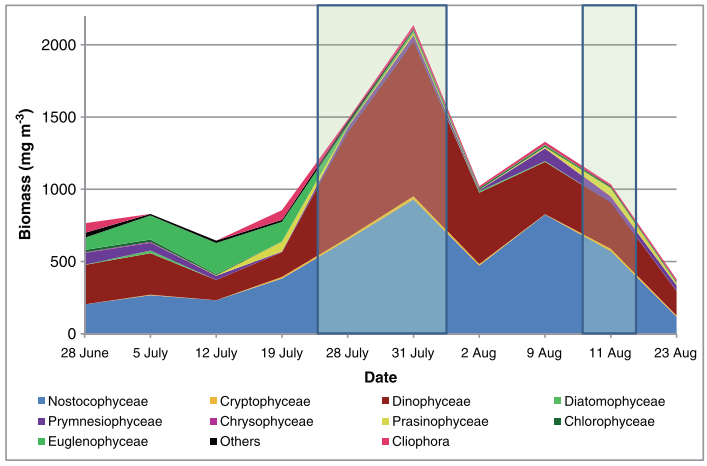

Fig. 5 Temporal dynamics of phytoplankton in the Gulf of Finland in summer 2009 in the vicinity of the buoy profiler. Ferrybox data collected from the depth of 4 m in the evening are complemented by research vessel data (marked as *shaded areas*) collected from the surface layer 1–5 m during daytime

period and for several distinct periods of atmospheric–oceanographic forcing and species composition. Due to the high variability at other time scales, the amplitude of the diurnal cycle, revealed using the data from the entire deployment period, was low in comparison to the overall variability (calculated as the standard deviation of Chl *a* at a fixed depth). Clear diurnal patterns in the Chl *a* dynamics were detected in the period of dominance of euglenophytes (*Eutreptiella* spp.) at the beginning of July and in the period of dominance of the dinoflagellate *H. triquetra* in late July–early August (Fig. 6). In the former period, the Chl *a* values were relatively low (mainly <5 mg m^{-3}), the maximum at the surface (3 m) was observed at 3 p.m. and the maximum at 15–17 m depth at 3 a.m. The changes in the Chl *a* distribution were restricted to the upper 20 m layer where the water temperature and density anomaly were >4°C and <5 kg m^{-3}, respectively. We

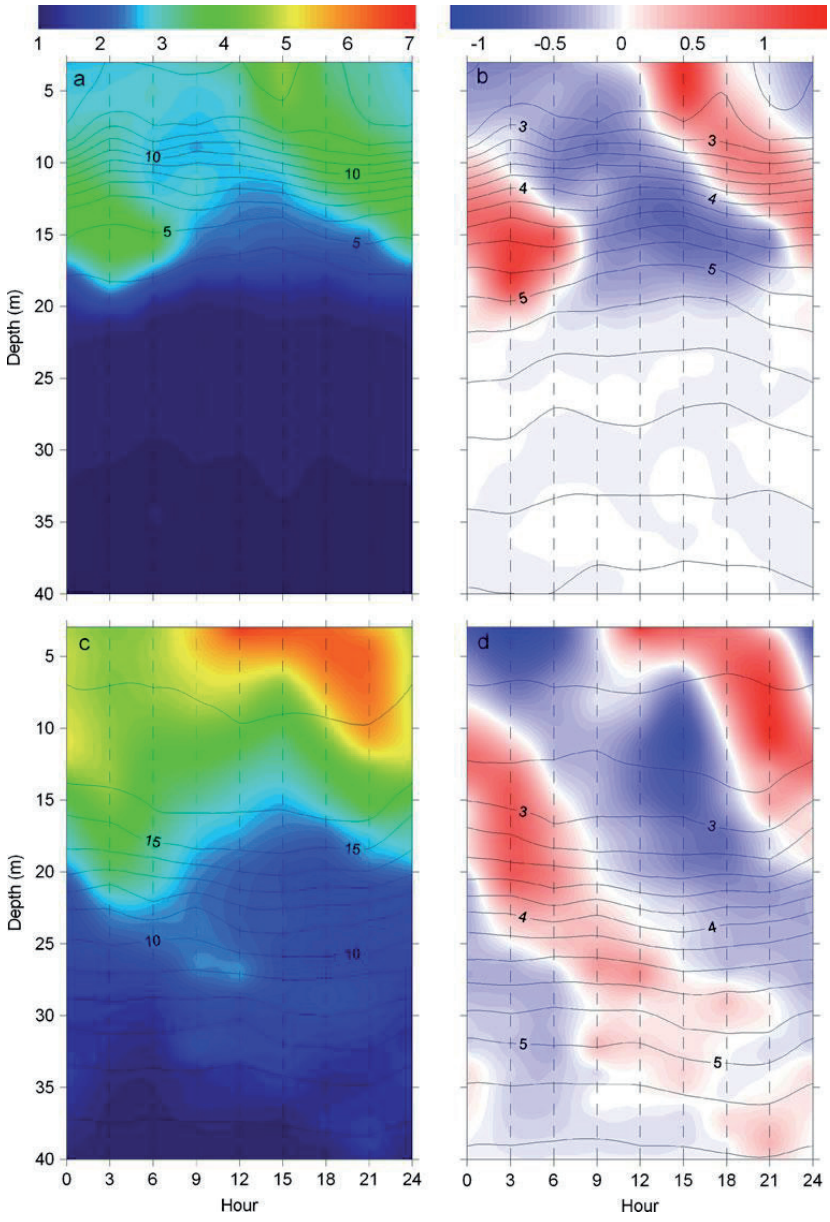

Fig. 6 The daily average variations of Chl *a* and deviations from the mean Chl *a* at each depth in the layer 3–40 m from 5 July to 9 July (**a** and **b**, respectively) and from 25 July to 2 August (**c**, **d**). Both Chl *a* scales are in milligram per cubic metre. Average temperature (degree Celsius; **a**, **c**) and density anomaly (kilogram per cubic metre; **b**, **d**) distributions are shown by *solid lines*

interpret the observed Chl *a* dynamics as diurnal vertical migration of phytoplankton with a clear downward migration at night. Two features of the Chl *a* dynamics in the time–depth plot (Fig. 6a, b) are consistent with the upward migration of phytoplankton—the upward directed branches of slightly higher values with the starting points at 3 a.m., 8–10 m and at 6 a.m., 15 m (Fig. 6a, b). However, we note that the related temporal changes were statistically not significant due to the high day-to-day variability and too short period with this migration pattern observed at the buoy profiler.

In late July–early August, the maximum Chl *a* concentrations at the surface were observed between noon and 6 p.m. and the minimum at 3 a.m. (Fig. 6c, d). Clear diurnal cycles, but with the daily maximum and minimum at the different times of day, occurred also in the sub-surface layer, while below the depth of the strongest density gradient (on average at 21–23 m), a possible cyclical migration pattern was masked by occasionally observed patches of high Chl *a*. It has to be noted that the daily maximum and minimum Chl *a* values were significantly different only in the upper 12-m layer. Due to a relatively strong vertical gradient of average Chl *a* in the upper 20 m layer (Fig. 6c), the diurnal cycle can be better examined with a graph of Chl *a* deviations (calculated against the daily averages at each depth) in a time–depth plot (Fig. 6d). The maximum Chl *a* values at 6–12 m were observed at 9 p.m. and the minimum at 3 p.m., while the maximum and minimum at 14–20 m were observed at 3 a.m. and 6–9 p.m., respectively. On the basis of the described Chl *a* dynamics, we suggest that, on average, after accumulation at the very surface at 3 p.m. the phytoplankton experienced downward migration reaching 20 m at 3 a.m., whereas sinking was faster in the almost mixed upper layer (see vertical density distribution in Fig. 6d). After 3 a.m., some part of the community continued downward migration and penetrated into the water layer below the strongest density gradient while some part returned, reaching the surface at noon. Although we do not have clear evidence that phytoplankton appearing below the thermocline returned, it can be assumed that part of the deep population could join the maximum at about 20 m depth at 3 a.m. the next day and thus could have a bi-diurnal migration pattern.

To illustrate the described diurnal (and possible bi-diurnal) migration pattern, a series of consecutive vertical profiles of Chl *a* collected from noon on 26 July to 6 p.m. on 27 July is presented (Fig. 7). According to this example, at 9 p.m., the maximum in the vertical profile of Chl *a* was measured at 4.6 m. During the night, the Chl *a* maximum was deeper and was at 10.4 m at midnight and 14.3 m at 3 a.m. Three hours later, Chl *a* was distributed almost evenly in the whole water layer from 3 to 25 m with local maxima at 5.5 and 19.2 m. Within the next 6 h, two clear maxima developed—one near the surface (at 3 m) and the other at 27 m. At the same time, Chl *a* concentration decreased in the water layer between 13 and 23 m. The strongest density gradient during the described period was at 21–23 m. The presented evolution of Chl *a* distribution showed that the Chl *a* maximum moves downward during the night with an approximate speed of 1.6 m h^{-1}. The splitting of the community into two at 9 a.m. could indicate that part of the community returns to the sea surface and the other part continues downward migration until getting below the thermocline.

On 11–12 August, vertical sampling was performed in the vicinity of the buoy profiler aboard the research vessel

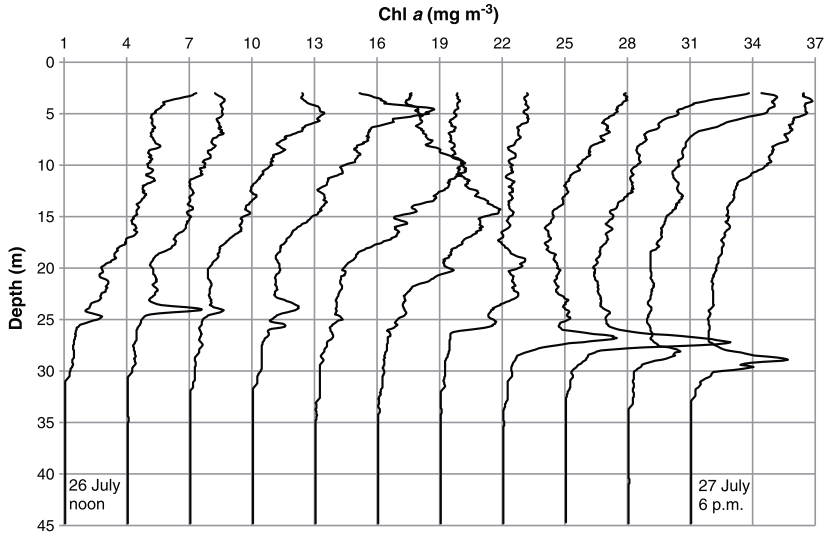

Fig. 7 Changes in the vertical distribution of Chl *a* at the buoy station from noon on 26 July until 9 p.m. on 27 July 2009. Values on the *x*-axis are correct for the first profile. Each subsequent profile is shifted to the right by 3 mg m^{-3} in relation to the preceding one

SALME—from 5 p.m. until 9 a.m. with a time resolution of 2–3 h. No Chl *a* fluorescence maxima were found below the seasonal thermocline and no temporal changes of profiles, which could be related to the vertical migration of phytoplankton, were observed. The contribution of cyanobacteria and dinoflagellates to the phytoplankton total wet weight biomass at 2 m was 53–87% and 6–27%, respectively, while *H. triquetra* biomass was low—it formed only 2–13% of phytoplankton biomass. However, the temporal changes in the vertical distribution of *H. triquetra* were in accordance with a diurnal migration pattern—the biomass maximum was at a depth of 2 m in the evening, at 10–15 m at midnight and at 3 a.m. and in the upper 5 m layer by 6 a.m. It has to be noted that although fluorescence profiles did not show maxima in the thermocline, we observed relatively high biomass of heterotrophic dinoflagellates at 20 m depth in all samples. The phytoplankton biomass was between 600 and 1,400 mg m^{-3} and the heterotrophic dinoflagellates formed 84–99% of the total wet weight.

3.5 Sub-surface patches of high phytoplankton biomass

On 28 July, when the maximum Chl *a* concentration was recorded by the autonomous profiler in the sub-surface layer (at 32 m at 9 a.m.), a north–south-oriented transect of four stations close to the mooring was sampled twice—2–3.5 h later and 5.5–7 h later. Extremely layered vertical distributions of temperature, salinity and Chl *a* with substantial horizontal gradients of all parameters in the thermocline were recorded (Fig. 8). Isopycnals below the thermocline (below the depth of the strongest density gradient) had a shallower position in the northern part of the section and a cold intrusion extended from the north towards the buoy profiler. There was a less saline layer (well visible at station 5) in the upper part of the thermocline beneath the more saline surface layer (Fig. 8b). A relatively intense sub-surface Chl *a* maximum layer, which was thinner and more intense in the northern part and thicker (consisting of a few sub-layers) near the buoy profiler (station 5), was detected. At the two northernmost stations, the maximum Chl *a* concentration and thickness of the layer (determined as described by Lips et al. (2010)) were 9.9 mg m^{-3} and 3.9 m and 9.2 mg m^{-3} and 5.0 m, respectively. The sub-surface Chl *a* maximum layer coincided with the cold intrusion. The vertical distribution of nutrients revealed that nitrates–nitrites were depleted (concentration <0.1 μM) and only low concentrations of phosphates were measured (0.15 μM) in the water column above the Chl *a* maximum layer while relatively high concentrations were measured in it (0.5 μM of $NO_3^- + NO_2^-$ and 0.54 μM of PO_4^{3-}).

Phytoplankton had the highest total biomass (2,300 mg m^{-3}) in the surface layer at the northernmost station (station 3), where at a depth of 2 m, 75% of the biomass was dinoflagellates (69% of total wet weight was formed by *H. triquetra*) and 20% cyanobacteria. At 28 m depth, in the Chl *a* maximum layer, a phytoplankton biomass of 1,700 mg m^{-3}

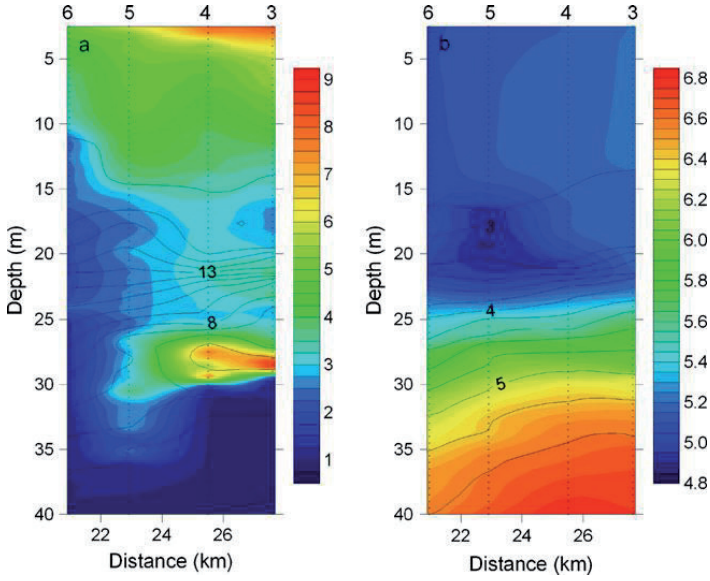

Fig. 8 Vertical sections of Chl *a* and temperature (**a**; colour scale, milligram per cubic metre and *solid lines*, degree Celsius, respectively), and salinity and density anomaly (**b**; colour scale, without units and *solid lines*, kilogram per cubic metre, respectively) along a north–south transect in the vicinity of the buoy profiler (station 5 was located close to the buoy) sampled on 28 July. Distance in kilometres corresponding to the distance in Fig. 4 is shown on the *x*-axis and station numbers are indicated above the plots

was measured. About 90% of biomass in this layer was formed by dinoflagellates—half of it by *H. triquetra* and the other half by larger heterotrophic species. By microscopic examination, it could be seen that heterotrophic species were feeding on *H. triquetra*. At the next station (located 2.2 km southward), the total biomass at 28 m depth was slightly lower (1,200 mg m^{-3}), but it was mostly (96%) formed by dinoflagellates with a clear dominance of *H. triquetra* (90%). Near the buoy profiler (station 5), the biomass maximum was thicker and the biomass values at the sampling depths of 25–31 m were lower (340–600 mg m^{-3}). *H. triquetra* formed 50–83% of total wet weight biomass. At the same time in the surface layer, the biomass (1,600 mg m^{-3}) was dominated by cyanobacteria (51%) while the contribution of dinoflagellates to the total wet weight biomass was 43% (*H. triquetra* formed 29% and *D. acuminata* 10%).

Similar to that described above, a layered structure of vertical temperature, salinity and Chl *a* distribution was observed during the second sampling on 28 July. A very intense sub-surface phytoplankton biomass maximum was detected at 33 m (at station 9, which was close to station 4 in Fig. 8). The maximum Chl *a* concentration and thickness of the layer detected at the measured vertical Chl *a* profile were 26.6 mg m^{-3} and 1.3 m, respectively. This Chl *a* maximum layer coincided with a warm intrusion, which occurred below the cold intrusion where the Chl *a* maximum at stations 3 and 4 was detected 4 h earlier (Fig. 8). Phytoplankton counting gave a very high abundance and biomass of *H. triquetra* in the water sample collected from the maximum layer at station 9—2,523,000 cells l^{-1} and 3,390 mg m^{-3} (forming 95% of the total phytoplankton biomass). The Chl *a* fluorescence value measured when the water bottle was closed corresponded to a Chl *a* value of 42.8 mg m^{-3}.

On 31 July, the transect consisting of four stations was sampled again. In the surface layer, dinoflagellates and cyanobacteria formed an equal share (close to 50%) of the total phytoplankton biomass at all stations. Only moderate sub-surface maxima were observed with a *H. triquetra* biomass of up to 300 mg m^{-3}. In most samples from 25 to 32 m, the heterotrophic dinoflagellates were dominant in the phytoplankton community with biomasses of between 500 and 600 mg m^{-3}.

4 Discussion

High-resolution vertical profiling has revealed remarkable variations of the vertical distribution of temperature, salinity and Chl *a* in the Gulf of Finland in July–August 2009. Vertical dynamics of phytoplankton was described to a large extent using Chl *a* fluorescence data. It is well known that the fluorescence quenching effect can influence the results at high daytime irradiances (Sackmann et al. 2008), even up to 30%. During our study, the daily maximum Chl *a* values near the sea surface were recorded at daytime and the minimum values at night (Fig. 6). Thus, if the quenching effect could influence the fluorescence data, the amplitude of diurnal variation at the sea surface could be underestimated, rather than overestimated. In addition, the Secchi depth measured aboard the research vessel on 28 July, 31 July and 11–12 August did not exceed 4 m. Consequently, the euphotic depth in the study area was about 12.8 m (or less) in late July–early August 2009. It allows us to assume that the quenching effect could not affect the Chl *a* fluorescence measurements in the sub-surface layer where, on average, the Chl *a* maximum was observed at 3 a.m. and the minimum at 3 p.m.

We explain the observed changes in vertical dynamics of phytoplankton by prevailing meteorological and oceanographic forcing and related shifts between dominant species/taxonomic groups of phytoplankton. The most prominent variations in the vertical Chl *a* distribution were observed in late July–early August when the phytoplankton community was dominated by *H. triquetra*. While at our measurement site this period was relatively short, *H. triguetra* was the dominant species in the community in the northern Gulf by early July and in the central Gulf by mid-July. Thus, similar migration patterns of phytoplankton as observed in the southern Gulf in late July–early August and formation of sub-surface layers of high phytoplankton biomass could have occurred in those areas for a longer period. This suggestion has to be taken into account when extrapolating our observational results over the larger area in the Gulf of Finland, e.g. when estimating the role of sub-surface biomass maxima in summer phytoplankton assemblages. One question to be answered is why the dominance of *H. triquetra* in the phytoplankton community at our measurement site was restricted only to late July and first days of August. Vertical migration of phytoplankton was evident also in the first half of July when euglenophytes (*Eutreptiella* spp.) dominated the phytoplankton community in the UML. Although we did not collect samples for phytoplankton counting from the sub-surface layer to confirm that *Eutreptiella* spp. were dominating there as well, the revealed diurnal migration pattern is in accordance with earlier findings on migration behaviour of these species. Figueroa et al. (1998) have shown that *Eutreptiella* sp. aggregated at the surface in maximum numbers at noon and migrated through the pycnocline (at depth of 6 m) at night. The winds favourable for the development of upwelling events near the southern coast of the Gulf of Finland prevailed, and the seasonal thermocline had a quite shallow position in early July. Most probably, the latter and related shallow position of nutriclines (e.g. Laanemets et al. 2004) created favourable conditions also for smaller sized species,

which should have lower swimming speeds than bigger sized species (e.g. Smayda 2010), to undertake nutrient-gathering migrations to nutrient-rich layers.

In the beginning of August, a secondary thermocline developed close to the sea surface and the UML temperature increased to 19.2°C. It resulted in the dominance of cyanobacteria and appearance of *N. spumigena* in the community. This observational result confirms that the vertical stratification in the surface layer is favourable for cyanobacteria, especially for *N. spumigena* (e.g. Kanoshina et al. 2003). Thus, the nitrogen uptake strategy of dinoflagellates by vertical migration through the secondary and seasonal thermoclines seems to be less competitive than the nitrogen fixation by cyanobacteria in warm stratified surface waters. Deepening of the UML, observed after 16 August at the buoy station due to the development of downwelling near the southern coast, did not result in *H. triquetra* dominance and related migration pattern. Most probably, in this case, the nutrient-rich waters were pushed too deep, to depths >35–40 m. A reason for the observed overall decline in phytoplankton biomass in the second half of August (Fig. 5) could be the deep UML as well; the UML depth was about two times deeper than the estimated euphotic depth.

Many dinoflagellates are known to be capable of vertical migration, and the measured maximum swimming speeds of different phytoplankton species range from 139 to 1,667 μm s^{-1} (Smayda 2010). Swimming enables nutrient-deficient cells to migrate to the deeper layers where they dark-assimilate NO_3^- for photosynthetic incorporation upon swimming back up into the euphotic zone (Fauchot et al. 2005). The ability of *H. triquetra* to uptake nitrate in the dark was shown by Paasche et al. (1984). The maximum swimming speed of *H. triquetra*, as measured by laboratory experiments, is as high as 467 μm s^{-1} (average 370 μm s^{-1}; Jeong et al. 2002). We presented in situ evidence that the summer phytoplankton dominated by the dinoflagellate *H. triquetra* in the stratified Gulf of Finland experiences vertical migration, and the speed of downward migration could be as high as 1.6 m h^{-1} (equal to 444 μm s^{-1}). During mesocosm experiments conducted by Olli and Seppälä (2001), clear diurnal vertical migration of *H. triquetra* was detected in the 11-m water column in 24 h. We observed a similar diurnal migration pattern by direct measurements on 11–12 August in a situation when *H. triquetra* had low biomass in the community dominated by cyanobacteria, and the vertical migration range of cells was only 15 m.

During the period of dominance of *H. triquetra* in late July–early August, the detectable amounts of nutrients were measured below the strongest density gradient at depths >25 m. The estimated mean spherical diameter of *H. triquetra* in the sub-surface biomass maxima layers was 21.5 μm. As motility progressively increases with cell size up to a threshold of 35 μm (Kamykowski et al. 1992), the depths of 28–34 m, where phytoplankton biomass maxima were observed, are in principle reachable by diurnal migratory behaviour. However, the observed swimming speed of 1.6 m h^{-1} is not enough for cells to sink to a depth >25 m, uptake nitrogen, and swim back to the surface in 24 h. Furthermore, we have measured many profiles with two vertically separated maxima of Chl *a* during daytime. Therefore, we suggest that the migration cycle for those cells of *H. triquetra* which reach the high nutrient resources below the thermocline could be longer, e.g. bi-diurnal. Ralston et al. (2007) have shown in their modelling exercise that asynchronous vertical migrations in cases when the migration cycle cannot be completed in 24 h could result in a bimodal vertical distribution of phytoplankton cells. As suggested by Townsend et al. (2005), the cells that swim downward would most likely stop upon encountering the nitracline, and likewise, those swimming upwards would concentrate near the surface. Our results indicate that the downward migration is clearly synchronous while the upward migration could be asynchronous and depend on the time period needed to reach the nutrient-rich layer and uptake enough nitrogen.

Dortch and Maske (1982) have proposed that only part of the population migrates to the full depth necessary to reach the nitracline in response to the depletion of internal stores of nitrogen. We also showed the splitting of the community into two. One half stayed in the upper mixed layer and was moving to the surface by noon, while the other half continued downward migration (Fig. 7). The downward migrating phytoplankton cells did not stop at the depths with the strongest density gradient and formed patches of high biomass just a few metres below h_{maxN}. The presence of phytoplankton maxima below h_{maxN} has been shown in the Adriatic Sea (Revelante and Gilmartin 1995), indicating that the formation of these maxima are not connected to the accumulation of organisms at a marked density gradient as it has been reported in many other studies (e.g. Velo-Suarez et al. 2010). The latter and the fact that in these layers high enough nutrient concentrations were measured support the suggestion that the downward migration was caused by physiological needs of phytoplankton. The split of one species community during migration and the formation of a double peak in vertical profiles was demonstrated by Olli and Seppälä (2001) in their mesocosm experiment and found by Holligan et al. (1984) in field measurements. The downward movement of dinoflagellates has been suggested to be triggered by inorganic nutrient depletion in the surface layers. However, laboratory experiments (Olli and Seppälä 2001; Jephson and Carlsson 2009) have shown downward migrations to be present also in nutrient-sufficient conditions.

In many studies, it has been argued that physical processes are able to shape the vertical distribution of phytoplankton into thin layers of high biomass (e.g. Velo-Suarez et al. 2010). Sullivan et al. (2010) have concluded that even though physical forcing affects the spatial–temporal dynamics of thin phytoplankton layers, biological processes and behaviour can be equally, if not more important. Ross and Sharples (2007) showed that motility could give an advantage to the phytoplankton in competing for the nutrients in the thermocline. Our results indicate that the sub-surface maxima of *H. triquetra* are fuelled by synchronous downward migration of cells at night. Since the physical processes in the tideless Gulf of Finland do not reveal a diurnal cycle, we suggest that this migration pattern occurs as an adaptation of phytoplankton to migrate to the deeper nutrient resources at low irradiances (when photosynthesis rate is low) in response to the inorganic nutrient depletion at the surface. On the other hand, we suggest that the success of this strategy depends on hydrophysical background, mostly at a mesoscale, e.g. the appearance of a more saline water mass, which could be interpreted as an anticyclonic eddy, at the study site coincided with the clear vertical migration of phytoplankton and formation of biomass maxima in the sub-surface layer. Similar suggestions on the importance of mesoscale processes were made in the earlier studies by Kononen et al. (2003) and Lips et al. (2010).

The most intense sub-surface maxima observed in our study area were associated with the intrusions (with both, warm and cold ones) indicating that physical processes at a sub-mesoscale are also important. However, since on some occasions the biomass is much higher in the sub-surface maxima than that in the surface layer, it is not possible to explain the phenomenon by physical processes alone. The question in this context is why the downward migration of cells stops at a very restricted depth range? Thus, we still do not know the exact mechanisms of formation of these very thin layers with a very high biomass. We have not discussed the possible influence of grazing, although direct evidence of feeding of large heterotrophic dinoflagellates on *H. triquetra* was found. A topic which has to be studied in more detail in the future is related to the heterotrophic communities in the sub-surface layers in general. Local biomass maxima of heterotrophic phytoplankton at most sampling stations were detected in the thermocline, but the observed biomasses were not as high as for *H. triquetra*. Equipment suitable to locate similar layers of very high biomass of heterotrophic phytoplankton has to be used in these studies.

5 Conclusions

We have observed pronounced oceanographic processes and related changes in the horizontal and vertical distributions of temperature; salinity; and Chl *a* in the Gulf of Finland in July and August 2009. Based on our observations, we suggest that the conditions caused by the prevailing atmospheric and oceanographic forcing (wind, dynamics of vertical stratification, basin-wide, mesoscale and sub-mesoscale processes) are preferred by certain species/taxonomic groups (small flagellates, dinoflagellate *H. triquetra* or cyanobacteria) and explain the migration patterns of phytoplankton. Downward migration of *H. triquetra* with a speed up to 1.6 $m h^{-1}$ and splitting of the community into two, resulting in a bimodal vertical distribution of organisms were documented. The areas and periods where and when this migration pattern and the sub-surface biomass maxima occur are suggested to be defined by mesoscale processes and vertical stratification of the water column. To understand the role of the sub-surface phytoplankton biomass maxima in the total primary production and internal nutrient cycling in stratified estuaries, further studies are needed.

Acknowledgements This work was financially supported by the Estonian Science Foundation (grant no. 6955). We thank the Finnish Meteorological Institute for providing wind data at Kalbådagrund station, AS Tallink Group for cooperation on Ferrybox measurements and our colleagues and crew members for participation in the field measurements.

References

Alenius P, Myrberg K, Nekrasov A (1998) The physical oceanography of the Gulf of Finland: a review. Boreal Environ Res 3:97–125

APHA (1992) APHA, AWWA, and WPCF standard methods for the examination of water and wastewater, 18th edn. American Public Health Association, Washington

Dortch Q, Maske H (1982) Dark uptake of nitrate and nitrate reductase activity of a red-tide population off Peru. Mar Ecol Prog Ser 9:299–303

Elken J, Raudsepp U, Lips U (2003) On the estuarine transport reversal in deep layers of the Gulf of Finland. J Sea Res 49:267–274

Fauchot J, Levasseur M, Roy S (2005) Daytime and nighttime vertical migrations of *Alexandrium tamarense* in the St. Lawrence estuary (Canada). Mar Ecol Prog Ser 296:241–250

Figueroa FL, Niell FX, Figueiras FG, Villarino ML (1998) Diel migration of phytoplankton and spectral light field in the Ría de Vigo NW Spain. Mar Biol 130:491–499

HELCOM (1988) Guidelines for the Baltic monitoring programme for the third stage. Part D. Biological determinants. Baltic Sea Environ Proc 27D:1–161

HELCOM (2002) Environment of the Baltic Sea area 1994–1998; background document. Baltic Sea Environ Proc 82B:1–215

Holligan PM, Balch WM, Yentsch CM (1984) The significance of subsurface chlorophyll, nitrate and ammonium maxima in relation to nitrogen for phytoplankton growth in stratified waters of the Gulf of Maine. J Mar Res 42:1051–1073

Jeong HJ, Yoon JY, Kim JS, Yoo YO, Seong KA (2002) Growth and grazing rates of the prostomid ciliate *Tiarina fusus* on red tide and toxic algae. Aquat Microb Ecol 28:289–297

Jephson T, Carlsson P (2009) Species- and stratification-dependent diel vertical migration behaviour of three dinoflagellate species in a laboratory study. J Plankton Res 31:1353–1362

Kamykowski D, Reed RE, Kirkpatrick GJ (1992) Comparison of sinking velocity, swimming velocity, rotation and path characteristics among six marine dinoflagellate species. Mar Biol 113:319–328

Kanoshina I, Lips U, Leppänen JM (2003) The influence of weather conditions (temperature and wind) on cyanobacterial bloom development in the Gulf of Finland (Baltic Sea). Harmful Algae 2:29–41

Kononen K, Kuparinen J, Mäkelä K, Laanemets J, Pavelson J, Nõmmann S (1996) Initiation of cyanobacterial blooms in a frontal region at the entrance of the Gulf of Finland, Baltic Sea. Limnol Oceanogr 41:98–112

Kononen K, Huttunen M, Hällfors S, Gentien P, Lunven M, Huttula T, Laanemets J, Lilover M, Pavelson J, Stips A (2003) Development of a deep chlorophyll maximum of *Heterocapsa triquetra* Ehrenb. at the entrance to the Gulf of Finland. Limnol Oceanogr 48:594–607

Laanemets J, Kononen K, Pavelson J, Poutanen EL (2004) Vertical location of seasonal nutriclines in the western Gulf of Finland. J Mar Syst 52:1–13

Lips I, Lips U (2008) Abiotic factors influencing cyanobacterial bloom development in the Gulf of Finland (Baltic Sea). Hydrobiologia 614:133–140

Lips I, Lips U (2010) Phytoplankton dynamics affected by the coastal upwelling events in the Gulf of Finland in July–August 2006. J Plankton Res 32:1269–1282

Lips I, Lips U, Liblik T (2009) Consequences of coastal upwelling events on physical and chemical patterns in the central Gulf of Finland (Baltic Sea). Cont Shelf Res 29:1836–1847

Lips U, Lips I, Liblik T, Kuvaldina N (2010) Processes responsible for the formation and maintenance of sub-surface chlorophyll maxima in the Gulf of Finland. Estuar Coast Shelf Sci 88:339–349

Olli K, Seppälä J (2001) Vertical niche separation of phytoplankton: large-scale mesocosm experiments. Mar Ecol Prog Ser 217: 219–233

Paasche E, Bryceson I, Tangen K (1984) Interspecific variation in dark nitrogen uptake by dinoflagellates. J Phycol 20:394–401

Pavelson J, Kononen K, Laanemets J (1999) Chlorophyll distribution patchiness caused by hydrodynamical processes: a case study in the Baltic Sea. ICES J Mar Sci 56S:87–99

Ralston DK, McGillicuddy DJ, Townsend DW (2007) Asynchronous vertical migration and bimodal distribution of motile phytoplankton. J Plankton Res 29:803–821

Revelante N, Gilmartin M (1995) The relative increase of larger phytoplankton in a subsurface chlorophyll maximum in Northern Adriatic Sea. J Plankton Res 17:1535–1562

Ross ON, Sharples J (2007) Phytoplankton motility and the competition for nutrients in the thermocline. Mar Ecol Prog Ser 347:21–38

Sackmann BC, Perry MJ, Eriksen CC (2008) Seaglider observations of variability in daytime fluorescence quenching of chlorophyll-*a* in Northeastern Pacific coastal waters. Biogeosciences Discuss 5:2839–2865

Shlitzer R (2010) Ocean data view, http://odv.awi.de. Accessed 15 Jul 2010

Smayda TJ (2010) Adaptation and selection of harmful and other dinoflagellate species in upwelling system. Motility and migratory behaviour. Prog Oceanogr 85:71–91

Sullivan JM, Donaghay PL, Rines JEB (2010) Coastal thin layer dynamics: consequences to biology and optics. Cont Shelf Res 30:50–65

Townsend DW, Bennett SL, Thomas MA (2005) Diel vertical distributions of the red tide dinoflagellate *Alexandrium fundyense* in the Gulf of Maine. Deep Sea Res Pt II 52:2593–2602

Utermöhl H (1958) Zur Vervollkommnung der quantitativen Phytoplanktonmetodic. Mittelungen des Internationale Vereinigung für Theoretische und Angewandte Limnologie 9:1–38

Vahtera E, Laanemets J, Pavelson J, Huttunen M, Kononen K (2005) Effect of upwelling on the pelagic environment and bloom-forming cyanobacteria in the western Gulf of Finland, Baltic Sea. J Mar Syst 58:67–82

Velo-Suarez L, Fernand M, Gentien P, Reguera B (2010) Hydrodynamic conditions associated with the formation, maintenance and dissipation of a phytoplankton thin layer in a coastal upwelling system. Cont Shelf Res 30:193–202

Zhurbas V, Laanemets J, Vahtera E (2008) Modeling of the mesoscale structure of coupled upwelling/downwelling events and related input of nutrients to the upper mixed layer in the Gulf of Finland, Baltic Sea. J Geophys Res 113:C05004

Paper VI

Lips, Urmas; Lips, Inga; Liblik, Taavi; Kuvaldina, Natalja. (2010). Processes responsible for the formation and maintenance of sub-surface chlorophyll maxima in the Gulf of Finland. Estuarine, coastal and shelf science, 88, 339 - 349.

Estuarine, Coastal and Shelf Science 88 (2010) 339–349

Contents lists available at ScienceDirect

Estuarine, Coastal and Shelf Science

journal homepage: www.elsevier.com/locate/ecss

Processes responsible for the formation and maintenance of sub-surface chlorophyll maxima in the Gulf of Finland

Urmas Lips*, Inga Lips, Taavi Liblik, Natalja Kuvaldina

Marine Systems Institute, Tallinn University of Technology Akadeemia 21B, 12618 Tallinn Estonia

ARTICLE INFO

Article history:
Received 28 December 2009
Accepted 21 April 2010
Available online 10 May 2010

Keywords:
sub-surface chlorophyll maxima
seasonal thermocline
nutrients
meso-scale processes
Gulf of Finland
Baltic Sea

ABSTRACT

Vertical cross-sections of temperature, salinity and Chl *a* fluorescence distributions in the Gulf of Finland were mapped on 11, 19–20 and 25 July 2006. The sub-surface Chl *a* maximum layers with thickness varying between 1.5 and 9 m and intensity up to 7.6 μg l^{-1} were observed in the lower part of the seasonal thermocline within the depth range of 14.5–35 m. Nutrient ($PO4^{3-}$, $NO2^{-} + NO3^{-}$) analyses of water samples collected from the thermocline revealed the coincidence of the location of Chl *a* maxima and nutriclines. We suggest that the observed Chl *a* maxima were formed by dinoflagellate *Heterocapsa triquetra* capable for vertical migration and nutrient uptake in dark. The upward flux of nutrients caused by estuarine circulation and vertical turbulent mixing created favourable conditions for the formation and maintenance of sub-surface Chl *a* maxima. We explain the observed horizontal patchiness of sub-surface Chl *a* maxima by meso-scale processes – by the accumulation of phytoplankton along the depressed isopycnals at the base of anti-cyclonic circulation cells and by the horizontal convergence of waters in the downwelling area.

1. Introduction

The distribution of phytoplankton in water bodies (including the Baltic Sea) is highly heterogeneous, both horizontally and vertically. Horizontal distribution of phytoplankton in the euphotic layer is often related to the meso-scale hydrophysical processes and structures – meso-scale eddies, fronts and coastal upwelling events (in the Gulf of Finland e.g. Talpsepp et al., 1994; Kononen et al., 1996; Kanoshina et al., 2003; Lips et al., 2005). Vertical distribution of phytoplankton is determined by availability of major resources – light and nutrients – as well as grazing and divergence/convergence of sinking and buoyancy (see e.g. Fennel and Boss, 2003). In a stratified water column the contrasting gradients of resources – light that is supplied from above and nutrients that are often supplied from below – will lead to the development of a sub-surface biomass/chlorophyll (Chl *a*) maximum (Klausmeier and Litchman, 2001).

The sub-surface Chl *a* maxima have been observed in the Baltic Sea quite often (e.g. Kahru et al., 1982; Kuosa, 1990; Kononen et al., 1998; Pavelson et al., 1999) and a variety of mechanisms of their formation has been suggested. It is known that the sub-surface Chl *a* maxima are located just above the nutricline(s) which could be developed by an intrusion of nutrient rich water into the sea area under consideration (Lund-Hansen et al., 2006). In some cases the sub-surface Chl *a* maxima are observed well below the euphotic layer (e.g. Kononen et al., 2003). As mechanisms of the formation of such deep maxima, the hydrodynamic processes (Pavelson et al., 1999) and changing migratory behavior of *Heterocapsa triquetra* after an upwelling event (Kononen et al., 2003) have been proposed.

Sub-surface Chl *a* maxima are commonly observed in the summer stratified North Sea (Weston et al., 2005) and in the Celtic Sea (Hickman et al., 2009). It has been argued that accumulated new production in these layers in summer may be greater than that occurring in the spring bloom in the same regions (Richardson et al., 2000). No estimates of the role of sub-surface maxima in the total primary production during summer months are available yet for the Baltic Sea.

Development of measuring equipment in the last years has triggered an enhanced interest to sub-surface maximum layers of phytoplankton and zooplankton biomass, their fine-scale structure and ecology. Typical fine-scale layers range in thickness from a few centimetres to a few meters and they are described in the literature as “thin layers” (e.g. McManus et al., 2003). Physical processes can play an important role in the formation and dynamics of thin layers of phytoplankton and zooplankton (Dekshenieks et al., 2001; McManus et al., 2003). The measurements in the East Sound

* Corresponding author.
E-mail addresses: urmas.lips@phys.sea.ee (U. Lips), inga@sea.ee (I. Lips), taavi.liblik@phys.sea.ee (T. Liblik), natalja.kuvaldina@phys.sea.ee (N. Kuvaldina).

0272-7714/$ – see front matter © 2010 Elsevier Ltd. All rights reserved.
doi:10.1016/j.ecss.2010.04.015

revealed that over 71% of thin layers where located in the base of, or within, the pycnocline (Dekshenieks et al., 2001). The regions of occurrence of thin layers are relatively sheltered bays or straits with two-layer vertical structure. A two-layer current, temporal and spatial variation of pycnocline depth, caused by meso-scale hydrophysical processes and estuarine structure of hydrographic fields, and minimum of turbulent mixing are conditions favourable for formation of thin layers (McManus et al., 2003; Lund-Hansen et al., 2006). Recent observations have shown that thin layers of Chl *a* maxima can exist in both weak and strong turbulent conditions, however, under strong turbulence a weakening of the thin layer was evident (Wang and Goodman, 2010).

The Gulf of Finland as an elongated basin has a weak, characteristic to an estuary, circulation pattern superimposed by quite energetic, wind-driven meso-scale motions. In summer, the upper layer of the gulf is nutrient depleted while in the layers below the seasonal thermocline high nutrient reserves are available. Meso-scale processes cause vertical movements and mixing of water masses – upwelling events bring water from below the thermocline into the upper layer (e.g. Lips et al., 2009) and downwelling events generate downward transport of upper layer waters containing phytoplankton (Pavelson et al., 1999; Laanemets et al., 2005). Vertical stratification characterised by two strong pycnoclines serves as a pre-requisite for formation of layered current structure in the gulf. Thus, we can assume that a coincidence of certain factors could lead to favourable conditions for the formation of sub-surface Chl *a* maxima and thin layers in the Gulf of Finland.

The aim of the present paper is to define the pre-conditions and physical processes responsible for the formation and maintenance of sub-surface Chl *a* maxima observed in the Gulf of Finland in July 2006. We show that similarly to the horizontal distribution of phytoplankton in the euphotic layer, the distribution pattern of sub-surface Chl *a* maxima and occurrence of maxima complying with the "thin layer" definition are affected by the meso-scale processes.

2. Material and methods

Three surveys of hydrographic, -chemical and -biological fields were carried out in the central part of the Gulf of Finland in July 2006 – on 11, 19–20 and 25 July. Vertical profiles of temperature, salinity and Chl *a* fluorescence were recorded at 27 stations (Fig. 1, distance between stations 2.6 km) and water samples for inorganic nutrient (PO_4^{3-}, $NO_2^- + NO_3^-$) analyses were collected at 14 stations (distance between stations 5.2 km) from the upper mixed layer and from the thermocline with a vertical resolution of 2.5–5 m. In order to convert fluorescence values to Chl *a* content, the water samples at 6 to 10 stations per survey were collected from different depths. Full sampling program was completed on 11 and 25 July while on 19–20 July we were able to take water samples only at the northernmost stations (TH19-TH27). Samples for phytoplankton analyses were collected mainly from the upper mixed layer, except a few samples collected in the thermocline on 11 and 25 July.

Vertical profiles of temperature, salinity and Chl *a* fluorescence in the upper 50-m layer were recorded using an SBE 19 CTD probe (Sea-Bird) equipped with a WETStar flourometer (WET Labs). Sampling rate and lowering speed of the probe were 2 Hz and 0.5–1 m s^{-1}, respectively. In data processing, standard software package SEASOFT (Sea-Bird) was used where constant time shifts of 0.5 s for conductivity sensor, 1.0 s for temperature sensor and 2.5 s for Chl *a* fluorescence sensor were applied in order to compensate the time constant differences and different location of sensors while water was pumped through the sensors. The time shifts used in data processing were defined as the values ensuring the best conformity between downcast and upcast profiles (by visual comparison of them). Salinity data were quality checked against the water sample analyses by a high precise salinometer AUTOSAL (Guildline). In order to assure that the measured fluorescence peaks reflect the stable structures, the downcast and upcast profiles were both taken into account and an average profile at every station was analysed.

Nutrient analyses were carried out according to the guidelines of American Public Health Association (APHA, 1992; methods 4500-NO3 F and 4500-P F). Samples for phosphates (PO_4^{3-}) were mostly analysed immediately after the sampling onboard research vessel and samples for dissolved nitrogen compounds ($NO_2^- + NO_3^-$; henceforth called as NO_x) determination were deep-frozen after collection and analysed later in the on-shore laboratory. Phosphates and nitrates + nitrites were analysed using automatic nutrient analyzer μMac 1000 (Systea S.r.l.). The lower detection range for phosphate-phosphorus and nitrate + nitrite-nitrogen was 2 ppb (parts per billion; 0.06 mmol m^{-3} and 0.14 mmol m^{-3}, respectively).

Chl *a* concentration in the water samples was determined on Millipore APFF glass-fibre filters following the extraction at the room temperature in dark with 96% ethanol for 24 h. Chl *a* content from the extract was measured spectrophotometrically (Thermo Helios γ) in laboratory (Helsinki Commission, 1988). Results of analyses of 16 water samples collected on 11 and 25 July were used to get a calibrations line for converting measured fluorescence values to the Chl *a* content. The corresponding fluorescence values were obtained as 2-m average values around the water sampling depth. We applied only one calibration line for the whole data set: $Chl = 0.58 \times F + 1.37$ ($r^2 = 0.75$, where F is fluorescence in arbitrary units and Chl *a* content (Chl) is obtained in μg l^{-1}).

Phytoplankton samples were preserved with acid Lugol solution and analysed using the Utermöhl (1958) technique and PhytoWin software by Kahma Ky. Cyanobacterial filaments were counted as 100-μm segments and other phytoplankton species as single cells or colonies.

The intensity and thickness of sub-surface Chl *a* maxima were detected as shown in a sketch in Fig. 2. The maximum Chl *a* value (Chl_{max}) below 10 m depth and the minimum above it (Chl_1) were defined at every profile. The intensity of Chl *a* maximum was estimated as the difference between the values of Chl_{max} and Chl_1. The thickness of maximum layer was defined as the difference between the depth of local minimum Chl_1 (h_1) and the depth h_2 where the Chl *a* values below the maximum decreased back to the same concentration (Chl_1). The depth, temperature, salinity and density values associated to the maximum were recorded as these values at the depth of Chl_{max} (h_{max}). Only Chl *a* maxima with an intensity of ≥0.5 μg l^{-1} were taken into account.

The upper mixed layer (UML) depth at each station was determined using smoothed (2.5 m moving average) vertical density profiles. First, the density difference (Δd_{tot}) between the cold intermediate layer and the surface layer was estimated as the density at the depth of minimum temperature minus the minimum density value in the surface layer. The UML depth was defined as the shallowest depth at which the vertical density gradient exceeded a criterion calculated as $C_{up} \times \Delta d_{tot}$, where $C_{up} = 1/30$ m^{-1}. In order to determine the base of thermocline, the temperature difference between the UML and the cold intermediate layer was found. The shallowest depth, at which the temperature differs from the maximum value in the UML more than 90% of this difference, was defined as the base of thermocline.

The upper boundary of phosphacline and nitracline was defined as the deepest depth at which the nutrient (PO_4^{3-} or NO_x, respectively) concentration below the lower detection range was measured. When comparing the depths of Chl *a* maximum, thermocline and nutriclines it has to be kept in mind that the water

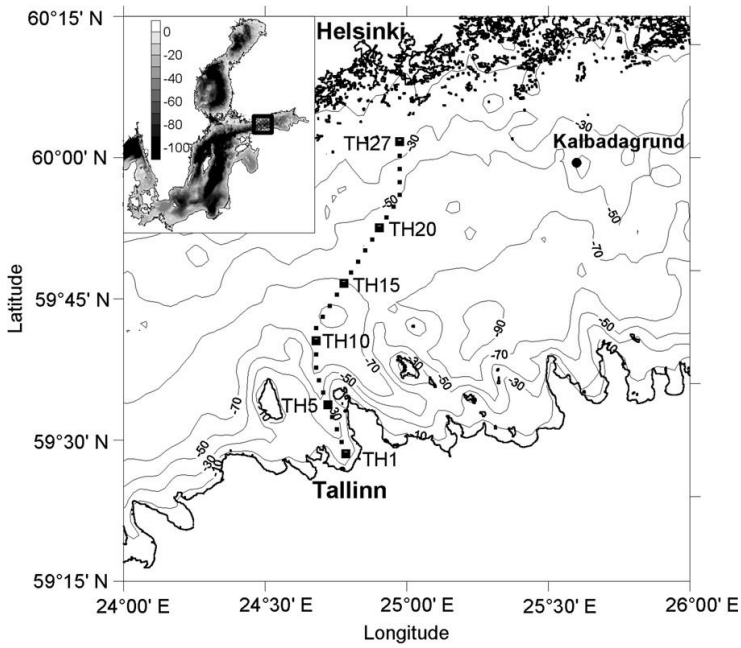

Fig. 1. Map of the study area and location of stations.

samples were collected with a vertical resolution of 2.5 m while the analysed temperature, salinity and fluorescence profiles had a vertical resolution of 0.5 m.

A primitive equation, sigma coordinate, free surface, hydrostatic model with a second moment turbulent closure sub-model embedded – Princeton Ocean Model (POM; Blumberg and Mellor, 1983) – was used with the aim to simulate the hydrophysical processes and related nutrient transport in the Gulf of Finland from 10 July until 31August 2006 (Laanemets et al., in press). Since the nutrient uptake by phytoplankton was not taken into account in the model calculations, the difference between the modelled and measured changes of nutrient concentrations in the upper water layer (comprising UML and thermocline) was taken as an estimate of the amount of consumed nutrients.

Fine structure of vertical stratification related to the observed Chl *a* maxima was analysed using vertical profiles of Brunt–Väisälä frequency estimated as $N^2 = -g/\rho \cdot \partial\rho/\partial z$, where g is acceleration due to gravity, ρ is density and $\partial\rho/\partial z$ is vertical density gradient. The flow structure in the study area at the time of surveys was characterised by vertical profiles of relative cross-transect geostrophic velocity, which were estimated on the basis of CTD data as: $u = 1/fL\int_{p_{ref}}^{p}(\delta_{p,i} - \delta_{p,i+2})dp$, where f is the Coriolis parameter, L – the distance between the stations i and $i+2$ (about 5.2 km) and $\delta_{p,i}$ and $\delta_{p,i+2}$ – vertical profiles of specific volume anomaly at stations i and $i+2$. The reference level of no motion (p_{ref}) was chosen at 40 dbar in the open gulf and at the seabed in the shallower areas.

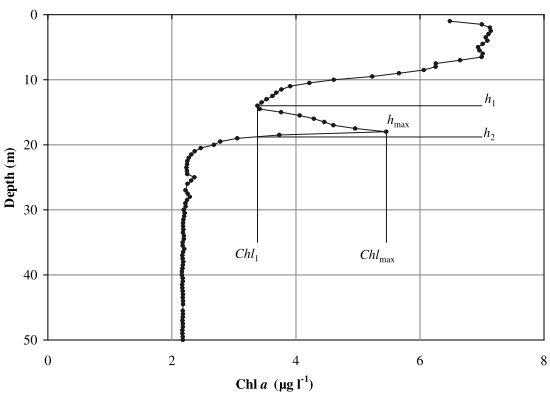

Fig. 2. Sketch used to define the parameters of sub-surface Chl *a* maxima (vertical profile is obtained at station TH8 on 11 July). Chl_{max}, h_{max} – maximum Chl *a* value below 10 m depth and depth of this maximum; Chl_1, h_1– minimum Chl *a* value above h_{max} and depth of this minimum; h_2 – depth where the Chl *a* values below the maximum decrease back to Chl_1.

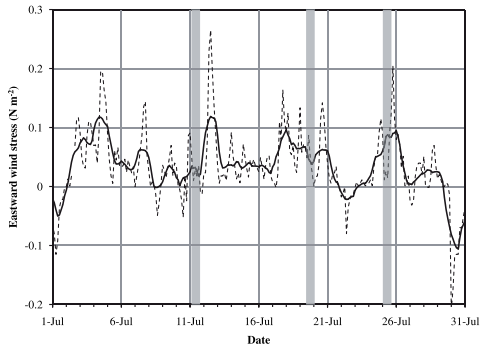

Fig. 3. Eastward wind stress (dashed line) in July 2006 estimated using wind data from Kalbådagrund meteorological station. Daily average wind stress is shown as solid line and vertical grey areas indicate the periods of sampling.

3. Results

According to the wind stress estimates southward cross-gulf Ekman drift (due to the eastward wind stress; Fig. 3) prevailed in the surface layer of the Gulf of Finland in July 2006. The surveys on 11 July and on 25 July were conducted after the periods of relatively weak winds from varying direction. The survey on 19–20 July was conducted when moderate westerly winds have been prevailed for a week. It resulted in an upwelling near the northern coast and a downwelling near the southern coast of the gulf. A more detailed description of upwelling and downwelling events in the Gulf of Finland in summer 2006 is given by Lips et al. (2009).

Vertical profiles of Chl *a* registered in July 2006 in the Gulf of Finland revealed the occurrence of sub-surface maximum layers of phytoplankton at many sampling stations (Fig. 4). Even if in most cases the maximum Chl *a* values were observed in UML, local maxima in the thermocline layer were quite common on the vertical profiles during all surveys. The Chl *a* content in UML on 11 July was higher in the open gulf – up to 6–8 $\mu g\ l^{-1}$ – than that in the coastal areas. On 19–20 July, the UML Chl *a* content was $<6\ \mu g\ l^{-1}$ except in the upwelling front at the northernmost part of the study transect where the maximum values exceeded 10 $\mu g\ l^{-1}$. On 25 July, higher Chl *a* values were observed in the northern part – reaching 7–8 $\mu g\ l^{-1}$ and lower values in the southern part – mostly $<6\ \mu g\ l^{-1}$.

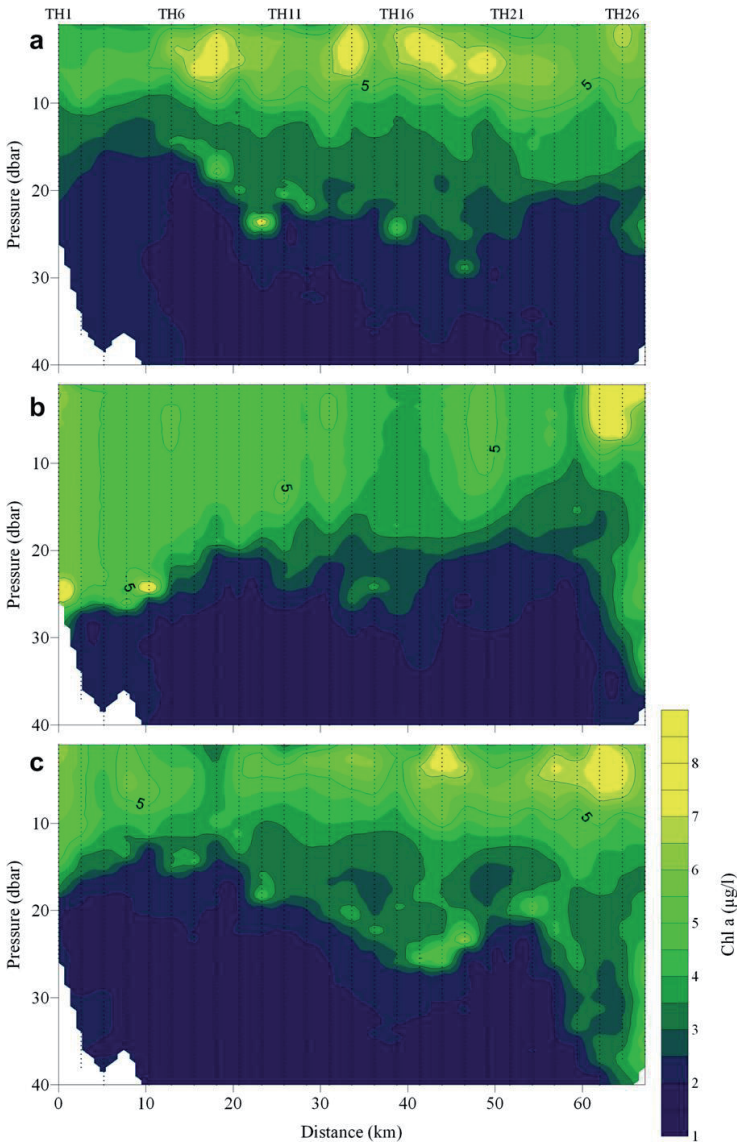

Fig. 4. Vertical sections of Chl *a* on 11 (a), 19–20 (b) and 25 (c) July 2006. Dotted lines indicate profiles; values on *x*-axis are distance from the southernmost station (TH1); station numbers are shown above.

In total the sub-surface Chl *a* maxima with intensities ≥0.5 μg l^{-1} were observed at 37 stations out of analysed 80 stations, ≥1.0 μg l^{-1} at 19, ≥2.0 μg l^{-1} at 7 and ≥5.0 μg l^{-1} at 4 stations. The characteristics of observed sub-surface Chl *a* maximum layers are summarised in Table 1. The highest observed Chl *a* values in these maximum layers were 10.5 μg l^{-1} on 11 July (at station TH10), 12.2 μg l^{-1} and 11.4 μg l^{-1} on 19–20 July (at stations TH1 and TH5, respectively) and 8.2 μg l^{-1} on 25 July (at station TH19). If excluding the sub-surface Chl *a* maximum observed close to the seabed at the shallowest station (TH1) on 19–20 July, all other three most intense maximum layers comply with the "thin layer" definition in regard of the optical signal (Dekshenieks et al., 2001). While their intensities estimated as shown in Fig. 2 were 7.6 μg l^{-1}, 6.9 μg l^{-1} and 5.1 μg l^{-1}, the Chl *a* fluorescence values measured in maxima where at least three times greater than the background Chl *a* fluorescence level. The depth of maxima varied between 14.5 and 35 m while the average depth of maxima was 23.0 ± 4.6 m (arithmetic mean and standard deviation are given, median was 23.5 m). Average values of temperature, salinity and density anomaly (density minus 1000 in kg m^{-3}) in the observed maxima were 4.73 ± 1.75 °C (median 4.46 °C), 5.85 ± 0.30 (median 5.86) and 4.61 ± 0.28 kg m^{-3} (median 4.65 kg m^{-3}), respectively.

The occurrence of Chl *a* maximum layers was found to be very well related to the registered vertical temperature structure (Fig. 5). An ordinary vertical distribution of temperature was observed on 11 July 2006 with sea surface temperature >20 °C at almost all stations and the seasonal thermocline situated at the depths of 10–20 m. Eight days later an upwelling event was observed near the northern coast and downwelling in the southernmost part of the study transect. On 25 July, the sea surface temperature was between 19 and 20 °C and the thermocline was steeper than in the beginning of study period. The UML depth was on average 7 m on 11 July, 12 m on 19–20 July and 8 m on 25 July. The base of thermocline was situated at 24 m on 11 July, 23 m on 19–20 July and 21 m on 25 July. While on 19–20 July the thermocline characteristics were affected by a coupled upwelling-downwelling event, on 11 and 25 July the observed thermocline characteristics could be considered as typical ones in July in the Gulf of Finland. According to these two surveys the UML was shallower in the northern gulf than that in the southern part. In contrary, the base of thermocline was shallower in the southern gulf. As a consequence a very pronounced (steep) thermocline with vertical temperature and density gradients up to 2.43 °C m^{-1} and 0.48 kg m^{-4} was observed in the southern gulf while thermocline was thicker in the northern gulf.

As seen from the vertical cross-sections of temperature (Fig. 5) the Chl *a* maxima followed almost precisely the base of thermocline. On 11 July, the maxima were situated just above the base of

Table 1
Characteristics of sub-surface Chl *a* maximum layers with intensities ≥0.5 μg l^{-1} observed in the Gulf of Finland in July 2006. The maxima with fluorescence signal more than three times greater than the background signal are indicated in bold.

Date	Station	Chl *a* fluores. (a.u.)	Chl *a* (μg l^{-1})	Depth (m)	Intensity fluores. (a.u.)	Intensity Chl *a* (μg l^{-1})	Thickness (m)	Temp. (°C)	Salin.	Density anomaly (kg m^{-3})
11/07	TH6	4.3	3.8	14.5	0.9	0.5	2.5	6.67	5.58	4.34
11/07	TH7	4.8	4.1	15.0	1.5	0.8	2.5	5.77	5.66	4.44
11/07	TH8	8.1	6.0	18.0	4.8	2.8	4.5	4.39	5.52	4.38
11/07	TH9	4.8	4.1	20.0	1.7	1.0	4.0	5.35	5.74	4.53
11/07	**TH10**	**15.9**	**10.5**	**23.5**	**13.2**	**7.6**	**2.5**	**4.38**	**5.99**	**4.75**
11/07	TH11	6.0	4.8	20.5	3.1	1.8	5.5	5.36	5.69	4.48
11/07	TH12	4.8	4.1	22.0	1.5	0.9	4.5	5.68	5.39	4.24
11/07	TH14	3.7	3.5	22.0	1.0	0.6	3.5	5.43	5.53	4.35
11/07	TH16	5.7	4.6	24.5	2.8	1.6	4.5	4.79	5.60	4.43
11/07	TH18	3.5	3.4	22.5	0.9	0.5	6.0	6.19	5.36	4.19
11/07	TH19[a]	3.7	3.5	25.0	1.1	0.6	2.5	5.02	5.84	4.61
11/07	TH19[a]	5.0	4.3	29.0	2.8	1.6	3.0	3.73	6.13	4.88
11/07	TH26	3.0	3.1	24.5	1.0	0.6	4.0	3.87	5.88	4.68
11/07	TH27	4.4	3.9	23.5	1.6	0.9	6.5	3.81	5.95	4.73
19/07	TH1	18.9	12.2	25.0	11.0	6.4	5.0[b]	11.81	5.73	3.97
19/07	TH4	8.9	6.5	26.0	3.9	2.2	2.0	5.67	6.08	4.78
19/07	**TH5**	**17.4**	**11.4**	**24.5**	**11.9**	**6.9**	**3.0**	**6.52**	**6.01**	**4.68**
19/07	TH8	5.3	4.4	19.0	1.2	0.7	1.5	8.19	5.80	4.40
19/07	TH14	3.4	3.3	25.5	1.2	0.7	6.0	2.54	6.31	5.03
19/07	TH15	4.5	4.0	24.0	2.4	1.4	3.0	2.79	6.21	4.95
19/07	TH16	2.9	3.0	25.0	1.0	0.6	5.5	2.99	6.20	4.94
19/07	TH24	4.1	3.7	15.5	0.9	0.5	4.0	6.39	5.15	4.01
19/07	TH26	4.3	3.8	20.5	1.0	0.6	4.0	4.5	5.81	4.60
19/07	TH27[a]	6.5	5.1	25.5	1.2	0.7	7.0	3.58	5.99	4.77
19/07	TH27[a]	5.9	4.7	32.0	1.4	0.8	5.0	3.04	6.19	4.93
25/07	TH7	5.4	4.4	14.5	2.2	1.3	2.5	4.42	6.32	5.02
25/07	TH10	6.2	4.9	18.5	3.2	1.8	6.5	4.09	5.91	4.69
25/07	TH14	4.6	4.0	20.5	1.6	0.9	3.5	4.83	5.71	4.52
25/07	TH15	4.3	3.8	22.5	2.0	1.1	4.5	4.61	5.76	4.57
25/07	TH16	4.0	3.7	19.5	1.1	0.6	7.0	6.67	5.56	4.31
25/07	TH17	6.7	5.2	25.5	3.4	2.0	5.0	3.29	6.03	4.81
25/07	TH18	6.8	5.3	26.0	3.5	2.0	5.0	3.53	5.95	4.73
25/07	**TH19**	**11.9**	**8.2**	**23.5**	**8.9**	**5.1**	**5.5**	**3.52**	**5.88**	**4.68**
25/07	TH21	4.1	3.7	20.5	1.3	0.8	5.0	4.34	5.68	4.51
25/07	TH22	5.8	4.7	19.5	3.0	1.7	5.5	4.80	5.49	4.35
25/07	TH23	4.9	4.2	22.5	1.8	1.0	8.0	4.63	5.66	4.48
25/07	TH24[a]	4.2	3.8	26.0	1.0	0.6	7.0	3.97	5.93	4.71
25/07	TH24[a]	3.6	3.4	33.0	1.0	0.6	4.5	2.27	6.46	5.15
25/07	TH25	3.6	3.4	35.0	1.4	0.8	5.0	2.41	6.47	5.16
25/07	TH27	6.1	4.9	27.5	2.2	1.3	9.0	3.53	6.02	4.79

[a] Two sub-surface Chl *a* maxima were found on the profile.
[b] Lower border of Chl *a* maximum layer was defined as the deepest measurement point on the profile.

thermocline and were related to the isotherm 5 °C (average temperature at maxima was 5.0 ± 0.9 °C), except a secondary maximum at station TH19. On 19 July, the most intensive maxima were observed in the thermocline in the downwelling area and less pronounced maxima in the central part of the study transect below the thermocline. The initial pattern of maxima distribution was re-established on 25 July; however, the maxima were less pronounced and they were registered almost precisely at the base of thermocline and at slightly lower temperatures than those on 11 July (average temperature at maxima on 25 July was 4.1 ± 1.1 °C).

The vertical structure of salinity field was characterised by low values in the surface layer – from 4.5 to 5.3 on 11 July, from 4.7 to 5.2 on 19–20 July and from 4.5 to 5.1 on 25 July – and by a continuous increase of salinity in the seasonal thermocline and below it. The Chl *a* maxima were mostly observed in the salinity range from 5.8 to 6.2.

The vertical sections of nutrients on 11 and 25 July revealed low nutrient concentrations in the upper layer – UML and upper part of the thermocline – and higher values with relatively patchy distribution in the deeper layer below the thermocline (Fig. 6). According to both surveys the nitrates + nitrites were completely consumed

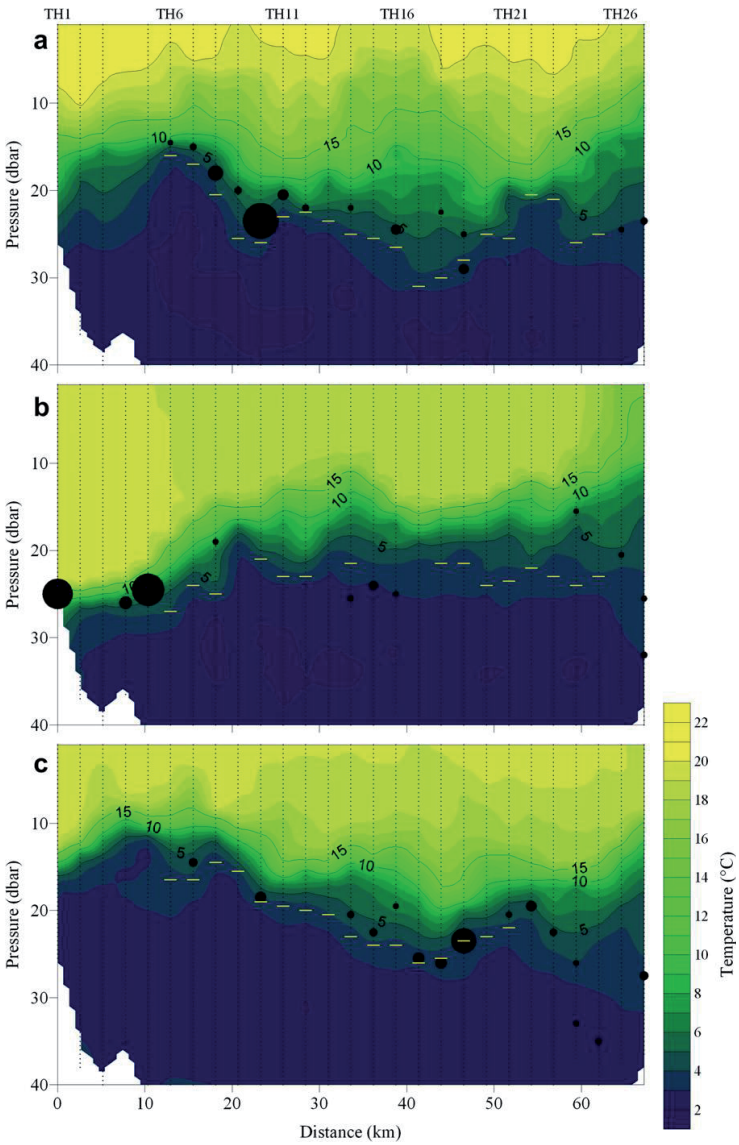

Fig. 5. Vertical sections of temperature on 11 (a), 19–20 (b) and 25 (c) July 2006. Dotted lines indicate profiles; values on *x*-axis are distance from the southernmost station (TH1); station numbers are shown above. Observed sub-surface Chl *a* maxima are indicated as black circles scaled proportionally to the intensity of maxima; the base of thermocline is shown by yellow/light dashes (the base of thermocline was not determined if the profile did not reach the minimum temperature).

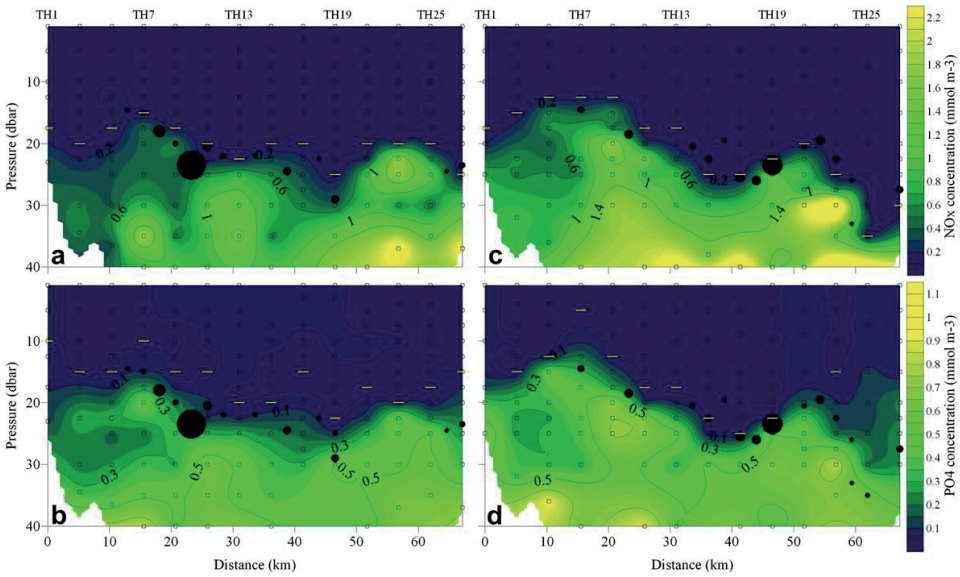

Fig. 6. Vertical sections of nutrient concentrations: (a) – NO_x on 11 July, (b) – PO_4 on 11 July, (c) – NO_x on 25 July and (d) – PO_4 on 25 July. Dots indicate the sampling points; values on *x*-axis are distance from the southernmost station (TH1); station numbers are shown above. Observed sub-surface Chl *a* maxima are indicated as black circles scaled proportionally to the intensity of maxima; the depth of nutriclines (nitracline and phosphacline, respectively) is shown by yellow/light dashes.

from the UML while detectable concentrations of phosphates were measured at some stations in the central part on 11 July and at some stations in the coastal areas on 25 July. A comparison of corresponding nutrient distributions in the deeper layer on 11 and 25 July shows that slightly higher concentrations, especially in the southern part and for nitrates + nitrites, were observed during the latter survey. The registered sub-surface Chl *a* maxima coincided well with the nutriclines, especially with the nitracline. Since the vertical resolution of water sampling was 2.5 m or more and the samples were taken not at all stations it is not possible to indicate the exact nutrient concentrations in the maximum layers. However, at most of the stations with sub-surface maxima the concentrations of NO_x were below the lower detection range in the samples taken above the Chl *a* maximum layer and detectable concentrations were measured in the samples taken just below the maxima.

According to the model results the average NO_x concentration in the upper 0–25 m layer increased in a two-week period from 11 to 25 July by 0.16 mmol m^{-3} (Laanemets et al., in press), which corresponds to an average nitrate flux at the 25 m depth level of 0.3 mmol N m^{-2} d^{-1}. On the basis of measurements, the increase of NO_x concentration in the upper 0–25 m layer between surveys on 11 and 25 July was only 0.04 mmol m^{-3}. If assuming that this discrepancy between measurements and model might be related to the nutrients transported upward and taken up by phytoplankton in the thermocline one can suppose that about $^3/_4$ of nitrates was consumed. Given that the local wind forcing before 11 July was similar to that within the period from 11 to 25 July (see Fig. 3) we may assume that an upward nutrient flux of similar intensity (0.3 mmol N m^{-2} d^{-1}) occurred also before our first survey on 11 July.

Filamentous cyanobacteria species/groups and dinoflagellate *H. triquetra* (Ehrenberg) Stein were dominating in the UML phytoplankton community in the Gulf of Finland in July 2006 (more detailed description of phytoplankton dynamics in the UML can be found in (Lips and Lips, 2010)). Wet weight biomass up to 1039 mg m^{-3} (54% of total phytoplankton biomass) on 11 July, up to 1013 mg m^{-3} (56%) on 19–20 July and up to 542 mg m^{-3} (39%) on 25 July of the latter species known to be forming sub-surface maxima was observed. Only one quantitative phytoplankton sample from a sub-surface Chl *a* maximum was analysed. The sample was collected at station TH19 on 25 July from 22.5 m depth where the Chl *a* fluorescence value was a half of that at the fluorescence peak registered at 23.5 m depth (see Fig. 7a; relative depth 1 m). The phytoplankton community at this sampling point was dominated by *H. triquetra* (288 mg m^{-3}, 33%), *Aphanizomenon* sp. (L.) Ralfs (203 mg m^{-3}, 23%) and *Dinophysis acuminata* Claparède and Lachmann (147 mg m^{-3}, 17%). The two former species had a similar share while the latter species was absent in the UML community at the same station.

Vertical profiles of Brunt–Väisälä frequency estimated over 2 m intervals and presented as functions of the relative depth (calculated as the distance from the depth of maximum Chl *a* value – h_{max}) revealed a quite high variability (Fig. 7b). Nevertheless, an average profile indicates a clear weakening of stratification with the depth in the vicinity of h_{max}. The two most intense Chl *a* maxima were associated with the weakest stratification in the water layer from 1 to 3 m below h_{max}. While a sharp drop of Chl *a* values below h_{max} was observed at almost all stations (Fig. 7a) the profiles were more variable above h_{max}. At some stations, where the stratification was stronger just above h_{max}, the Chl *a* maximum layers were thicker (station TH19 on 25 July as an example) and at stations with a weaker stratification above h_{max}, thinner Chl *a* maximum layers were observed (among them the most intense sub-surface Chl *a* maximum sampled at station TH10 on 25 July).

According to the cross-transect geostrophic velocity distributions in the upper 40-m layer (Fig. 8), an outflow prevailed in the central part of the gulf and an inflow in the southernmost and northernmost areas on 11 July. Next survey on 19–20 July revealed a cross-transect jet current associated with the upwelling front in the northern part of the study transect and another jet current

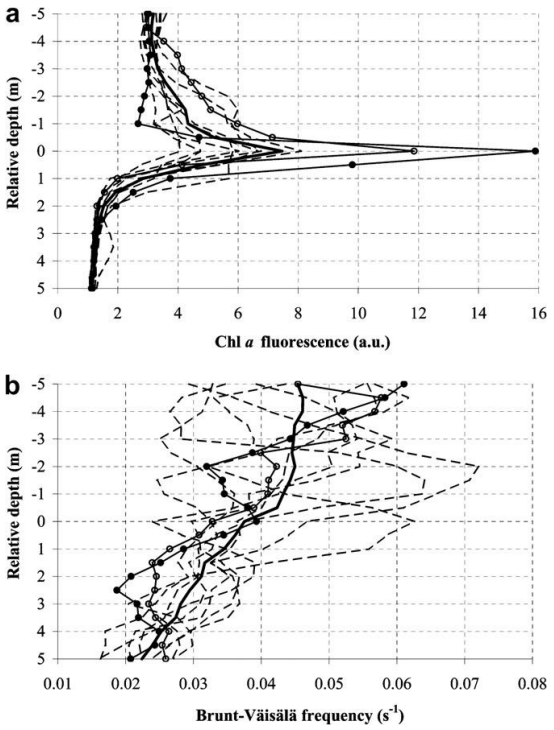

Fig. 7. Vertical profiles of Chl *a* fluorescence (a) and Brunt–Väisälä frequency (b) at selected stations (TH8-TH12 on 11 July and TH17-TH19, TH21-TH22 on 25 July) as functions of the relative depth (calculated as the vertical distance from the depth of maximum Chl *a* value – h_{max}). Brunt–Väisälä frequency was estimated over 2 m intervals. Average profiles are shown as thick solid lines, profiles at station TH10 on 11 July as thin solid lines with filled circles and at station TH19 on 25 July as thin solid lines with empty circles.

coupled with the downwelling in the southern gulf. Only a narrow outflow region in the central gulf was evident on 19–20 July. The geostrophic current structure was characterised mainly by an outflow in the upper layer except narrow inflow regions in the northernmost, southernmost and central parts of the study transect on 25 July.

Presented geostrophic velocity distributions with alternating flow directions along the study transect could be interpreted as a sequence of meso-scale eddies or as a sequence of cyclonic and/or anti-cyclonic circulation cells. On 11 July, two of such anti-cyclonic circulation cells were evident – first in the southern part between 15 and 30 km and second in the central part within the thermocline between 33 and 48 km. On 25 July a similar to the latter circulation cell with higher velocities in the thermocline was observed between 33 and 48 km. As seen in Fig. 8, most of the detected sub-surface maximum layers, especially those with the highest intensities, were located at the base of the described meso-scale features (anti-cyclonic circulation cells). On 19–20 July, the Chl *a* maxima were observed mainly in the downwelling area which could be also characterised as an anti-cyclonic circulation cell with horizontal convergence of water masses.

4. Discussion

Our measurements in July 2006 along the study transect Tallinn-Helsinki in the Gulf of Finland confirm that the sub-surface Chl *a* maximum layers can exist in a stratified water column in summer when the upper layer is depleted of nutrients while high reserves of nutrients are available below the seasonal thermocline. The detected maxima were almost all located at the base of thermocline and coincided well with the depth of nutriclines. The former indicates that the vertical stratification and related hydrodynamic conditions, such as mixing and/or current shear, could play an important role in formation of the observed Chl *a* maxima. The latter points either to the nutrient availability as a major factor controlling the formation of sub-surface Chl *a* maximum layers or to the nutrient uptake by the phytoplankton in the Chl *a* maxima at the base of thermocline that maintained the nutriclines exactly at these depths.

The Chl *a* maxima were located at the depths between 14.5 and 35 m with an average of 23 m. Since the Secchi disk depth in the study area during all surveys did not exceed 5 m, very low irradiances could be assumed at the depths of the observed maxima. We estimated PAR attenuation coefficient K_d on the basis of optical measurements in the upper 3 m layer in the study area on 11 July (T. Kutser and L. Metsamaa, personal communication). According to these estimates of K_d (from 0.33 to 0.55 m^{-1}) the photic depth varied between 8.4 and 13.9 m, which are clearly less than the average depth of observed sub-surface maxima. Similar relatively deep Chl *a* maxima observed in the Gulf of Finland in July 1998 at low irradiances (<0.1% of the sea surface irradiance) were formed by *H. triquetra* (Kononen et al., 2003). Phytoplankton community data suggest that the Chl *a* maximum layers observed in July 2006 were also dominated by *H. triquetra*, as it was the dominating species in the sample collected close to a sub-surface Chl *a* fluorescence peak and one of the dominant species in the UML in our study area. Since the Chl *a* maximum layers were observed during all three surveys conducted within two weeks in July 2006, the favourable conditions should have existed for a relatively long period to support their formation and maintenance. Among these favourable conditions the hydrodynamic processes producing upward flux of nutrients and/or the nutrient conditions or hydrodynamic processes triggering downward migration of phytoplankton could be referred.

Several estimates based on the field measurements are available indicating that in certain conditions the upward nutrient fluxes may support formation and maintenance of sub-surface Chl *a* maxima. In the studies by Sharples et al. (2001) and Hales et al. (2009) the vertical turbulent nitrate fluxes were estimated at 0.8–5.2 mmol N m^{-2} d^{-1} which could support a net phytoplankton productivity of 64–360 mg C m^{-2} d^{-1}. In the southwest Kattegat, Baltic Sea where a sub-surface Chl *a* maximum was observed in October 2003 the nitrate flux as high as 17 mmol N m^{-2} d^{-1} was estimated (Lund-Hansen et al., 2006). One of the favourable conditions supporting the development of sub-surface maxima is the functioning of estuarine circulation with opposite flow directions in the layers above and below the thermocline resulting in an upward volume (and nutrient) flux in the gulf interior (Elken et al., 2003; Lips et al., 2008). A modelling study (Laanemets et al., in press) gave an estimate of average nitrate flux of 0.3 mmol N m^{-2} d^{-1} at the 25 m depth level in the central Gulf of Finland in July 2006, which according to our assumption was in a large extent consumed by phytoplankton in the sub-surface layer. This estimate of nitrate flux is one order of magnitude lower than those referred above. It has to be noted that the contribution of vertical ammonium flux (ammonium was not measured in our study) could double the flux of available dissolved inorganic nitrogen due to the high concentrations of ammonium in the Gulf of Finland deep layers (e.g. Pitkänen et al., 2008). However, it appears that the upward nutrient flux was still not large enough to maintain the sub-surface Chl *a* maxima along the entire study

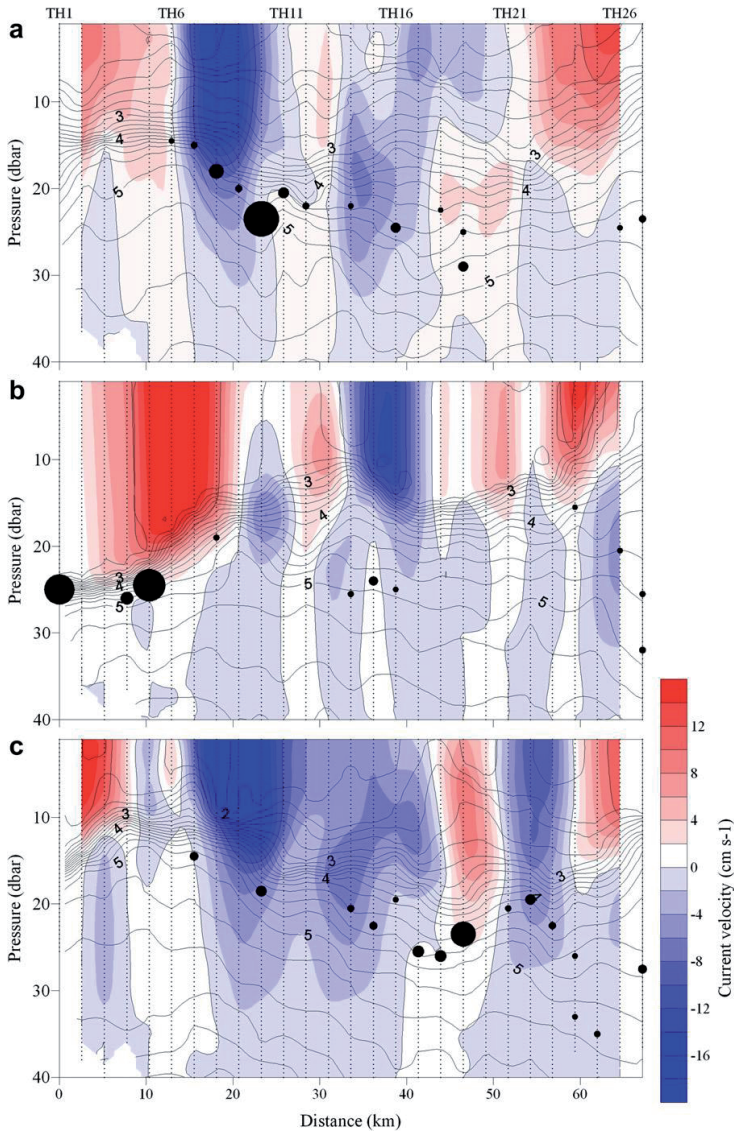

Fig. 8. Vertical sections of cross-transect geostrophic current velocity on 11 (a), 19–20 (b) and 25 (c) July 2006. The reference level of no motion was chosen at 40 dbar in the open gulf and at the seabed in the shallower areas. Corresponding density anomaly distribution (density − 1000 kg m^{-3}) is shown by black contour lines. Dotted lines indicate profiles; values on *x*-axis are distance from the southernmost station (TH1); station numbers are shown above. Observed sub-surface Chl *a* maxima are indicated as black circles scaled proportionally to the intensity of maxima.

transect at all three surveys in July 2006. As a result the sub-surface maxima were observed at about 50% of stations and only a few of them revealed at least three times greater optical signal than the background level. Thus, it needs to be analysed what processes were responsible for the observed patchiness of horizontal distribution of sub-surface maxima.

Many earlier studies have revealed evidences that the mesoscale processes shape the horizontal distribution of phytoplankton both in the surface layer and in the sub-surface layer whereas pure advection of biomass as well as local growth enhancement might cause the observed patchiness. It is well documented that eddy/wind interactions can generate high sub-surface diatom biomass in mode-water eddies (McGillicuddy et al., 2007). The tracer measurements were used to estimate the vertical advection and turbulent diffusion of deep-water nutrients into a sub-surface Chl *a* layer and the flux of dissolved inorganic nitrogen was found to be large enough to maintain the observed high diatom biomass (Ledwell et al., 2008). On the other hand, Johnston et al. (2009) related the appearance of thin layers in a coastal upwelling zone to the advection and current shear and argued that initially thick

sub-surface Chl *a* maxima were transformed into thin layers by current shear on the flanks of the eddies, filaments, and fronts. The peak values in the observed thin layers exceeded concentrations in the upwelled source waters and stayed unexplained by the available data.

The cross-transect geostrophic velocity distributions revealed that the sub-surface Chl *a* maximum layers detected in the Gulf of Finland in July 2006 were located mostly at the base of anticyclonic circulation cells. Although the highest Chl *a* maxima observed on 11 and 25 July were related to the meso-scale circulation cells similar to mode-water eddies, our results differ from those referred above (McGillicuddy et al., 2007; Ledwell et al., 2008), first, the scales are non-comparable and, secondly, the maxima were found at the base of circulation cells where the isopycnlas were depressed (not at the domed isopycnals above, see Fig. 8). On 19–20 July, the most intense sub-surface Chl *a* maxima were found in the downwelling area where the thermocline had the deepest position but the horizontal convergence of waters could be expected. Therefore, we conclude that the most intense maxima could be formed due to the accumulation of downward migrated phytoplankton cells near the base of the meso-scale features.

The formation of such patches of high biomass of phytoplankton could be favoured both by the ability of cells to reach and maintain these depths (the shallowest depth where high enough nutrient concentrations were available for the growth) and by the horizontal convergence of waters along the depressed isopycnals at the base of anti-cyclonic circulation cells. It has been reported that the swimming speed of *H. triquetra* in a turbulent environment could be as high as 0.5–0.75 m h^{-1} (Anderson and Stolzenbach, 1985). We have recorded downward migration of phytoplankton community dominated by *H. triquetra* in the Gulf of Finland in July 2009 of about 20 m during a 24 h period (unpublished data). Thus, the phytoplankton can reach the observed depths of Chl *a* maxima within a day. A clear weakening of stratification with the depth just below the observed maxima could be considered as an indirect indication of vertical mixing and nutrient fluxes supporting the possible nutrient uptake there. Unlike to many other dinoflagellates *H. triquetra* might assimilate nitrate in the dark as efficiently as in the light (Paasche et al., 1984) and that explains the coinciding depth of Chl *a* maxima and nitracline.

5. Conclusions

Our measurements in July 2006 showed that the sub-surface Chl *a* maximum layers are common in the Gulf of Finland stratified water column in summer. The Chl *a* maxima were mostly located at the base of thermocline and coincided well with the depths of nutriclines. We suggest that downward migration of phytoplankton capable for nutrient uptake in dark and upward flux of nutrients caused by estuarine circulation and vertical turbulent mixing created favourable conditions for the formation and maintenance of sub-surface Chl *a* maxima. The observed horizontal patchiness of sub-surface Chl *a* maximum layers could be related to the meso-scale processes. The accumulation of phytoplankton was observed along the depressed isopycnals at the base of anti-cyclonic circulation cells and in the downwelling area characterised by the horizontal convergence of waters.

Acknowledgments

This work was financially supported by the Estonian Science Foundation (grants no. 6752 and 6955) and Foundation Innove (grant no. 1.0101-0279). Authors appreciate the help of colleagues and crew members who participated in the field measurements. We express our gratitude to Dorrit Talts who first analysed the fluorescence profiles presented here during her Master studies. We thank Liisa Metsamaa and Tiit Kutser for providing us with data of optical measurements and the Finnish Meteorological Institute for wind data at Kalbådagrund station.

References

Anderson, D.M., Stolzenbach, K.D., 1985. Selective retention of two dinoflagellates in a well-mixed estuarine embayment: the importance of diel vertical migration and surface avoidance. Marine Ecology Progress Series 25, 39–50.

APHA, 1992. APHA, AWWA, and WPCF Standard Methods for the Examination of Water and Wastewater, 18th ed. American Public Health Association, Washington, DC.

Blumberg, A.F., Mellor, G.L., 1983. Diagnostic and prognostic numerical calculation studies of the South Atlantic Bight. Journal of Geophysical Research 88 (C8), 4579–4592.

Dekshenieks, M.M., Donaghay, P.L., Sullivan, J.M., Rines, J.E.B., Osborn, T.R., Twardowski, M.S., 2001. Temporal and spatial occurrence of thin phytoplankton layers in relation to physical processes. Marine Ecology Progress Series 223, 261–271.

Elken, J., Raudsepp, U., Lips, U., 2003. On the estuarine transport reversal in deep layers of the Gulf of Finland. Journal of Sea Research 49, 267–274.

Fennel, K., Boss, E., 2003. Subsurface maxima of phytoplankton and chlorophyll: steady-state solutions from a simple model. Limnology and Oceanography 48, 1521–1534.

Hales, B., Hebert, D., Marra, J., 2009. Turbulent supply of nutrients to phytoplankton at the New England shelf break front. Journal of Geophysical Research 114, C05010. doi:10.1029/2008JC005011.

Helsinki Commission, 1988. Guidelines for the Baltic Monitoring Programme for the third stage. Part D. Biological determinands. Baltic Sea Environment Proceedings 27D, 1–161.

Hickman, A.E., Holligan, P.M., Moore, C.M., Sharples, J., Krivtsov, V., Palmer, M.R., 2009. Distribution and chromatic adaptation of phytoplankton within a shelf sea thermocline. Limnology and Oceanography 54, 525–536.

Johnston, T.M.S., Cheriton, O.M., Pennington, J.P., Francisco, P.C., 2009. Thin phytoplankton layer formation at eddies, filaments, and fronts in a coastal upwelling zone. Deep-Sea Research II 56, 246–259.

Kahru, M., Aitsam, A., Elken, J., 1982. Spatio-temporal dynamics of chlorophyll in the open Baltic Sea. Journal of Plankton Research 4, 779–790.

Kanoshina, I., Lips, U., Leppänen, J.-M., 2003. The influence of weather conditions (temperature and wind) on cyanobacterial bloom development in the Gulf of Finland (Baltic Sea). Harmful Algae 2, 29–42.

Klausmeier, A., Litchman, E., 2001. Algal games: the vertical distribution of phytoplankton in poorly mixed water columns. Limnology and Oceanography 46, 1998–2007.

Kononen, K., Kuparinen, J., Mäkelä, K., Laanemets, J., Pavelson, J., Nõmmann, S., 1996. Initiation of cyanobacterial blooms in a frontal region at the entrance of the Gulf of Finland, Baltic Sea. Limnology and Oceanography 41, 98–112.

Kononen, K., Hällfors, S., Kokkonen, M., Kuosa, H., Laanemets, J., Pavelson, J., Autio, R., 1998. Development of a subsurface chlorophyll maximum at the entrance to the Gulf of Finland, Baltic Sea. Limnology and Oceanography 43, 1089–1106.

Kononen, K., Huttunen, M., Hällfors, S., Gentien, P., Lunven, M., Huttula, T., Laanemets, J., Lilover, M., Pavelson, J., Stips, A., 2003. Development of a deep chlorophyll maximum of *Heterocapsa triquetra* Ehrenb. At the entrance to the Gulf of Finland. Limnology and Oceanography 48, 594–607.

Kuosa, H., 1990. Subsurface chlorophyll maximum in the northern Baltic Sea. Archive für Hydrobiologie 118, 437–447.

Laanemets, J., Väli, G., Zhurbas, V., Elken, J., Lips, I., Lips, U., Simulation of mesoscale structures and nutrient transport during summer upwelling events in the Gulf of Finland in 2006. Boreal Environment Research, in press.

Laanemets, J., Pavelson, J., Lips, U., Kononen, K., 2005. Downwelling related mesoscale motions at the entrance to the Gulf of Finland: observations and diagnosis. Oceanological and Hydrobiological Studies 34 (2), 15–36.

Ledwell, J.R., McGillicuddy, D.J., Anderson, L.A., 2008. Nutrient flux into an intense deep chlorophyll layer in a mode-water eddy. Deep-Sea Research II 55, 1139–1160.

Lips, I., Lips, U., Kononen, K., Jaanus, A., 2005. The effect of hydrodynamics on the phytoplankton primary production and species composition at the entrance to the Gulf of Finland (Baltic Sea) in July 1996. Proceedings of Estonian Academy of Sciences. Biology. Ecology 54 (3), 210–229.

Lips, I., Lips, U., Liblik, T., 2009. Consequences of coastal upwelling events on physical and chemical patterns in the central Gulf of Finland (Baltic Sea). Continental Shelf Research 29, 1836–1847.

Lips, I., Lips, U., 2010. Phytoplankton dynamics affected by the coastal upwelling events in the Gulf of Finland in July–August 2006. Journal of Plankton Research, doi:10.1093/plankt/fbq049.

Lips, U., Lips, I., Liblik, T., Elken, J., 2008. Estuarine Transport versus Vertical Movement and Mixing of Water Masses in the Gulf of Finland (Baltic Sea). US/EU-Baltic International Symposium, 27–29 May 2008. Institute of Electrical and Electronics Engineers/Oceanic Engineering Society (IEEE/OES), Tallinn. doi:10.1109/BALTIC. 4625535.

Lund-Hansen, L.C., Ayala, P.C.A., Reglero, A.F., 2006. Bio-optical properties and development of a sub-surface chlorophyll maxima (SCM) in south-west Kattegat, Baltic Sea. Estuarine. Coastal and Shelf Science 68, 372–378.

McGillicuddy, D.J., Anderson, L.A., Bates, N.R., Bibby, T., Buesseler, K.O., Carlson, C., Davis, C.S., Ewart, C., Falkowski, P.G., Goldthwait, S.A., Hansell, D.A., Jenkins, W.J., Johnson, R., Kosnyrev, V.K., Ledwell, J.R., Li, Q.P., Siegel, D.A., Steinberg, D.K., 2007. Eddy-wind interactions stimulate extraordinary mid-ocean plankton blooms. Science 316, 1021–1026.

McManus, M.A., Alldredge, A.L., Barnard, A., Boss, E., Case, J., Cowles, T.J., Donaghay, P. L., Eisner, L., Gifford, D.J., Greenlaw, C.F., Herren, C., Holliday, D.V., Johnson, D., MacIntyre, S., McGehee, D., Osborn, T.R., Perry, M.J., Pieper, R., Rines, J.E.B., Smith, D.C., Sullivan, J.M., Talbot, M.K., Twardowski, M.S., Weidemann, A., Zaneveld, J.R.V., 2003. Characteristics, distribution and persistence of thin layers over a 48 hours period. Marine Ecology Progress Series 261, 1–19.

Paasche, E., Bryceson, I., Tangen, K., 1984. Interspecific variation in dark nitrogen uptake by dinoflagellates. Journal of Phycology 20 (3), 394–401.

Pavelson, J., Kononen, K., Laanemets, J., 1999. Chlorophyll distribution patchiness caused by hydrodynamical processes: a case study in the Baltic Sea. ICES Journal of Marine Science 56 (S), 87–99.

Pitkänen, H., Lehtoranta, J., Peltonen, H., 2008. The Gulf of Finland. In: Schiewer, U. (Ed.), Ecology of Baltic Coastal Waters. Ecological Studies 197. Springer, Berlin, pp. 285–308.

Richardson, K., Visser, A.W., Pedersen, F.B., 2000. Subsurface phytoplankton blooms fuel pelagic production in the North Sea. Journal of Plankton Research 22, 1663–1671.

Sharples, J., Moore, C.M., Rippeth, T.P., Holligan, P.M., Hydes, D.J., Fisher, N.R., Simpson, J.H., 2001. Phytoplankton distribution and survival in the thermocline. Limnology and Oceanography 46, 486–496.

Talpsepp, L., Nõges, T., Raid, T., Kõuts, T., 1994. Hydrophysical and hydrobiological processes in the Gulf of Finland in summer 1987: characterization and relationship. Continental Shelf Research 14, 749–763.

Utermöhl, H., 1958. Zur Vervollkommnung der quantitativen Phytoplanktonmetodic. Mittelungen des Internationale Vereinigung für Theoretische und Angewandte Limnologie 9, 1–38.

Wang, Z., Goodman, L., 2010. The evolution of a thin phytoplankton layer in strong turbulence. Continental Shelf Research 30, 104–118.

Weston, K., Fernand, L., Mills, D.K., Delahunty, R., Brown, J., 2005. Primary production in the deep chlorophyll maximum of the central North Sea. Journal of Plankton Research 27, 909–922.

ABSTRACT

The main aim of the thesis was to improve the present knowledge on the thermohaline structure of the Gulf of Finland in summer – on its variability and driving factors, and to reveal the consequences of processes shaping the thermohaline structure as well as the vertical stratification on the nutrient distribution and phytoplankton community dynamics.

Long-term changes in the thermohaline structure are related to the variations in the large-scale atmospheric circulation patterns. Such long-term changes were revealed on the basis of data from 1987-2009 in the deep layer and the cold intermediate layer. The increase of salinity and temperature in the deep layer of the Gulf of Finland is connected to the more intense water exchange between the North Sea and the Baltic Sea. An important feature for the pelagic primary production has been shown – the significant shift in vertical stratification at the halocline depth was not accompanied by similar changes in the intermediate and upper layer. The temperature of cold intermediate layer in the Gulf of Finland in summer depends strongly on the severity of the previous winter in the Baltic Sea area, whereas the temperature increases slowly in summer from June to August.

The Gulf of Finland as a typical estuary is stratified water body, and estuarine circulation scheme is prevailing here in the long-term. The most intense estuarine circulation and the strongest stratification of the water column exist in the Gulf when north-easterly, northerly and north-westerly winds are dominating in the region. For the Gulf's ecosystem, it is important that intensified estuarine circulation causes a considerable flux of nutrients (especially phosphorus) into the near bottom layer of the Gulf. Local, along-axis winds generate also coastal upwelling events, which besides redistributing of heat and salt, transport nutrients into the upper layer. In summer, when the nutrient concentrations are mostly below the detection limit in the surface layer, these events can supply additional resources for phytoplankton growth. For instance, the major upwelling event observed along the Estonian coast in August 2006 created flux of phosphate-phosphorus equal to the total monthly phosphorus load into the Gulf of Finland. In addition, the observations revealed that upwelling events are associated with remarkable vertical mixing of waters and could enlarge the separation of nitracline and phosphacline in the Gulf of Finland.

Vertical profiles of temperature, salinity and Chl *a* collected with high temporal resolution using an autonomous buoy profiler showed that atmospheric forcing at a synoptic scale leads to distinct prevailing physical processes and stratification patterns, which clearly differ from each other. The analysed data set revealed stratification patterns dominated by the following processes in summer 2009: upwelling, relaxation of the upwelling, reversal of the estuarine

circulation, ordinary estuarine circulation and downwelling. The changes of vertical stratification were simulated reasonably well by a simple model, where the heat flux through the sea surface, wind mixing, wind induced transport parallel to the horizontal salinity gradient and estuarine circulation were taken into account. The largest discrepancies between the observations and model results were evident when water movement across the Gulf and associated vertical displacement of isopycnals (upwelling or downwelling) prevailed.

The dominant physical processes and related thermohaline structures directly influenced the summer phytoplankton vertical dynamics. It was shown that the formation and maintenance of sub-surface chlorophyll a maxima layers were dependant on the vertical stratification – the maxima followed the base of thermocline and coincided with the nutriclines in the stratified Gulf of Finland in summer. Clear diurnal patterns in the vertical dynamics of phytoplankton were detected in certain periods. Autonomous profiler enabled measuring the downward movement of Chl *a* maximum with the speed of up to 1.6 m h^{-1} in the period of dominance of the dinoflagellate *Heterocapsa triquetra*.

RESÜMEE

Käesoleva uurimustöö eesmärgiks oli kirjeldada Soome lahe termohaliinsete väljade struktuuri suvekuudel ning määrata kindlaks peamised seda kujundavad ja selle muutlikkust põhjustavad protsessid. Teiseks, töös on püütud hinnata termohaliinsete väljade ja nende varieeruvuse mõju toitainete vertikaalsele jaotusele veesambas ja toitainete voogudele ning fütoplanktoni koosluste dünaamikale. Töös on kasutatud aastatel 1987-2009 kogutud temperatuuri ja soolsuse vertikaalsete profiilide andmeid, aastatel 2006, 2007 ja 2009 teostatud interdistsiplinaarsete mõõdistuste andmeid ja veesamba autonoomse profileerijaga suure ajalise lahutusega juulis-augustis 2009 kogutud andmeid Soome lahest.

Töö tulemusena on näidatud, et termohaliinsete väljade pikaajalised muutused on seotud suuremastaabiliste tsirkulatsioonimustrite varieeruvusega atmosfääris. Soome lahes on need muutused selgelt näha põhjalähedases veekihis ja külmas vahekihis. Põhjalähedase kihi soolasemaks ja soojemaks muutumine alates üheksakümnendate keskpaigast on seotud intensiivsema veevahetusega Läänemere ja Põhjamere vahel. Pelagiaali ökosüsteemi seisukohalt on oluline, et sellise nihkega stratifikatsioonis halokliini sügavusel ei kaasnenud olulist muutust (töös kasutatud andmestiku põhjal aastatest 1987-2009) ülemises veekihis ja külmas vahekihis, kuigi mõlemas nimetatud kihis esines märkimisväärne aastatevaheline muutlikkus. Vahekihi suvised temperatuurid sõltuvad suures osas eelnenud talve karmusest, kuigi ka suve vältel leiab seal aset vee aeglane soojenemine.

Soome lahes esineb stratifitseeritud estuaaridele iseloomulik voolamine, kus ülemises kihis liigub vesi lahest välja ja sügavamtes kihtides lahte sisse. Enim estuaari tüüpi voolamist intensiivistavateks ja see läbi ka stratifikatsiooni tugevdavateks tuulteks on kirde-, põhja- ja loodetuuled. Oluline on, et intensiivse estuaari tüüpi voolamisega kantakse Soome lahe põhjakihti Läänemere avaosast tavalisest enam toitaineid (eelkõige fosfaate). Nimetatud tuuled kutsuvad esile ka süvaveekerkeid, mis lisaks soojuse ja soolade ümberjaotamisele lahes, tõstavad ülemisse kihti toitaineid. Kesksuvisel ajal, kui toitainete väärtused on mere pinnakihis sisuliselt langenud alla määramispiiri, on selline voog märkimisväärne lisaressurss fütoplanktoni kasvuks. 2006. aastal mõõdistatud massiivne apvelling tõi pinnakihti ligikaudu samaväärse hulga toitaineid, mis saabub lahte kõikidest jõgedest kokku ühe kuu jooksul. Lisaks näitasid vaatlused apvellingu tekkimisest kuni tavapärase stratifikatsiooni taaskujunemiseni, et süvaveekerked soodustavad vertikaalset segunemist ning nitrakliini ja fosfokliini vertikaalse eraldatuse suurenemist.

Veesamba autonoomse profileerija abil suure ajalise lahutusega teostatud mõõtmised näitasid, et atmosfääri mõjud sünoptilises ajamastaabis põhjustavad teatud füüsikaliste protsesside domineerimise meres, mille tulemusena

eksisteerivad selgelt üksteisest erineva vertikaalse stratifikatsiooniga perioodid. Juulis-augustis kogutud andmete põhjal olid domineerivateks füüsikalisteks protsessideks apvelling, apvellingu taandumine, estuaari tüüpi tsirkulatsiooni ümberpööramine, estuaari tüüpi tsirkulatsioon ja daunvelling. Muutusi vertikaalses stratifikatsioonis on võimalik modelleerida suhteliselt täpselt kasutades selleks loodud lihtsat mudelit, kus on arvesse võetud soojusvood mere pinnal, tuule poolt põhjustatud vertikaalne segunemine, soolsuse horisontaalse gradiendiga samas sihis toimuv tuulest tingitud vee liikumine pinnakihis ja estuaarne tsirkulatsioon. Suurimad erinevused mõõdetud ja modelleeritud stratifikatsiooni muutuste vahel esinesid, kui valdavaks protsessiks oli risti lahte liikumine pinnakihis ja sellega kaasnevad tiheduse samajoonte vertikaalsed nihked (apvelling või daunvelling).

Erinevad domineerinud füüsikalised protsessid avaldasid olulist mõju fütoplanktoni vertikaalsele jaotusele. On näidatud, et pinna-aluste klorofülli maksimumide teke ja jaotus on tihedalt seotud vertikaalse stratifikatsiooniga – maksimumid paiknevad termokliini alaosas ja ühtivad nitrakliiniga. Fütoplanktoni vertikaalses migratsioonis domineerib teatud füüsikaliste tingimuste puhul ööpäevane tsükkel. Dinoflagelladi *Heterocapsa triquetra* domineerimise perioodil õnnestus autonoomse profileerija abil registreerida klorofülli maksimumi liikumist sügavamale kiirusega kuni 1,6 m h^{-1}.

ELULOOKIRJELDUS

1. Isikuandmed

Ees- ja perekonnanimi: Taavi Liblik
Sünniaeg ja –koht: 10.03.1981, Kuressaare
Kodakondsus: Eesti

2. Kontaktandmed

Aadress: Akadeemia tee 15a, 12618 Tallinn, Eesti.
Telefon: 6204315
E-posti aadress: taavi.liblik@msi.ttu.ee

3. Hariduskäik

Õppeasutus	Aasta	Haridus (eriala/kraad)
Tallinna Tehnikaülikool	2008	Tehniline füüsika/magistrikraad
Eesti Mereakadeemia	2004	Hüdrograafia/rakenduskõrgharidus
Saaremaa Ühisgümnaasium	1999	Keskharidus

4. Keelteoskus

Keel	Tase
Eesti keel	Emakeel
Inglise keel	Keskmine

5. Teenistuskäik

Töötamise aeg	Tööandja nimetus	Ametikoht
2006-…	TTÜ Meresüsteemide Instituut	Insener
2008-2010	Ramboll Eesti AS	Keskkonnaekspert
2004-2006	Eesti Mereakadeemia	Assistent

6. Publikatsioonid Eesti Teadusinfosüsteemi klassifikaatori järgi

1.1.

Liblik, T; Lips, U. (2011). Characteristics and variability of the vertical thermohaline structure in the Gulf of Finland in summer. Boreal Environment Research, 16A, 73 - 83.

Liblik, T; Lips, U. (2011). Spreading of suspended matter in a shallow sea area influenced by dredging activities and variable atmospheric forcing: results of in-situ measurements. Journal of Coastal Research, SI 64, 561 - 566.

Lips, U; Lips, I; Liblik, T; Kikas, V; Altoja, K; Buhhalko, N; Rünk, N (2011). Vertical dynamics of summer phytoplankton in a stratified estuary (Gulf of Finland, Baltic Sea). Ocean Dynamics, 61, 903 - 915.

Kuvaldina, N., Lips, I., Lips, U., Liblik, T. (2010). The influence of a coastal upwelling event to the spatio-temporal distribution of nutrients and chlorophyll a in the Gulf of Finland, Baltic Sea: observational results. Hydrobiologia, 639(1), 221 - 230.

Lips, U., Lips, I., Liblik, T., Kuvaldina, N. (2010). Processes responsible for the formation and maintenance of sub-surface chlorophyll maxima in the Gulf of Finland. Estuarine, coastal and shelf science, 88, 339 - 349.

Lips, I.; Lips, U.; Liblik, T. (2009). Consequences of coastal upwelling events on physical and chemical patterns in the central Gulf of Finland (Baltic Sea). Continental Shelf Research, 29, 1836 - 1847.

1.3.

Liblik, T; Lips, U (2006). Analysis of hydrometeorological conditions for environmental impact assessment of reconstruction of Rohuküla and Heltermaa harbors. Eesti Mereakadeemia Toimetised, 3, 32 - 43.

Liblik, T; Lips, U (2004). Soela sadama rajamise ja ekspluateerimise keskkonnamõjude eelhinnang. Eesti Mereakadeemia Toimetised, 1, 82 - 98.

Liblik, T.; Lips, U.; Keevallik, S. (2004). Soome lahe tuulerežiimi analüüs Kalbådagrundi meteojaama andmete põhjal. Eesti Mereakadeemia Toimetised, 1, 108 - 120.

3.1.

Lips, U; Lips, I; Liblik, T; Elken, J (2008). Estuarine transport versus vertical movement and mixing of water masses in the Gulf of Finland (Baltic Sea). US/EU-Baltic Symposium "Ocean Observations, Ecosystem-Based Management & Forecasting", Tallinn, 27-29 May, 2008. IEEE, 2008, (IEEE Conference Proceedings), 1 - 8.

3.2.

Elken, J; Kõuts, T; Lips, U; Raudsepp, U; Lagemaa, P; Liblik, T (2007). Performance of the Operational HIROMB Model in Relation to the Oceanographic Extreme Events and Seasonal Fluxes in the Gulfs of

Finland and Riga. Hans-Jörg Isemer (Toim.). Fifth Study Conference on BALTEX, Kuressaare, Saaremaa, Estonia, 4 - 8 June 2007. (77 - 78). Geesthacht: International BALTEX Secretariat

3.4.

Lips, U.; Lips, I.; Liblik, T.; Kikas, V.; Altoja, K.; Kuvaldina, N.; Norit, N. (2010). Multiparametric in-situ observations in the Gulf of Finland. Proceedings of the 2nd International Conference (school) on DYNAMICS OF COASTAL ZONE OF NON-TIDAL SEAS, Baltiysk, 26-30 June 2010 (284 - 289). Kaliningrad: Terra Baltica

Erm, A; Elken, J; Pavelson, J; Kask, J; Voll, M; Kört, M; Roots, O; Liblik, T; Lagemaa, P; Buschmann, F (2010). Observation of High-Speed Deep Currents and Resuspension of Soft Sediments in the Central Part of the Gulf of Finland. *In: The Baltic Sea Geology-10. The 10-th International Marine Geological Conference. 24-28 August 2010, VSEGEI, St. Petersburg, Russia. Abstract volume, 164 p.:* SPb.: Press VSEGEI, 2010, 25 - 26.

6.3.

Liblik, T (2010). Retk merepõhja sügavusse. Tarkade Klubi, 1, 54 - 59.

7. Kaitstud lõputööd

Temperatuuri ja soolsuse vertikaalse jaotuse iseärasused Soome lahes suvekuudel. Magistritöö Tallinna Tehnikaülikoolis, 2008.

Soela sadama rajamise ja ekspulateerimise keskkonnamõjude eelhinnang. Lõputöö Eesti Mereakadeemias, 2004.

8. Teadustöö põhisuunad

Hüdrofüüsikalised protsessid Läänemeres ja neid mõjutavad tegurid.

9. Uurimisprojektid Eesti Teadusinfosüsteemi järgi

Eesti Teadusfondi grandid

Hüppekihid stratifitseeritud estuaaride ökosüsteemis, 2012 - 2015.

Upwellingud Soome lahes ja nendega seotud toitainete transport, 2008 - 2011.

Fütoplanktoni biomassi pinna-alused maksimumid Soome lahes: esinemise ulatus, teket soodustavad tingimused ja nende roll, 2007 - 2010.

Soome lahe hüdrofüüsikaliste iseärasuste mõju fütoplanktoni biomassi ja liigilise koosseisu laigulisusele, 2006 - 2009.

Miksotroofsuse suhteline osatähtsus eutroofses Läänemeres, 2011-2014.

Siseriiklikud rakenduslikud uurimisprojektid

Avamere seire 2011. a, 2011- 2012.

Nord Streami gaasijuhtme rajamise mõju-uuring Soome lahe merekeskkonnale, 2010-2011.

Aegna sadama rekonstrueerimise keskkonnamõju hindamine, 2010.

Hundipea sadama rekonstrueerimise keskkonnamõju hindamine. Meteoroloogiline ja hüdroloogiline režiim. Heljumi levik, 2009.

Virtsu sadama kai nr 8 ehituse süvendus ja kaadamistööde seire, 2009.

Kuressaare jahisadama laevatee süvendamise KMH peatükid 3.5 Meteoroloogiline ja hüdroloogiline režiim, 5.3 Hinnang heljumi levikule, 2008.

Heltermaa sadama rekonstrueerimise süvendus- ja kaadamistöödega seotud seire teostamine, 2008-2010.

Tehniline abi laevateede süvendamiseks ja rekonstrueerimiseks Lääne-Eesti saarestikus. Keskkonnamõju hindamine, 2008-2009.

Virtsu sadama 8. kai tööprojekti keskkonnamõju hindamine - hüdrometeoroloogia ja heljumi levik, 2007.

Avamere tuuleparkide rajamisega Loode-Eesti rannikumerre kaasnevate keskkonnamõjude hindamine, peatükid 3.6, 5.2, 5.3, 5.10, 2007.

Naissaare sadama-ala uuringud, 2007.

Mere õlireostuse varase avastamise ja leviku prognoosi tehnoloogia, 2006-2008.

Kärdla piirkonna keskkonnamõjude hindamise hüdrometeoroloogia ja heljumi leviku osad, 2006.

Välisprojektid

Good environmental status through regional coordination and capacity building, 2011-2013.

Measurements and analyses for the assessment of environmental state of the Baltic Sea, 2010.

BalticSeaNow.info - Innovative participatory forum for the Baltic Sea, 2009-2012.

CURRICULUM VITAE

1. Personal data

Name: Taavi Liblik
Date and place of birth: 10.03.1981, Kuressaare
Citizenship: Estonia

2. Contact information

Aadress: Akadeemia tee 15a, 12618 Tallinn, Estonia.
Phone: 6204315
E-mail: taavi.liblik@msi.ttu.ee

3. Education

Institution	Year	Education (field of study/degree)
Tallinn University of Technology	2008	Physics/master's degree
Estonian Maritime Academy	2004	Hydrography/professional higher education
Saaremaa Gymnasium	1999	Secondary

4. Language competence/skills

Language	Level
Eesti keel	Native langue
Inglise keel	Average

5. Professional Employment

Period	Organisation	Position
2006-…	Marine Systems Institute at Tallinn University of Technology	Engineer
2008-2010	Ramboll Eesti AS	Environmental expert
2004-2006	Estonian Maritime Academy	Assistant

6. Publications according to the Estonian Research Information System

1.1.

Liblik, T; Lips, U. (2011). Characteristics and variability of the vertical thermohaline structure in the Gulf of Finland in summer. Boreal Environment Research, 16A, 73 - 83.

Liblik, T; Lips, U. (2011). Spreading of suspended matter in a shallow sea area influenced by dredging activities and variable atmospheric forcing: results of in-situ measurements. Journal of Coastal Research, SI 64, 561 - 566.

Lips, U; Lips, I; Liblik, T; Kikas, V; Altoja, K; Buhhalko, N; Rünk, N (2011). Vertical dynamics of summer phytoplankton in a stratified estuary (Gulf of Finland, Baltic Sea). Ocean Dynamics, 61, 903 - 915.

Kuvaldina, N., Lips, I., Lips, U., Liblik, T. (2010). The influence of a coastal upwelling event to the spatio-temporal distribution of nutrients and chlorophyll a in the Gulf of Finland, Baltic Sea: observational results. Hydrobiologia, 639(1), 221 - 230.

Lips, U., Lips, I., Liblik, T., Kuvaldina, N. (2010). Processes responsible for the formation and maintenance of sub-surface chlorophyll maxima in the Gulf of Finland. Estuarine, coastal and shelf science, 88, 339 - 349.

Lips, I.; Lips, U.; Liblik, T. (2009). Consequences of coastal upwelling events on physical and chemical patterns in the central Gulf of Finland (Baltic Sea). Continental Shelf Research, 29, 1836 - 1847.

1.3.

Liblik, T; Lips, U (2006). Analysis of hydrometeorological conditions for environmental impact assessment of reconstruction of Rohuküla and Heltermaa harbors. Eesti Mereakadeemia Toimetised, 3, 32 - 43.

Liblik, T; Lips, U (2004). EIA of the Soela harbor reconstruction (in Estonian). Eesti Mereakadeemia Toimetised, 1, 82 - 98.

Liblik, T.; Lips, U.; Keevallik, S. (2004). Analysis of the wind regime in the Gulf of Finland on the basis of Kalbådagrund wind data (in Estonian). Eesti Mereakadeemia Toimetised, 1, 108-120.

3.1.

Lips, U; Lips, I; Liblik, T; Elken, J (2008). Estuarine transport versus vertical movement and mixing of water masses in the Gulf of Finland (Baltic Sea). US/EU-Baltic Symposium "Ocean Observations, Ecosystem-Based Management & Forecasting", Tallinn, 27-29 May, 2008. IEEE, 2008, (IEEE Conference Proceedings), 1 - 8.

3.2.

Elken, J; Kõuts, T; Lips, U; Raudsepp, U; Lagemaa, P; Liblik, T (2007). Performance of the Operational HIROMB Model in Relation to the Oceanographic Extreme Events and Seasonal Fluxes in the Gulfs of

Finland and Riga. Hans-Jörg Isemer (Toim.). Fifth Study Conference on BALTEX, Kuressaare, Saaremaa, Estonia, 4 - 8 June 2007. (77 - 78). Geesthacht: International BALTEX Secretariat

3.4.

Lips, U.; Lips, I.; Liblik, T.; Kikas, V.; Altoja, K.; Kuvaldina, N.; Norit, N. (2010). Multiparametric in-situ observations in the Gulf of Finland. Proceedings of the 2nd International Conference (school) on DYNAMICS OF COASTAL ZONE OF NON-TIDAL SEAS, Baltiysk, 26-30 June 2010 (284 - 289). Kaliningrad: Terra Baltica

Erm, A; Elken, J; Pavelson, J; Kask, J; Voll, M; Kört, M; Roots, O; Liblik, T; Lagemaa, P; Buschmann, F (2010). Observation of High-Speed Deep Currents and Resuspension of Soft Sediments in the Central Part of the Gulf of Finland. *In: The Baltic Sea Geology-10. The 10-th International Marine Geological Conference. 24-28 August 2010, VSEGEI, St. Petersburg, Russia. Abstract volume, 164 p.:* SPb.: Press VSEGEI, 2010, 25 - 26.

6.3.

Liblik, T (2010). Retk merepõhja sügavusse. Tarkade Klubi, 1, 54 - 59.

7. Defended theses

Characteristics of vertical distribution of temperature and salinity in the Gulf of Finland in summer (in Estonian). Master thesis in Tallinn University of Technology, 2008.

Environmental impact assesment of the Soela harbor reconstruction (in Estonian). Diploma work in Estonian Maritime Academy, 2004.

8. Main areas of scientific work/Current research topics

Hydrophysical processes in the Baltic Sea.

9. Research projects

Estonian Science Foundation grants

Clines in stratified estuaries – implications to ecosystem functioning, 2012 - 2015.

Upwelling events and the related nutrient transport in the Gulf of Finland, 2008 - 2011.

Subsurface maxima of phytoplankton biomass in the Gulf of Finland: occurrence, favorable conditions for formation and their role, 2007 - 2010.

Influence of hydrographical features to the patchiness of phytoplankton biomass and species composition in the Gulf of Finland, 2006 - 2009.
The relative importance of mixotrophy in the eutrophic Gulf of Finland, 2011-2014.

National engineering projects

Open sea monitoring 2011. a, 2011- 2012.
Study of impact of Nord Stream gas pipeline construction to the Gulf of Finland environment, 2010-2011.
Environmental impact assesment of Aegna harbour reconstruction, 2010.
Environmental impact assessment of reconstruction of Hundipea harbour. Meteorological and hydrographic conditions. Spreading of suspended matter, 2009.
Monitoring of dredging and dumping during costruction of quay 8 in Virtsu harbour, 2009.
Technical assistance for dredging and reconstruction of shipping roites in the Western-Estonian archipelago. Environmental impact assesment, 2008-2009.
EIA of dredging of Kuressaare harbour fairway, chapters 3.5 Meteorological and hydrological regime, 5.3 Estimate of spreading of suspended matter, 2008.
Environmental monitoring of dredging and dumping activities related to the reconstruction of Heltermaa harbour, 2008-2010.
Environmental impact assessment of quay No 8 in Virtsu harbor - hydrometeorological conditions and transport of suspended matter, 2007.
Environmental impact assessment of construction of off-shore wind parks in the north-western Estonian coastal waters, chapters 3.6, 5.2, 5.3, 5.10, 2007.
Investigations of Naissaare harbor area, 2007.
Early detection and drift forecast of marine oil pollution, 2006-2008.
Environmental impact assessment in Kardla coastal area, hydrometeorological conditions and spreading of suspended matter, 2006.

EU projects

Good environmental status through regional coordination and capacity building, 2011-2013.
Measurements and analyses for the assessment of environmental state of the Baltic Sea, 2010.
BalticSeaNow.info - Innovative participatory forum for the Baltic Sea, 2009-2012.

DISSERTATIONS DEFENDED AT TALLINN UNIVERSITY OF TECHNOLOGY ON *NATURAL AND EXACT SCIENCES*

1. **Olav Kongas**. Nonlinear Dynamics in Modeling Cardiac Arrhytmias. 1998.

2. **Kalju Vanatalu**. Optimization of Processes of Microbial Biosynthesis of Isotopically Labeled Biomolecules and Their Complexes. 1999.

3. **Ahto Buldas**. An Algebraic Approach to the Structure of Graphs. 1999.

4. **Monika Drews**. A Metabolic Study of Insect Cells in Batch and Continuous Culture: Application of Chemostat and Turbidostat to the Production of Recombinant Proteins. 1999.

5. **Eola Valdre**. Endothelial-Specific Regulation of Vessel Formation: Role of Receptor Tyrosine Kinases. 2000.

6. **Kalju Lott**. Doping and Defect Thermodynamic Equilibrium in ZnS. 2000.

7. **Reet Koljak**. Novel Fatty Acid Dioxygenases from the Corals *Plexaura homomalla* and *Gersemia fruticosa.* 2001.

8. **Anne Paju**. Asymmetric oxidation of Prochiral and Racemic Ketones by Using Sharpless Catalyst. 2001.

9. **Marko Vendelin**. Cardiac Mechanoenergetics *in silico*. 2001.

10. **Pearu Peterson**. Multi-Soliton Interactions and the Inverse Problem of Wave Crest. 2001.

11. **Anne Menert**. Microcalorimetry of Anaerobic Digestion. 2001.

12. **Toomas Tiivel**. The Role of the Mitochondrial Outer Membrane in *in vivo* Regulation of Respiration in Normal Heart and Skeletal Muscle Cell. 2002.

13. **Olle Hints**. Ordovician Scolecodonts of Estonia and Neighbouring Areas: Taxonomy, Distribution, Palaeoecology, and Application. 2002.

14. **Jaak Nõlvak**. Chitinozoan Biostratigrapy in the Ordovician of Baltoscandia. 2002.

15. **Liivi Kluge**. On Algebraic Structure of Pre-Operad. 2002.

16. **Jaanus Lass**. Biosignal Interpretation: Study of Cardiac Arrhytmias and Electromagnetic Field Effects on Human Nervous System. 2002.

17. **Janek Peterson**. Synthesis, Structural Characterization and Modification of PAMAM Dendrimers. 2002.

18. **Merike Vaher**. Room Temperature Ionic Liquids as Background Electrolyte Additives in Capillary Electrophoresis. 2002.

19. **Valdek Mikli**. Electron Microscopy and Image Analysis Study of Powdered Hardmetal Materials and Optoelectronic Thin Films. 2003.

20. **Mart Viljus**. The Microstructure and Properties of Fine-Grained Cermets. 2003.

21. **Signe Kask**. Identification and Characterization of Dairy-Related *Lactobacillus.* 2003

22. **Tiiu-Mai Laht**. Influence of Microstructure of the Curd on Enzymatic and Microbiological Processes in Swiss-Type Cheese. 2003.

23. **Anne Kuusksalu**. 2–5A Synthetase in the Marine Sponge *Geodia cydonium*. 2003.

24. **Sergei Bereznev**. Solar Cells Based on Polycristalline Copper-Indium Chalcogenides and Conductive Polymers. 2003.

25. **Kadri Kriis**. Asymmetric Synthesis of C_2-Symmetric Bimorpholines and Their Application as Chiral Ligands in the Transfer Hydrogenation of Aromatic Ketones. 2004.

26. **Jekaterina Reut**. Polypyrrole Coatings on Conducting and Insulating Substracts. 2004.

27. **Sven Nõmm**. Realization and Identification of Discrete-Time Nonlinear Systems. 2004.

28. **Olga Kijatkina**. Deposition of Copper Indium Disulphide Films by Chemical Spray Pyrolysis. 2004.

29. **Gert Tamberg**. On Sampling Operators Defined by Rogosinski, Hann and Blackman Windows. 2004.

30. **Monika Übner**. Interaction of Humic Substances with Metal Cations. 2004.

31. **Kaarel Adamberg**. Growth Characteristics of Non-Starter Lactic Acid Bacteria from Cheese. 2004.

32. **Imre Vallikivi**. Lipase-Catalysed Reactions of Prostaglandins. 2004.

33. **Merike Peld**. Substituted Apatites as Sorbents for Heavy Metals. 2005.

34. **Vitali Syritski**. Study of Synthesis and Redox Switching of Polypyrrole and Poly(3,4-ethylenedioxythiophene) by Using *in-situ* Techniques. 2004.

35. **Lee Põllumaa**. Evaluation of Ecotoxicological Effects Related to Oil Shale Industry. 2004.

36. **Riina Aav**. Synthesis of 9,11-Secosterols Intermediates. 2005.

37. **Andres Braunbrück**. Wave Interaction in Weakly Inhomogeneous Materials. 2005.

38. **Robert Kitt**. Generalised Scale-Invariance in Financial Time Series. 2005.

39. **Juss Pavelson**. Mesoscale Physical Processes and the Related Impact on the Summer Nutrient Fields and Phytoplankton Blooms in the Western Gulf of Finland. 2005.

40. **Olari Ilison**. Solitons and Solitary Waves in Media with Higher Order Dispersive and Nonlinear Effects. 2005.

41. **Maksim Säkki**. Intermittency and Long-Range Structurization of Heart Rate. 2005.

42. **Enli Kiipli**. Modelling Seawater Chemistry of the East Baltic Basin in the Late Ordovician–Early Silurian. 2005.

43. **Igor Golovtsov**. Modification of Conductive Properties and Processability of Polyparaphenylene, Polypyrrole and polyaniline. 2005.

44. **Katrin Laos**. Interaction Between Furcellaran and the Globular Proteins (Bovine Serum Albumin β-Lactoglobulin). 2005.

45. **Arvo Mere**. Structural and Electrical Properties of Spray Deposited Copper Indium Disulphide Films for Solar Cells. 2006.

46. **Sille Ehala**. Development and Application of Various On- and Off-Line Analytical Methods for the Analysis of Bioactive Compounds. 2006.

47. **Maria Kulp**. Capillary Electrophoretic Monitoring of Biochemical Reaction Kinetics. 2006.

48. **Anu Aaspõllu.** Proteinases from *Vipera lebetina* Snake Venom Affecting Hemostasis. 2006.

49. **Lyudmila Chekulayeva**. Photosensitized Inactivation of Tumor Cells by Porphyrins and Chlorins. 2006.

50. **Merle Uudsemaa**. Quantum-Chemical Modeling of Solvated First Row Transition Metal Ions. 2006.

51. **Tagli Pitsi**. Nutrition Situation of Pre-School Children in Estonia from 1995 to 2004. 2006.

52. **Angela Ivask**. Luminescent Recombinant Sensor Bacteria for the Analysis of Bioavailable Heavy Metals. 2006.

53. **Tiina Lõugas**. Study on Physico-Chemical Properties and Some Bioactive Compounds of Sea Buckthorn (*Hippophae rhamnoides* L.). 2006.

54. **Kaja Kasemets**. Effect of Changing Environmental Conditions on the Fermentative Growth of *Saccharomyces cerevisae* S288C: Auxo-accelerostat Study. 2006.

55. **Ildar Nisamedtinov**. Application of ^{13}C and Fluorescence Labeling in Metabolic Studies of *Saccharomyces* spp. 2006.

56. **Alar Leibak**. On Additive Generalisation of Voronoï's Theory of Perfect Forms over Algebraic Number Fields. 2006.

57. **Andri Jagomägi**. Photoluminescence of Chalcopyrite Tellurides. 2006.

58. **Tõnu Martma**. Application of Carbon Isotopes to the Study of the Ordovician and Silurian of the Baltic. 2006.

59. **Marit Kauk**. Chemical Composition of $CuInSe_2$ Monograin Powders for Solar Cell Application. 2006.

60. **Julia Kois**. Electrochemical Deposition of $CuInSe_2$ Thin Films for Photovoltaic Applications. 2006.

61. **Ilona Oja Açik**. Sol-Gel Deposition of Titanium Dioxide Films. 2007.

62. **Tiia Anmann**. Integrated and Organized Cellular Bioenergetic Systems in Heart and Brain. 2007.

63. **Katrin Trummal**. Purification, Characterization and Specificity Studies of Metalloproteinases from *Vipera lebetina* Snake Venom. 2007.

64. **Gennadi Lessin**. Biochemical Definition of Coastal Zone Using Numerical Modeling and Measurement Data. 2007.

65. **Enno Pais**. Inverse problems to determine non-homogeneous degenerate memory kernels in heat flow. 2007.

66. **Maria Borissova**. Capillary Electrophoresis on Alkylimidazolium Salts. 2007.

67. **Karin Valmsen**. Prostaglandin Synthesis in the Coral *Plexaura homomalla*: Control of Prostaglandin Stereochemistry at Carbon 15 by Cyclooxygenases. 2007.

68. **Kristjan Piirimäe**. Long-Term Changes of Nutrient Fluxes in the Drainage Basin of the Gulf of Finland – Application of the PolFlow Model. 2007.

69. **Tatjana Dedova**. Chemical Spray Pyrolysis Deposition of Zinc Sulfide Thin Films and Zinc Oxide Nanostructured Layers. 2007.

70. **Katrin Tomson**. Production of Labelled Recombinant Proteins in Fed-Batch Systems in *Escherichia coli*. 2007.

71. **Cecilia Sarmiento**. Suppressors of RNA Silencing in Plants. 2008.

72. **Vilja Mardla**. Inhibition of Platelet Aggregation with Combination of Antiplatelet Agents. 2008.

73. **Maie Bachmann**. Effect of Modulated Microwave Radiation on Human Resting Electroencephalographic Signal. 2008.

74. **Dan Hüvonen**. Terahertz Spectroscopy of Low-Dimensional Spin Systems. 2008.

75. **Ly Villo**. Stereoselective Chemoenzymatic Synthesis of Deoxy Sugar Esters Involving *Candida antarctica* Lipase B. 2008.

76. **Johan Anton**. Technology of Integrated Photoelasticity for Residual Stress Measurement in Glass Articles of Axisymmetric Shape. 2008.

77. **Olga Volobujeva**. SEM Study of Selenization of Different Thin Metallic Films. 2008.

78. **Artur Jõgi**. Synthesis of 4'-Substituted 2,3'-dideoxynucleoside Analogues. 2008.

79. **Mario Kadastik**. Doubly Charged Higgs Boson Decays and Implications on Neutrino Physics. 2008.

80. **Fernando Pérez-Caballero**. Carbon Aerogels from 5-Methylresorcinol-Formaldehyde Gels. 2008.

81. **Sirje Vaask**. The Comparability, Reproducibility and Validity of Estonian Food Consumption Surveys. 2008.

82. **Anna Menaker**. Electrosynthesized Conducting Polymers, Polypyrrole and Poly(3,4-ethylenedioxythiophene), for Molecular Imprinting. 2009.

83. **Lauri Ilison.** Solitons and Solitary Waves in Hierarchical Korteweg-de Vries Type Systems. 2009.

84. **Kaia Ernits.** Study of In_2S_3 and ZnS Thin Films Deposited by Ultrasonic Spray Pyrolysis and Chemical Deposition. 2009.

85. **Veljo Sinivee**. Portable Spectrometer for Ionizing Radiation "Gammamapper". 2009.

86. **Jüri Virkepu**. On Lagrange Formalism for Lie Theory and Operadic Harmonic Oscillator in Low Dimensions. 2009.

87. **Marko Piirsoo.** Deciphering Molecular Basis of Schwann Cell Development. 2009.

88. **Kati Helmja**. Determination of Phenolic Compounds and Their Antioxidative Capability in Plant Extracts. 2010.

89. **Merike Sõmera**. Sobemoviruses: Genomic Organization, Potential for Recombination and Necessity of P1 in Systemic Infection. 2010.

90. **Kristjan Laes**. Preparation and Impedance Spectroscopy of Hybrid Structures Based on $CuIn_3Se_5$ Photoabsorber. 2010.

91. **Kristin Lippur**. Asymmetric Synthesis of 2,2'-Bimorpholine and its 5,5'-Substituted Derivatives. 2010.

92. **Merike Luman**. Dialysis Dose and Nutrition Assessment by an Optical Method. 2010.

93. **Mihhail Berezovski**. Numerical Simulation of Wave Propagation in Heterogeneous and Microstructured Materials. 2010.

94. **Tamara Aid-Pavlidis**. Structure and Regulation of BDNF Gene. 2010.

95. **Olga Bragina**. The Role of Sonic Hedgehog Pathway in Neuro- and Tumorigenesis. 2010.

96. **Merle Randrüüt**. Wave Propagation in Microstructured Solids: Solitary and Periodic Waves. 2010.

97. **Marju Laars**. Asymmetric Organocatalytic Michael and Aldol Reactions Mediated by Cyclic Amines. 2010.

98. **Maarja Grossberg**. Optical Properties of Multinary Semiconductor Compounds for Photovoltaic Applications. 2010.

99. **Alla Maloverjan**. Vertebrate Homologues of Drosophila Fused Kinase and Their Role in Sonic Hedgehog Signalling Pathway. 2010.

100. **Priit Pruunsild**. Neuronal Activity-Dependent Transcription Factors and Regulation of Human *BDNF* Gene. 2010.

101. **Tatjana Knjazeva**. New Approaches in Capillary Electrophoresis for Separation and Study of Proteins. 2011.

102. **Atanas Katerski**. Chemical Composition of Sprayed Copper Indium Disulfide Films for Nanostructured Solar Cells. 2011.

103. **Kristi Timmo.** Formation of Properties of $CuInSe_2$ and $Cu_2ZnSn(S,Se)_4$ Monograin Powders Synthesized in Molten KI. 2011.

104. **Kert Tamm**. Wave Propagation and Interaction in Mindlin-Type Microstructured Solids: Numerical Simulation. 2011.

105. **Adrian Popp**. Ordovician Proetid Trilobites in Baltoscandia and Germany. 2011.

106. **Ove Pärn**. Sea Ice Deformation Events in the Gulf of Finland and This Impact on Shipping. 2011.

107. **Germo Väli**. Numerical Experiments on Matter Transport in the Baltic Sea. 2011.

108. **Andrus Seiman**. Point-of-Care Analyser Based on Capillary Electrophoresis. 2011.

109. **Olga Katargina**. Tick-Borne Pathogens Circulating in Estonia (Tick-Borne Encephalitis Virus, *Anaplasma phagocytophilum*, *Babesia* Species): Their Prevalence and Genetic Characterization. 2011.

110. **Ingrid Sumeri**. The Study of Probiotic Bacteria in Human Gastrointestinal Tract Simulator. 2011.

111. **Kairit Zovo**. Functional Characterization of Cellular Copper Proteome. 2011.

112. **Natalja Makarytsheva**. Analysis of Organic Species in Sediments and Soil by High Performance Separation Methods. 2011.

113. **Monika Mortimer**. Evaluation of the Biological Effects of Engineered Nanoparticles on Unicellular Pro- and Eukaryotic Organisms. 2011.

114. **Kersti Tepp**. Molecular System Bioenergetics of Cardiac Cells: Quantitative Analysis of Structure-Function Relationship. 2011.

115. **Anna-Liisa Peikolainen**. Organic Aerogels Based on 5-Methylresorcinol. 2011.

116. **Leeli Amon**. Palaeoecological Reconstruction of Late-Glacial Vegetation Dynamics in Eastern Baltic Area: A View Based on Plant Macrofossil Analysis. 2011.

117. **Tanel Peets**. Dispersion Analysis of Wave Motion in Microstructured Solids. 2011.

118. **Liina Kaupmees**. Selenization of Molybdenum as Contact Material in Solar Cells. 2011.

119. **Allan Olspert**. Properties of VPg and Coat Protein of Sobemoviruses. 2011.

120. **Kadri Koppel**. Food Category Appraisal Using Sensory Methods. 2011.

121. **Jelena Gorbatšova**. Development of Methods for CE Analysis of Plant Phenolics and Vitamins. 2011.

122. **Karin Viipsi**. Impact of EDTA and Humic Substances on the Removal of Cd and Zn from Aqueous Solutions by Apatite. 2012.

123. **David Schryer**. Metabolic Flux Analysis of Compartmentalized Systems Using Dynamic Isotopologue Modeling. 2012.

124. **Ardo Illaste**. Analysis of Molecular Movements in Cardiac Myocytes. 2012.

125. **Indrek Reile**. 3-Alkylcyclopentane-1,2-Diones in Asymmetric Oxidation and Alkylation Reactions. 2012.

126. **Tatjana Tamberg**. Some Classes of Finite 2-Groups and Their Endomorphism Semigroups. 2012.